From Trees to Seas

Phylogeny and Ecology as Predictors for Semicircular Canal Morphology

---

Dissertation

zur

Erlangung der naturwissenschaftlichen Doktorwürde
(Dr. sc. nat.)

vorgelegt der

Mathematisch-naturwissenschaftlichen Fakultät

der

Universität Zürich

von

Ashley E. Latimer

aus

Frankreich und Neuseeland

Promotionskomission
PD Dr. Torsten Scheyer
(Leitung der Dissertation)
Prof. Dr. Marcelo Sánchez-Villagra (Vorsitz)
Prof. Dr. Wolf Blankenhorn
Dr. Renaud Lebrun

Zürich, 2018

From Trees to Seas

Phylogeny and Ecology as Predictors for Semicircular Canal Morphology

Image: Lepidosaur inner ears
Ashley Latimer
Digital media 2017

Ashley Latimer, 2018

Summary

Sensory systems are the interface between organisms and their environment and they must collect the information an organism needs to survive. All vertebrates have one sense that is never lost, despite radical changes in body morphology and ecological transitions: balance and orientation. That basic sense is mediated by the semicircular canal system, which in addition balance and orientation, also allow for gaze stabilization, visually tracking moving objects, posture, and motion. The semicircular canals systems include soft tissue semicircular ducts as well as their impression in the skull, the semicircular canals. The ducts are filled with viscous fluid and receptive hair cells that transmit the motion of the fluid in impulses along nerves to the brain. The canals record that trace in any skull even without soft tissue, to a greater or lesser extent. The shape of these ducts and canals varies in all vertebrates, but the causes for these shapes are not explicitly known. Studies suggest that environment and phylogeny influence the shape, but investigations are often patchy, and mostly focusing on mammals. Understanding of the causes for semicircular canal shape have been directly applied to extinct organisms to predict their life history, with special interest on transitions from terrestrial to aquatic environments, however these changes may not be as powerful as thought.

In this thesis, with collaborators, I test several ideas and hypotheses related to semicircular canals across vertebrates, focusing on adaptations to aquatic environments. I use a fish an example from a lineage that has never left the water, and clades that have returned to the water in both mammals and reptiles. We use three-dimensional computed tomography to image the semicircular canals and compare them using phylogenetic methods and statistical modeling techniques.

In Chapter 2, I investigate the inner ear of the most aquatic seal, the Antarctic Ross seal *Ommatophoca rossii*, and identify reduced semicircular canal length and radius. This morphology is convergent with the morphology in whales but is not accompanied by a reduction in neck length. This suggests that there is something about semiaquatic habit that produces this morphology.

In Chapter 3, I describe a new fish from the Triassic of Switzerland using only a neurocranium. I show that the semicircular canals of this new, previously undescribed fish are useful in identifying phylogenetic relationships, and reconfirm that neurocranial characters are powerful predictors for phylogeny.

In Chapter 4, I investigate habit and phylogeny as predictors for semicircular canal morphology in squamates. I show that phylogeny and size alone predict semicircular canal morphology, and there is no effect of habit on the inner ear of squamates in this sample. In

Chapter 5, I extend this model to reptiles including living crocodylians, turtles, and extinct species: sauropterygians, one of the main lineages of Mesozoic marine reptiles, a sea turtle, and the Triassic archosauriform reptile *Euparkeria*. I find that the length of the semicircular canals can predict body mass, that neck length is not the universal cause of reduced semicircular canal radius across vertebrates, that the effects of habit on inner ear size are caused by sample inclusion, and the semicircular canal morphology is a useful predictor for phylogenetic relationship across reptiles.

These analyses show that phylogeny is the main predictor of semicircular canal morphology across vertebrates and should always be corrected for models investigating other predictors. Furthermore, habit cannot be usefully predicted across phylogenetic groups for extinct taxa.

Zusammenfassung

Sensorische Systeme sind die Schnittstelle zwischen Organismen und ihrer Umwelt und sie müssen die Informationen sammeln, die ein Organismus zum Überleben benötigt. Alle Wirbeltiere haben einen Sinn, der trotz radikaler Veränderungen der Körpermorphologie und ökologischer Übergänge nie verloren geht: der Gleichgewichts- und Orientierungssinn. Dieser Grundsinn wird durch das Bogengangsystem im Innenohr (Vestibularsystem) vermittelt, das neben Balance und Orientierung auch Blickstabilisierung, die visuelle Verfolgung sich bewegender Objekte, Haltung und auch Bewegung ermöglicht. Zu dem Vestibularsystem gehören halbkreisförmige Weichgewebegänge sowie deren Abdrücke im Schädel, den Bogengängen. Die Kanäle sind mit einer viskosen Flüssigkeit und empfänglichen Haarzellen gefüllt, welche die Bewegung der Flüssigkeit in Impulsen entlang Nerven zum Gehirn übertragen. Die Kanäle zeichnen mehr oder weniger präzise diese Spuren in jedem Schädel auch ohne das Vorhandensein der Weichgewebe auf. Die Form der Kanäle und Gänge variiert in allen Wirbeltieren, aber die Ursachen für diese Formenvariabilität sind nicht explizit bekannt. Studien deuten darauf hin, dass Umwelt und Stammesgeschichte die Form beeinflussen, aber Untersuchungen sind oft lückenhaft und konzentrieren sich hauptsächlich auf Säugetiere. Das Verständnis der Ursachen für die Formen der Bogengänge wurde direkt auf ausgestorbene Organismen angewendet, um ihre Lebensgeschichte vorherzusagen, mit besonderem Interesse an den Übergängen von terrestrischen zu aquatischen Umgebungen; jedoch sind diese Veränderungen möglicherweise nicht so stark wie bisher angenommen.
In dieser Arbeit teste ich mehrere Ideen und Hypothesen in Bezug auf die Morphologie der Bogengänge in Wirbeltieren mit Schwerpunkt auf Anpassungen an aquatisches Milieu. Ein Fisch wird hier als Beispiel aus einer Linie verwendet, die nie das Wasser verlassen hat, während aus den Säugetieren und Reptilien mehrere Gruppen untersucht wurden, die wieder ins Wasser zurückgekehrt sind. Die dreidimensionale Computertomographie ermöglicht die Abbildung der Bogengänge und erlaubt Vergleiche durch phylogenetische Methoden und statistische Modellierungstechniken.

In Kapitel 2 wurde das Innenohr der am stärksten aquatischen Robbe, der antarktischen Rossrobbe *Ommatophoca rossii*, untersucht, wobei eine Reduktion der Länge und des Radius der Bogengänge festgestellt wurde. Diese Morphologie ist konvergent mit der Morphologie des Innenohrs der Wale, aber sind geht nicht einher mit einer Verringerung der Halslänge. Dies deutet darauf hin, dass es etwas an der semiaquatischen Lebensweise gibt, welche diese Morphologie bei der Robbe hervorbringt.

Kapitel 3 beschreibt einen neuen Fisch aus der Trias der Schweiz basierend auf einem isolierten Neurocranium. Es kann gezeigt werden, dass die Bogengänge dieses neuen, bisher

unbeschriebenen Fisches nützlich sind, um phylogenetische Beziehungen zu identifizieren, was nochmals bestätigt, dass neurokraniale Merkmale starke Prädiktoren in phylogenetischen Untersuchungen sind.

Kapitel 4 untersucht Habitus und Phylogenie als Prädiktoren für die Bogengangmorphologie innerhalb der Squamaten. Phylogenie und Größe scheinen allein für die Morphologie der Bogengänge ausschlaggebend zu sein, und in der untersuchten Probe gibt es keinen Effekt der Lebensgewohnheiten auf das Innenohr.

In Kapitel 5 wurde dieses Modell auf Reptilien einschließlich lebender Krokodile, Vögel, und Schildkröten, sowie ausgestorbener Reptilarten ausgedehnt: Sauropterygier, eine der Hauptlinien mesozoischer Meeresreptilien, eine Meeresschildkröte, sowie das triassische archosauriforme Reptil *Euparkeria.* Die Ergebnisse zeigen, dass man mittels der Länge der Bogengänge die Körpermasse der Tiere vorhersagen kann, dass die Halslänge nicht die universelle Ursache für den reduzierten Radius der Bogengänge innerhalb der Wirbeltiere ist, dass die Auswirkungen von Lebensgewohnheiten auf die Innenohrgröße von den untersuchten Taxa abhängt, und dass die Morphologie der Bogengänge ein nützlicher Prädiktor für phylogenetische Untersuchungen innerhalb der Reptilien darstellt.

Diese Analysen zeigen, dass die Stammesgeschichte der wichtigste Prädiktor für die Morphologie der Bogengänge in Wirbeltieren ist und somit immer in anderen Modellen, welche andere Prädiktoren untersuchen, hierfür korrigiert werden sollte. Darüber hinaus können Lebensgewohnheiten für phylogenetische Gruppen für ausgestorbene Taxa nicht sinnvoll vorhergesagt werden.

Acknowledgements

Thank you to my supervisor Torsten Scheyer for giving a chance to an unpublished student from Texas, thank you for letting me follow my own project as it developed, and thank you for your patience and kindness when life took me on some interesting unforeseen adventures. Among many other things, thanks for translating my summary. Thank you to Marcelo Sanchez for your guidance, bringing me into interesting projects, and your patience when I double checked everything. Thank you to Renaud Lebrun for help with his program Meshtools and submissions to Morphomuseum. Thank you to the people who helped me get here, especially Ernie and Judy Lundelius, Martin Sander, and Christopher J. Bell. Although every person I mention deserves at least a paragraph, the following will have to do or these thanks risk becoming a novel.

Thanks to my co-authors for accepting me on their project, Mara Cleopatra Loza and Alfredo A. Carlini. Thank you for agreeing to help with my projects Emma Sherratt and Sam Giles. Emma, thank you for your patience with a statistics novice and your encouragement that it could be done. Sam, thank you for helping make some manky fish scribblings into something more palatable. Thanks to M. Plamondon (EMPA, Dübendorf) for scanning that fish. Two paragons Gertrud Rössner and Adriana Lopez-Arbarello, thank you. Thank you to Jessie Maisano (UTCT), without the scans you provided this thesis would look very different. Thank you to collections managers Erin Maxwell (Stuttgart), Pat Holroyd (Berkeley), Ingmar Werneburg (Tubingen), and William F. Simpson (Chicago) who let me search among the dead. Thank you to Josh and Julia Popp for opening your home in Chicago. Thank you to the discoverers, excavators, motivators, and teachers I cannot name.

Thank you to the lovely people I had the good luck to meet in Zurich, that made my time there a pleasure, and that made it difficult to leave. In no particular order, thanks to PIM mates Juan David Carrillo, Christian Kolb, Amane Tajika, Carlo Romano, Romain Jaittiot, Anita Schweizer, Carole Meier, Linda Frey, Anna Sanson Barrera, Alexandra Wegmann, Madlen Stange, Madeleine Geiger, Wei Wang, and Gabriel Aguirre Fernandez, Morgane Brosse, Marc Leu, Thodoris Argyriou, Borhan Bagherpour, Laura Heck, Jorge Carillo, Christian Klug, Markus Hebeisen, Heinz Furrer, Beat Scheffold, Heike Götzmann, Heinrich Walter, and Laura Wilson. Extra thanks to Anita Schweizer for being my partner-in-ears and checking my German! Thanks for sharing good times and good food Glauco Camensh, Tasneem Ariswala, Tina Cornioley, Chelsea Little, Alexandra Van Regensberg, Koen van Benthem, Judith Bachmann, Nina Vasiljevic and many more.

A big thank you to my supportive and generous adoptive phd family at ANU. Thanks to Loekse Kruuk and Scott Keogh for both making me feel welcome and providing a place for

me to work. Thank you to Simone Blomberg for a friendly chance mistaken identity and sound advice. Thanks to my adoptive lab and to the EE for their support and interest in my projects, shut up and write sessions, parties, game nights, adventures, discussions, and more: Marta Vidal Garcia, Damien Esquerre, Nina McLean, Claire Taylor, Jéssica Fenker, Leonardo Gonçalves Tedeschi, Brani Igić, Pierre Chuard, Jessie Au, Sonya Geange, Carlos Pavón, Regina Vega Trejo, Robyn Shaw, Pip Beale, Tomas Rowell, Dan Starrs, Alyssa Weinstein, Frances Amelia Jacomb, Daniela Malgarini-Perez, Rita Chou, Megan Head, Wendy King, and many more. Thanks to Josh Penalba for a little axolotl who cheered me up during a lot of writing days.

Timothée Bonnet, thank you for your friendship and especially your support on dark days. Thank you for the birds, your stimulating discussions, help with puzzling statistics, and playing "find the missing comma" in R.

This PhD also gave me the opportunity to live near family in Alsace, and they deserve a special thank you for letting me in their lives while I was near. Thanks to my brother Mike Latimer for supporting an insufferable little sister. Ronald Latimer, I know you would be proud. Thank you to my mother, Monique Latimer, for being my friend, listening, and cheering my adventures. Your support and encouragement mean so much more than words can express.

Table of Contents

Chapter 1 Introduction

All animals must correct for their motion and that of their environment to interact with their world. Balance, orientation, head position, and gaze stabilization are all mediated by the semicircular system, a sensory receptor common to all vertebrates and, exceptionally, never lost. There are three canals on each side of the head, each describing something close to an arc, in every vertebrate animal [1,2].

The semicircular system consists of soft tissue semicircular ducts filled with fluid and receptor hair cells enclosed by bones of the skull. The semicircular canals refer the bone that surrounds soft tissue, but the actual sensing is done by the soft tissue semicircular ducts. Semicircular ducts, as the name suggests, are fluid filled tubes with a swollen end containing a jelly-like cup covering small hair cells [1]. When an animal moves, or is moved by its environment, the fluid moves too, and displaces the cup and the associated hair cells. That information, along with information from the eyes, is transferred to the brain to give the animal a sense of how it has moved. This systems also allows for an organism to move its head while keeping its eyes fixed on an object, known as the vestibulo-ocular reflex, and adjust its posture [2]. Conveniently, the semicircular canals follow the semicircular ducts and allow non-invasive three-dimensional computed tomography to image the trace of the soft tissue from only bone. This allows the comparison of semicircular canals to some extent, be they from skulls recent or fossil.

The inner ears of mammals are the most extensively studied. In mammals each canal describes close to a semicircular arc. The degree of orthogonality, or how close the three canals come to being at right angles with each other, is usually highest in mammals of the groups although deviates from perfectly orthogonal [3], with a few notable exceptions such a sloths [3]. In mammals, eye size is linked with visual acuity [4], running speed and locomotion [5,6], and has been tested for flight and echolocation in bats, and a surprising number of groups have been investigated in depth [7–10]. This information has been used to inform the life history of extinct mammals [11].

The semicircular canals of reptiles have been associated with ecological traits such as burrowing and the origin of snakes [12,13], gliding in lizards [14], assisted walking in dwarf chameleons [15], and the ecomorph of *Anolis* lizards [16]. Often work on reptiles focuses on using extant taxa to predict life history of extinct taxa, such as sauropterygians [17,18], mosasaurs [19], flying reptiles [20,21], extinct dinosaurs [22,23], crocodylians [24], and *Euparkeria* [25].

The shape of the semicircular canals certainly carry information, but so does their size. In vertebrates, the size of the semicircular canals can predict the body mass of that taxon [26]

including reptiles and mammals, but size of the canals have not been used to predict body mass of extinct taxa.

Transitions

Both reptiles and mammals have conquered land and returned to the sea [27,28], and these transitions are associated with changes in the inner ear. The striking anatomy of whale inner ears is a prime example, the canals are much shorter and smaller than would be predicted for their size [29]. One hypothesis for the evolution of these small semicircular canals in whales is a concurrent shortening of cetacean necks [3]. These changes are not found in semiaquatic mammals, and semiaquatic habit does not predict ear shape when corrected for phylogeny in otters [8]. Although mammals and reptiles convergently evolved similar body proportions in similar habits, such as ichthyosaurs and dolphins, reptiles also evolved radically divergent long-necked morphologies such a plesiosaurs and thalattosaurs. Despite different body plans, shrunken semicircular canals are observed in both cetaceans and plesiosaurs [17].

The reptiles that radiated back into semiaquatic and aquatic habits in the Triassic are unfortunately extinct, and few living reptiles have regained that level of aquatic adaptation[30]. Two that have are sea snakes and sea turtles. Sea turtles still emerge from the water to lay eggs and are therefore not ideal to compare with fully pelagic taxa. On the other hand, sea snakes give birth to live young in the water but are not ideal to test convergences in the influence of neck length on the inner ear for obvious reasons. Other reptiles can swim in the ocean, such as the marine iguana and the saltwater crocodile, but neither are quite the right comparison for fully pelagic marine reptiles.

Lacking living fully pelagic reptiles with variable neck lengths, comparisons between the various living taxa can at least be undertaken. The living semiaquatic taxa include a host of monitor lizards in the genus *Varanus*, the marine iguana *Amblyrhynchus*, as well as other taxa that swim and live near water, as well as living crocodiles and turtles. Shape convergences in the semicircular canals, or lack thereof, would provide a starting point for the comparison of shape between taxa which are not closely related. Aside from snakes [12], comparisons of semicircular canal shape from reptiles with semiaquatic and aquatic habit that are corrected for phylogeny are lacking.

Study Aims and methods.

This study focuses on the semicircular canals of fish, reptiles, and mammals with aquatic habits. In doing so I hope to understand the convergent evolution of the semicircular canals in independently aquatic lineages of vertebrates. I specifically test the hypothesis of

neck reduction predicting reduction in semicircular canals, the applicability of body mass predictions, and the influence of phylogeny on semicircular canal morphology.

I accomplish this by combining non-destructive imaging techniques, comparative anatomy, and three dimensional morphometrics. Surfaces of the inner ears of diverse vertebrates were extracted from three-dimensional computed tomography scans of skulls or fossils. These surfaces were either examined using traditional comparative anatomy or three-dimensional morphometrics. Traditional comparative anatomy was used to described a new fossil fish and to compare the inner ears of Antarctic seals. For reptiles, three-dimensional landmarks were placed on the central streamlines of the canals to capture their shape, and comparison of those canals was facilitated using statistical methods such as phylogenetic least squares analysis.

Thesis outline

Along with co-authors I describe inner ear morphology in relation to phylogeny, habitat, and body morphology and compare it to predictions based on those variables in the literature. I focus on transitions to aquatic environments in different clades, and look at the outgroup, fish which never left the water.

In Chapter 1 I investigate the inner ear of the most pelagic seal, the Antarctic Ross seal *Ommatophoca rossi*, for clues to the pelagic ear described above. Indeed, I identify shorter semicircular canal length and radii than would be predicted for the body size of the Ross seal when compared with other seals. Although the semicircular canals are larger than those in whales, the convergent reduction in pelagic habits is striking. This convergent reduction is not, however, accompanied by a reduction in neck length. This suggest that there is something about semiaquatic habit that produces shorter canals independent of neck length.

In Chapter 2 I describe a new fish from the Triassic of Switzerland from a neurocranium alone. I show that the semicircular canals of this formerly undescribed fish are useful in identifying phylogenetic relationships and reconfirm that neurocranial characters are powerful predictors for phylogeny, less homoplastic than characters outside the braincase. This new fish does not exhibit reduced canal radii as seen in other pelagic taxa, consistent with all other fish investigated in this course of this study.

In Chapter 3 I investigate habit and phylogeny as predictors for semicircular canal morphology in squamates. I show that phylogeny alone predicts semicircular canal shape, and habit has no discernable effect on the inner ear shape of squamates in our sample. This suggests that prediction of habit from inner ears of unrelated taxa is not advisable and extended to the next chapter.

In Chapter 4 I extend this model to reptiles including living crocodylians, turtles, and extinct species: Sauropterygians, a sea turtle, and *Euparkeria*. I find that the length of the semicircular canals can predict body mass, that short neck length does not universally reduce semicircular canal radius across vertebrates, that the effects of habit on inner ear size are caused by sample inclusion, and the semicircular canal morphology is a useful predictor for phylogenetic relationship across reptiles.

These analyses show that phylogeny is the main predictor of semicircular canal morphology across vertebrates and should always be corrected for models investigating other predictors. Furthermore, habit cannot be usefully predicted across phylogenetic group for extinct taxa.

References

1. Federative Committee on AnatomicalTerminology. 1998 *Terminologia Anatomica*. Stuttgart: Georg Thieme Verlag.

2. Henn V. 1988 Visual-Vestibular Interaction. In *Sensory Systems I Vision and Visual Systems* (ed G Aldeman), pp. 114–115. Basel: Birkhäuser. (doi:978-1-4899-6647-6)

3. Berlin JC, Kirk EC, Rowe TB. 2013 Functional implications of ubiquitous semicircular canal non-orthogonality in mammals. *PLoS One* **8**, 24–26. (doi:10.1371/journal.pone.0079585)

4. Kemp AD, Kirk EC. 2014 Eye Size and Visual Acuity Influence Vestibular Anatomy in Mammals. *Anat. Rec. Integr. Anat. Evol. Biol.* **297**, 781–790. (doi:10.1002/ar.22892)

5. Grohé C, Lee B, Flynn JJ. 2018 Recent inner ear specialization for high-speed hunting in cheetahs. , 1–8. (doi:10.1038/s41598-018-20198-3)

6. Malinzak MD, Kay RF, Hullar TE. 2012 Locomotor head movements and semicircular canal morphology in primates. *Proc. Natl. Acad. Sci. U. S. A.* **109**, 17914–17919. (doi:10.1073/pnas.1206139109)

7. Davies KTJ, Bates PJJ, Maryanto I, Cotton JA, Rossiter SJ. 2013 The Evolution of Bat Vestibular Systems in the Face of Potential Antagonistic Selection Pressures for Flight and Echolocation. *PLoS One* **8**, 8–10. (doi:10.1371/journal.pone.0061998)

8. Grohe C, Tseng ZJ, Lebrun R, Boistel R, Flynn JJ. 2016 Bony labyrinth shape variation in extant Carnivora: a case study of Musteloidea. *J. Anat.* **228**, 366–383. (doi:10.1111/joa.12421)

9. Loza CM, Latimer AE, Sánchez-Villagra MR, Carlini AA. 2017 Sensory anatomy of the most aquatic of carnivorans: the Antarctic Ross seal, and convergences with other mammals. *Biol. Lett.* **20170489**. (doi:http://dx.doi.org/10.1098/rsbl.2017.0489)

10. Pfaff C, Martin T, Ruf I. 2015 Bony labyrinth morphometry indicates locomotor adaptations in the squirrel-related clade (Rodentia, Mammalia). *Proc. R. Soc. B-Biological Sci.* **282**. (doi:ARTN 2015074410.1098/rspb.2015.0744)
11. Kirk EC, Hoffmann S, Kemp AD, Krause DW, O'Connor PM. 2014 Sensory Anatomy and Sensory Ecology of *Vintana Sertichi* (Mammalia, Gondwanatheria) from the Late Cretaceous of Madagascar. *J. Vertebr. Paleontol.* **34**, 203–222. (doi:10.1080/02724634.2014.963232)
12. Palci A, Hutchinson MN, Caldwell MW, Lee MSY. 2017 The morphology of the inner ear of squamate reptiles and its bearing on the origin of snakes. *R. Soc. Open Sci.* **4**, 170685. (doi:10.1098/rsos.170685)
13. Yi H, Norell MA. 2015 The burrowing origin of modern snakes. *Sci. Adv.* **1**, 1–5. (doi:10.1126/sciadv.1500743)
14. Boistel R, Herrel A, Lebrun R, Daghfous G, Tafforeau P, Losos JB, Vanhooydonck B. 2011 Shake rattle and roll: The bony labyrinth and aerial descent in squamates. *Integr. Comp. Biol.* **51**, 957–968. (doi:10.1093/icb/icr034)
15. Boistel R, Herrel A, Daghfous G, Libourel P-A, Boller E, Tafforeau P, Bels V. 2010 Assisted walking in Malagasy dwarf chamaeleons. *Biol. Lett.* **6**, 740–743. (doi:10.1098/rsbl.2010.0322)
16. Dickson B V., Sherratt E, Losos JB, Pierce SE. 2017 Semicircular canals in *Anolis* lizards: ecomorphological convergence and ecomorph affinities of fossil species. *R. Soc. Open Sci.* **4**, 170058. (doi:10.1098/rsos.170058)
17. Neenan JM, Reich T, Evers SW, Druckenmiller PS, Voeten DFAE, Choiniere JN, Barrett PM, Pierce SE, Benson RBJ. 2017 Evolution of the Sauropterygian Labyrinth with Increasingly Pelagic Lifestyles. *Curr. Biol.* , 1–7. (doi:10.1016/j.cub.2017.10.069)
18. Neenan JM, Scheyer TM. 2014 New specimen of Psephoderma alpinum (Sauropterygia, Placodontia) from the Late Triassic of Schesaplana Mountain, Graubünden, Switzerland. *Swiss J. Geosci.* **107**, 349–357. (doi:10.1007/s00015-014-0173-9)
19. Cuthbertson RS, Maddin HC, Holmes RB, Anderson JS. 2015 The Braincase and Endosseous Labyrinth of Plioplatecarpus peckensis (Mosasauridae, Plioplatecarpinae), With Functional Implications for Locomotor Behavior. *Anat. Rec.* **298**, 1597–1611. (doi:10.1002/ar.23180)
20. Domínguez Alonzo P, Milner AC, Ketcham RA, Cookson MJ, Rowe TB. 2004 The avian nature of the brain and inner ear of Archaeopteryx. *Nature* **430**, 666–669. (doi:10.1038/nature02706)

21. Whitmer LM, Chatterjee S, Franzosa J, Rowe T. 2003 Neuroanatomy of flying reptiles and implications for flight, posture, and behavior. *Nature* **425**, 951.
22. Witmer LM, Ridgely RC. 2009 New insights into the brain, braincase, and ear region of tyrannosaurs (Dinosauria, Theropoda), with implications for sensory organization and behavior. *Anat. Rec.* **292**, 1266–1296. (doi:10.1002/ar.20983)
23. Georgi JA, Sipla JS, Forster CA. 2013 Turning Semicircular Canal Function on Its Head: Dinosaurs and a Novel Vestibular Analysis. *PLoS One* **8**. (doi:10.1371/journal.pone.0058517)
24. Brusatte SL, Muir A, Young MT, Walsh S, Steel L, Witmer LM. 2016 The Braincase and Neurosensory Anatomy of an Early Jurassic Marine Crocodylomorph: Implications for Crocodylian Sinus Evolution and Sensory Transitions. *Anat. Rec.* **299**, 1511–1530. (doi:10.1002/ar.23462)
25. Sobral G, Sookias RB, Bhullar B-AS, Smith R, Butler RJ, Müller J. 2016 New information on the braincase and inner ear of *Euparkeria capensis* Broom: implications for diapsid and archosaur evolution. *R. Soc. Open Sci.* **3**, 160072. (doi:10.1098/rsos.160072)
26. Jones GM, Spells KE. 1963 A theoretical and comparative study of the functional dependence of the semicircular canal upon its physical dimensions. *Proc. R. Soc. London. Ser. B* **157**, 403–419. (doi:10.1098/rspb.1963.0019)
27. Vermeij GJ, Motani R. 2018 Land to sea transitions in vertebrates: the dynamics of colonization. *Paleobiology* , 1–14. (doi:10.1017/pab.2017.37)
28. Georgi JA, Sipla JS. 2008 Comparative and Functional Anatomy of Balance in Aquatic Reptiles and Birds. *Sens. Evol. Threshold Adapt. Second. Aquat. Vertebr.* , 233–256.
29. Spoor F, Bajpal S, Hussaim ST, Kumar K, Thewissen JGM. 2002 Vestibular evidence for the evolution of aquatic behaviour in early cetaceans. *Nature* **417**, 163–166. (doi:DOI 10.1038/417163a)
30. Spoor F, Thewissen JGM. 2008 Comparative and Functional Anatomy of Balance in Aquatic Mammals. *Sens. Evol. Threshold Adapt. Second. Aquat. Vertebr.* , 257–284.

Chapter 2 Ross Seal Sensory Anatomy

2.1 Sensory anatomy of the most aquatic of carnivorans: the Antarctic Ross seal and convergences with other mammals

[1] Cleopatra Mara Loza, [2] Ashley E. Latimer [#2] , Marcelo R. Sánchez-Villagra[*1], Alfredo A. Carlini

[#] Second first author

[1] División Paleontología de Vertebrados, Museo de La Plata, Facultad de Ciencias Naturales y Museo, Universidad Nacional de La Plata, La Plata, Argentina. CONICET.

[2] Paläontologisches Institut und Museum der Universität Zürich, Karl-Schmid Strasse 4, 8006 Zürich, Switzerland.

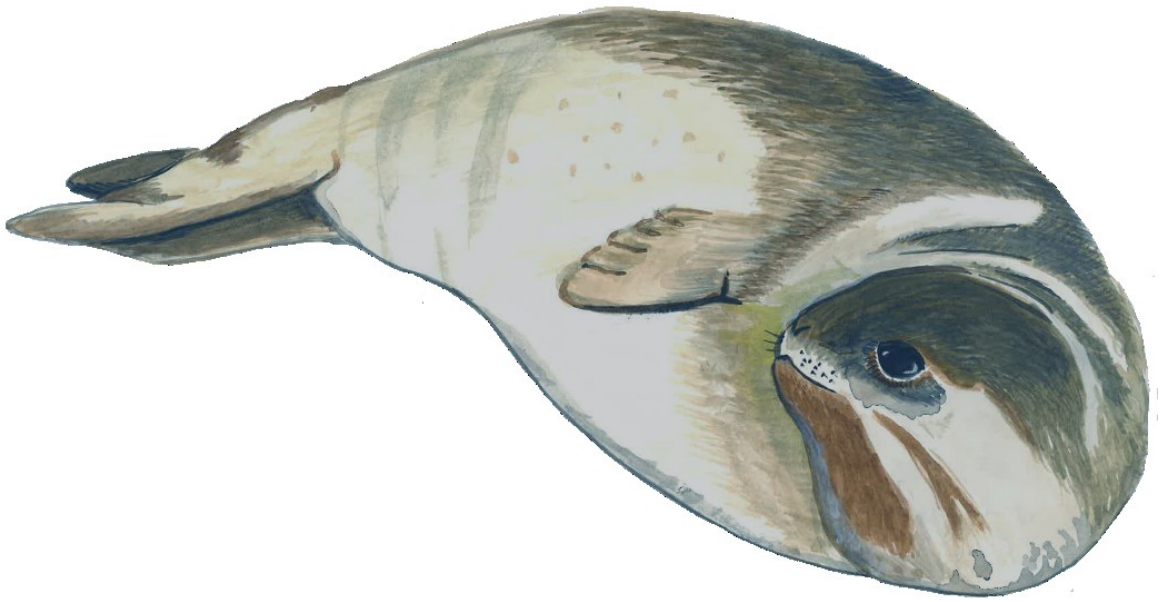

Image: Ross Seal
Ashley Latimer 2017
Watercolor

Author Contributions All authors conceived the study, conducted analyses, contributed to interpretation of the data and preparation of the manuscript, approved the final version of the manuscript and agree to be held accountable for the content therein.

BIOLOGY LETTERS

rsbl.royalsocietypublishing.org

Research

Cite this article: Loza CM, Latimer AE, Sánchez-Villagra MR, Carlini AA. 2017 Sensory anatomy of the most aquatic of carnivorans: the Antarctic Ross seal, and convergences with other mammals. *Biol. Lett.* **13**: 20170489. http://dx.doi.org/10.1098/rsbl.2017.0489

Received: 1 August 2017
Accepted: 12 September 2017

Subject Areas:
behaviour, ecology, evolution, palaeontology

Keywords:
petrosal, sensory ecology, Carnivora, Cetartiodactyla

Author for correspondence:
Marcelo R. Sánchez-Villagra
e-mail: m.sanchez@pim.uzh.ch

†Second first author.

Electronic supplementary material is available online at https://dx.doi.org/10.6084/m9.figshare.c.3893854.

THE ROYAL SOCIETY PUBLISHING

Evolutionary biology

Sensory anatomy of the most aquatic of carnivorans: the Antarctic Ross seal, and convergences with other mammals

Cleopatra Mara Loza[1], Ashley E. Latimer[2,†], Marcelo R. Sánchez-Villagra[2] and Alfredo A. Carlini[1]

[1]División Paleontología de Vertebrados, Museo de La Plata, Facultad de Ciencias Naturales y Museo, Universidad Nacional de La Plata, La Plata, Argentina. CONICET, La Plata, Argentina
[2]Paläontologisches Institut und Museum der Universität Zürich, Karl-Schmid Strasse 4, 8006 Zürich, Switzerland

MRS-V, 0000-0001-7587-3648

Transitions to and from aquatic life involve transformations in sensory systems. The Ross seal, *Ommatophoca rossii*, offers the chance to investigate the cranio-sensory anatomy in the most aquatic of all seals. The use of non-invasive computed tomography on specimens of this rare animal reveals, relative to other species of phocids, a reduction in the diameters of the semicircular canals and the parafloccular volume. These features are independent of size effects. These transformations parallel those recorded in cetaceans, but these do not extend to other morphological features such as the reduction in eye muscles and the length of the neck, emphasizing the independence of some traits in convergent evolution to aquatic life.

1. Background

A glimpse of a Ross seal (*Ommatophoca rossii*) on an ice floe in the Antarctic summer, with its short flippers and thick neck, is vaguely whale-like, hinting at the eight months of the year it spends exclusively at sea [1,2]. Spending months at sea distinguishes this animal from the other three earless Lobodontini seals: the crabeater seal, leopard seal and Weddell seal. Ross seals leave the water for only two weeks to give birth and moult and have unarguable external specializations for their extreme aquatic lifestyle [3]. Until now, scarce sampling of these rare animals has inhibited further exploration of their internal anatomical specializations [3]. As species specialize for aquatic habitats, their sensory organs undergo major transitions, recorded for other carnivoran mammals besides the Ross seal [4]. Comparisons with groups that independently invaded marine environments, such as cetaceans (whales and dolphins) [5], provide insights on evolutionary convergences, even at the genomic level [6].

Specializations for aquatic habitats are reflected in vestibular anatomy, a complex area of the head that can be studied using virtual endocasts. Such endocranial volumes approximate the soft tissue morphology (e.g. ducts, vessels and nerves), and thus provide information useful to reconstruct sensory ecology, locomotion, behaviour and phylogeny [7,8]. Although the function of changes in the vestibular system—concerned with balance, orientation and motion sensation—in aquatic vertebrates are debated [9], reductions in marine vertebrates' semicircular canals have been associated with increased time in the water but not with axial body rotations [10]. The canals of the bony labyrinth of aquatic taxa are recorded to be shorter dorsoventrally and more elongate rostro-caudally than in terrestrial relatives [11]. Smaller semicircular canals may be related to reduced neck lengths [9]. Furthermore, the volume of the dorsal paraflocculus, a lobe of the cerebellum associated with the vestibular system,

© 2017 The Author(s) Published by the Royal Society. All rights reserved.

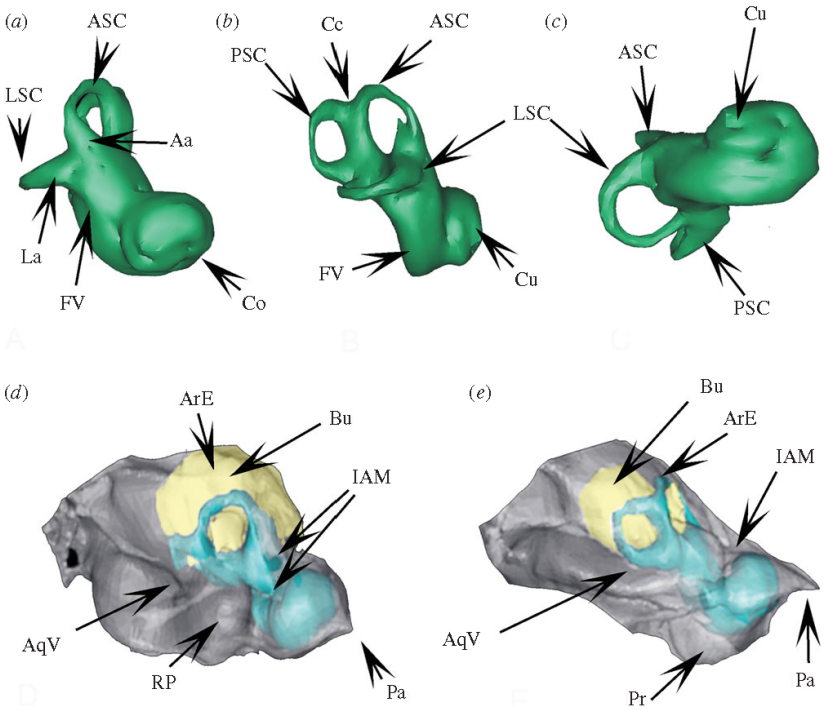

Figure 1. Virtual reconstruction of the right inner ear of the Ross seal, *Ommatophoca rossii* MACN 48.259 in isolation and within the petrosal bone: (*a*) anterior, (*b*) lateral, and (*c*) ventral view, and with the parafloccului in (*d*) dorsal, and (*e*) medial views. Aa: anterior ampulla; AqV: vestibular aqueduct; ASC: anterior semicircular canal; Bu: subarcuate fossa housing the dorsal lobe of the paraflocculus; Cc: commune crus; Cu: cupula; Co: cochlear canal; ArE: arched eminence; FV: vestibular fenestra; IAM: internal acoustic meatus; La: lateral ampulla; LSC: lateral semicircular canal; RP: Ross prominence; Pa: petrosal apex; Pr: promontorium; PSC: posterior semicircular canal.

is also reduced given its relation to agility and coordination of movements using vision and balance [12,13].

2. Methods

A list of museum sources and accession numbers of specimens examined is provided in the electronic supplementary material. A total of 68 petrosal bones from six species of phocids were investigated. All four members of the Lobodontini were sampled: two specimens of the Ross seal (an adult female MACN 48.259 and a newborn MACN 48.260), seven leopard seals (*Hydrurga leptonyx*), 11 Weddell seals (*Leptonychotes weddellii*) and 15 crabeater seals (*Lobodon carcinophagus*). The extant phylogenetic bracket is represented by 30 elephant seals (*Mirounga leonina*), one harbour seal (*Phoca vitulina*), one walrus (*Odobenus rosmarus*), one South American sea lion (*Otaria byronia*; Otariidae), a Tibetan wolf (*Canis lupus filchneri*), a hyena (*Crocuta crocuta*), and a sea otter (*Enhydra lutris*) (electronic supplementary material). We compiled body length data from the literature [14]. Statistics and graphs were generated using R [15]. We reconstructed the bony labyrinth and the petrosal in three-dimensional CT scans using VGStudio MAX v. 2.2, Mimics v. 10.1 and Avizo v. 6.2 (figure 1; electronic supplementary material).

We measured the volume of the subarcuate fossae, which houses the dorsal cerebellar paraflocculus, also called the dorsal portion of the petrosal lobe. Histological preparations confirmed the correspondence of the two structures (electronic supplementary material). The three-dimensional models are available at (http://morphomuseum.com/).

3. Results

The Lobodontini, in order of largest to smallest arc radius of the loops of the semicircular canals and common crus, are leopard seals, crabeater seals, Weddell seals and Ross seals. The maximum diameter of each of the three semicircular canals and the length of the common crus of the Ross seal are significantly shorter than in other Phocidae (Welch *t*-test Ross seal = 0.7003617, other seals = 1.03011095, $t = -6.9386$, d.f. = 6.5762, $p = 0.0002965$; graph 1 in electronic supplementary material). Elephant seals exhibit less reduction of the semicircular canals versus the Lobodontini. In all Phocidae the horizontal canal is consistently the shortest and the anterior canal the longest.

A comparison of the Ross seal with other phocids also reveals reduced parafloccular volume with a simpler shape (figure 2). This difference persists after correction for body mass; a linear regression of the ratio of the parafloccular volume to the natural log average mass for the species still results in significant differences (*t*-test $p = 0.03073$; electronic supplementary material). The parafloccului of the other Lobodontini, besides being larger, have several individual digitiform projections extending around the horizontal semicircular canal, absent in the Ross seal (figure 2). The endocast of the subarcuate fossa of the Ross seal clearly exhibits less surface rugosity as well as greater simplicity and roundness.

The Ross seal has a double internal acoustic foramen, common to all phocids. The cochlea has two and a half turns, similar to the other Lobodontini, but it ends in a poorly demarcated cupula (figure 1). Additionally, Lobodontini and phocids have fewer cochlear turns than mustelids [17].

The Ross seal shares features characteristic of Cetacea that are absent in other lobodontines: a reduced parafloccular volume and lack of surface projections. Both also share a secondary basal lamina on the first turn of cochlea [18,19] that is

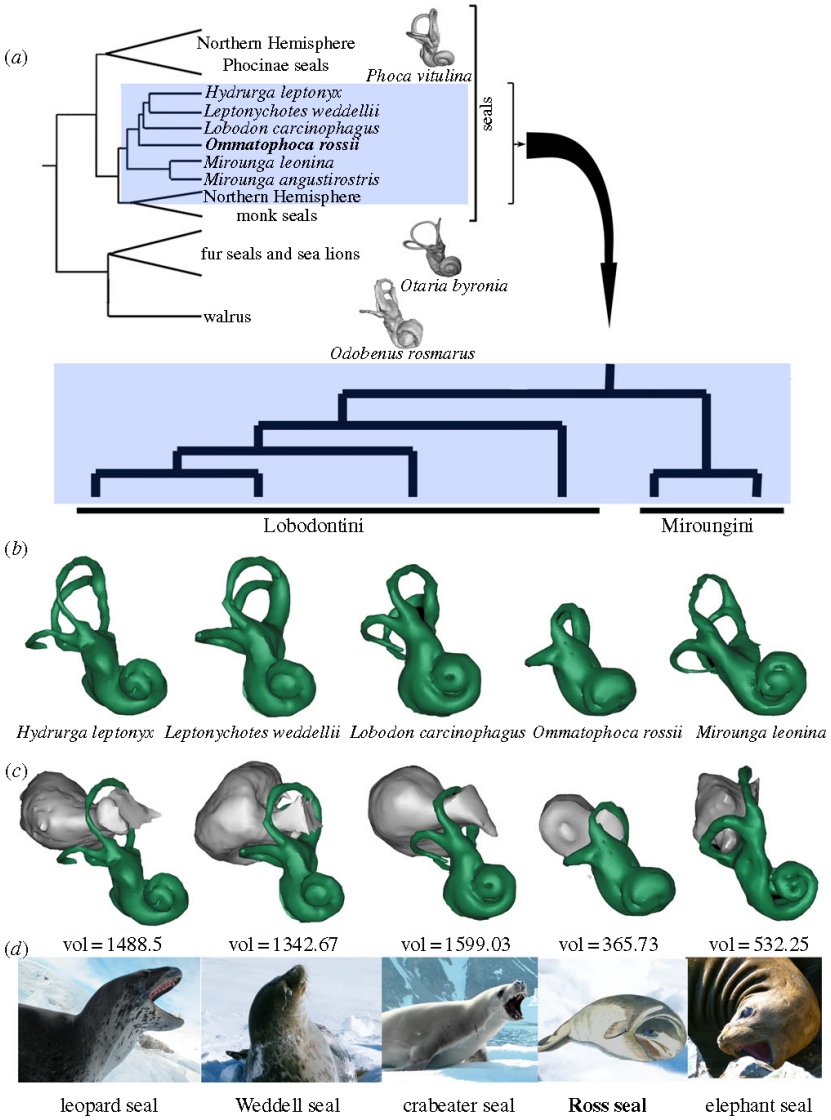

Figure 2. Three-dimensional models of relative labyrinth and parafloccular volume among the Antarctic true seals (Lobodontini) in the context of the phylogenetic relationships among pinniped carnivorans [16]. Photographs by C. M. Loza, drawing of the Ross seal by A. E. Latimer.

antero-ventral to the rest of the labyrinth, and is separated from the rest of the coil. An extremely thick squamosal portion of the temporal bone is present in Ross seals and cetaceans [3]. Likewise is a thickening of the anterior half of the petrosal which develops a rostral projection, a reduced arcuate eminence (probably due to the small size of the anterior semicircular canal), and an expanded medial side, as in some cetaceans [8]; see also electronic supplementary material. In the Ross seal the vestibular fenestra is visible on the lateral face of the vestibule, and the vestibule is smaller and more globular than in other species of phocids. Further anatomical comparisons are in the electronic supplementary material.

4. Discussion

The exceptionally aquatic lifestyle of the Ross seal among carnivoran mammals is reflected in anatomical specializations that are hypothesized to be related to sensory function and which in some cases are similar to those recorded in whales. The semicircular canals of the Ross seal exhibit an extreme size reduction among phocids, as recorded also for cetaceans within Cetartiodactyla. This similarity does not extend to all other aspects of inner ear anatomy and correlated anatomical features.

Neck mobility and neck length have been proposed to affect the morphology of semicircular canals. Reduced vertebral mobility restricts the degrees of freedom of the neck, and the semicircular canals reduce in size accordingly [9]. In pinnipeds, otarids have thinner canals and longer necks than phocids [20,21] and exhibit more neck mobility both during swimming and while moving on land [21]. However, among phocids including the Ross seal, correlation between the parallel reduction of the semicircular canals and neck length is not straightforward (electronic supplementary

material), and neck mobility may play a larger role. Among phocids, leopard seals have the longest neck and practice wide three-dimensional movements of the head, the fastest and most precise of which are related to prey capture [21–23]. Its large semicircular canals contrast with the reduction in the Ross seal.

Lobodontini have thick semicircular canals and ducts, as is characteristic of seals, but different from other aquatic mammals, e.g. sea lions, with thinner canals [20]. The semicircular canals in the Ross seal are smaller in radius than in other phocids, but larger than canals in cetaceans.

The Ross seal has a proportionally reduced paraflocculus with respect to other phocids; the simplicity of the paraflocculus and the semicircular canal may be coupled functionally, as is hypothesized for cetaceans. Not all the features of the Ross seal are consistent with whale anatomy. Reduced semicircular canals in cetaceans have been linked with a reduced need for the vestibulo-ocular reflex with reduction of extra-ocular muscles [24,25]. Ross seals, in contrast, have well developed ocular musculature and large eyes, and likely rely on vision for prey capture. The mechanism for the reduced paraflocculus and semicircular canals therefore cannot be coupled solely on the musculature of the eyes.

Ethics. No special permission was needed to use the existing collections of skulls and histological materials in the museums visited, other than the agreement of the curators listed in the Acknowledgements.

Data accessibility. All specimens studied are in existing osteological and anatomical collections of universities. Data can be accessed at: http://morphomuseum.com/

Authors' contributions. All authors conceived the study, conducted analyses, contributed to interpretation of the data and preparation of the manuscript, approved the final version of the manuscript and agree to be held accountable for the content therein.

Competing interests. We declare we have no competing interests.

Funding. Project funded by UNLP-N-724 to A.A.C.

Acknowledgements. We thank the curators I. Olivares and D. Verzi (MLP); D. Flores and S. Lucero (MACN); M. Haffner (UZH); M. Jardim (MCN); E. Crespo and N. García (CENPAT); and Dr J. Negrete (IAA): the technicians at CIMED La Plata for their assistance during CT scanning; T. Bonnet; J. Maisano (Digimorph.org), and T. Rowe's NSF Digital Libraries Grant for the *Odobenus* scan; C. Zollikofer, A. Schweizer, A. Wegmann (UZH) and T. Schmelzle for technical help and two anonymous reviewers and the editor for constructive suggestions.

References

1. Blix AS, Nordoy ES. 2007 Ross seal (*Ommatophoca rossii*) annual distribution, diving behaviour, breeding and moulting, off Queen Maud Land, Antarctica. *Polar Biol.* **30**, 1449–1458. (doi:10.1007/s00300-007-0306-y)
2. Arcalís-Planas A, Sveegaard S, Karlsson O, Harding KC, Wåhlin A, Harkonen T, Teilmann J. 2015 Limited use of sea ice by the Ross seal (Ommatophoca rossii), in Amundsen Sea, Antarctica, using telemetry and remote sensing data. *Polar Biol.* **38**, 445–461. (doi:10.1007/s00300-014-1602-y)
3. King JE. 1969 Some aspects of the anatomy of the Ross seal, *Ommatophoca rossi* (Pinnipedia: Phocidae). *Br. Antarct. Surv. Sci. Rep.* **63**, 1–50.
4. Berta A. 2012 *Return to the sea: the life and evolutionary times of marine mammals*. Berkeley, CA: University of California Press.
5. Thewissen JGM. 2014 *The walking whales: from land to water in eight million years*. Berkeley, CA: University of California Press.
6. Zhou X, Seim I, Gladyshev VN. 2015 Convergent evolution of marine mammals is associated with distinct substitutions in common genes. *Sci. Rep.* **5**, 16550. (doi:10.1038/srep16550)
7. Ekdale EG. 2016 Form and function of the mammalian inner ear. *J. Anat.* **228**, 324–337. (doi:10.1111/joa.12308)
8. O'Leary MA. 2010 An anatomical and phylogenetic study of the osteology of the petrosal of extant and extinct Artiodactylans (Mammalia) and relatives. *Bull. Am. Museum Nat. Hist.* **335**, 1–206. (doi:10.1206/335.1)
9. Spoor F, Bajpal S, Hussaim ST, Kumar K, Thewissen JGM. 2002 Vestibular evidence for the evolution of aquatic behaviour in early cetaceans. *Nature* **417**, 163–166. (doi:10.1038/417163a)
10. Kandel BM, Hullar TE. 2010 The relationship of head movements to semicircular canal size in cetaceans. *J. Exp. Biol.* **213**, 1175–1181. (doi:10.1242/jeb.040105)
11. Georgi JA, Sipla JS. 2008 Comparative and functional anatomy of balance in aquatic reptiles and birds. *Sens. Evol. Threshold Adapt. Second. Aquat. Vertebr.* **28**, 233–256.
12. Gannon PJ, Eden AR, Laitman JT. 1988 The subarcuate fossa and cerebellum of extant primates—comparative-study of a skull–brain interface. *Am. J. Phys. Anthropol.* **77**, 143–164. (doi:10.1002/ajpa.1330770202)
13. Jeffery N, Ryan TM, Spoor F. 2008 The primate subarcuate fossa and its relationship to the semicircular canals part II: adult interspecific variation. *J. Hum. Evol.* **55**, 326–339. (doi:10.1016/j.jhevol.2008.02.010)
14. Food & Agriculture Orgainzation (FAO). 1979 Pinniped species summaries and report on sirenians. In *Mammals in the seas*, vol. II, pp. 120–124. Rome, Italy: Food and Agriculture Organization of the United Nations.
15. R core team. 2014 *R: a language and environment for statistical computing*. Vienna, Austria: R Foundation for Statistical Computing.
16. Arnason U, Gullberg A, Janke A, Kullberg M, Lehman N, Petrov EA, Väinölä. 2006 Pinniped phylogeny and a new hypothesis for their origin and dispersal. *Mol. Phylogenet. Evol.* **41**, 345–354.
17. Grohe C, Tseng ZJ, Lebrun R, Boistel R, Flynn JJ. 2016 Bony labyrinth shape variation in extant Carnivora: a case study of Musteloidea. *J. Anat.* **228**, 366–383. (doi:10.1111/joa.12421)
18. Luo ZX, Eastman ER. 1995 Petrosal and inner-ear of a squalodontoid whale—implications for evolution of hearing in Odontocetes. *J. Vertebr. Paleontol.* **15**, 431–442. (doi:10.1080/02724634.1995.10011239)
19. Geisler JH, Luo ZX. 1996 The petrosal and inner ear of *Herpetocetus* sp. (Mammalia: Cetacea) and their implications for the phylogeny and hearing of archaic mysticetes. *J. Paleontol.* **70**, 1045–1066. (doi:10.1017/S0022336000038749)
20. Gray AA. 1907 *The labyrinth of animals: including mammals, birds, reptiles and amphibians*. London, UK: J. & A. Churchill.
21. Beentjes MP. 1990 Comparative terrestrial locomotion of the Hooker's sea lion (*Phocarctos hookeri*) and the New Zealand fur seal (*Arctocephalus forsteri*): evolutionary and ecological implications. *Zool. J. Linn. Soc.* **98**, 307–325. (doi:10.1111/j.1096-3642.1990.tb01204.x)
22. Rogers T, Bryden MM. 1995 Predation of Adélie penguins (*Pygoscelis adeliae*) by leopard seals (*Hydrurga leptonyx*) in Prydz Bay, Antarctica. *Can. J. Zool. Can. Zool.* **73**, 1001–1004. (doi:10.1139/z95-119)
23. Laws RM. 1984 A decade of research on Antarctic and sub-Antarctic seals—introduction to the colloquium. *S. Afr. J. Sci.* **80**, 25–26.
24. Pilleri G, Wandeler A. 1964 Ontogenese Und Funktionelle Morphologie Des Auges Des Finnwals *Balaenoptera physalus* Linnaeus (Cetacea Mysticeti Balaenopteridae). *Acta Anat.* **57**, 3(Suppl. 50). (doi:10.1159/000142567)
25. Hosokawa H. 1951 On the extrinsic eye muscles of the whale, with special remarks upon the innervation and function of the musculus retractor bulbi. *Sci. Rep. Whales Res. Inst. Tokyo* **6**, 1–33.

Supplementary material Sensory anatomy of the most aquatic of carnivorans: the Antarctic Ross seal, and convergences with other mammals

Cleopatra Mara Loza, Ashley E. Latimer, Marcelo R. Sánchez-Villagra*, Alfredo A. Carlini

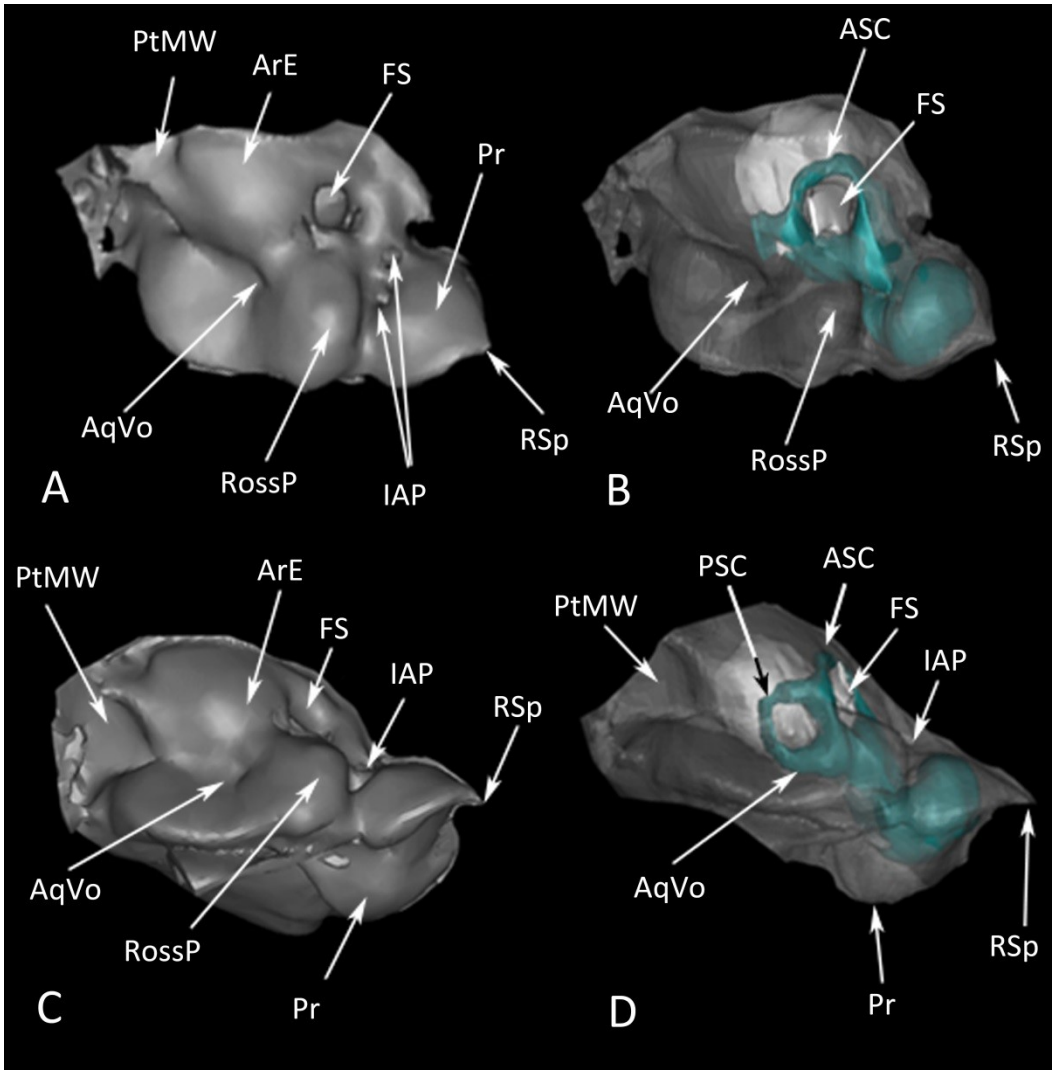

Supplemental Figure 1. 3D reconstruction of a left petrosal of an adult female of Ommatophoca rossii (MACN-48259) in: A, dorsal view; B, transparent dorsal view with the labyrinth; C, medial view; and D, transparent medial view with the labyrinth. ASC, anterior semicircular canal; AqVo, opening to the vestibular aqueduct; ArE, arched eminence; FS, subarcuate fossa; IAP, internal acoustic pore; PtMW, petromastoid wing; Pr, promontorium; PSC, posterior semicircular canal; RossP: Ross prominence; Rsp, rostral spine.

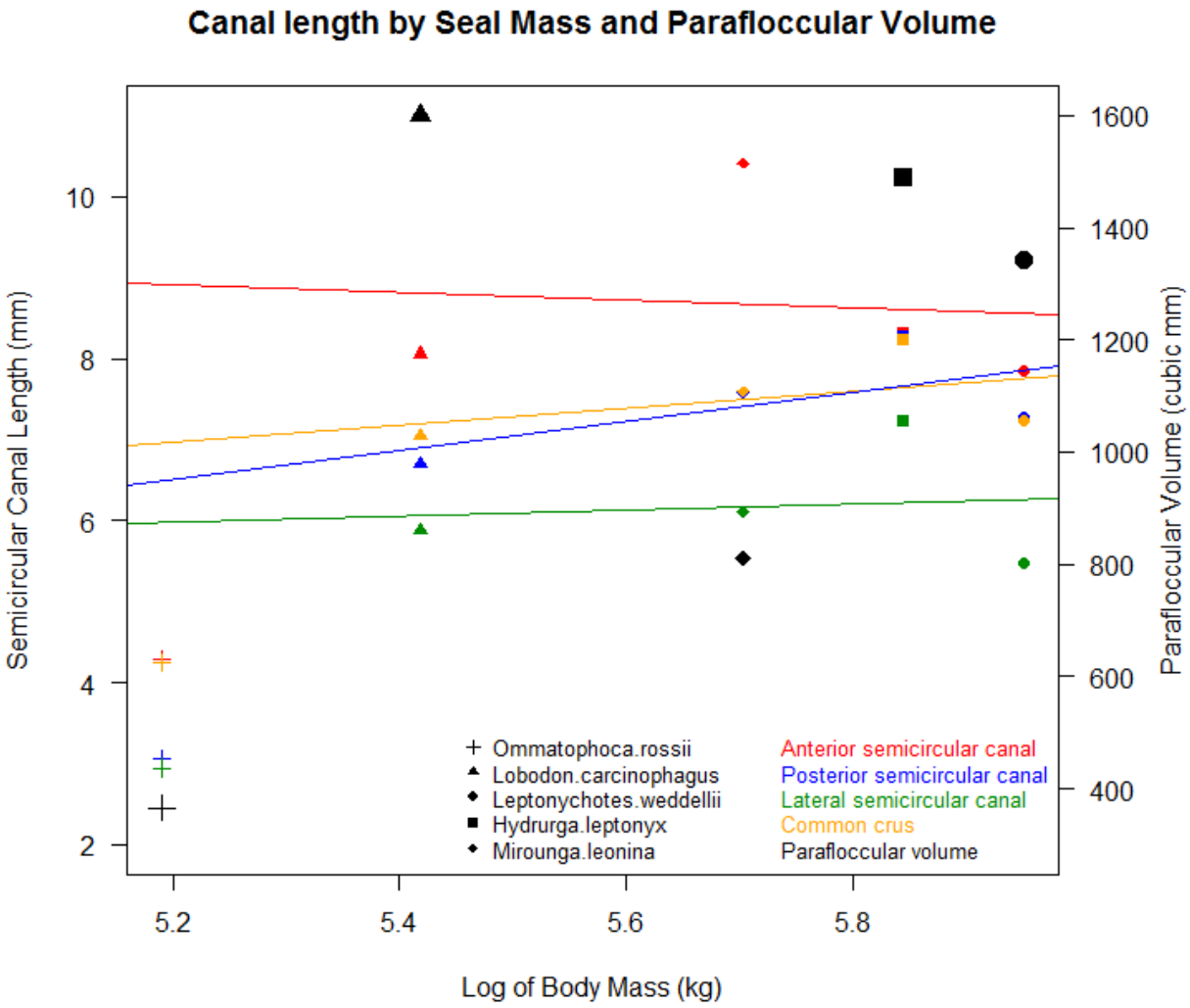

Supplemental Figure 2 Graph of semicircular canal size and parafloccular volume to log body mass. Parafloccular volume in black, semicircular canal lengths colored points. Regression lines for canal length to body mass.

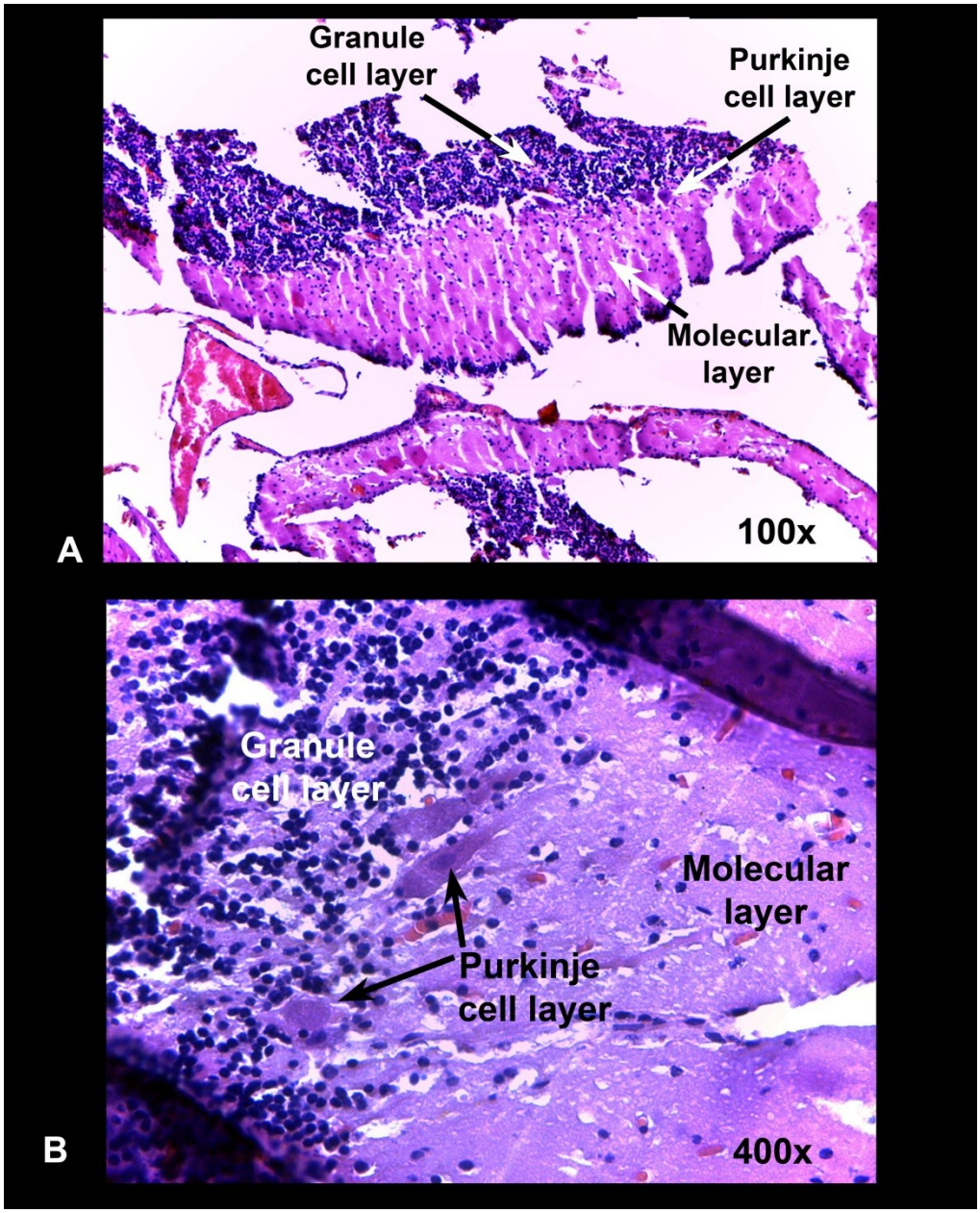

Supplemental Figure 3: Histological section through the paraflocculus of *Mirounga leonina* (pup).

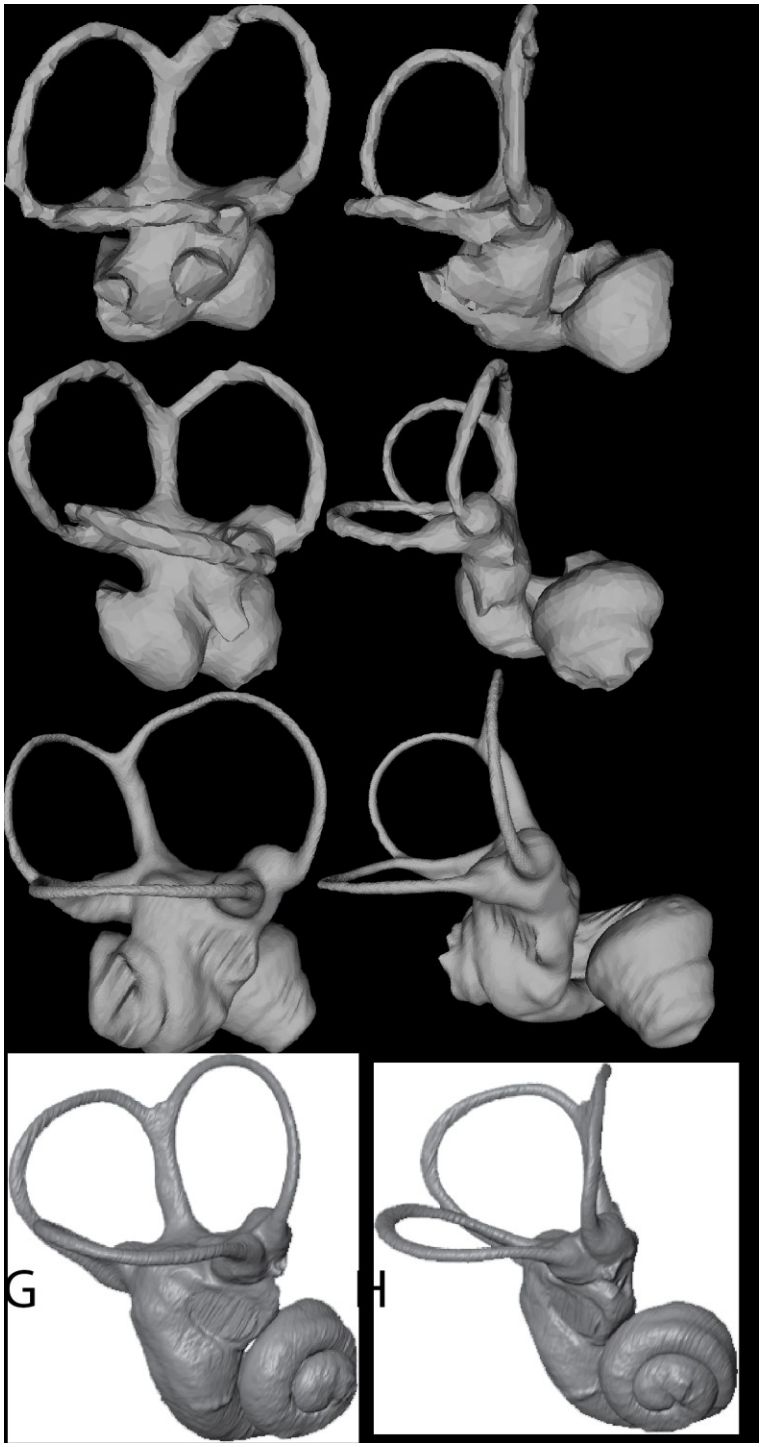

Supplemental Figure 4: Labyrinths of hyena (*Crocuta crocuta*) A- lateral and B- anterior view, sea otter (*Enhydra lutris*) C- lateral and D- anterior view, Tibetan wolf (*Canis lupus filchneri*) in E- lateral and F- anterior view, and South American sea lion (*Otaria byronia)*, G- anterior view; and H- lateral view, not to scale.

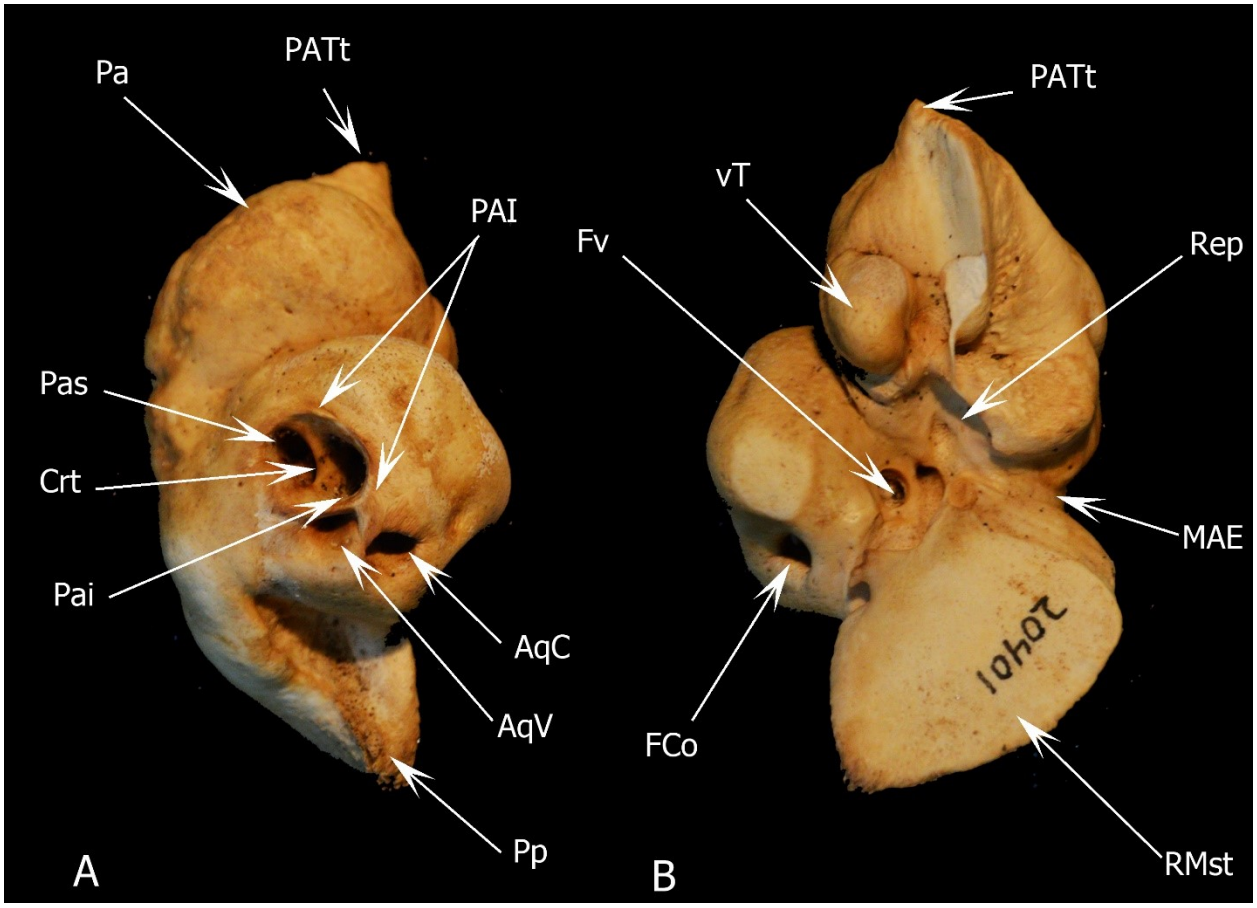

Supplemental Figure 5: Petrosal bone of Hector's beaked whale *Mesoplodon hectori* (Lucero and Loza 2016), a cetacean, in (A) dosomedial (cerebellar) and (B) ventrolateral (tympanic) views. Abbreviations: AqC: *aqueducto cochleae;* AqV: *aqueducto vestibuli ;* Crt: *crista interfenestralis;* FCo: *fenestra cochleae;* FV: *fenestra vestibuli;* MAE: *meatus acusticus externus;* Pa: Petrosal anterior process; PAI: *porus acusticus internus;* Pai: *foramen acusticus inferius;* Pas: *foramen acusticus superius;* PATt: Anterior process of the *Tegmen Tympani;* Pp: Petrosal Posterior Process; Rep: Epitympanic recessus; RMst: mastoid region; vT: ventral tubercle.

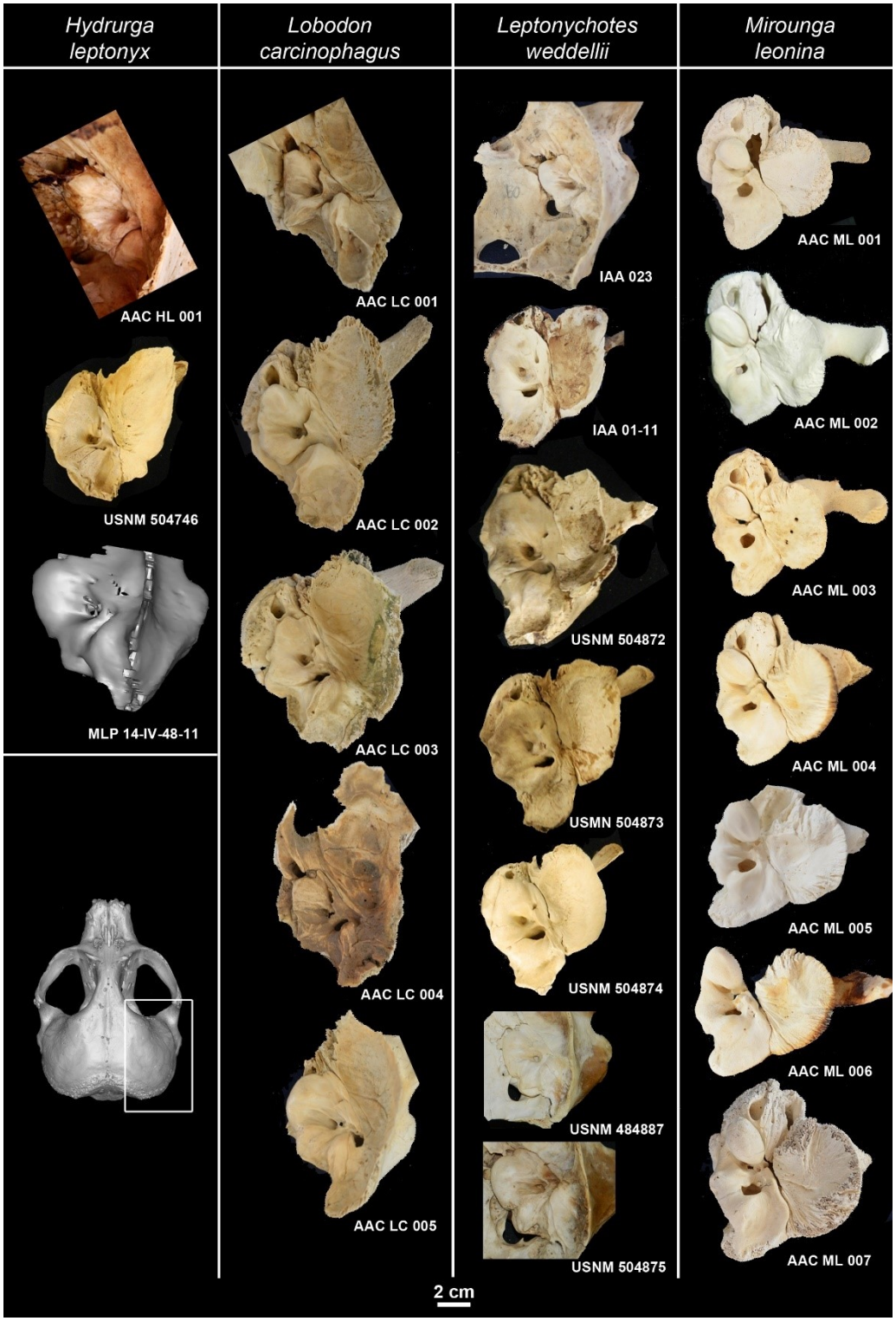

Supplemental Figure 6: Petrosal bones three leopard seals (*Hydrurga leptonyx)*, seven Weddell seals (*Leptonychotes weddellii),* seven crabeater seals (*Lobodon carcinophagus*) and seven Southern elephant seals (*Mirounga leonina*).

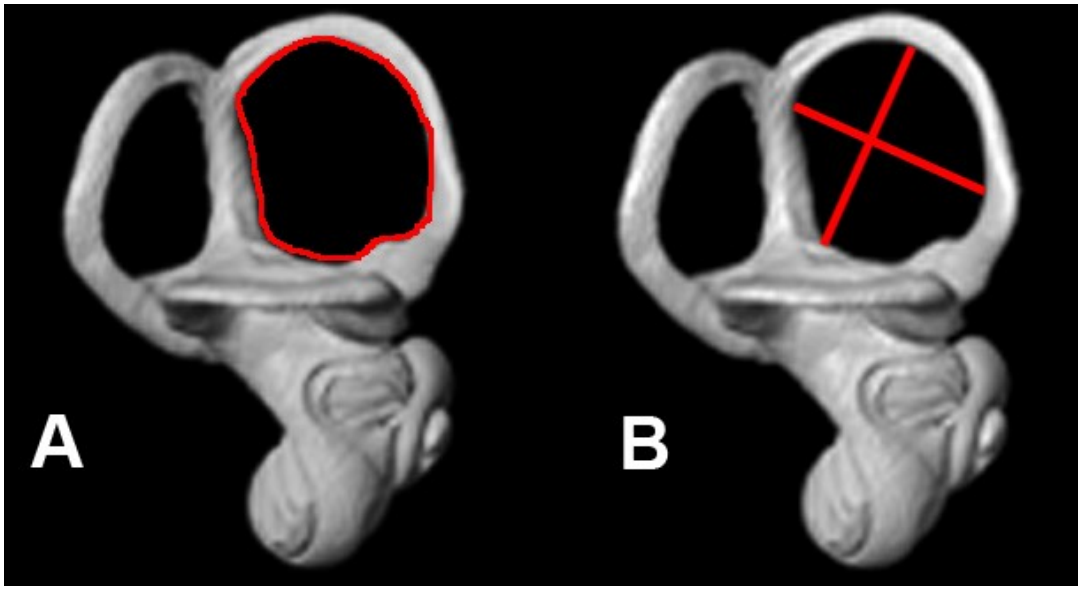

Supplemental Figure 7: Inner ear measurements as shown in a crabeater seal, *Lobodon carcinophagus*. A, Perimeter; B. Length and width.

Specimen number	Taxon	Institution
MLP 14.IV.48.11	Hydrurga leptonyx	Museo de La Plata, División Zoología Vertebrados
MLP 30.XII.02.1	Hydrurga leptonyx	Museo de La Plata, División Zoología Vertebrados
MLP 26.IV.00.14	Hydrurga leptonyx	Museo de La Plata, División Zoología Vertebrados
MACN 24636	Hydrurga leptonyx	Museo Cs. Naturales B. Rivadavia
MACN 20396	Hydrurga leptonyx	Museo Cs. Naturales B. Rivadavia
MACN 13.17	Hydrurga leptonyx	Museo Cs. Naturales B. Rivadavia
USNM 504746	Hydrurga leptonyx	Smithsonian Institution, USA
IAA 02-13	Leptonychotes weddellii	Instituto Antártico Argentino
IAA 08-13	Leptonychotes weddellii	Instituto Antártico Argentino
IAA 01-13	Leptonychotes weddellii	Instituto Antártico Argentino
IAA 02-15	Leptonychotes weddellii	Instituto Antártico Argentino
IAA 09-11	Leptonychotes weddellii	Instituto Antártico Argentino
USNM 395815	Leptonychotes weddellii	Smithsonian Institution, USA
USNM 504871	Leptonychotes weddellii	Smithsonian Institution, USA
USNM 395810	Leptonychotes weddellii	Smithsonian Institution, USA
USNM 504873	Leptonychotes weddellii	Smithsonian Institution, USA
USNM 504874	Leptonychotes weddellii	Smithsonian Institution, USA
USNM 504872	Leptonychotes weddellii	Smithsonian Institution, USA
IAA 530	Lobodon carcinophagus	Instituto Antártico Argentino
MLP 22.III.99.10	Lobodon carcinophagus	Museo de La Plata, División Zoología Vertebrados
USNM 310693	Lobodon carcinophagus	Smithsonian Institution, USA
AAC 542	Lobodon carcinophagus	Osteological Comparative Collection, Div. Paleontol Vert., MLP
AAC 769	Lobodon carcinophagus	Osteological Comparative Collection, Div. Paleontol Vert., MLP
IAA 03-5	Mirounga leonina	Instituto Antártico Argentino
IAA 00-8	Mirounga leonina	Instituto Antártico Argentino
IAA 01-14	Mirounga leonina	Instituto Antártico Argentino
IAA 00-9	Mirounga leonina	Instituto Antártico Argentino

IAA 02-16	Mirounga leonina	Instituto Antártico Argentino
IAA 02-24	Mirounga leonina	Instituto Antártico Argentino
IAA 02-14	Mirounga leonina	Instituto Antártico Argentino
IAA 02-28	Mirounga leonina	Instituto Antártico Argentino
IAA AA-B	Mirounga leonina	Instituto Antártico Argentino
IAA AA-2	Mirounga leonina	Instituto Antártico Argentino
IAA AA-7	Mirounga leonina	Instituto Antártico Argentino
IAA AA-6	Mirounga leonina	Instituto Antártico Argentino
IAA AA-8	Mirounga leonina	Instituto Antártico Argentino
IAA 01-15	Mirounga leonina	Instituto Antártico Argentino
AAC 776	Mirounga leonina	Osteological Comparative Collection, Div. Paleontol Vert., MLP
AAC 777	Mirounga leonina	Osteological Comparative Collection, Div. Paleontol Vert., MLP
AAC 778	Mirounga leonina	Osteological Comparative Collection, Div. Paleontol Vert., MLP
AAC 779	Mirounga leonina	Osteological Comparative Collection, Div. Paleontol Vert., MLP
AAC 780	Mirounga leonina	Osteological Comparative Collection, Div. Paleontol Vert., MLP
AAC781	Mirounga leonina	Osteological Comparative Collection, Div. Paleontol Vert., MLP
AAC 782	Mirounga leonina	Osteological Comparative Collection, Div. Paleontol Vert., MLP
AAC 783	Mirounga leonina	Osteological Comparative Collection, Div. Paleontol Vert., MLP
AAC 784	Mirounga leonina	Osteological Comparative Collection, Div. Paleontol Vert., MLP
MLP 14.IV.48.13	Mirounga leonina	Museo de La Plata, División Zoología Vertebrados
CNP 109	Mirounga leonina	Centro Nacional Patagónico, Pto. Madryn, Chubut
CNP S/N-A	Mirounga leonina	Centro Nacional Patagónico, Pto. Madryn, Chubut

CNP S/N-B	Mirounga leonina	Centro Nacional Patagónico, Pto. Madryn, Chubut
CNP S/N-C	Mirounga leonina	Centro Nacional Patagónico, Pto. Madryn, Chubut
CNP S/N-D	Mirounga leonina	Centro Nacional Patagónico, Pto. Madryn, Chubut
CNP ML 11	Mirounga leonina	Centro Nacional Patagónico, Pto. Madryn, Chubut
MLP 26.IV.00.6	Otaria byronia	Museo de La Plata, División Zoología Vertebrados
AMNH 232423	Phoca vitulina	American Museum of Natural History, NY, USA
USNM 550009	Odobenus rosmarus	Smithsonian Institution, USA

Supplemental Table 2: Studied specimens and their repository.

Species	ASC (mm)	PSC (mm)	LSC (mm)	*CC*(mm)	Ratio
Ommatophoca rossii	4.28	3.06	2.95	4.25	0.86
Lobodon carcinophagus	8.05	6.7	5.88	7.04	1.04
Leptonychotes weddellii	7.85	7.28	5.47	7.23	1.04
Hydrurga leptonyx	8.3	8.26	7.23	8.22	1
Mirounga leonina	10.41	7.58	6.11	7.6	1.08
Crocuta crocuta	6.98	6.8	4.87	4.81	0.88
Canis lupus filchneri	5.59	4.45	4.76	3.84	1.3
Enhidra lutris	4.05	4.27	3.87	2.7	1.51

Supplemental Table 2: Measurements of semicircular canal and common crus lengths by species. ASC – anterior semicircular canal, PSC – posterior semicircular canal, LSC lateral semicircular canal, CC – *Crus commune* (Common crus).

	Cervical Vertebral Height (mm)						
	1	2	3	4	5	6	7
Ommatophoca rossii	69.77	35.17	36.59	31.47	39.54	40.10	38.49
Lobodon carcinophagus	41.80	44.00	24.00	24.80	23.00	26.80	26.60
Leptonychotes weddellii	40.90	24.80	32.40	32.60	24.80	27.10	28.40
Hydrurga leptonyx	NA	NA	NA	NA	NA	NA	NA
Mirounga leonina	37.80	65.40	65.40	74.60	78.80	71.60	72.60
	Cervical Vertebral Width (mm)						
	1	2	3	4	5	6	7
Ommatophoca rossii	73.32	48.00	51.7	54.88	43.48	45.87	47.69
Lobodon carcinophagus	63.20	47.60	35.60	35.00	38.60	39.20	37.40
Leptonychotes weddellii	70.40	33.60	39.80	35.00	34.30	44.40	47.20
Hydrurga leptonyx	NA	NA	NA	47.00	NA	NA	NA
Mirounga leonina	144.00	81.20	83.80	84.60	89.40	91.80	93.40
	Cervical Vertebral Length (mm)						
	1	2	3	4	5	6	7
Ommatophoca rossii	22.22	39.90	36.8	41.33	41.92	35.68	28.07
Lobodon carcinophagus	11.40	26.00	31.60	31.40	27.00	34.60	29.40
Leptonychotes weddellii	15.40	45.10	34.20	35.60	38.60	41.60	40.60
Hydrurga leptonyx	NA	NA	NA	51.00	NA	NA	NA
Mirounga leonina	47.20	75.20	78.40	81.80	81.10	82.80	69.60

Supplemental Table 3: Measurements of cervical vertebrae 1-7 for select seals, dimensions: Height of the vertebral body at the midline of the anterior face of the vertebra, Length of the vertebral body between the articular faces, width of the vertebra measured at the medial edges of the vertebrarterial foramina.

On the thickness between the semicircular canals in pinnipeds and other aquatic mammals

Phocid semicircular canals are among the largest and thickest in mammals; destructive sampling by Gray [29] revealed soft tissue semicircular duct widths of 1.25-2.5mm in the Harbor seal, only approached by other marine mammals (0.75mm in a sea lion).

References Supplementary Information

Lucero, S.O., Loza C.M.(2016). Descripción del complejo tímpano-periótico del zifio de Hector, *Mesoplodon hectori* (Gray, 1871, Cetacea: Ziphiidae). Resumenes, XXIX Jornadas Argentinas de Mastozoologia: 23-24. Octubre 18 al 21, 2016. San Juan, Argentina.

Supplemental information: Sensory anatomy of the most aquatic of carnivorans: the Antarctic Ross seal, and convergences with other mammals

Dataset

Supplemental information for "Sensory anatomy of the most aquatic of carnivorans: the Antarctic Ross seal, and convergences with other mammals"

Latimer Ashley E.[1]*, Loza Cleopatra Mara[2], Sánchez-Villagra Marcelo[1], Carlini Alfredo A.[2]

[1]*University of Zurich, Department of Paleontology and Paleontological Museum*

[2]*División Paleontología de Vertebrados, Museo de La Plata, Facultad de Ciencias Naturales y Museo, Universidad Nacional de La Plata, La Plata, Argentina. CONICET.*

***Corresponding author**: ashley.latimer@pim.uzh.ch

Abstract

Here, the semicircular canals of the most aquatic seal, the rare Antarctic Ross Seal (*Ommatophoca rossii*), are presented for the first time, along with representatives of every species in the Lobodontini: the leopard seal (*Hydrurga leptonyx*), Weddell seal (*Leptonychotes weddellii*), and crabeater seal (*Lobodon carcinophagus*). Because encounters with wild Ross seal are rare and few specimens are available in collections worldwide, this dataset increases accessibility to a rare species. For further comparison, we present the bony labyrinths of other carnivorans, the elephant seal (*Mirounga leonina*), harbor seal (*Phoca vitulina*), walrus (*Odobenus rosmarus*), South American sea lion (*Otaria byronia*).

Keywords: aquatic, inner ear, *Ommatophoca rossi*, *Phoca*, semicircular canals

Submitted:2017-10-09, published online:2017-11-28. https://doi.org/10.18563/m3.3.4.e7

INTRODUCTION

Marine mammals repeatedly converge on similar body shapes, but convergences in sensory systems are less well documented. Here we explore the convergences in the sensory anatomy of the Ross seal (*Ommatophoca rossii*) and compare with carnivorans including true seals (*Hydrurga leptonyx*, *Lobodon carcinophagus*, Leptonychotes weddellii), walrus (Odobenus rosmarus), and otter (Otaria byronia). Bony labyrinths of the species cited above are presented here (Fig. 1 and table 1). This publication accompanies "Sensory anatomy of the most aquatic of carnivorans: the Antarctic Ross seal, and convergences with other mammals"(Loza et al., 2017).

METHODS

The Lobodontini specimens and all South American taxa were scanned using MRI (Magnetic Resonance Imaging), the harbor seal was scanned at the University of Zurich in the Anthropological Institue, using a Nikon X TH 225ST in the Anthropological department at the University of Zurich., and the walrus scan was obtained from Digimorph (Ekdale, 2006). The 3D surfaces were extracted using VG StudioMax 2.2 (https://www.volumegraphics.com/ Volume Graphics, Heidelberg, Germany) and Mimics (http://biomedical.materialise.com/mimics; Materialise, Leuven, Belgium) after either manual or semi-automatic region selection. They were post-processed using MeshLab to remove isolated pieces, merge close vertices, remove non-manifold edges and vertices, remove unreferenced vertices, and close holes. Where the files were unnecessarily large, they were also optimized in MeshLab (http://meshlab.sourceforge.net) using Laplace smoothing and quadratic edge decimation. The surfaces can be opened and viewed using MeshLab, Blender (http://blender.org; Stitching Blender Foundation, Amsterdam, the Netherlands), or any programs with support of .ply format files.

ACKNOWLEDGEMENTS

We thank the curators of the consulted collections: I. Olivares and D. Verzi (MLP); D. Flores and S. Lucero (MACN); M. Haffner (UZVC); M. Jardim (MCN); E. Crespo and N. García (CENPAT); to Dr. J. Negrete (IAA). To the technicians at CIMED La Plata, for their assistance during CT scanning; to J. Maisano (Digimorph.org), and T. Rowe's NSF Digital Libraries Grant for the *Odobenus* scan; to C. Zollikofer (UZH), to T. Bonnet (ANU), A. Schweizer, A. Wegmann (UZH) and T. Schmelzle for technical help. Project funded by UNLP-N-724 to A.A.C. and Swiss National Science Foundation grant 31003A-149506 to Torsten M. Scheyer.

BIBLIOGRAPHY

Loza CM, Latimer AE, Sánchez-Villagra MR, Carlini AA, 2017. Sensory anatomy of the most aquatic of carnivorans: the Antarctic Ross seal, and convergences with other mammals. Biol. Lett. 2017;20170489. https://doi.org/10.1098/rsbl.2017.0489

Ekdale E. 2006. *Odobenus rosmarus* [Internet]. Digit. Morphol. Available from: http://digimorph.org/specimens/Odobenus_rosmarus/adult/

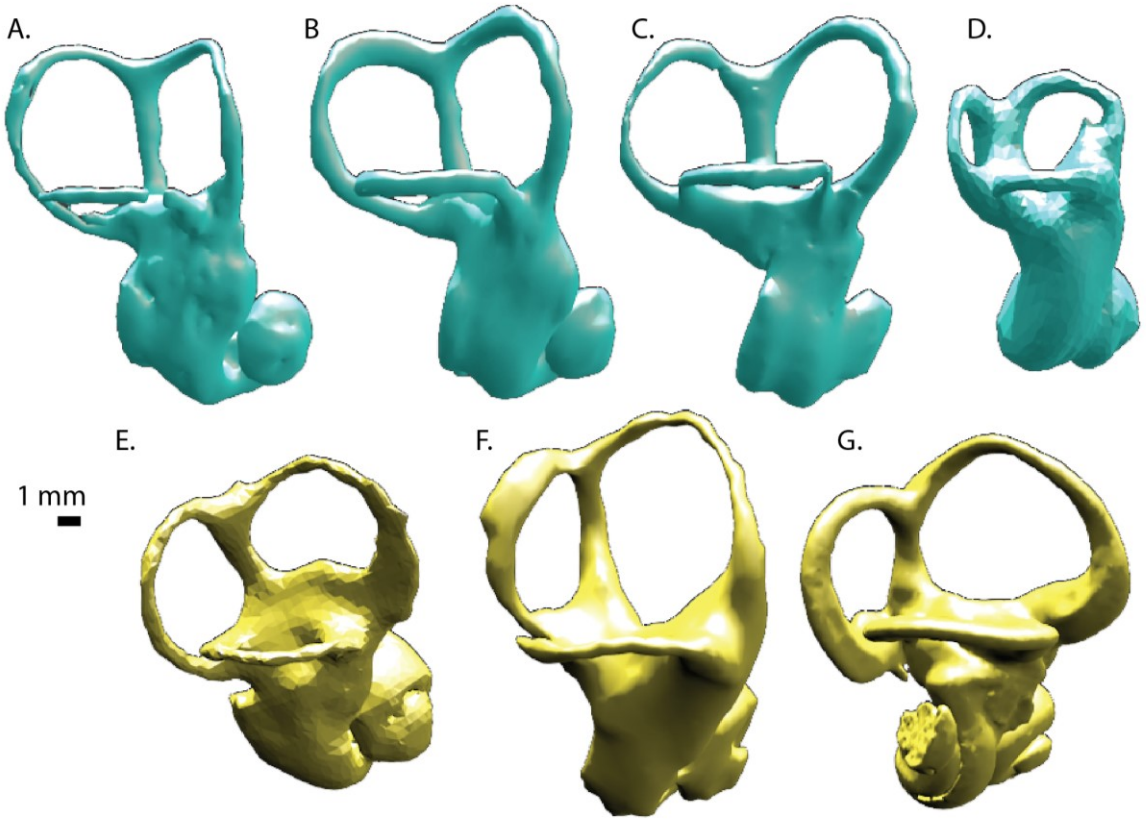

Figure 1. Bony labyrinths in lateral view of A. *Hydrurga leptonyx* B. *Leptonychotes weddellii,* C. *Lobodon carcinophagus,* D. *Ommatophoca rossii,* E. *Odobenus rosmarus,* F. *Mirounga leonia,* G. *Phoca Vitulina.* Scale bar is 1mm.

Chapter 3 A Giant Dapediid Braincase from Switzerland

3.1 A giant dapediid from the Late Triassic of Switzerland and insights into neopterygian phylogeny

Ashley E. Latimer 1* & Sam Giles2*

[1] Paleontological Institute and Museum, University of Zurich, Zurich 8052, Switzerland, latimer.ae@pim.uzh.ch

[2] Department of Earth Sciences, University of Oxford, Oxford, OX1 3AN, UK

Image: The rock-headed cliff fish
Ashley Latimer 2018
Watercolor

Author contributions AEL designed the project. AEL and SG segmented the data, produced figures, ran phylogenetic analyses, interpreted the results and wrote the manuscript.

ABSTRACT

A new Triassic neopterygian is described on the basis of a large three-dimensional neurocranium from the Rhaetian (Late Triassic) of the Kössen Formation (Schesaplana, Grisons, Switzerland). CT scanning reveals neurocranial features similar to *Dapedium*, suggesting that this new genus, *Scopulipiscis saxciput* gen. et sp. nov., was deep bodied and potentially durophagous, although no associated dental material is known. An expanded phylogenetic analysis of actinopterygians resolves Dapediidae as a clade (inclusive of *Tetragonolepis*), although fails to recover any characters supporting the monophyly of the genus *Dapedium*. Dapediids are resolved as stem holosteans, filling a conspicuous gap in early neopterygian relationships. Similarities between this new taxon and *Dapedium* provide new insights into morphological disparity within early members of the group--suggesting that the ecological expansion of dapediids originated prior to the end-Triassic extinction--as well as contributing to a growing understanding of endocranial anatomy in Palaeozoic and early Mesozoic actinopterygians.

INTRODUCTION

Ray finned fishes (Actinopterygii) constitute the majority of living vertebrate diversity, displaying a huge disparity of body forms filling a wide variety of ecological niches [1,2]. Almost all extant actinopterygians (>30,000) belong to a single group, the Teleostei, with non-teleostean actinopterygians comprising just 56 living species [3]. The distribution of extant species belies past diversity: teleosts have not always been the dominant group, having reached their current status only after the end of the Cretaceous [4]. Indeed, their sister group, the holosteans, outstripped teleosts in terms of diversity and disparity in the earliest part of their history [5], despite only eight species surviving to the modern. Understanding of relationships amongst early holosteans remains poor, however, with no taxa currently identified as branching from the holostean stem [6–9].

Representing an early experiment in body form and ecological diversity, *Dapedium* is a modestly diverse (~20 species) radiation of neopterygians known from the Late Triassic (Rhaetian) to mid Jurassic (earliest Aalenian), most notable for its adaptations for durophagy. Members of this genus possess thick, interlocking ganoid scales; dense, pustular ornament; and a small mouth with styliform teeth borne on the stout lower jaw. Other genera closely associated with *Dapedium*, and typically united into Dapediidae (or Dapediiformes), include *Aetholepis* [10], *Dandya* [11], *Hemicalypterus* [12,13], *Heterostrophus* [14], *Paradapedium* [15], *Sargodon* [11], and *Tetragonolepis* [15,16], although the dapediid affinity of at least *Heterostrophus* and *Dandya* has been called into question [12,15]. Most *Dapedium* species

have a standard length of around 15–35 cm [17], although other dapediids range in size from ~8 cm (*Dapedium noricum* [11] to ~1 m (*Sargodon tomicus* [11]). Only around five of the 30 or so known species of dapediid are present in the Triassic, and are exclusively represented by disarticulated (two isolated teeth [18]) or two-dimensional [11,13,19] remains. Consequently, their adaptation for durophagy is thought to have facilitated the group's success in the aftermath of the end-Triassic extinction, a time at which many other durophagous taxa went extinct [20,21].

Despite representing an important expansion into a new ecological niche, the phylogenetic position of dapediids is unclear. Initially classed as 'semionotids' [11,22,23], a waste-basket taxon of primitive neopterygians, *Dapedium* was moved to Dapediidae by Lehman [24]. This family was erected largely on the basis of a deep-bodied phenotype [24–26], and a formal diagnosis was not provided until several decades later ([27]: these authors note that a previous diagnosis, formulated by Wenz [25], was largely inaccurate). Dapediids are poorly sampled in formal phylogenetic analyses (but see [13]), typically being represented by a single, often composite, terminal [28–37]). Despite—or perhaps in consequence of—their limited phylogenetic consideration, dapediids have variably been considered stem teleosts [8,28,29,32,35,36,38–40] and total group holosteans (generally sister to ginglymodians: [11,12,17,31,37]). Further uncertainty surrounds the identity of the sister taxon of dapediids, with a close relationship variably found with pycnodonts [26,29,30,33], pholidophorids + leptolepids [28,35] and pachycormids [32,33]). Historical difficulties in defining apomorphies for dapediids stem from a lack of diagnoses teamed with characters of dubious merit (such as the distribution of scale serrations and multicuspid teeth [10]) being used to distinguish between species, and the monophyly of *Dapedium* has previously been questioned [27]. Furthermore, material from the Sinemurian of Dorset is sorely in need of taxonomic revision, as has recently been carried out for German dapediid material [27,31,41].

This equivocal phylogenetic signal is in part due to the conflicting datasets used to resolve relationships. The phylogenetically informative endoskeleton [30,42,43], in particular the braincase, is described for only a small number of dapediids (*Dapedium punctatum*, *D. caelatum*: [17]), and exhaustively in just a single taxon (*Dapedium* sp: [26,38,40,44]). While three-dimensional crania are known in a number of taxa (e.g. *Tetragonolepis semicincta*: [16]; *Dapedium granulatum*: [21], the majority of dapediids are preserved as laterally compressed fossils, with heavy dermal ornament obscuring most of the internal skeleton. In particular, no neurocrania are described from the Triassic, when the group first appeared.

Here we present a new, large (~17cm length) braincase from the Rhaetian (Late Triassic) of the Kössen Formation (Schesaplana, Grisons, Switzerland; figure. 1). This site is prolific, with marine reptiles and pterosaurs previously described [45–47]). Actinopterygian

remains attributed to *Birgeria* have also been described from a lateral extension of the formation into Austria [48], but no dapediids have previously been identified. This new specimen expands our knowledge of the taxonomic richness of the locality and increases the size range known for dapediids, with implications for the diversification of the group and the timing of their radiation. Furthermore, CT scanning of this well-preserved neurocranium presents an opportunity to revisit the phylogenetic affinities of the group.

MATERIALS AND METHODS

CT scanning

PIMUZ A/I 3026 was scanned at EMPA using a 300kV micro-focus source (Finetec FOMR300.0) and flat-panel detector (Perkin-Elmer XRD 1621 AN14 ES, 200 µm pixels) at 100 µm resolution. VGStudio Max V2.2.5 and Mimics v.19 were used for digital segmentation and meshes were exported into and imaged in Blender (blender.org). Scan data and 3D surface files (.PLYs) are available on MorphoMuseuM (link-at-publication).

Phylogenetic analysis

Our dataset is based on [8], with additional characters both novel and taken from the literature [13,34]. 12 taxa were added to the matrix in order to increase the sampling of dapediids. *Brachydegma caelatum* was removed pending a redescription of this taxon. This gives a total of 278 characters and 104 taxa. An equally weighted parsimony analysis was conducted using a heuristic search in PAUP* v. 4.0a158 [49] with the following settings: 1000 random addition sequences, five trees held at each step, maxtrees set to automatically increase, nchuck = 10 000, chuckscore = 1, tree bisection and reconstruction strategy enabled. Six characters were ordered. Taxonomic equivalence [50] was assessed using Claddis [51]. The outgroup was constrained using the topology [*Dicksonosteus*[*Entelognathus* [*Acanthodes*, *Cladodoides*, *Ozarcus*][ingroup]]]. Bootstrap values were calculated in PAUP with the following settings: 1000 replicates of a heuristic search, tree branching and reconstruction strategy enabled, 25 replicates, five trees held at each step, rearrlimit = 50 000 000, limitperrep = yes, nchuck = 10000, chuckscore = 1. Bremer support values were calculated in PAUP.

Measurements

Four full body *Dapedium pholidotum* fossils (PIMUZ A/I 3111, PIMUZ A/I 1290, PIMUZ A/I 422, PIMUZ A/I 421) and *Sargodon tomicus* (PIMUZ cast, figures [11]) were measured in order to calculate body length estimates. The following measurements were taken: tip of the snout to the caudal margin of the tail (body length); tip of the snout to the

anterior-most point of the operculum (skull length); and the angle of inclination of the skull roof from horizontal.

Abbreviations

EMPA: Swiss Federal Laboratories for Materials Science and Technology, Dübendorf, Switzerland; PIMUZ: Paleontological Institute and Museum, University of Zurich, Switzerland.

RESULTS

Systematic palaeontology

OSTEICHTHYES Huxley 1880

ACTINOPTERYGII Cope 1887

SCOPULIPISCIS SAXCIPUT gen. et sp. nov.

Etymology

Generic name describes the marine deposits on the alpine cliff sides of Schesaplana Scopuli- from scopulus (Latin) - meaning a lookout place, cliff or crag, in or under the sea-, piscis (Latin) for fish. In the specific epithet, sax- (Latin) is for 'rock' and -ciput from caput (Latin) for head because the holotype specimen PIMUZ A/I 3026 is a well ossified neurocranium.

Holotype

PIMUZ A/I 3026 (figure 2), a neurocranium and associated dermal elements infilled by a fine carbonate matrix including small (~2-8mm) bivalves. Collected in 1976 by Dr. Heinz Furrer, PIMUZ, the specimen was subsequently prepared mechanically.

Locality and Horizon

The specimen was collected as float from the Kössen Formation of Schesaplana mountain, in Canton Grisons/Graubünden, Switzerland (figure 1), in the lowest part of the Alplihorn Member, Late Triassic [45], where the boundary between the Late Norian and Early Rhaetian is currently undefined (Heinz Furrer pers. comm). Other fish from the same locality include fragmentary elements and teeth from Birgeria [52] and isolated elements in the collections at PIMUZ assigned to Sargodon and Lepidotes. The Austrian portion of the Kössen Formation has produced other fish remains [48]. Other taxa from Schesaplana include marine reptiles [45,46] and pterosaurs [53].

Diagnosis

Large neopterygian with a well ossified neurocranium and the following combination of characters: spiracular canal extending through postorbital process to open on ventral surface of braincase; elongate hyomandibular facet ~1/4 of neurocranial length; pronounced median occipital crest, large sinus between lateral cranial canals, parasphenoid keel extending dorsally between orbits.

Anatomical description

General PIMUZ A/I 3026 preserves a partial skull roof and a near-complete neurocranium (17cm preserved length), missing the nasal capsules and anterior portion of the orbit. There is some distortion, with the right orbit partially crushed and the basiocciput sheared slightly to the right. The skull roofing bones have also collapsed in the region of the anterior dorsal fontanelle. The complete ossification of the braincase and partial obliteration of dermal sutures suggests the cranium belonged to an adult specimen. Sutures between braincase ossifications are not apparent; the neurocranium appears to be ossified as a single unit. Some areas of perichondral bone were weathered away prior to collection, exposing cancellous bone, particularly in the occipital region and along the parasphenoid.

Skull roof

The dermal bones of the skull roof are heavily ornamented with pustular tubules, from 0.5–1 mm in diameter, radiating from ossification centres and increasing in size towards element margins (figure 2, 3). The tubules are particularly large around the midline where the frontals and parietals meet. Such dense ornament means that sutures between bones are typically difficult to trace, although can sometimes be followed in CT scans. The frontal is relatively short, accounting for a little under half the length of the skull roof (fr, figure 3d). It is widest anterior to the parietal contact, and tapers anteriorly. There is no pineal foramen, and the frontals appear to be fused at the midline. Only a small fragment of the left nasal is preserved, but an unornamented area at the anteriormost point of the left frontal represents the overlap area for this bone (n.ov, figure 3d). A series of pores marks the passage of the supraorbital sensory canal through the frontal and into the parietal (soc, figure 3d), and the path of the canal can be followed in CT sections. Very little of the midline suture is preserved between the elongate parietals (pa, figure 3d), which have partially collapsed into the anterior dorsal fontanelle (adf, figure 3c). The suture between the rectangular dermopterotic and parietal (dpt, figure 3d) is obscured by ornament externally, but can be traced in CT sections.

However, it is unclear whether the dermopterotic contacts the frontal anteriorly. As with the supraorbital canal, the path of the infraorbital canal through the dermopterotic and into the dermosphenotic is indicated by a line of pores (ioc, figure 3d), with the canal visible in CT slices.

Braincase

Occipital region. The occipital region is the deepest part of the braincase, with the basiocciput accounting for half the vertical height of the specimen (figs 4c,d and 5). It is narrower than either the otic or orbitotemporal regions (fig 6a,b). A 'bulge' on the midline projects dorsally above the skull roof (bul, figs 4d and 5b,d), and houses a large cavity within the perichondrium of the braincase (cav, figure 7a). The posterior face of the occiput is developed into a broad median occipital crest, punctuated by a large ligamentous pit (lig, figs 4d, 7a). A process lateral to this pit is pierced by small anastomosing branches for the occipital nerve (focn, figs 4d and 5b). Medial to the posterodorsal angle of the braincase is a deep posttemporal fossa (ptf, figs 4d and 5b,d), which is continuous anteriorly with the fossa bridge (fb, figure 4d). The foramen magnum is small and triangular, and both its floor and roof are well ossified (fm, figs 4a, 7a). Two foramina for the occipital arteries open onto the lateral face of the braincase just above the parasphenoid (foca, figs 4d and 5b), with the smaller opening for the occipital nerve dorsal to these (focn, figs 4d and 5d). The notochordal facet is large and rounded (not, figure 4d), and leads into a narrow notochordal canal that pinches out approximately halfway along the length of the basiocciput (not, figs 7a,b and 8b). Ventral to the opening for the notochord is the circular aortic canal, which is enclosed ventrally by the parasphenoid (da, figs 4a, 6a, 7a). A dorsally-directed canal leaves the dorsal margin of the aorta to open on the lateral wall of the braincase above the parasphenoid. There is no indication of either a posterior dorsal fontanelle or otoccipital fissure.

Otic region. The otic region is the widest part of the braincase (figure 6a,b). Much of its dorsal surface is unossified to accommodate the large anterior dorsal fontanelle, which extends from the posterior margin of the hyoid facet to above the orbits (adf, figs 3c, 4b, 9d). Lateral to the fontanelle is an excavation for the fossa bridgei (figs 8a,b and 9), which extends posteriorly to the posttemporal fossa and anteriorly to the postorbital process. The lateral margin of the fossa bridgei is strongly concave, wrapping around the hyomandibular facet. The medial margin is convex, with multiple small projections giving an irregular edge. A total of five canals connect with the fossa bridgei. Two canals issue from its anteromedial corner. The more ventral, for the spiracular canal, enters the top of the postorbital process and travels along its entire length, opening just posterior to the lateral commissure on the ventral surface

of the braincase (spic, figs 5b, 6a, 8a, 9d). On the left side, the lateral commissure is broken, and consequently this canal appears to open midway along its length. The more dorsal of the two anteromedial canals opens into the posterolateral corner of the orbit, just below the orbital roof, and transmitted the otic nerve (otn, figs 4a, 6d, 8b,d). An additional canal leaves more posteriorly from the medial margin and opens into the roof of the hyomandibular facet, and may have transmitted the recurrent lateralis branch of the facial nerve (frla, figs 6b, 8a). Two narrow canals exit the anterolateral corner to open on the side of braincase just below the skull roof, and likely housed branches of the otic nerve (otn, figs 5b,d, 8b, 9b,d). Dorsal to the fossa bridgei is a separate small cavity, which also lies within the perichondrium of the braincase. Due to specimen preservation, the chamber is only fully observable on the right side. The chamber has a medial connection to the orbit, opening into the dorsolateral corner of the posterior wall (soph2, figure 4b). An additional small canal leaves the lateral margin of the chamber to open onto the lateral surface of the braincase dorsal to the otic nerve canals (ca, figure 5b).

The articular facet for the hyomandibular is elongate and horizontally oriented (hmf, figs 5b,d and 6b), and a deep dilatator fossa lies dorsal to the hyoid articulation (dil, figs 5b,d and 6b). Ventral to the facet, the lateral wall of the braincase narrows towards the midline, and this face is pierced by a number of canals. The most posterior of these is the lenticular opening for the vagus nerve (X, figs 5b,d and 6b), positioned ventral to the posterior margin of the hyoid facet. A shallow depression between the vagus nerve and hyoid facet is the supratemporal fossa (stf, figs 5d and 6f), delimited anteriorly by a vertical strut. The glossopharyngeal nerve (likely its supratemporal branch) exits the braincase via a small canal at the base of this strut (IXst, figs 5b,d and 6b), adjacent to an elliptical pit. This pit appears to be at least partly the result of mechanical preparation, as it punches through the perichondrium to reach the saccular chamber on one side, but comparison of both sides shows that the perichondral lining of the endocavity is complete, and there is no vestibular fontanelle. The original morphology of the pit is unclear, but it may represent an articular facet for the first suprapharyngobranchial (sup.ph, figure 5). A shallow groove for the jugular marks the lateral face of the braincase anterior to this facet, and can be traced to a foramen in the lateral commissure (jug, figs 5b,d and 6b). A large opening on the ventral margin of the jugular groove marks the exit of a stout canal, which originates on the on the lateral face of the sacculus near its anterior margin. This canal may be the main trunk of the glossopharyngeal nerve (IX, figs 5b,d and 6b). More anteriorly, a large opening for the hyomandibular branch of the facial neve (VIIfhm, figs 5b,d and 6b) pierces the roof of the jugular groove. The jugular vein and main trunk of the facial nerve continue through the postorbital process into the orbit.

Orbitotemporal region. The posterior margin of the orbitotemporal region is formed by the lateral commissure and postorbital process (por, figs 4a, 5b,d, 6b,d). The lateral commissure is reduced to a thin splint laterally, and the extent to which it is covered by the ascending process of the parasphenoid is difficult to discern. The orbital walls are pierced by a complex anastomosing series of canals, some of which are difficult to identify.

These canals can roughly be separated into four groups: on the roof and posterolateral corner of the orbit; on the posteromedial corner of the orbit; on the medial wall of the orbit; and midway up the posterior orbital wall. Of the canals that open onto the roof of the orbit, around four to six transmit the superficial ophthalmic branches of the facial and trigeminal nerves dorsally through the braincase to contact the visceral surface of the skull roof (soph, figs 4b, 6d). The two canals in the posterolateral corner of the orbit have different point of origin: the more ventral, for the otic nerve (otn, figs 4b, 6d, 8b, 9b,e) connects to the fossa bridgei, and the more dorsal, which may also carry branches of the superficial ophthalmic (soph2, figs 4b, 6d) to the chamber that lies above the fossa bridgei. Of the two canals in the posteromedial corner of the orbit, the more anterior and dorsal carries the trochlear nerve from the optic lobes (IV, figs 6d, 8b, 9b). The more posterior originates from the dorsal part of the midbrain, above and some way posterior to the trochlear nerve, but its identity is unclear (v?, figs 6d, 8b,9e). Two canals open on the medial wall of the orbit via a single foramen. These canals have a single root on the forebrain on the right of the specimen and a double root on the left, and transmitted the oculomotor and profundus nerves into the orbit (III and Vprof, figs 6d, 8b). The final set of canals, approximately midway up the posterior orbital wall, is centered about the trigeminofacialis chamber (tfc, figure 4b), which is continuous posteroventrally with the jugular canal. Two canals exit from the same point on the anterior face of the utriculus before separating into separate canals. These canals enter the orbit separately, but both are continuous within the trigeminofacialis chamber. The more dorsal transmits the trigeminal nerve (V, figs 4b, 6d, 8b, 9e) and the more ventral the facial nerve (VII, figs 4b, 6d, 8b,f). Two grooves extend from the dorsal margin of the chamber. The groove on the posterior margin of the orbit is short, with no canal at its dorsal limit. It terminates some way ventral and medial to any of the canals that connect to the skull roof, but may have transmitted the superficial ophthalmic nerves, which entered the orbit via the underlying chamber. The groove on the medial orbital wall is deeper, and a canal at its dorsal margin connects to the cranial cavity via two closely positioned openings. This likely transmitted the internal carotid artery (ica, figs 4b, 6d, 8b). A ventral connection links the trigeminofacialis chamber and the median posterior myodome (myo 4b, 6d, 8b,f,h). The pituitary vein enters the orbit ventral to the trigeminofacialis chamber (pv, 4b, 6d, 8b,f,h). There is no obvious opening for the palatine branch of the facial nerve into the orbit.

The braincase is broken midway along the orbit, and the skull roof has partially collapsed. A single opening on the midline represents where the braincase is broken through the endocranial cavity of the forebrain (endo, figs 4b, 6d); neither the exit of the optic (II) or olfactory (I) nerve is preserved. The basisphenoid is well-ossified, contributing to the medial walls and floor of the orbit, although the interorbital septum is formed entirely by the parasphenoid (psp, figs 4b, 5d, 6d, 7a). The basipterygoid process, which has both a dermal and endoskeletal component, is robust. The internal carotid opens into the posterior margin of basisphenoid via a foramen anterior to the posterior myodome. The subocular shelf is narrow and formed entirely by the parasphenoid.

Parasphenoid

The parasphenoid extends the full length of the preserved braincase, although a fragment is missing in the middle where the specimen is broken between the midpoint of the basiocciput and the postorbital process. The posterior margin of the parasphenoid is weathered, exposing the basioccipital, but a midline aortic notch appears to have been absent (figs 4 and 6). Although housed entirely within the basiocciput posteriorly, most of the floor of the aortic canal is formed by the parasphenoid (da, figure 7a). As the parasphenoid is broken midway along the basiocciput, the nature of the bifurcation into the lateral aortae is unknown. A narrow median keel on the ventral surface of the parasphenoid (ke, figs 5b,d and 6b) is flanked by a shallow groove (gr, figs 5b and 6b); the depth of the left groove has been exaggerated during specimen preparation. As the dorsal and lateral aortae are enclosed within the braincase, the purpose of these grooves is unclear. The parasphenoid extends up the lateral walls of the braincase to the level of the foramen magnum, effectively cloaking the basiocciput. The ascending processes of the parasphenoid are narrow and strut-like, although it is difficult to assess how far they extend dorsally up the postorbital process. The basipterygoid processes are robust, projecting dorsally as well as laterally (bpt, figs 4b, 5b,d, 6b,d), and the ophthalmic artery pierces the orbital floor posteromedial to the process (opa, figs 4a, 5d, 6d,e). An opening at the anterior limit of the basipterygoid process marks the exit of the palatine nerve and artery from the basisphenoid (pal, figs 4a, 5b,d, 6b,d,e). A v-shaped ridge is present on the ventral surface of the parasphenoid, and the efferent pseudobranchial artery exits posterior to where the two arms of the ridge converge on the midline (epsa, figs 5d, 6b,e). Anteriorly, the buccohypophyseal canal exits the parapshenoid on the midline (bhc, figure 6e). The internal carotid foramen is not preserved, and presumably entered the parasphenoid through the missing section. A broad parasphenoid keel extends dorsally between the orbits, forming the interorbital septum (psp, figs 4a, 5d, 6d, 7a). No teeth are present on the parasphenoid.

Endocast

The regions of the endocranial cavity corresponding to the midbrain, hindbrain and bony labyrinth are almost completely preserved, although only a short portion corresponding to the narrow forebrain is present in the specimen (tel, fig 8). As the internal walls of the braincase are sometimes poorly mineralised (figure 7a), contrast between the braincase and infilling sediment is low, and the exact boundary of some regions of the endocranial cavity are difficult to discern.

Midbrain. The optic lobes (midbrain) are large, representing the widest part of the endocast (optl, figure 9b). Much of the dorsal surface is unfinished, indicating the position of the extensive anterior dorsal fontanelle (adf, fig 9a). Two closely associated canals leave from the anterolateral face of the midbrain, entering the orbit via a single (on the right of the specimen) or double (on the left) opening. These likely transmitted the oculomotor and profundus nerves (III/Vprof, figure 8b). The trochlear nerve leaves the cranial cavity posteriorly and dorsally (IV, figs 8b and 9b).

Hindbrain. There is no clear division between the midbrain and hindbrain, although the portion of the hindbrain positioned behind the crus commune sits far ventral relative to the rest of the endocavity, perhaps indicating that the cerebellum projected into the fourth ventricle [54]. Cerebellar auricles cannot be identified. Several canals exit the cranial cavity in the anterior part of the hindbrain. Dorsally, a stout canal transmits an unidentified vessel into the dorsal part of the orbit (v?, figure 8b). The middle cerebral vein exits the cranial cavity some way ventral to this (mcv, figure 8b), and the internal carotid enters more ventrally still (mcv, figure 8b). The trigeminal and facial nerves exit from the angle between the midbrain and utricular recess (V and VII, figure 8b). Posterior to the labyrinth, the vagus nerve leaves the ventral margin of the hindbrain through a large, anteroposteriorly elongate canal (X, figure 8b). The region corresponding to the spinal cord is by far the narrowest portion of the endocast, and from its lateral margins issue a dorsal, bifurcating canal for the occipital nerves (focn, figs 8b and 9b,d), and a ventral, single canal for the occipital artery (foca, figs 8b and 9b,d).

Labyrinth. The walls of the bony labyrinth are fairly well ossified, except in the region of the sinus superior and anterior ampulla. The three semicircular canals are narrow, and all are fully enclosed in bone (asc, hsc, psc, figs 8b and 9b,e). Both the anterior and posterior canals are anteroposteriorly short, and the horizontal canal is almost isoclinal in its curvature

(hsc, figure 9c). The orientation of the anterior ampulla is unclear (aa, figure 8b). The utriculus is dorsoventrally tall, and there is a slight suggestion of division into dorsal and ventral components (utr, figure 8b). A small saccular notch is present (sac, figure 8b). Although incompletely ossified, the sinus superior is long (ssu, figure 8b), and the crus commune projects above the roof of the hindbrain and slightly towards the midline (cc, figs 8b and 9b). The lateral cranial canal is very well developed (lcc, figs 8b and 9b,d). As well as anterior and posterior connections to the cranial cavity, it has a dorsal extension that almost reaches the underside of the skull roof. At least a single canal, likely for the endolymphatic ducts (end.d, fig 7a), connects the cranial cavity to the median sinus positioned between the lateral cranial canals.

Circulatory system. The buccohypophyseal canal is elongate, leaving the anteriormost point of the posterior myodome and continuing anteroventrally (bhc, figure 8). A narrow canal branches from its lateral margin level with the exit of the internal carotids into the orbit (can.bsp: unidentified canal in the region of the basiphenoid, figure 8*f*,*h*). Further anteriorly, the buccohypophyseal canal bends dorsally in a 's' shape, before opening onto the ventral surface of the parasphenoid. The path of the internal carotid artery is incompletely known, largely due to the loss of part of the parasphenoid. It presumably entered the parasphenoid posterior to the basipterygoid process (?ica, figure 6*e*) and continued via an anterodorsally directed canal. This canal opens onto the orbital floor posteromedial to the basipterygoid processes (ica, figs 6*e* and 8*e*,*h*), and enters the cranial cavity through a foramen in a dorsally directed groove medial to the trigeminofacialis chamber (ica, fig 6*d*,*e*). The efferent pseudobranchial pierces the parasphenoid beneath the basipterygoid process (epsa, figs 5*d*, 6*d*, 8*f*,*h*) and is transmitted through a vertical canal, exiting onto the floor of the orbital as the ophthalmic artery (opa, figs 4*b*, 5*b*,*d*, 6*d*,*e*, 8*f*,*h*). The internal carotid and efferent pseudobranchial communicate via a short anastomosing canal (anas, fig 6*e* and 8*f*), and are also linked via the parabasal canal (pbc, fig 6*e*), which seems to have housed the palatine nerve and artery. The path of the palatine into the orbit is not known, but it appears to have entered the parabasal canal though the same opening as the internal carotid, and opens anteriorly on the lateral margin of the parasphenoid (pal, figs 4*b*, 5*b*,*d*, 6*b*,*d*,*e*, 8*f*,*h*). The internal carotids and efferent pseudobranchials do not anastomose with their antimeres, but a narrow transverse canal connects the two ophthalmic arteries.

Body size.

The neurocranium of *Dapedium* is inclined at approximately 50° from the horizontal in articulated specimens, and body size typically ranges from around 15–35cm [17]. Skull length accounts for approximately 16-18% of body length in *Dapedium*, but accounts for a much smaller proportion (~10%) in the largest known dapediids. Body length of a large *Sargondon tomicus* is estimated about 1m [11], with absolute head length of a medium sized specimen ~6cm and of the large specimen ~10cm [55]. We measured head-body proportion of 19-21% in large *Sargodon.*

The length of the preserved portion of PIMUZ A/I 3026 is 17cm. Based on the proportions of the skull of *Dapedium*, a conservative estimate for the length of the unbroken skull is 20 cm. Because head to body proportion ranges between 10-20%, estimates for body length of this individual range from 1-2m.

Because this individual is large, and larger animals have smaller heads in proportion to their bodies, we would expect the true length to be within the upper range of our estimate, 1.5-2m. Importantly, the estimated skull length of 20cm is much larger than the estimated skull lengths for *Sargodon* (~10cm in the largest individual [55]), suggesting that the new taxon and *Sargodon* are indeed separate.

DISCUSSION

Scopulipiscis saxciput gen. et sp. nov. as a dapediid

Although represented only by an isolated neurocranium, this specimen bears conspicuous similarities to dapediids, in particular the braincase described for *Dapedium* sp. [26,40]: short aortic canal, parasphenoid 'wings' cloaking the basiocciput, median occipital crest punctuated by a large ligamentous pit, parasphenoid extending dorsally between the orbits fossa bridgei continuous posteriorly with the posttemporal fossa, a median sinus between the lateral cranial canals, canals for endolymphatic ducts connecting the cranial cavity to the median sinus, and being formed of a single ossified unit. Similar likenesses are found with the endocast of *Dapedium* sp. [40], including a large lateral cranial canal extending dorsal to the endocranial roof, narrow semicircular canals, and a lenticular utriculus. The majority of actinopterygian material from Schesaplana has been identified as either *Birgeria* or *Lepidotes* [56] although unpublished elements in the collections at PIMUZ have been referred to the giant dapediid taxon *Sargodon* (A Latimer pers. obs), known from the Late Triassic (Norian) of Italy [11]. The limited overlap between described specimens of *Sargodon* and the braincase described here makes comparisons difficult: *Sargodon* is known from articulated but laterally compressed fossils, with no part of the braincase, and only small portions of the skull roof, described. Differences are evident in some of the few comparable regions, for example

the parietals and dermopterotic of *Sargodon* are quadrate, and those of the specimen described here are markedly rectangular. Furthermore, the cranium of even the largest *Sargodon* specimen known is only around 10 cm in length, with a standard length of 90–100 cm. In contrast, the braincase described here is approximately 17cm, and is incomplete anterior to the orbit, suggesting a total cranial length of at least 20cm. Consequently, we feel justified in erecting a new genus for this specimen: *Scopulipiscis saxciput*. It is possible that undescribed cranial elements at PIMUZ belong to *Scopulipiscis saxciput* rather than *Sargodon*, as their identification was most likely based on size.

In the strict consensus tree of our phylogenetic analysis (Fig. 10*a*), *Scopulipiscis saxciput* is resolved in a polytomy with all included *Dapedium* species, *Heterostrophus phillipsi*, *Sargodon tomicus*, *Dandya ovalis*, *Hemicalypterus weiri* and *Paradapedium egertoni*. This clade is supported by two homoplastic characters: c.18, nasals contacting on the midline; c.43, three or more pairs of extrascapulars. The monophyly of *Dapedium* is not upheld, and the genus is recovered as paraphyletic even in the Adams consensus tree (Fig. 10*b*). *Tetragonolepis oldhami* falls as the sister taxa to this clade, supported by a single homoplastic character (c.112: anterodorsal process of suboperculum absent). *Tetragonolepis semicincta* is placed as the earliest diverging dapediid lineage, and the monophyl y of dapediids is supported by seven homoplastic characters: c.156, braincase ossifications not differentiated; c.247, complete set of dorsal ridge scales between skull roof and dorsal fin; c.258, posterior margin of caudal fin forked; c.269, suborbitals extend ventral to orbit; c.275, hem-like median fins; c.276, anal fin insertion long; c.277, denticulate ridge scales present. Additional characters found in dapediid taxa to the exclusion of immediate outgroups, but which cannot be optimized due to uncertainty over the primitive condition in the clade, include: c.89, more than two infradentaries present; c.270, coronoids contribute to lateral dentition field; c. 272, parasphenoid wings extend around basiocciput; c. 273, dorsal extension of parasphenoid between orbits; c.274, ligament pit on posterior face of braincase; c.278, ossified centra absent.

The failure to resolve *Dapedium* as monophyletic is hardly surprising, given that placement of material in the genus traditionally largely relied on the presence of a deep-bodied morphology and differentiation of species on characters that could co-vary in individual specimens [11]. Doubt over the monophyly of the genus have been raised before [41], and it is possible that more detailed investigation of Sinemurian material from Dorset may raise further objections. Only two dapediid taxa are excluded in the agreement subtree, suggesting that only some of the uncertainty is a result of conflicting endoskeletal and dermal character sets. The monophyly of dapediids, in contrast, seems well supported, albeit with a different set of characters to those identified in previous phylogenetic analyses [13,31].

Placement of dapediids

Dapediids (along with a clade comprising *Hulettia americana* + *Ichthykentema purbeckensis*) form a clade of stem holosteans, sharing with other holosteans the following six homoplastic characters: c.11, short nasal process of premaxilla; c.29, frontals not broads and tapering anteriorly; c.89, two infradentaries; c.112, anterodorsal process of suboperculum present; c.135, anterodorsal myodome single; c.178 aortic notch in parasphenoid absent. Remaining holosteans share six characters, the first of which has a CI of 1: c.10, olfactory nerve pierces premaxilla; c.14, single median dermal bone capping snout absent; c.50, tube-like canal bearing anterior arm of antorbital; c.61, circumorbital ring; c.107, vomers paired, c.161, sphenotic with small dermal component.

While dapediids have been recovered as total group holosteans before, they are more typically resolved as the sister group to ginglymodians [31,37]. A position deep on the holostean stem goes some way to explaining the peculiar combination of apparent holostean and teleost features that have influenced their past phylogenetic relationships. The position of Hulettia + Ichthyokentema as sister taxa to dapediids is unexpected, and supported only by three homoplastic characters: c.27, parietals rectangular; c.247, dorsal scutes limited to region anterior to dorsal fin; c.249, ventral scutes anterior to anal fin. We note that both Hulettia and Ichthyokentema show large numbers of character reversals, suggesting that this position may not be robust. However, Hulettia has previously been associated with Dapedium [30]. Conspicuously absent from our analysis are pycnodonts, a clade of deep-bodied neopterygians with heterodont dentition [57] commonly recovered as the sister taxon to Dapedium [26,29,30,33]. Despite an extensive fossil record stretching from the Late Triassic to the Eocene, few pycnodont neurocrania are described: the most comprehensive description of an early-occurring pycnodont braincase is based on a specimen that now appears to be lost (Mesturus sp: [58]). Derived pycnodont neurocrania are known from well- preserved Cretaceous specimens of Neoproscinetes penlavi and Iemanja palma from Brazil, but are poorly ossified [59,60]. The earliest pycnodonts are named from dental elements found in isolation in Norian and Rhaetian deposits [57,61], with Late Triassic remains from the alpine regions of Germany, Italy, and Austria including isolated teeth and articulated but two-dimensional specimens [60–62]. Pycnodonts are excluded from this analysis pending a redescription of three dimensional neurocranial material from the early Cretaceous.

Dapedid diversity

Ray-finned fishes with an adaptation to durophagy were well represented in the Triassic [20,63], although dapediids are thought to have made up a fairly small proportion of this diversity. Although many durophages were wiped out during the end-Triassic extinction,

dapediids survived and went on to radiate in the Jurassic, presumably filling vacated ecospace [64]. The discovery of this new, exceptionally large [65] dapediid in the Late Triassic indicates that dapediids may have been more diverse before the end-Triassic extinction than previously thought. Although dental elements are not preserved for *Scopulipiscis saxciput*, many of the similarities in braincase anatomy to *Dapedium* seem likely to perform a functional role in strengthening the skull during durophagy, including the pronounced midline occipital crest, the deep insertion point for a longitudinal ligament, and the extension of the parasphenoid between the orbit and around the basioccipital.

CONCLUSION

This paper presents a new genus and species of a giant dapediid from the Schesaplana (Canton Grisons, Switzerland), and is the first actinopterygian neurocranium to be described from this locality. Although represented only by a three-dimensional neurocranium, *Scopulipiscis saxciput* can be confidently identified as a dapediid. CT scanning reveals important internal neurocranial anatomy, including a largely complete endocast, and similarities with the braincase of *Dapedium* suggest that this taxon was also adapted for durophagy. The very large size of this taxon—inferred to be well over 1.5 m in length—increases the known size range of dapediids, and suggests that dapediids reached higher levels of diversity than previously anticipated prior to the end-Triassic extinction. An expanded phylogenetic analysis incorporating most dapediid taxa and this new specimen fails to support the monophyly of *Dapedium*, but recovers Dapediidae as a clade of early-diverging holosteans, filling a conspicuous gap on the holostean stem [7].

ACKNOWLEDGEMENTS

H. Furrer (Zurich), C. Klug (Zurich), I. Werneburg (Tübingen), and T. Mörs (Uppsala) provided specimen and collections access. M. Plamondon (EMPA, Dübendorf) conducted CT scanning. T. M. Scheyer (Zurich), C. Romano (Zurich), T. Argyriou (Zurich), R. Socha (Warsaw) and M. Friedman (Michigan) provided helpful discussion. Thanks to A. Müller and J. Mansfield.

Ethical Statement

n/a

Funding Statement

This funding was supported by a Swiss National Science Foundation grant no. 31003A_149506 to T. M. Scheyer and L'Oréal-UNESCO International Rising Talents Fellowship and Royal Society Dorothy Hodgkin Research Fellowship to S. Giles.

Data Accessibility

3D surface files (.ply) and scan data (.tiff stack) are available from MorphoMuseuM (link-after-publication). Other data files, including the data matrix, are provided as Supplementary Materials.

Competing Interests

We have no competing interests.

Authors' Contributions

AEL designed the project. AEL and SG segmented the data, produced figures, ran phylogenetic analyses, interpreted the results and wrote the manuscript.

References

1. Nelson JS. 2006 *Fishes of the world, 600 pp.* 4th edn. Hoboken: John Wiley and Sons.
2. Sallan LC. 2014 Major issues in the origins of ray-finned fish (Actinopterygii) biodiversity. *Biol. Rev.* 89, 950–971. (doi:10.1111/brv.12086)
3. Broughton RE, Betancur-R. R, Li C, Arratia G, Ortí G. 2013 Multi-locus phylogenetic analysis reveals the pattern and tempo of bony fish evolution. *PLoS Curr.* 5. (doi:10.1371/currents.tol.2ca8041495ffafd0c92756e75247483e)
4. Friedman M, Brazeau MD. 2010 A reappraisal of the origin and basal radiation of the Osteichthyes. *J. Vertebr. Paleontol.* 30, 36–56. (doi:10.1080/02724630903409071)
5. Clarke JT, Lloyd GT, Friedman M. 2016 Little evidence for enhanced phenotypic evolution in early teleosts relative to their living fossil sister group. *Proc. Natl. Acad. Sci.* 113, 11531–11536. (doi:10.1073/pnas.1607237113)
6. Xu G, Gao K, Finarelli JA. 2014 A revision of the Middle Triassic scanilepiform fish *Fukangichthys longidorsalis* from Xinjiang, China, with comments on the phylogeny of the Actinopteri. *J. Vertebr. Paleontol.* 34, 747–759. (doi:10.1080/02724634.2014.837053)
7. Friedman M. 2015 The early evolution of ray-finned fishes. *Palaeontology* 58, 213–228. (doi:10.1111/pala.12150)
8. Giles S, Xu GH, Near TJ, Friedman M. 2017 Early members of 'living fossil' lineage imply later origin of modern ray-finned fishes. *Nature* 549, 265–268. (doi:10.1038/nature23654)

9. Xu G, Ma X. 2018 Redescription and phylogenetic reassessment of Asialepidotus shingyiensis (Holostei : Halecomorphi) from the Middle Triassic (Ladinian) of China. *Zool. J. Linn. Soc.* XX, 1–20. (doi:10.1093/zoolinnean/zlx105/4827721)
10. Woodward AS. 1895 *Catalogue of the fossil fishes in the British Museum (Natural History)*. British Museum.
11. Tintori A. 1983 Hypsisomatic semionotidae (Pisces, Actinopterygii) from the Upper Triassic of Lombardy (N. Italy). *Riv. Ital. di Paleontol. e Stratigr.* 88, 417–442.
12. Schaeffer B. 1967 Late Triassic fishes from the western United States. *Bull. Am. Museum Nat. Hist.* 135, 285–342.
13. Gibson SZ. 2016 Redescription and phylogenetic placement of †*Hemicalypterus weiri* Schaeffer, 1967 (Actinopterygii, Neopterygii) from the Triassic Chinle formation, southwestern United States: New insights into morphology, ecological niche, and phylogeny. *PLoS One* 11, 1–23. (doi:10.1371/journal.pone.0163657)
14. Woodward AS. 1929 The Upper Jurassic Ganoid Fish Heterostrophus. *J. Zool.* 99, 561–566.
15. Jain S. 1973 New specimens of Lower Jurassic holostean fishes from India. *Palaeontology* 16, 149–177.
16. Thies D. 1991 The osteology of the bony fish *Tetragonolepis semicincta* BRONN 1830 (Actinopterygii, †Semionotiformes) from the Early Jurassic (Lower Toarcian) of Germany. *Geol. Palaeontol.* 25, 251–297.
17. Thies D, Herzog A. 1999 New information on †*Dapedium* LEACH 1822 (Actinopterygii, †Semionotiformes). In *Mesozoic Fishes 2 - Systematics and Fossil Record* (eds G Arratia, H-P Schultze), pp. 143–152. Munich: Verlag Dr. Friedrich Pfeil.
18. Godefroit P, Cuny G, Delsate D, Roche M. 1998 Late Triassic vertebrates from Syren (Luxembourg). *Neues Jahrb. Fur Geol. und Palaontologie Abhandlungen* 210, 305–343.
19. Gibson SZ. 2015 Evidence of a specialized feeding niche in a Late Triassic ray-finned fish: evolution of multidenticulate teeth and benthic scraping in †*Hemicalypterus*. *Naturwissenschaften* 102, 10. (doi:10.1007/s00114-015-1262-y)
20. Lombardo C, Tintori A. 2005 Feeding specializations in Norian fishes. *Ann. dell'Università degli Stud. di Ferrara* , 1–9.
21. Smithwick FM. 2015 Feeding ecology of the deep-bodied fish *Dapedium* (Actinopterygii, Neopterygii) from the Sinemurian of Dorset, England. *Palaeontology* 58, 293–311. (doi:10.1111/pala.12145)
22. Patterson C. 1973 Interrelationships of holosteans. In *Interrelationships of Fishes.* (eds PH Greenwood, RS Miles), pp. 233–305. London.

23. Woodward AS. 1890 *The fossil fishes of the Hawkesbury Series at Gosford.* C. Potter, Government Printer.
24. Lehman J-P. 1966 Actinopterygii. *Trait. Paléontologie* 4, 1–242.
25. Wenz S. 1968 *Compléments à l'étude des poissons actinoptérygiens du Jurassique français.* Paris: Éditions du Centre national de la recherche scientifique.
26. Patterson C. 1975 The braincase of pholidophorid and leptolepid fishes, with a review of the actinopterygian braincase. *Phil. Trans. R. Soc. B* 269, 275–579. (doi:10.1098/rstb.1975.0001)
27. Thies D, Hauff RB. 2011 A new species of *Dapedium* LEACH, 1822 (Actinopterygii, Neopterygii, Semionotiformes) from the Early Jurassic of South Germany. *Palaeodiversity* 4, 185–221.
28. Olsen PE. 1984 The skull and pectoral girdle of the parasemionotid fish *Watsonulus eugnathoides* from the Early Triassic Sakamena group of Madagascar, with comments on the relationships of the Holostean fishes. *J. Vertebr. Paleontol.* 4, 481–499. (doi:10.1080/02724634.1984.10012024)
29. Gardiner BG, Maisey JG, Littlewood DTJ. 1996 Interrelationships of basal neopterygians. In *Interrelationships of Fishes.* (eds MLJ Stiassny, LR Parenti, GD Johnson), pp. 117–146. San Diego: Academic Press.
30. Hurley IA *et al.* 2007 A new time-scale for ray-finned fish evolution. *Proc. R. Soc. B Biol. Sci.* 274, 489–498. (doi:10.1098/rspb.2006.3749)
31. Thies D, Waschkewitz J. 2015 Redescription of *Dapedium pholidotum* (Agassiz, 1832) (Actinopterygii, Neopterygii) from the Lower Jurassic Posidonia Shale, with comments on the phylogenetic position of *Dapedium* Leach, 1822. *J. Syst. Palaeontol.* , 1–26. (doi:10.1080/14772019.2015.1043361)
32. Arratia G. 1999 The monophyly of Teleostei and stem-group teleosts. Consensus and disagreements. In *Mesozoic Fishes 2 - Systematics and Fossil Record*, pp. 265–334. Munich.
33. Arratia G. 2013 Morphology, taxonomy, and phylogeny of Triassic pholidophorid fishes (Actinopterygii, Teleostei). *J. Vertebr. Paleontol.* 33, 1–138. (doi:10.1080/02724634.2013.835642)
34. López-Arbarello A. 2012 Phylogenetic interrelationships of Ginglymodian Fishes (Actinopterygii: Neopterygii). *PLoS One* 7, 1–44.
35. Wen W, Zhang Q-Y, Hu S-X, Zhou C-Y, Xie T, Huang J-Y, Chen ZQ, Benton MJ. 2012 A new basal Actinopterygian fish from the Anisian (Middle Triassic) of Luoping, Yunnan Province, southwest China. *Acta Palaeontol. Pol.* 57, 149–160. (doi:10.4202/app.2010.0089)

36. Xu GH, Wu FX. 2012 A deep-bodied ginglymodian fish from the Middle Triassic of eastern Yunnan Province, China, and the phylogeny of lower neopterygians. *Chinese Sci. Bull.* 57, 111–118. (doi:10.1007/s11434-011-4719-1)
37. Bermúdez-Rochas DD, Poyato-Ariza FJ. 2015 A new semionotiform actinopterygian fish from the Mesozoic of Spain and its phylogenetic implications. *J. Syst. Palaeontol.* 13, 265–285. (doi:10.1080/14772019.2014.881928)
38. Gardiner BG. 1960 A revision of certain actinopterygian and coelacanth fishes, chiefly from the Lower Lias. *Bull. Br. Museum (Natural Hist.* 4, 239–384.
39. Arratia G. 2001 The sister-group of Teleostei: consensus and disagreements. *J. Vertebr. Paleontol.* 21, 767–773.
40. Giles S, Rogers M, Friedman M. 2016 Bony labyrinth morphology in early neopterygian fishes (Actinopterygii: Neopterygii). *J. Morphol.* 0, 1–15. (doi:10.1002/jmor.20551)
41. Thies D, Hauff RB. 2008 A neotype for *Dapedium caelatum* QUENSTEDT, 1858 (Actinopterygii, Neopterygii, Semionotiformes) from the Early Jurassic (Early Toarcian) of South Germany. *Geol. Palaeontol.* 42, 23–38.
42. Coates MI. 1999 Endocranial preservation of a Carboniferous actinopterygian from Lancashire, UK, and the interrelationships of primitive actinopterygians. *Philos. Trans. R. Soc. B Biol. Sci.* 354, 435–462. (doi:10.1098/rstb.1999.0396)
43. Giles S, Friedman M, Brazeau MD. 2015 Osteichthyan-like cranial conditions in an Early Devonian stem gnathostome. *Nature* 520, 82–85. (doi:10.1038/nature14065)
44. Frost GA. 1913 The Internal Cranial Elements and Foramina of *Dapedius granulatus*, from a Specimen recently found in the Lias at Charmouth. *Q. J. Geol. Soc.* 69, 219–222.
45. Furrer H. 1993 Stratigraphie und Facies der Trias/Jura-Grenzschichten in den Oberostalpinen Decken Graubündens. Universität Zürich.
46. Neenan JM, Scheyer TM. 2014 New specimen of Psephoderma alpinum (Sauropterygia, Placodontia) from the Late Triassic of Schesaplana Mountain, Graubünden, Switzerland. *Swiss J. Geosci.* 107, 349–357. (doi:10.1007/s00015-014-0173-9)
47. Fröbisch NB, Fröbisch J. 2006 A new basal pterosaur genus from the upper Triassic of the northern calcareous Apls of Switzerland. *Palaeontology* 49, 1081–1090.
48. Bürgin T, Furrer H. 1993 Kieferreste eines grossen Strahlenflossers (Osteichthyes; Actinopterygii) aus der ostalpinen Obertrias der Bergüner Stöcke (Kanton Graubünden, Schweiz) und Diskussion der Validität von ?*Birgeria costata* (Münster 1893). *Eclogae Geol. Helv.* 86, 1015–1029.

49. Swofford DL. 2003 PAUP*: phylogenetic analysis using parsimony (*and other methods). Version 4.
50. Wilkinson M. 1995 Coping with Abundant Missing Entries in Phylogenetic Inference Using Parsimony. *Syst. Biol.* 44, 501–514.
51. Lloyd GT. 2015 Claddis: an R package for performing disparity and rate analysis on cladistic-type data sets. *Online GitHub. See https//github. com/graemetlloyd/Claddis*
52. Bürgin T, Furrer H. 2004 Fossile Knochenfische aus der Kössen-Formation (Obertrias; Rhaet) von Lorüns (Vorarlberg, Österreich). *Vor. Naturschau* 14, 67–86.
53. Frobisch NB, Frobisch J, Sander PM, Schmitz L, Rieppel O. 2013 Macropredatory ichthyosaur from the Middle Triassic and the origin of modern trophic networks. *Proc. Natl. Acad. Sci. U. S. A.* 110, 1393–1397. (doi:10.1073/pnas.1216750110)
54. Nieuwenhuys R. 1982 An Overview of the Organization of the Brain of. *Am. Zool.* 22, 287–310.
55. Tintori A. 1998 Fish biodiversity in the marine Norian (Late Triassic) of northern Italy: The first neopterygian radiation. *Ital. J. Zool.* 65, 193–198. (doi:10.1080/11250009809386812)
56. Bürgin T, Furrer H. 1992 Zähne und Kieferreste der Gattung *Birgeria* (Osteichthyes, Actinopterygii) aus der ostalpinen Obertrias der Bergüner Stöcke (Kanton Graubünden, Schweiz). *Eclogae Geol. Helv.* 85, 931–946.
57. Poyato-Ariza FJ. 2005 Pycnodont fishes: morphologic variation, ecomorphologic plasticity, and a new interpretation of their evolutionary history. *Bull. Kitakyushu Museum Nat. Hist. Hum. Hist.* A, 169–184.
58. Nursall J. 1999 The family †Mesturidae and the skull of pycnodont fishes. In *Mesozoic Fishes 2 - Systematics and Fossil Record* (eds G Arratia, H-P Schultze), pp. 135–188. Munich.
59. Machado LP. 2008 The braincase of Neoproscinetes penalvai (Pycnodontiformes, Pycnodontidae). In *Meszoic fishes 4 - homology and phylogeny* (eds G Arratia, H-P Schultze), pp. 167–180. Munich: Verlag Dr. Friedrich Pfeil.
60. Kriwet J. 2005 A comprehensive study of the skull and dentition of pycnodont fishes. *Zitteliana R. A Mitteilungen der Bayer. Staatssammlung für Palaontologie und Geol.* 45, 135–188.
61. Tintori A. 1981 Two new Pycnodonts (Pisces Actinopterygii) from the Upper Triassic of Lombardy. *Riv. It. Paleont. Strat* 86, 19–30.
62. Delsate D, Kriwet J. 2004 Late Triassic pycnodont fish remains (Neopterygii, Pycnodontiformes) from the Germanic basin. *Eclogae Geol. Helv.* 97, 183–191. (doi:10.1007/s00015-004-1125-6)

63. Tintori A. 1995 Biomechanical fragmentation in shell-beds from the late Triassic of the Lombardian Basin (northern Italy). Preliminary report. *Riv. Ital. di Paleontol. e Stratigr.* 101, 371–379.
64. Bellwood DR, Hoey AS. 2004 Feeding in Mesozoic fishes: a functional perspective. In *Mesozoic fishes 3*, pp. 639–649. Verlag Dr. Friedrich Pfeil.
65. Romano C, Koot MB, Kogan I, Brayard A, Minikh A V., Brinkmann W, Bucher H, Kriwet J. 2016 Permian-Triassic Osteichthyes (bony fishes): Diversity dynamics and body size evolution. *Biol. Rev.* 91, 106–147. (doi:10.1111/brv.12161)

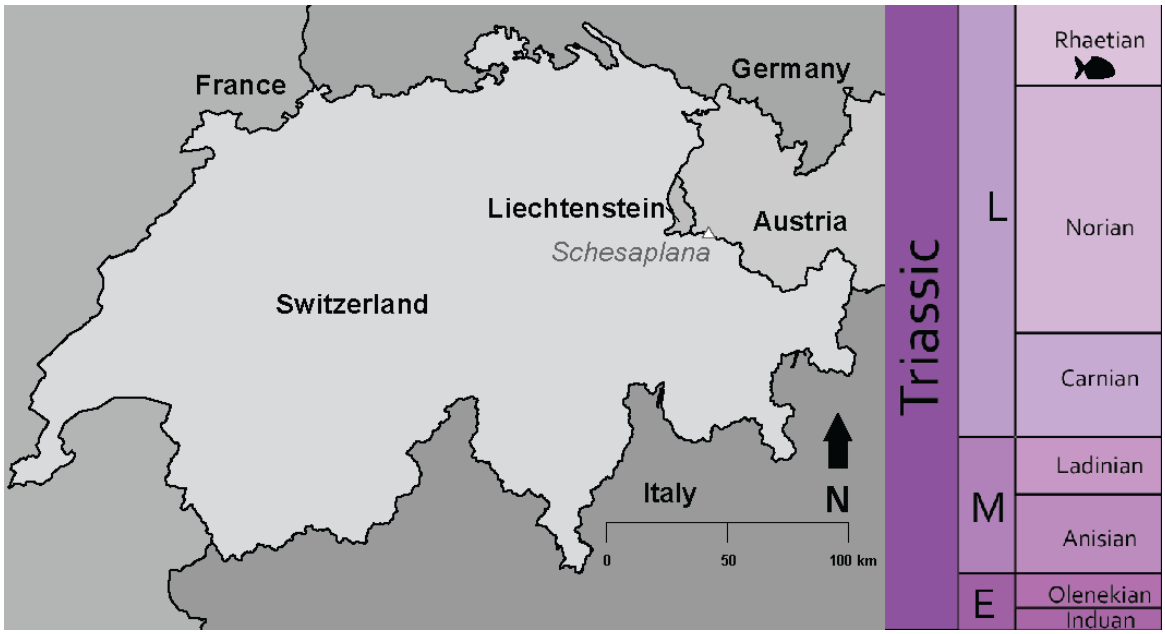

Figure 1. Map showing specimen locality (Schesaplana, white triangle) and putative age of deposit (Rhaetian).

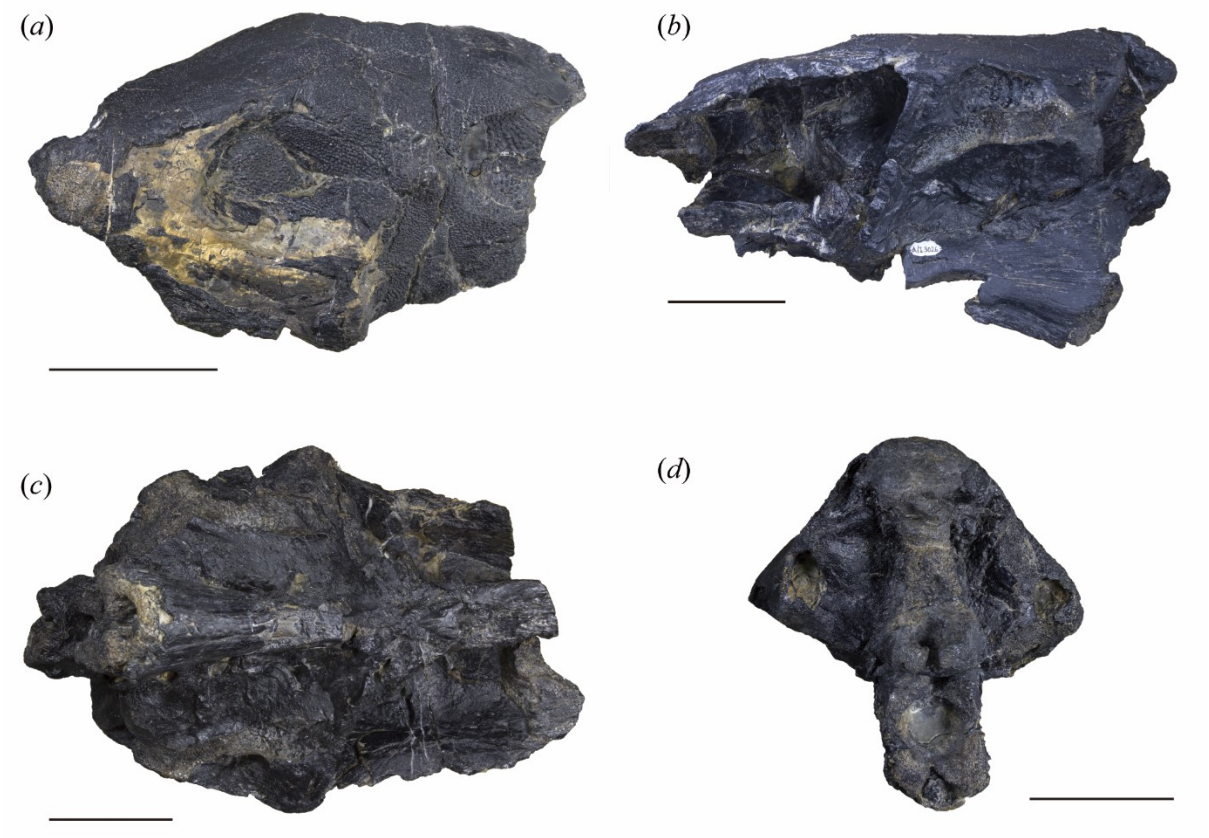

Figure 2. Photographs of the holotype of *Scopulipiscis saxciput* gen. et sp. nov. (PIMUZ A/I 3026). Specimen in dorsal (*a*), left lateral (*b*), ventral (*c*) and posterior (*d*) view. Scale bars are 50 mm.

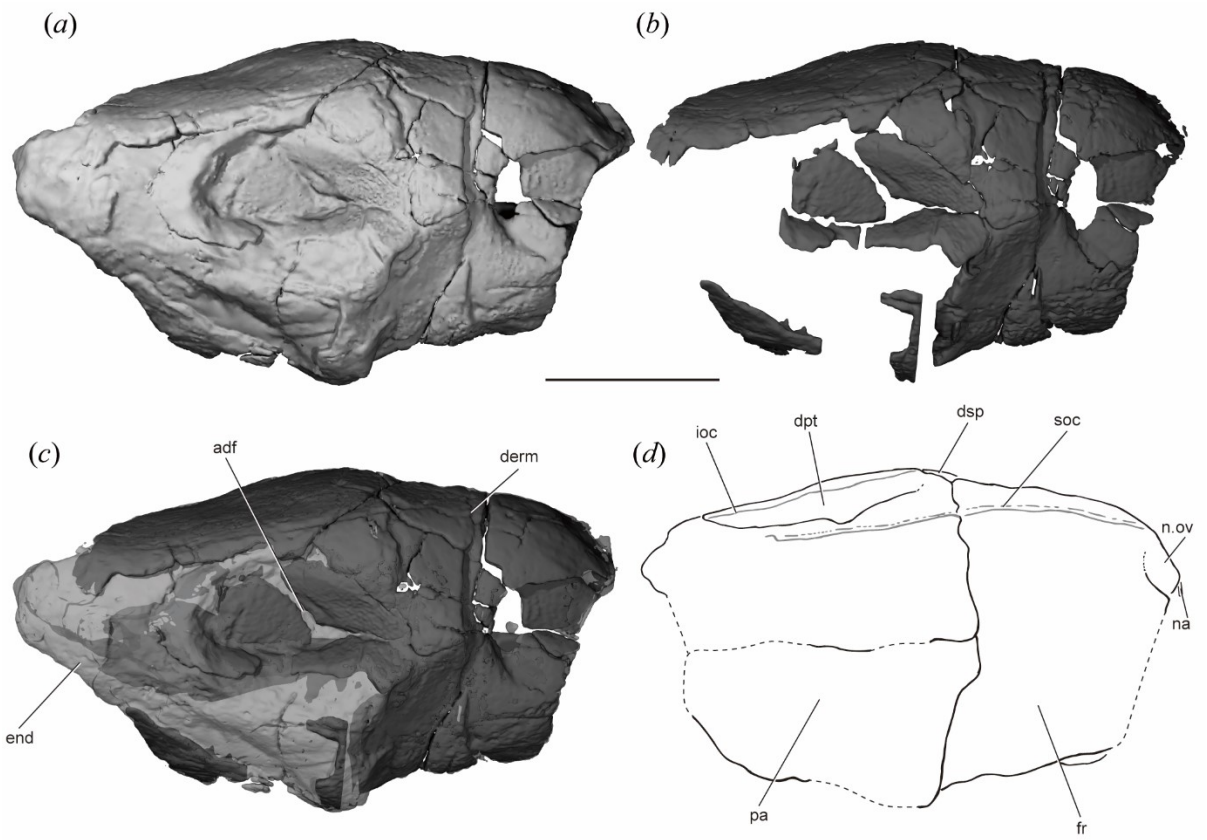

Figure 3. The skull roof of PIMUZ A/I 3026 in dorsal view. Rendering of entire specimen (*a*), dermal bone only (b) and position of preserved dermal bone (*c*). Interpretive drawing of skull roof (*d*). Dermal bone in dark grey, endochondral bone and matrix in light grey. Sensory canals in (*d*) in grey. Scale bar is 50 mm. adf, region of anterior dorsal fontanelle; derm, dermal bone; dpt, dermopterotic; dsp, dermosphenotic; end, endochondral bone; fr, frontal; ioc, infraorbital canal; na, nasal; n.ov, nasal overlap; pa, parietal; soc, supraorbital canal.

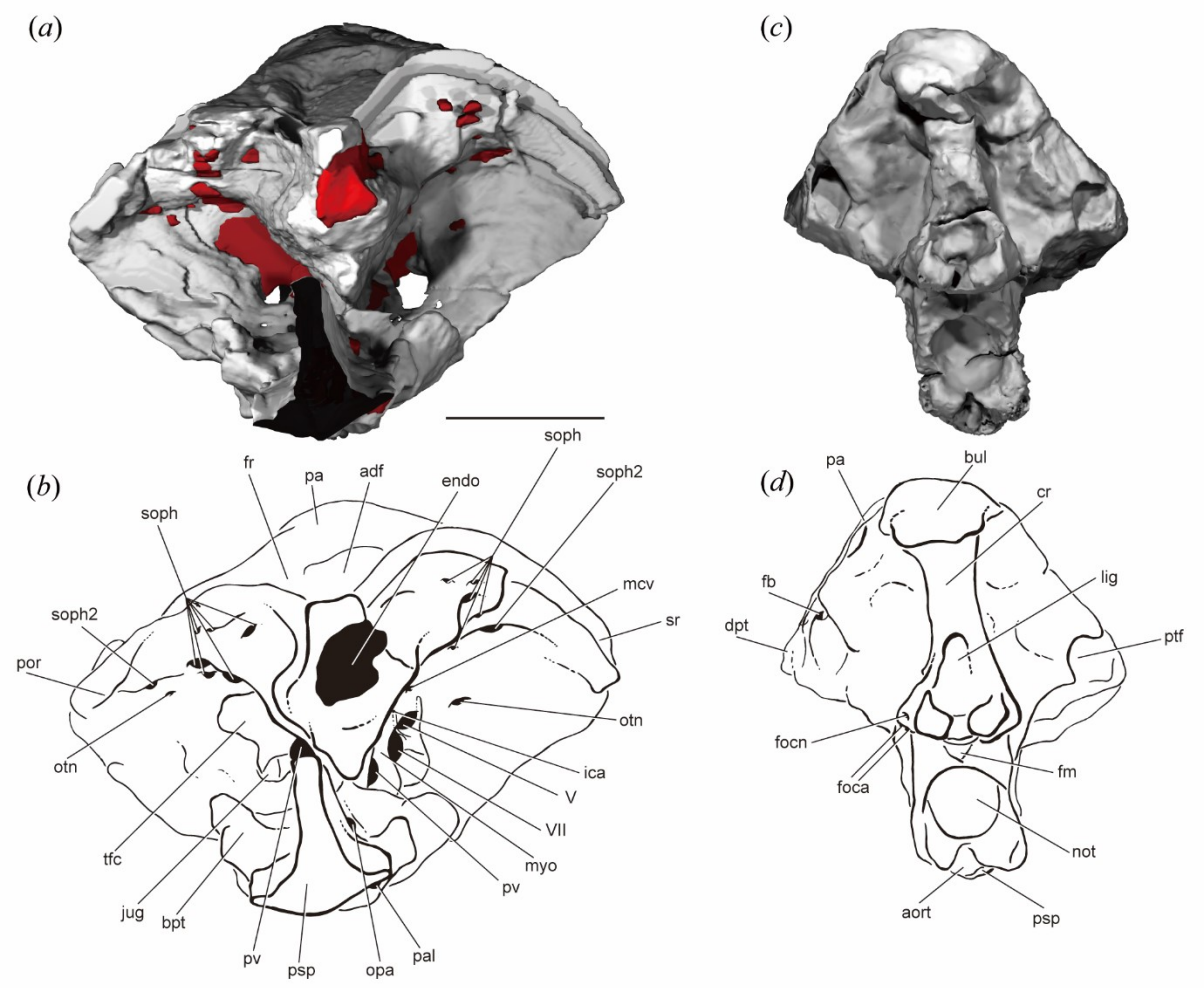

Figure 4. The braincase of PIMUZ A/I 3026. Rendering (*a*) and interpretive drawing (*b*) of cranium in anterior view, with the dermal skull roof digitally removed anterior to the postorbital process and the anterior corpus of the parasphenoid cropped. Rendering (*c*) and interpretive drawing (*d*) of cranium in posterior view. Braincase and dermal bones in light grey, endocast and canals in red. Scale bar is 50 mm. adf, region of anterior dorsal fontanelle; aort, dorsal aorta; bpt, basipterygoid process; bul, bulge; cr, crest; dpt, dermopterotic; endo, endocavity; fb, fossa bridgei; fm, foramen magnum; foca, occipital artery; focn, occipital nerve; fr, frontal; ica, internal carotid; jug, jugular vein; lig, ligament pit; mcv, middle cerebral vein; myo, myodome; not, notochord; opa, ophthalmic artery; otn, otic nerve; pa, parietal; pal, palatine artery; por, postorbital process; psp, parasphenoid; ptf, posttemporal fossa; pv, pituitary vein; soph, supraophthalmic artery; sr, skull roof; tfc, trigeminofacialis chamber; V, trigeminal nerve; VII, facial nerve.

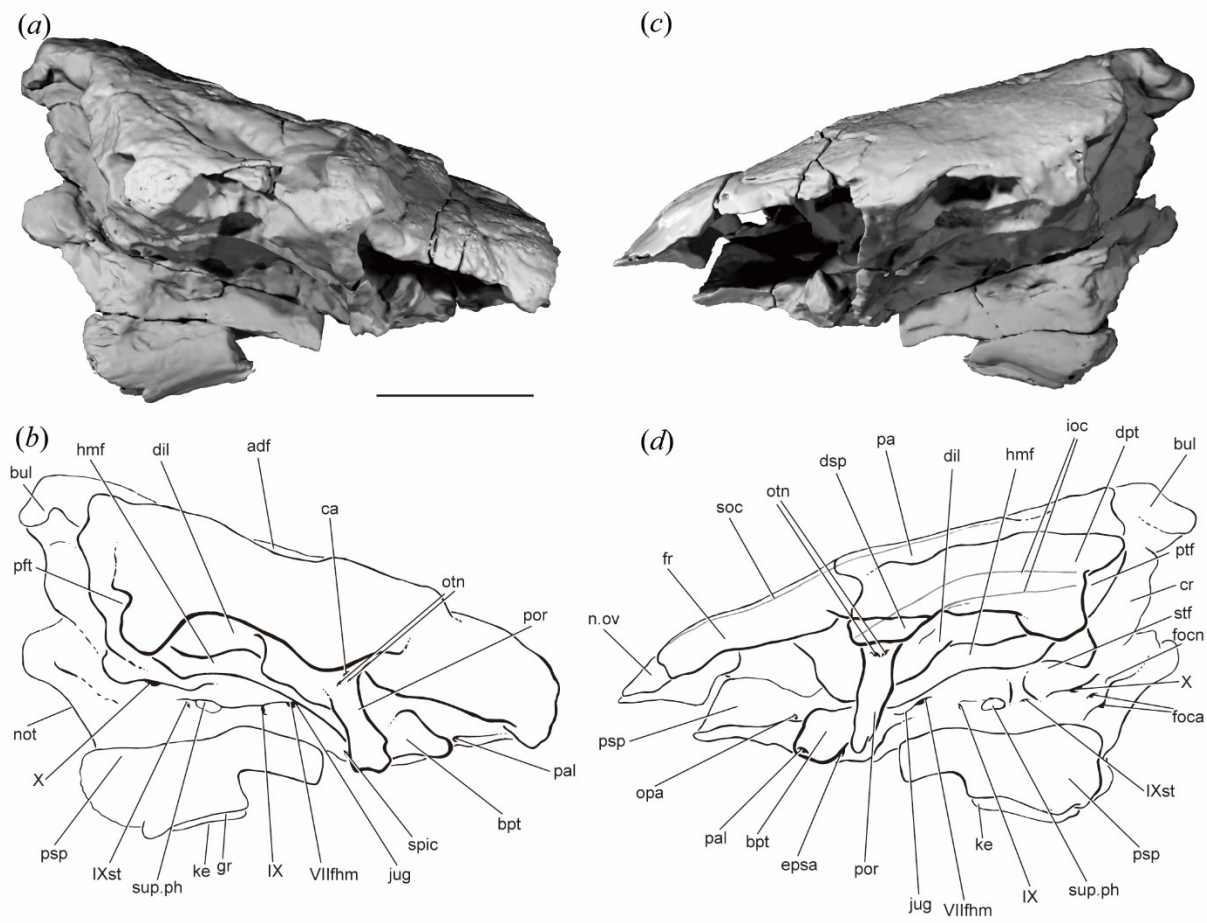

Figure 5. The braincase of PIMUZ A/I 3026. Rendering (*a*) and interpretive drawing (*b*) of cranium in right lateral view. Rendering (*c*) and interpretive drawing (*d*) of cranium in left lateral view. Sensory canals in (*d*) in grey. Scale bar is 50 mm. adf, region of anterior dorsal fontanelle; bpt, basipterygoid process; bul, bulge; ca, canal; cr, crest; dil, dilatator facet; dpt, dermopterotic; dsp, dermosphenotic; epsa, efferent pseudobranchial; foca, occipital artery; focn, occipital nerve; fr, frontal; gr, groove; hmf, hyomandibular facet; ioc, infraorbital canal; jug, jugular vein; ke, keel; n.ov, nasal overlap; not, notochord; opa, ophthalmic artery; otn, otic nerve; pa, parietal; pal, palatine artery; por, postorbital process; psp, parasphenoid; ptf, posttemporal fossa; soc, supraorbital canal; spic, spiracular canal; stf, supratemporal fossa; sup.ph, suprapharyngobranchial articulation; VIIfhm, hyomandibular branch of the facial nerve; IX, glossopharyngeal nerve; IXst, supratemporal branch of glossopharyngeal nerve, X, vagus nerve.

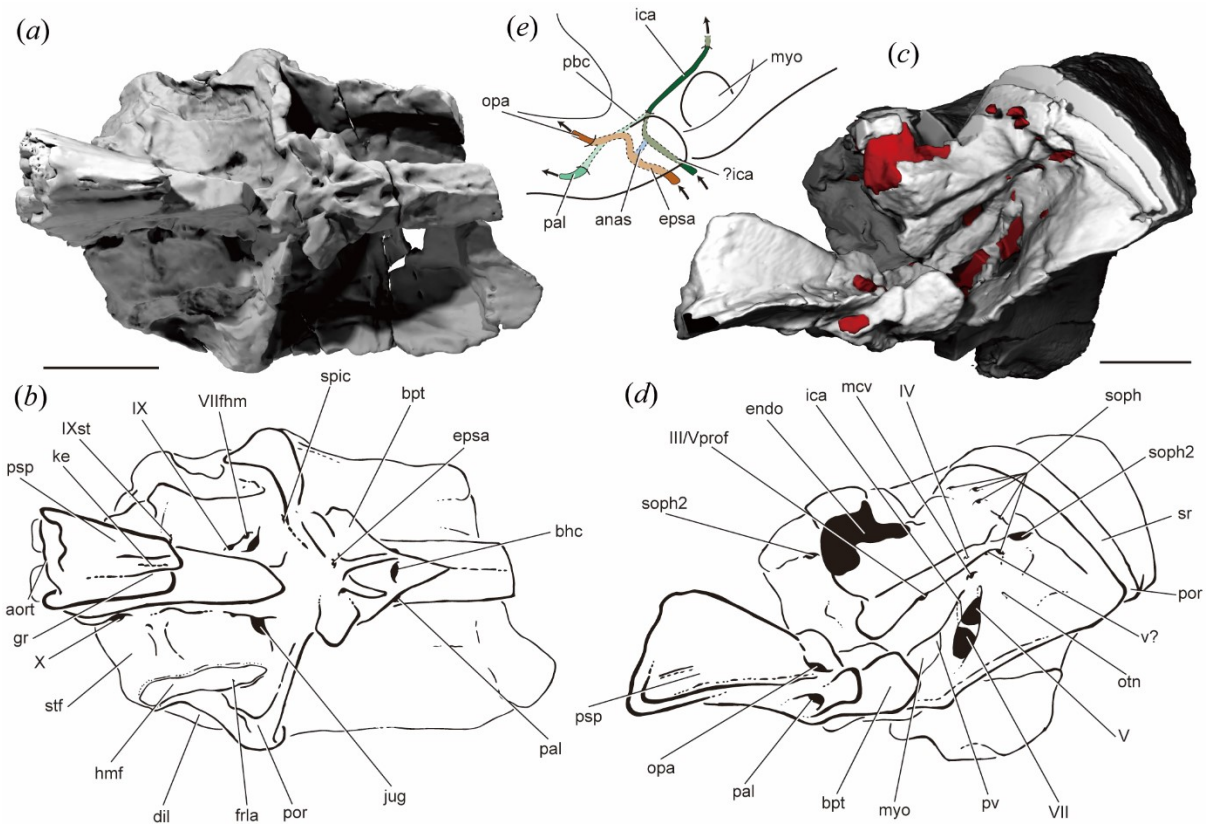

Figure 6. The braincase of PIMUZ A/I 3026. Rendering (*a*) and interpretive drawing (*b*) of cranium in ventral view. Rendering (*c*) and interpretive drawing (*d*) of cranium in left anterolateral view, with dermal skull roof digitally removed anterior to the postorbital process. (*e*) Schematic drawing of circulatory system in basisphenoid and parasphenoid in anterolateral view. The position of the entrance of the internal carotid in (*e*) is uncertain due to breakage. Braincase and dermal bones in light grey, endocast and canals in red. Scale bar is 50 mm. anas, anastomosis; aort, dorsal aorta; bhc, buccohypophyseal canal; bpt, basipterygoid process; dil, dilatator facet; endo, endocavity; epsa, efferent pseudobranchial; frla, recurrent lateralis branches of the facial nerve; gr, groove; hmf, hyomandibular facet; ica, internal carotid; jug, jugular vein; ke, keel; pal, palatine artery; mcv, middle cerebral vein; myo, myodome; opa, ophthalmic artery; otn, otic nerve; pbc, parabasal canal; por, postorbital process; psp, parasphenoid; pv, pituitary vein; soph, supraophthalmic artery; spic, spiracular canal; sr, skull roof; stf, supratemporal fossa; v?, unknown vein; III/Vprof, oculomotor nerve and profundus branch of the trigeminal nerve; IV, trochlear nerve; V, trigeminal nerve; VII, facial nerve; VIIfhm, hyomandibular branch of the facial nerve; IX, glossopharyngeal nerve; IXst, supratemporal branch of glossopharyngeal nerve; X, vagus nerve.

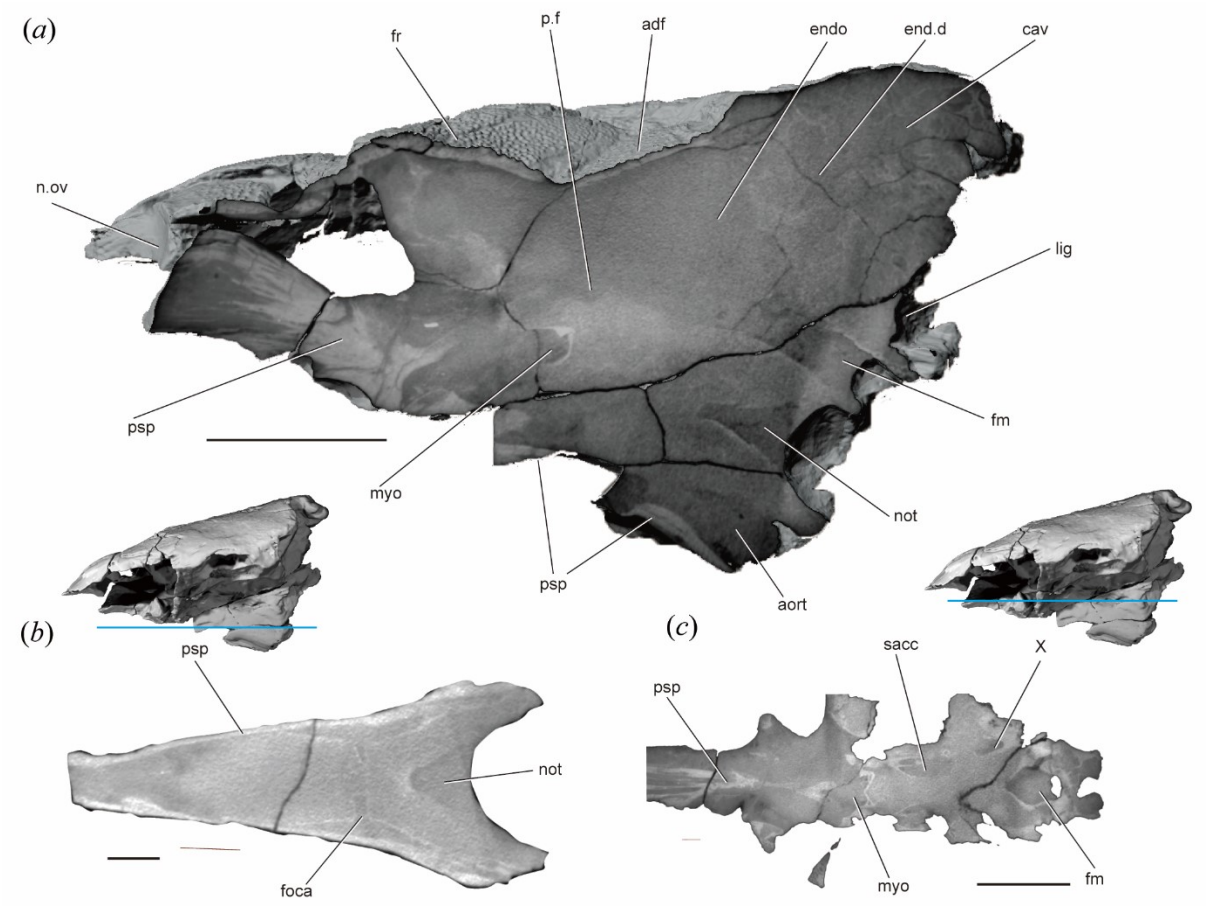

Figure 7. CT slices through the braincase of PIMUZ A/I 3026. (*a*) Sagittal section through the midline. Transverse planes through the basioccipital (*b*) and floor of the orbit and basisphenoid (*c*). Scale bars are 50 mm for (*a*,*c*) and 20 mm for (*b*). adf, region of anterior dorsal fontanelle; aort, dorsal aorta; cav, cavity; endo, endocavity; end.d, endolymphatic foca, occipital artery; fr, frontal; fm, foramen magnum; myo, myodome; n.ov, nasal overlap; not, notochord; p.f, pituitary fossa; psp, parasphenoid; sacc, sacculus; X, vagus nerve.

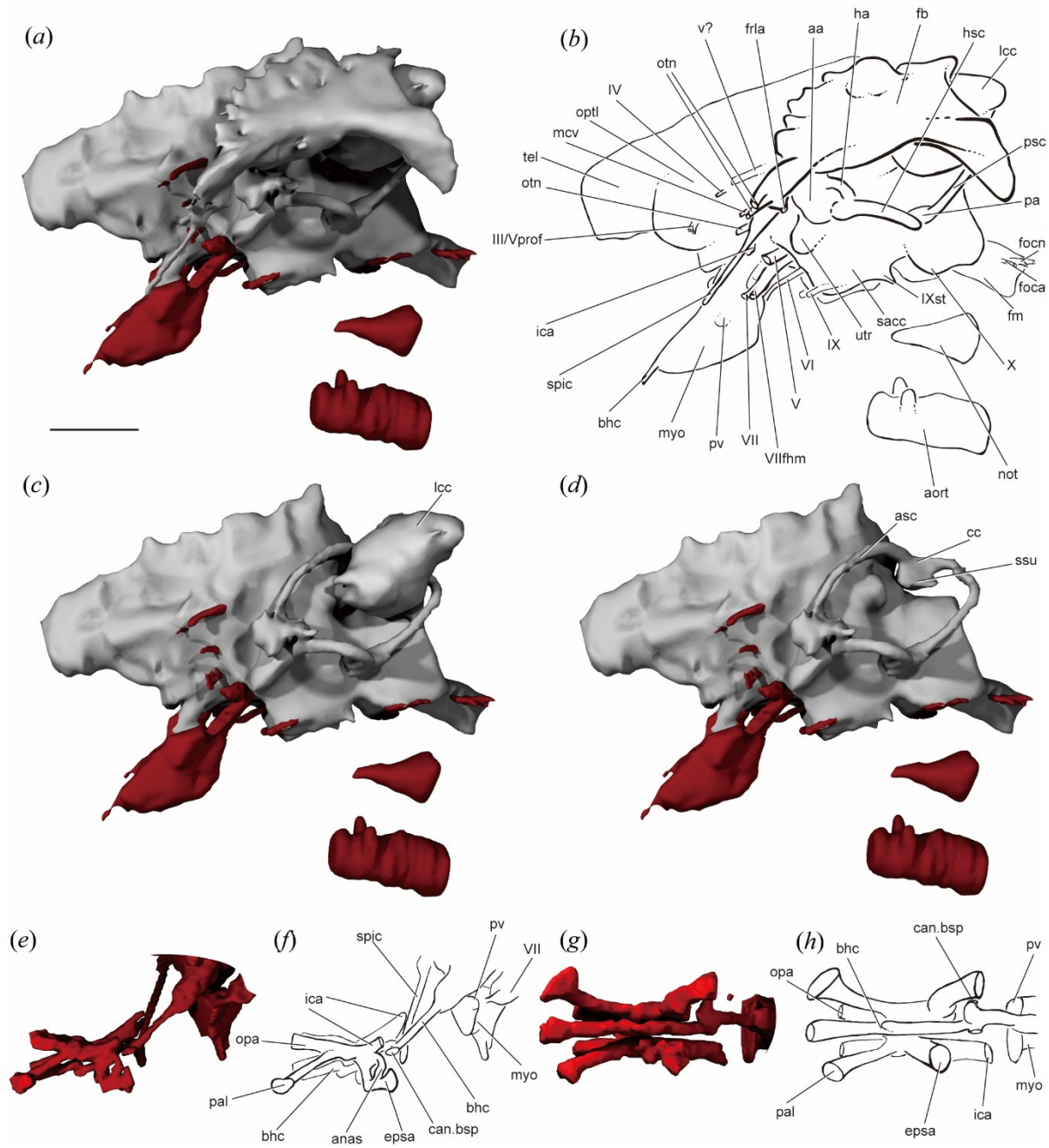

Figure 8. The endocast and cranial circulation of PIMUZ A/I 3026. Rendering (*a*) and interpretive drawing (*b*) of endocast, fossa bridgei and lateral cranial canal in left lateral view, and with fossa bridgei (*c*) and lateral cranial canal (*d*) digitally removed. Rendering (*e*,*g*) and interpretive drawing (*f*,*h*) of basisphenoid and parasphenoid circulatory system in left lateral (*e*, *f*) and ventral (*g*,*h*) view. Endocast in grey, canals in red. Scale bar is 50 mm. aa, anterior ampulla; aort, dorsal aorta; bhc, buccohypophyseal canal; can.bsp, unidentified canal in basisphenoid; cc, crus commune; fb, fossa bridgei; foca, occipital artery; focn, occipital nerve; fm, foramen magnum; fore, forebrain; ha, horizontal ampulla; hsc, horizontal semicircular canal; ica, internal carotid; lcc, lateral cranial canal; mcv, middle cerebral vein; myo, myodome; not, notochord; optl, optic lobe; otn, otic nerve; pa, posterior ampulla; psc,

posterior semicircular canal; pv, pituitary vein; sacc, sacculus; spic, cpiracular canal; ssu, sinus superior; tel, telencephalon; utr, utriculus; v?, unknown vein; III/Vprof oculomotor nerve and profundus branch of the trigeminal nerve; IV, trochlear nerve; V, trigeminal nerve; VI, abducens nerve; VII, facial nerve; VIIfhm, hyomandibular branch of the facial nerve; IX, glossopharyngeal nerve; IXst, supratemporal branch of glossopharyngeal nerve; X, vagus nerve.

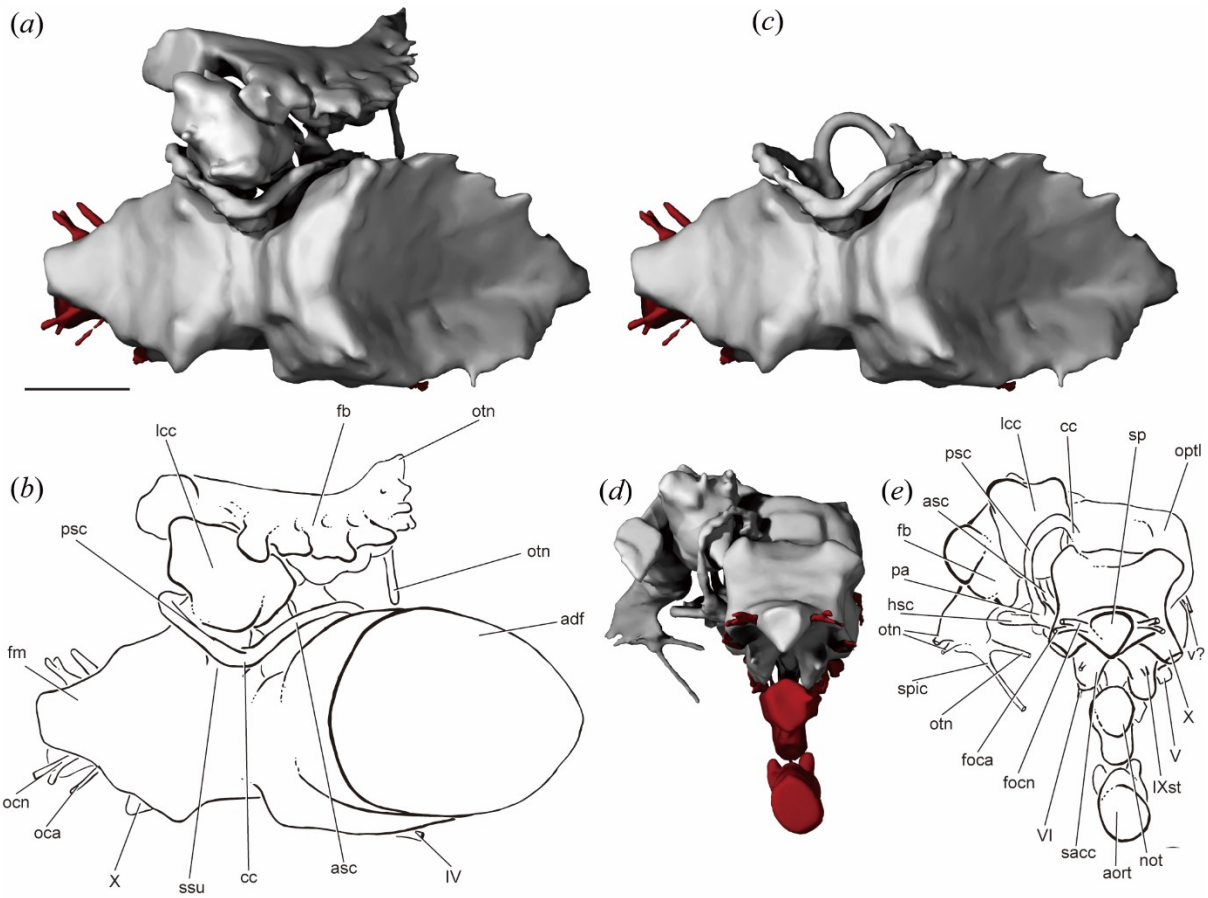

Figure 9. The endocast of PIMUZ A/I 3026. Rendering (*a*) and interpretive drawing (*b*) of endocast, fossa bridgei and lateral cranial canal in dorsal view. Rendering (*c*) and interpretive drawing (*d*) of endocast, fossa bridgei and lateral cranial canal in posterior view. Endocast in grey, canals in red. Scale bar is 50 mm. adf, anterior dorsal fontanelle; aort, dorsal aorta; asc, anterior semicircular canal; cc, crus commune; fb, fossa bridgei; fm, foramen magnum; hsc, horizontal semicircular canal; lcc, lateral cranial canal; not, notochord; oca, occipital artery; ocn, occipital nerve; optl, optic lobe; otn, otic nerve; pa, posterior ampulla; psc, posterior semicircular canal; sacc, sacculus; sp, spinal nerve cord; spic, spiracular canal; ssu, sinus superior; v?, unknown vein; IV, trochlear nerve; V, trigeminal nerve; VI, abducens nerve; IXst, supratemporal branch of glossopharyngeal nerve; X, vagus nerve.

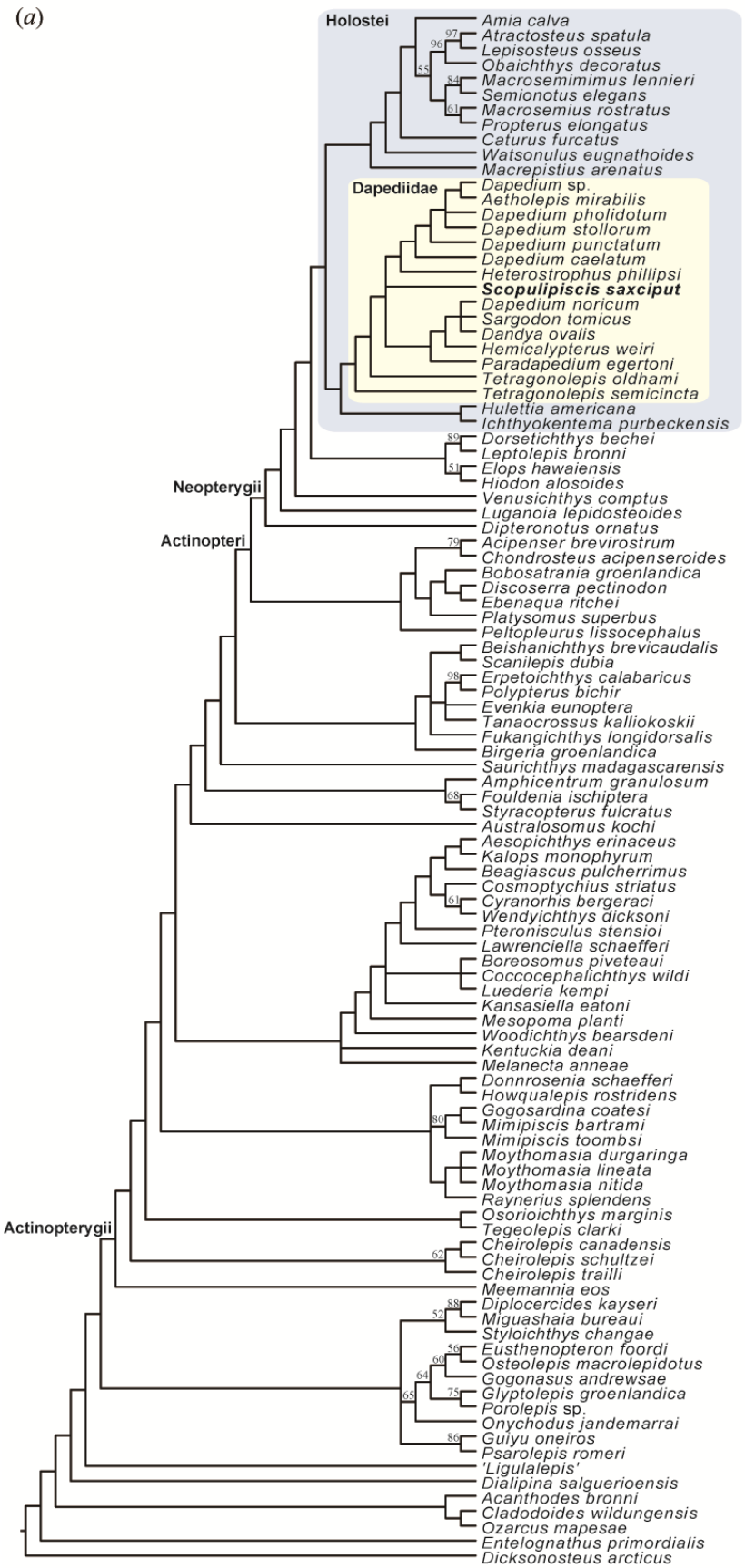

Figure 10. Consensus tree with holoseans in blue, dapediids in yellow.

3.2 Supplement for: “A giant dapediid from the Late Triassic of Switzerland and insights into neopterygian phylogeny”

Character List

1. [G 1] Large dermal plates (Forey, 1980; Gardiner, 1984; Zhu & Schultze, 2001; Zhu et al., 2001; Zhu & Yu, 2002; Zhu et al., 2006; Friedman, 2007; Brazeau, 2009; Zhu et al., 2009; Friedman & Brazeau; 2010; Davis et al., 2012; Zhu et al., 2013; Brazeau & Friedman, 2014; Giles et al., 2015b.)

0 absent
1 present

2. [G 2] Sensory lines (Brazeau, 2009; Zhu et al., 2013; Giles et al., 2015b.)

0 preserved as open grooves
1 pass through canals

3. Premaxilla as distinct ossification (Hurley et al. 2007; Xu et al. 2014. Typically, the premaxilla is a short, paired or median bone that contributes to the orbital margin anterior to the maxilla. However, considerable variation is present, and we have attempted to consistently code this variation as laid out here and in the following character descriptions. A premaxilla may be completely absent (e.g. Acipenser, Cyranorhis) or dorsally expanded into a midline bone (possibly fused with the rostral; e.g. Bobasatrania, Styracopterus). These two latter states are coded as ?1? here.)

0 present
1 absent

4. [CH 1; G3] Premaxillae, contact at midline (Cloutier & Ahlberg, 1996; Taverne, 1997; SchultzeCloutier & Ahlberg, 1996; Taverne, 1997; Schultze & Cumbaa, 2001; Zhu & Schultze, 2001; Zhu & Yu, 2002; Cloutier & Arratia, 2004; Friedman & Blom, 2006; Zhu et al., 2006; Friedman, 2007; Long et al., 2008; Swartz, 2009; Choo, 2011. Coded as inapplicable in taxa lacking any ossification in the position typically occupied by the premaxilla (e.g. Acipenser, Cyranorhis) and where the premaxilla appears fused with the rostral (e.g. Bobasatrania, Styracopterus). The premaxillae in Mansfieldiscus (Long, 1988) are thought to have contacted at the midline but have not been observed, and so the coding for this taxon is conservatively changed from '0' to ???. The snout is not preserved in Novagonatodus (Long, 1988; Holland et al., 2007), so the coding is changed from ?1? to ???. Although a median dentigerous 'rostral' is preserved in Luederia (Schaeffer & Dalquest, 1978), the lack of associated bones means its identity is uncertain, and it may well represent fused premaxillae. This taxon is conservatively coded ???. The premaxilla is absent in Wendichthys (Lund & Poplin, 1997), so the coding is revised from '0' to '-'. The coding for Moythomasia lineata is revised to '0' (Choo, 2015).)

0 present
1 absent

5. Premaxilla fused at midline (Xu et al., 2012; Xu et al., 2015; Xu & Zhao, 2016. Coded as inapplicable in taxa lacking any ossification in the position typically occupied by the premaxilla (e.g. Acipenser, Cyranorhis) and where the premaxilla appears fused with the rostral (e.g. Bobasatrania, Styracopterus) and where the premaxilla appears fused with the rostral (e.g. Bobasatrania, Styracopterus).)

0 absent
1 present

6. [G 4] Premaxilla (Friedman, 2007; Giles et al., 2015b. Coded as inapplicable in taxa lacking any ossification in the position typically occupied by the premaxilla (e.g. Acipenser, Cyranorhis) and in taxa where the premaxillae do not contact at the midline. The coding for Moythomasia lineata is revised to '0' (Choo, 2015).)

0 Reaches or extends past anterior margin of orbit
1 Confined to region anterior to orbit

7. [G 5] Premaxilla contributes to orbital margin (Cloutier & Ahlberg, 1996; Schultze & Cumbaa, 2001; Zhu & Schultze, 2001; Zhu et al., 2001; Zhu & Yu, 2002; Cloutier & Arratia, 2004; Zhu et al., 2006; Friedman, 2007; Long et al., 2008; Swartz, 2009; Zhu et al., 2009; Xu & Gao, 2011; Zhu et al., 2013; Xu et al., 2014. Coded as inapplicable in taxa lacking any ossification in the position typically

occupied by the premaxilla (e.g. Acipenser, Cyranorhis), where the premaxilla appears fused with the rostral (e.g. Bobasatrania, Styracopterus) and where the premaxilla appears fused with the rostral (e.g. Bobasatrania, Styracopterus), and where the premaxilla is restricted anterior to the orbit. The coding for Moythomasia lineata is revised to '1' (Choo, 2015).)

0 absent
1 present

8. Teeth on premaxillae (Cloutier & Arratia 2004, Xu et al. 2014. Coded as inapplicable in taxa lacking any ossification in the position typically occupied by the premaxilla (e.g. Acipenser, Cyranorhis).)

0 present
1 absent

9. Mobile premaxilla (Arratia 1999; Cavin & Suteethorn 2006; Hurley et al. 2007. Coded as inapplicable in taxa lacking any ossification in the position typically occupied by the premaxilla (e.g. Acipenser, Cyranorhis) and where the premaxilla appears fused with the rostral (e.g. Bobasatrania, Styracopterus).)

0 absent
1 present

10. Olfactory nerve pierces premaxilla (Grande 2010; Xu et al., 2015; Xu & Shen, 2015; Xu & Zhao, 2016. Coded as inapplicable in taxa lacking any ossification in the position typically occupied by the premaxilla (e.g. Acipenser, Cyranorhis) and where the premaxilla appears fused with the rostral (e.g. Bobosatrania, Styracopterus).)

0 absent
1 present

11. Nasal process of premaxilla (Gardiner & Schaeffer 1989; Gardiner et al. 1996; Gardiner et al. 2005; Cavin & Suteethorn 2006; Hurley et al. 2007; Grande 2010; Lopez-Arbarello 2011; Xu & Wu 2012; Xu et al. 2014; Xu & Shen, 2015; Xu & Zhao, 2016Xu & Zhao, 2015; Xu & Zhao, 2015. Coded as inapplicable in taxa lacking any ossification in the position typically occupied by the premaxilla (e.g. Acipenser, Cyranorhis) and where the premaxilla appears fused with the rostral (e.g. Bobasatrania, Styracopterus).)

0 absent
1 short
2 long, reaches skull roof

12. Sensory canal on premaxilla (New character. Coded as inapplicable in taxa lacking any ossification in the position typically occupied by the premaxilla (e.g. Acipenser, Cyranorhis) and where the premaxilla appears fused with the rostral (e.g. Bobasatrania, Styracopterus).)

0 present
1 absent

13. [CH 3; G 6] Postrostrals (element[s] immediately anterior to frontals but not in contact with premaxillae) (Cloutier & Ahlberg, 1996; Taverne, 1997; Lund, 2000; Schultze & Cumbaa, 2001; Zhu & Schultze, 2001; Lund & Poplin, 2002; Cloutier & Arratia, 2004; Friedman & Blom, 2006; Long et al., 2008; Swartz, 2009; Choo, 2011; Xu et al., 2014. Choo's (2011) codes for this character appear reversed.)

0 present
1 absent

14. [CH 4; G 7] Single median dermal bone capping snout (Gardiner & Schaeffer, 1989; Taverne, 1997; Friedman & Blom, 2006; Long et al., 2008; Swartz, 2009; Choo, 2011.)

0 absent
1 present

15. Median rostal (Gardiner et al. 1996; Hurley et al. 2007.)

0 plate-like
1 tube-like

16. [G 8] Pores for rostral organ (Friedman, 2007.)

0 absent
1 present

17. [CH 8; G 10] Nasal bone as single consolidated ossification (i.e. bone(s) carrying supraorbital canal between premaxilla and anterior margin of frontals) (Taverne, 1997; Schultze & Cumbaa, 2001; Friedman & Blom, 2006; Long et al., 2008; Swartz, 2009; Choo, 2011.)

0 absent
1 present

18. Contact of nasals on midline

0 separated by dermal bones

1 contacting or separated by gap unfilled by bone

19. Nasal contributes to orbital margin (Xu & Wu 2012; Xu et al. 2014; Xu & Zhao, 2016.)
0 absent
1 present

20. [CH 57; G 11] Mesial margin of (anterior) nasal (Lund et al., 1995; Ahlberg & Johanson, 1998; Ahlberg et al., 2000; Lund, 2000; Poplin & Lund, 2000; Schultze & Cumbaa, 2001; Lund & Poplin, 2002; Cloutier & Arratia, 2004; Zhu & Ahlberg, 2004; Daeschler et al., 2006; Long et al., 2006; Zhu et al., 2006; Zhu et al., 2009; Choo, 2011. The nasal is poorly preserved in Cheirolepis canadensis (Pearson & Westoll, 1979; Arratia & Cloutier, 1996), and coding for this taxon is revised from ?0? to ???. The position of the nostrils is not clear in Tegeolepis, and the coding for this taxon is revised from '1' to '?'.)
0 not notched
1 notched

21. [CH 6; G12] Posterior nostril in complete communication with orbital fenestra (Friedman & Blom, 2006; Long et al., 2008; Choo, 2011. The position of the nostrils is not clear in Tegeolepis, and the coding for this taxon is revised from '0' to '?'.)
0 absent
1 present

22. [CH 7; G 13] Posterior nostril ? contribution to margin by premaxillae (Friedman & Blom, 2006; Long et al., 2008; Choo, 2011. The coding for Howqualepis rostridens (Long, 1988) and Gogosardina (Choo et al., 2009) is revised from ?0? to ?1?. The premaxilla is not preserved in Novagonatodus (Long, 1988; Holland et al., 2007), so the coding is changed from ?0? to ???. The premaxilla is absent in Wendichthys (Lund & Poplin, 1997), so the coding is revised from '0' to '-'. The position of the nostrils is not clear in Tegeolepis, and the coding for this taxon is revised from '0' to '?'. The coding for Moythomasia lineata is revised to '0' (Choo, 2015).'?'.)
0 absent
1 present

23. [G 14] Tectals (sensu Cloutier & Ahlberg 1996, not counting the posterior tectal of Jarvik) (Lund et al., 1995; Cloutier & Ahlberg, 1996; Lund, 2000; Schultze & Cumbaa, 2001; Zhu & Schultze, 2001; Zhu et al., 2001; Lund & Poplin, 2002; Zhu & Yu, 2002; Cloutier & Arratia, 2004; Zhu et al., 2006; Friedman, 2007; Swartz, 2009; Zhu et al., 2009; Zhu et al., 2013.)
0 absent
1 present

24. [CH 75; G 36] Dermal intracranial joint (Cloutier & Ahlberg, 1996; Ahlberg & Johanson, 1998; Zhu & Ahlberg, 2004; Zhu & Schultze, 2001; Zhu et al., 2001; Zhu & Yu, 2002; Daeschler et al., 2006; Long et al., 2006; Zhu et al., 2006; Friedman, 2007; Brazeau, 2009; Zhu et al., 2009; Choo, 2011; Davis et al., 2012; Zhu et al., 2013. Choo?s coding for this character appears to be inaccurate, and codes have been changed where appropriate.)
0 absent
1 present

25. [CH 9; G 15] Pineal foramen (Cloutier & Ahlberg, 1996; Taverne, 1997; Schultze & Cumbaa, 2001; Zhu & Schultze, 2001; Zhu & Yu, 2002; Friedman & Blom, 2006; Friedman, 2007; Long et al., 2008; Brazeau, 2009; Swartz, 2009; Davis et al., 2012; Zhu et al., 2013; Xu et al., 2014; Giles et al., 2015b. A pineal foramen is variably present in Cheirolepis canadensis (Pearson & Westoll, 1979; Arratia & Cloutier, 1996), C. trailli (Pearson & Westoll, 1979), Kentuckia deani (Rayner, 1951) and Meemannia (Zhu et al., 2010), and these taxa are coded '0/1' to reflect this polymorphism. The coding for Moythomasia lineata is revised to '0' (Choo, 2015).)
0 present
1 absent

26. [G 16] Pineal eminence (Friedman, 2007; Zhu et al., 2009. Can only be coded in taxa that lack a pineal foramen.)
0 absent
1 present

27. [CH 10; G17] Shape of parietals (sarcopterygian postparietals): (Dietze, 2000; Schultze & Cumbaa, 2001; Cloutier & Arratia, 2004; Friedman & Blom, 2006; Long et al., 2008; Swartz, 2009; Choo, 2011; Xu et al., 2014. The coding for Cuneognathus

(Friedman & Blom, 2006), Kentuckia hlavini (Dunkle, 1964) and Stegotrachelus (Swartz, 2009) is revised from ?0? to ?1?. The coding for Melanecta (Coates, 1998) is revised from ?1? to ?0?. Wendichthys (Lund & Poplin, 1997) was erroneously coded by Choo (2011) as state ?2?, for which there is no description, and is recoded here as ?1?. The coding for Moythomasia lineata is revised to '0' (Choo, 2015).)

0 rectangular, with long axis parallel to midline

1 quadrate

28. [CH 11; G 18] Relative lengths of frontals and parietals (sarcopterygian parietals and postparietals) (Lund et al., 1995; Taverne, 1997; Dietze, 2000; Lund, 2000; Poplin & Lund, 2000; Schultze & Cumbaa, 2001; Lund & Poplin, 2002; Cloutier & Arratia, 2004; Friedman & Blom, 2006; Zhu et al., 2006; Long et al., 2008; Swartz, 2009; Choo, 2011; Lopez-Arbarello, 2011; Xu et al., 2014. The coding for Mimipiscis toombsi (Gardiner, 1984; Choo, 2011) is changed from ?1? to ?2?. The coding for Moythomasia lineata is revised to '2' (Choo, 2015).)

0 frontal shorter than parietal

1 frontal approximately equal to parietal

2 frontal longer than parietal

29. Frontals broad posteriorly and tapering anteriorly (Arratia 1999; Lopez-Arbarello 2011.)

0 absent

1 present

30. [G 19] Anterior pit line (Giles et al., 2015b. Although not figured, an anterior pit line is described for Miguashaia (Cloutier 1996).)

0 absent

1 present

31. [G 20] Otic canal extends through parietals (Giles et al., 2015b.)

0 absent

1 present

32. Junction between supraorbital and infraorbital canals (New character. The supraorbital canal may terminate in the frontal/parietal, or it may become confluent with the infraorbital canal. The exact position of this junction is highly variable, and typically occurs in the region of the frontal, dermosphenotic, dermopterotic.)

0 absent

1 present

33. Anterior branch of infraorbital sensory canal (New character. In some taxa (e.g. Dapedium), the infraorbital canal continues anteriorly above the orbit a short way.)

0 absent

1 present

34. [G 21] Tabular (Lund et al., 1995; Cloutier & Ahlberg, 1996; Schultze & Cumbaa, 2001; Zhu & Schultze, 2001; Cloutier & Arratia, 2004; Long et al., 2008; Swartz, 2009.)

0 present

1 absent

35. [G 22] Tabular pit line (Giles et al., 2015b.)

0 absent

1 present

36. [CH 64; G 28] Number of bones carrying otic portion of lateral line canal between dermosphenotic and posterior edge of skull roof. (Gardiner & Schaeffer 1989; Cloutier & Arratia, 2004; Hurley et al. 2007; Choo, 2011; Xu & Zhao, 2016. This character is reformulated from Choo's character 'Dermopterotic: present/absent'. Rather than designating bones as an intertemporal (or supratemporal or dermosphenotic) a priori, we consider the number of bones carrying the otic portion of the lateral line canal between the dermosphenotic and the posterior edge of the skull roof. Where two bones are present, these are treated as the intertemporal and supratemporal; where only one is present, this is treated as the dermopterotic. Anamestic bones between the dermosphenotic and frontal are not included in this count. The coding in Melanecta (Coates, 1998) has been revised from '0' to '1'. The coding in Moythomasia nitida (Jessen, 1968) has been revised from '1' to '0'. The coding for Moythomasia lineata is revised to '0' (Choo, 2015).)

0 at least two (i.e. intertemporal and supratemporal)

1 one (i.e. dermopterotic)

37. [CH 12; G 23] Intertemporal ? relative length (Taverne, 1997; Friedman & Blom, 2006; Choo,

2011. Coded as inapplicable in taxa with a dermopterotic. The coding for Moythomasia durgaringa (Gardiner, 1984) and Moythomasia nitida (Jessen, 1968) is revised from '1' to '0'. The intertemporal appears to be absent in Cheirolepis schultzei (Arratia & Cloutier, 2004), so is coded '-'. The coding for Moythomasia lineata is revised to '0' (Choo, 2015). NOTE - n/a etc)

0 shorter than supratemporal
1 of similar length to supratemporal
2 longer than supratemporal

38. [CH 13; G 24] Intertemporal ? contact with supratemporal anterior to that between frontal and parietal (Friedman & Blom, 2006; Choo, 2011. Coded as inapplicable in taxa with a dermopterotic. The coding for Moythomasia lineata is revised to '0' (Choo, 2015).)

0 absent
1 present

39. [G 27] Intertemporal contacts nasal (Xu & Gao, 2011; Xu et al., 2014. Coded as inapplicable in taxa with a dermopterotic.)

0 absent
1 present

40. [CH 69; G 29] Supratemporal ? narrow anterolateral flange forming ventral margin of spiracular opening (Choo, 2011. Coded as inapplicable in taxa with a dermopterotic. The coding for Mimipiscis bartrami and M. toombsi (Gardiner, 1984; Choo, 2011) is revised from ?0? to ?1?. The coding for Moythomasia durgaringa (Gardiner, 1984) and Moy. nitida (Jessen, 1968) is revised from ?1? to ?0?. The position of the spiracular space in Stegotrachelus is uncertain, so this taxon is coded as ???. The posterior and ventral borders of the supratemporal are poorly preserved in Krasnoyarichthys (Prokofiev, 2002), so the coding is changed from ?0? to ???. The coding for Moythomasia lineata is revised to '0' (Choo, 2015).)

0 absent
1 present

41. Parietal fused to dermopterotic (Xu & Gao 2011; Xu et al. 2014. Coded as inapplicable in taxa with a separate intertemporal and supertemporal, and in taxa lacking these bones entirely.)

0 absent
1 present

42. Bone carrying otic portion of lateral line canal extends past posterior margin of parietals

0 absent
1 present

43. [CH 15; G 30] Number of paired extrascapulars (Gardiner & Schaeffer, 1989; Lund et al., 1995; Cloutier & Ahlberg, 1996; Coates, 1998; Lund, 2000; Poplin & Lund, 2000; Schultze & Cumbaa, 2001; Zhu & Schultze, 2001; Lund & Poplin, 2002; Cloutier & Arratia, 2004; Friedman & Blom, 2006; Long et al., 2008; Swartz, 2009; Choo, 2011; Lopez-Arbarello 2011; Zhu et al., 2013; Xu et al., 2015; Xu & Zhao, 2016. The coding for Moythomasia lineata is revised to '0' (Choo, 2015).)

0 one pair
1 two pairs
2 three or more pairs

44. [G 31] Extrascapular reaches lateral edge of skull roof (Giles et al., 2015b. The skull roof of Moythomasia as shown in Fig. 103 (Gardiner, 1984) is a restoration (see also Choo 2015: fig. 13). The only skull roof directly figured by Gardiner does not preserve the extrascapulars in situ (fig. 83). However, in specimens viewed by us, as well as in published photos of articulated material (e.g. Choo 2015: fig 8), the lateral extrascapular of M. durgaringa is clearly excluded from the lateral margin of the sull roof. The extrascapular in Cuneognathus is incomplete laterally. However, the extensive posterolateral extension of the supratemporal (Friedman & Blom, 2006: fig. 3) makes it unlikely that the extrascapular would have reached the lateral edge of the skull roof, and as such this character is coded ?0?. This convention is also followed for Tegeolepis (Dunkle, 1964), and Meemannia (Zhu et al., 2006). The coding for Moythomasia lineata is revised to '0' (Choo, 2015).)

0 absent
1 present

45. [CH 71; G 32] Single median extrascapular (Dietze, 2000; Cloutier & Arratia, 2004; Long et al., 2008; Swartz, 2009; Choo, 2011; Xu & Gao, 2011; Zhu et al., 2013; Xu et al., 2014. The coding in Mimipiscis bartrami, M. toombsi (Gardiner, 1984; Choo, 2011), Stegotrachelus (Swartz, 2009), Cheirolepis canadensis (Arratia & Cloutier, 1996), C. schultzei (Arratia & Cloutier, 2004), C. trailli

(Pearson & Westoll, 1979), Donnrosenia (Long et al., 2008), Howqualepis (Long, 1988), Mansfieldiscus (Long, 1988) and Woodichthys (Coates, 1998) is revised from ?0? to ?1?. The extrascapulars are not preserved in Gogosardina (Choo et al., 2009) and Melanecta (Coates, 1998), and the coding for these taxa is revised from ?0? to ???. The median extrascapular in Coccocephalichthys has an anterior and posterior series, as well as being paired about the midline, and is coded as ?0? here. The coding for Moythomasia lineata is revised to '1' (Choo, 2015).)

0 present
1 absent

46. [G 33] Extrascapulae contact each other at midline (Giles et al., 2015b. inapplicable for taxa that possess a median extrascapular, as it is logically impossible for the lateral extrascapulae to meet in the midline. It is unclear whether the extrascapulae met at the midline in Moythomasia durgaringa (Gardiner, 1984) or Cuneognathus (Friedman & Blom, 2006), so these taxa are coded '?'.)

0 absent
1 present

47. [CH 70; G 34] Medially-directed branch of sensory canal in extrascapulae (Choo, 2011. The codings for Mimipiscis bartrami, M. toombsi (Gardiner, 1984; Choo, 2011), Osorioichthys (Taverne, 1997), Cheirolepis canadensis (Arratia & Cloutier, 1996), C. trailli (Pearson & Westoll, 1979), Mansfieldiscus (Long, 1988), Woodichthys (Coates, 1998) and Wendichthys (Lund & Poplin, 1997) are revised from ?1? to ?0?. Although often figured as present in reconstructions, it is unclear whether these canals were present in Howqualepis rostridens (Long, 1988), Cuneognathus (Friedman & Blom, 2006), Donnrosenia (Long et al., 2008), Kentuckia hlavini (Dunkle, 1964), Limnomis (Daeschler, 2000), Stegotrachelus (Swartz, 2009) and Krasnoyarichthys (Prokofiev, 2002), and the coding for these taxa is revised from ?1? to ???. The coding for Moythomasia lineata is revised to '1' (Choo, 2015).)

0 present
1 absent

48. [G 35] Extratemporal (Cloutier & Ahlberg, 1996; Ahlberg & Johanson, 1998; Zhu & Schultze, 2001; Zhu et al., 2001; Zhu & Yu, 2002; Zhu & Ahlberg, 2004; Daeschler et al., 2006; Long et al., 2006; Zhu et al., 2006; Friedman, 2007; Zhu et al., 2009.)

0 absent
1 present

49. [CH 59; G 38] Antorbital bone (Gardiner & Schaeffer 1989; Lund et al. 2000; Cloutier & Arratia, 2004; Hurley et al. 2007; Choo, 2011; Xu & Gao, 2011; Xu et al., 2014. The coding for Moythomasia lineata is revised to '0' (Choo, 2015).H07: Discoserra has a large plate at the anterior of the infraorbital series, the antorbital or infraorbital identity of which is uncertain because the sensory canal pattern is unclear (a dorsally directed branch would indicate antorbital affinity). It is interpreted here as the anteriormost infraorbital (lachrymal) (figure 2a, la).)

0 absent
1 present

50. Tube-like canal bearing anterior arm of antorbital: (Grande 2010; Xu & Wu 2012; Xu et al. 2014; Xu & Shen, 2015; Xu & Zhao, 2016.)

0 absent
1 present

51. [CH 61; G 39] Infraorbitals (Cloutier & Arratia, 2004; Gardiner et al., 2005; Choo, 2011; Xu & Gao, 2011; Xu et al., 2014. Choo's (2011) codes for this character appear reversed. The coding for Gogosardina (Choo et al., 2009) is revised from '0' to '?'. The coding for Limnomis (Daeschler, 2000) is revised from '?' to '0'. The coding for Tegeolepis (Dunkle & Schaeffer, 1973) is revised from '0' 'to '?'. The coding for Moythomasia lineata is revised to '0' (Choo, 2015).)

0 one
1 two
2 more than two

52. [CH 16; G 40] Anterior expansion of lacrimal (Taverne, 1997; Friedman & Blom, 2006; Long et al., 2008; Swartz, 2009; Choo, 2011. The coding for Melanecta (Coates, 1998) is revised from ?0? to ???. The coding for Miguashaia (Cloutier, 1996) is revised from '1' to '?'.The coding for Novagonatodus (Long, 1988; Holland et al., 2007) and Onychodus (Andrews et al., 2006) is revised from ??? to ?1?. The coding for Tegeolepis (Dunkle & Schaeffer, 1973) is revised from '1' to '0'. The coding for

Wendichthys (Lund & Poplin, 1997) is revised from '0' to '1'.)

0 absent
1 present

53. [CH 17; G 41] Notch in anterior margin of jugal (Cloutier & Arratia, 2004; Friedman & Blom, 2006; Long et al., 2008; Swartz, 2009; Choo, 2011; Xu et al., 2014. Although the jugal of Moythomasia durgaringa is only faintly notched in its reconstruction (Gardiner, 1984: fig. 103), the notch is clearly visible on the medial face (Gardiner, 1984: fig. 73). As such the coding is revised from ?0? to ?1?. The coding in Cuneognathus (Friedman & Blom, 2006) is revised from?0? to ???. The coding in Novagonatodus (Long, 1988; Holland et al., 2007) is changed from ?1? to ?0?.The coding in Wendichthys (Lund & Poplin, 1997) is revised from '1' to '0'. The coding for Moythomasia lineata is revised to '0' (Choo, 2015).)

0 absent
1 present

54. [CH 18; G 42] Suborbitals (non-canal bearing ossifications separating jugal and maxilla) (Gardiner & Schaeffer 1989; Taverne, 1997; Schultze & Cumbaa, 2001; Friedman & Blom, 2006; Long et al., 2008; Choo, 2011; Lopez-Arbarello 2011; Xu & Gao 2011; Xu et al., 2015; Xu & Zhao, 2016Xu & Zhao, 2015.)

0 absent
1 one
2 two
3 three or more

55. [G 43] Multiple rami of infraorbital canal in jugal (Giles et al., 2015b. Multiple branches radiate from the infraorbital canal in the jugal of many Carboniferous actinopterygians.)

0 absent
1 present

56. [CH 54; G 25] Dermosphenotic with distinct posterior ramus (Gardiner & Schaeffer, 1989; Coates, 1998; Schultze & Cumbaa, 2001; Cloutier & Arratia, 2004; Friedman & Blom, 2006; Zhu et al., 2006; Long et al., 2008; Zhu et al., 2009; Choo, 2011; Xu & Zhao, 2015. The dermosphenotic of Moythomasia illustrated by (Gardiner 1984, fig 69) lacks a posterior limb, but this is from a small individual and most likely reflects ontogenetic variability, with a posterior limb being developed in larger individuals (B. Choo, pers. comm.; Choo 2015: fig. 8). The shape of the dermosphenotic in Cuneognathus (Friedman & Blom, 2006) is inferred, and the coding is thus revised from ?1? to ???. The coding in Melanecta (Coates, 1998) is revised from ?0? to ???. The posterior limb of the dermosphenotic is variably developed in Mesopoma (Coates, 1999), so this taxon is scored '0/1' to reflect this polymorphism.)

0 absent
1 present

57. [CH 14; G 26] Dermosphenotic ? contact with frontals blocked by intertemporal or dermopterotic (Friedman & Blom, 2006; Choo, 2011. The coding for Moythomasia lineata is revised to '0' (Choo, 2015).)

0 absent
1 present

58. Supraorbital (Gardiner & Schaeffer 1989; Hurley et al. 2007; Xu & Gao 2011; Xu et al. 2014; Xu et al., 2015; Xu & Zhao, 2016.)

0 absent
1 one or two
2 three or more

59. Anterior-most infraorbital anterior to orbit (i.e. does not contribute to orbital margin) (Cavin & Suteethorn 2006; Lopez-Arbarello 2011.)

0 absent
1 present

60. Three or more lachrymals (Grande 2010; Xu & Wu 2012; Xu et al. 2014, 2015; Xu & Zhao, 2016. The first lachrymal is regarded here as the anteriormost canal-bearing bone that contributes to orbital margin.)

0 absent
1 present

61. Circumorbital ring (Wiley 1976; Lopez-Arbarello 2010.)

0 Supraorbitals do not contact infraorbitals at the anterior rim of the orbit.
1 Supraorbitals contact infraorbitals, closing the orbit.

62. [CH 62; G 44] Jugal canal (Patterson, 1982; Lauder & Liem, 1983; Gardiner, 1984; Cloutier &

Arratia, 2004; Brazeau, 2009; Friedman & Brazeau, 2010; Choo, 2011; Davis et al., 2012; Zhu et al., 2013; Giles et al., 2015b. Choo's (2011) codes may be reversed for this character, but it is unclear. The coding for Cuneognathus (Friedman & Blom, 2006), Kentuckia hlavini, Krasnoyarichthys and Limnomis is revised from '1' to ?'. The coding for Donnrosenia, Gogosardina, Howqualepis, Masnfieldiscus, Melanecta, Mimipiscis bartrami, M. toombsi, Moythomasia durgaringa, Moy. nitida, Novagonatodus, Stegotrachelus and Woodichthys is revisied from '1' to '0'. The coding for Onychodus is revised from '0' to '1'. The coding for Miguashaia is revised from '-' to '1'. The coding for Moythomasia lineata is revised to '0' (Choo, 2015).)

0 absent
1 present

63. [CH 53; G 45] Dermohyal (Patterson, 1982; Gardiner & Schaeffer, 1989; Lund et al., 1995; Cloutier & Ahlberg, 1996; Coates, 1998; Dietze, 2000; Lund, 2000; Schultze & Cumbaa, 2001; Zhu & Schultze, 2001; Zhu et al., 2001; Lund & Poplin, 2002; Zhu & Yu, 2002; Cloutier & Arratia, 2004; Gardiner et al., 2005; Friedman & Blom, 2006; Zhu et al., 2006; Friedman, 2007; Long et al., 2008; Swartz, 2009; Zhu et al., 2009; Choo, 2011; Xu & Gao, 2011; Xu et al., 2014; 2015; Xu & Zhao, 2016. This region of the cheek is missing in Coccocephalichthys (Poplin, 1974; Poplin & V?ran, 1996), and was presumably removed by Watson (1925) when he first described the specimen. It is unclear from the surviving cast whether a dermohyal and/or accessory operculum were present, and as such this taxon is coded as ???. The presence of a dermohyal is only inferred in Donnrosenia (Long et al., 2008), and the coding for this taxon is revised from ?1? to ??'.)

0 absent
1 present

64. [G 46] Head of dermohyal projects above dorsal margin of operculum (Giles et al., 2015b. The dermohyal is not preserved in Melanecta (Coates, 1998), but it is clear from the surrounding bones that it would not have projected above the dorsal surface of the operculum.)

0 absent
1 present

65. [G 47] Dermohyal (Gardiner et al., 2005; Coates, 1999; Xu & Gao, 2011; Xu et al., 2014. The relevant part of the cheek is not preserved in Donnrosenia (Long et al., 2008), so the coding for this taxon is changed from '1' to '?'.)

0 fused to hyomandibular
1 separate from hyomandibular

66. [G 49] Complete enclosure of spiracle by bones bearing otic and infraorbital canals (Friedman, 2007; Zhu et al., 2009. The position of the spiracular space in Stegotrachelus (Swartz, 2009) is uncertain, so this taxon is coded as '?'. The coding for Moythomasia lineata is revised to '1' (Choo, 2015).)

0 absent
1 present

67. [G 57] Maxilla (Zhu & Yu, 2002; Friedman, 2007; Xu et al., 2014, 2015; Xu & Zhao, 2016.)

0 absent
1 present

68. [G 58] Expanded dorsal lamina of maxilla (Lund et al., 1995; Lund, 2000; Poplin & Lund, 2000; Schultze & Cumbaa, 2001; Zhu & Schultze, 2001; Zhu et al., 2001; Zhu & Yu, 2002; Lund & Poplin, 2002; Cloutier & Arratia, 2004; Zhu et al., 2006; Friedman, 2007; Zhu et al., 2009; Zhu et al., 2013; Giles et al., 2015b.)

0 absent
1 present

69. [G 60] Contribution by maxilla to posterior margin of cheek (Friedman, 2007; Zhu et al., 2009; Zhu et al., 2013; Giles et al., 2015b.)

0 absent
1 present

70. [G 61] Sensory canal/pit line associated with maxilla (Friedman, 2007; Zhu et al., 2009; Zhu et al., 2013.)

0 absent
1 present

71. Teeth on maxilla (Cloutier & Arratia, 2004; Lopez-Arbarello 2011; Xu et al. 2014; Xu et al. 2014, 2015; Xu & Zhao, 2016.)

0 present
1 absent

72. Mobile maxilla in cheek (Gardiner & Schaeffer 1989; Gardiner et al. 1996; Gardiner et al. 2005; Coates 1999; Hurley et al. 2007; Xu & Gao 2011; Xu et al. 2014, 2015; Xu & Zhao, 2016.)
0 absent
1 present

73. Peg-like anterior process of maxilla (Grande 2010; Xu & Wu 2012; Xu et al. 2014.)
0 absent
1 present

74. Posterior maxillary notch (Grande & Bemis 1998; Xu & Wu 2012; Xu et al. 2014, 2015. Arratia 2013; Xu & Zhao, 2016.)
0 absent
1 present

75. Supramaxilla (Gardiner & Schaeffer 1989; Gardiner et al. 1996; Gardiner et al. 2005; Coates 1999; Hurley et al. 2007; Xu & Gao 2011; Xu et al. 2014, 2015; Xu & Shen, 2015; Xu & Zhao, 2016.)
0 absent
1 one
2 two

76. [CH 21; G 63] Course of mandibular canal (Friedman & Blom, 2006; Long et al., 2008; Swartz, 2009; Choo, 2011. The coding for Moythomasia lineata is revised to '0' (Choo, 2015).)
0 traces ventral margin of jaw along entire length
1 arches dorsally in anterior half of jaw

77. [G 64] Mandibular canal reaches anterior margin of mandible (Giles et al., 2015b. The mandibular canal is reconstructed as reaching the anterior margin of the dentary in Cuneognathus (Friedman & Blom, 2006), but specimen photos appear to show it leaving through the dorsal margin. As such, this taxon is coded '1' for this character.)
0 present
1 absent

78. [CH 74; G 65] Mandibular canal (Patterson, 1982; Cloutier & Ahlberg, 1996; Coates, 1998; Schultze & Cumbaa, 2001; Zhu & Schultze, 2001; Zhu et al., 2001; Zhu & Yu, 2002; Cloutier & Arratia, 2004; Zhu et al., 2006; Friedman, 2007; Zhu et al., 2009; Choo, 2011; Zhu et al., 2013. The coding for Moythomasia lineata is revised to '1' (Choo, 2015).)
0 primarily carried by infradentaries
1 primarily carried by dentary

79. [G 66] Relative length of dentary (Ahlberg & Johanson, 1998; Zhu et al., 2001; Zhu & Yu, 2002; Zhu & Ahlberg, 2004; Friedman, 2007; Zhu et al., 2009.)
0 long (constitutes most of the length of the lower jaw)
1 short (constitutes less than half of jaw length)

80. Teeth on dentary (Cloutier & Arratia 2004, Xu et al. 2014.)
0 present
1 absent

81. [CH 22; G 67] Dentary with conspicuously reflexed distal tip (Friedman & Blom, 2006; Long et al., 2008; Swartz, 2009; Choo, 2011. The anterior extent of the dentary is not preserved in Limnomis (Daeschler, 2000), so the coding for this taxon is revised from '1' to '?'.)
0 absent
1 present

82. [CH 24; G 68] Enlarged series of parasymphysial teeth on dentary (Friedman & Blom, 2006; Long et al., 2008; Swartz, 2009; Choo, 2011. Choo's (2011) codes for this character appear reversed. The anterior extent of the dentary is not preserved in Limnomis (Daeschler, 2000), so the coding for this taxon is revised from '1' to '?'.)
0 absent
1 present

83. [CH 73; G69] Facet for parasymphysial tooth-whorl on anterior dentary (Choo, 2011. The anterior extent of the dentary is not preserved in Limnomis (Daeschler, 2000), so the coding for this taxon is revised from '1' to '?'.)
0 present
1 absent

84. [G 70] Teeth of outer dental arcade (Friedman, 2007. Coates (1998) states that the maxilla of Melanecta bears large teeth interspersed with smaller teeth, but it is unclear how these teeth are arranged. As such, this taxon is coded '?'.)

0 several rows of disorganized teeth
1 two rows, with large teeth lingually and small teeth labially
2 single row of teeth

85. Jaw margins overlain by lateral lamina (New character. In Styracopterus, Fouldenia and Amphicentrum, a lateral lamina of bone obscures the maxillary dentition (Sallan & Coates 2013).)
0 absent
1 present

86. [CH 25; G 71] Acrodin caps on teeth (Patterson, 1982; Gardiner, 1984; Maisey, 1986; Gardiner & Schaeffer, 1989; Cloutier & Ahlberg, 1996; Taverne, 1997; Coates, 1999; Poplin & Lund, 2000; Schultze & Cumbaa, 2001; Zhu & Schultze, 2001; Zhu et al., 2001; Zhu & Yu, 2002; Cloutier & Arratia, 2004; Gardiner et al., 2005; Friedman & Blom, 2006; Zhu et al., 2006; Friedman, 2007; Long et al., 2008; Zhu et al., 2009; Friedman & Brazeau, 2010; Choo, 2011; Xu & Gao, 2011; Zhu et al., 2013; Xu et al., 2014; Giles et al., 2015b. The presence of acrodin in Limnomis (Daeschler, 2000), Mansfieldiscus (Long, 1988), Melanecta (Coates, 1998) and Woodichthys (Coates, 1998) is uncertain, and the coding for these taxa is revised from '1' to '?'.)
0 absent
1 present

87. Plicidentine (Zhu & Yu 2002; Friedman 2007; Lopez-Arbarello 2011.)
0 absent
1 present

88. [CH 27; G 73] Ossification of mentomeckelian region: (Friedman & Blom, 2006; Long et al., 2008; Swartz, 2009; Grande 2010; Choo, 2011; Xu et al., 2014.)
0 present
1 absent

89. [CH 23; G 76] Number of infradentaries (Friedman & Blom, 2006; Friedman, 2007; Long et al., 2008; Choo, 2011; Xu & Gao, 2011; Xu et al., 2014. The coding for Kentuckia hlavini (Dunkle, 1964) and Guiyu (Zhu et al., 2009) is revised from '0' to '?'. The coding for Limnomis (Daeschler, 2000) and Stegotrachelus (Swartz, 2009) is revised from '1' to '?'. The coding in Mansfieldiscus (Long, 1988) is revised from '0' to '2'. The coding for Moythomasia lineata is revised to '1' (Choo, 2015).H07:)
0 more than two
1 two (angular and surangular)
2 one (angular only)

90. [G 74] Coronoids (sensu stricto, excluding parasymphysial tooth whorl or anterior coronoid) (Schultze and Cumbaa, 2001; Zhu and Schultze, 2001; Zhu et al., 2001; Zhu and Yu, 2002; Zhu et al., 2006; Friedman, 2007; Zhu et al., 2009.)
0 present
1 absent

91. [G 75] Number of coronoids (Ahlberg & Clack, 1998; Daeschler et al., 2006; Long et al., 2006; Friedman, 2007; Zhu et al., 2009; Zhu et al., 2013; Giles et al., 2015b. A single specimen of Pteronisculus stensioi has at least five or six coronoids anterior to the prearticular region. However, these appear to correspond to the three coronoids present in most specimens, so the taxon is coded here as '2'. Two coronoids are reported in Boreosomus (Nielsen, 1942).)
0 five
1 four or more
2 three
3 two
4 one

92. [G 76] Posterior coronoid (Cloutier & Ahlberg, 1996; Ahlberg & Johanson, 1998; Zhu & Ahlberg, 2004; Daeschler et al., 2006; Long et al., 2006.)
0 morphologically similar to anterior coronoids
1 expanded

93. [G 78] Coronoid process of lower jaw (Gardiner & Schaeffer 1989; Zhu & Yu, 2002; Friedman, 2007; Friedman, 2007; Xu & Gao 2011; Xu et al. 2014, 2015; Xu & Zhao, 2016.)
0 absent
1 present

94. Coronoid process contributed to by (Modified from Gardiner et al. 2005.)
0 prearticular only
1 surangular only
2 dentary plus postdentary bones
3 angular only

95. Leptolepid notch (Arratia 2013. A distinct notch in the posterior margin of the dentary is seen in taxa such as Leptolepis.)
0 absent
1 present

96. Symplectic involvement in jaw joint (Grande & Bemis 1998; Grande 2010; Xu & Wu 2012; Xu et al. 2014, 2015; Lopez-Arbarello 2011; Xu & Zhao, 2016.)
0 absent
1 present

97. [G 79] Retroarticular process (Friedman, 2007.)
0 present
1 absent

98. Palatal bite
0 absent
1 present

99. [G 82] Palatal articulation with basipterygoid process (Revised from Friedman, 2007; Brazeau, 2009; Zhu et al., 2009; Friedman & Brazeau, 2010; Davis et al., 2012; Zhu et al., 2013; Giles et al., 2015b. This character is expanded from previous formulations, which only considered whether a basipterygoid fenestra was absent or present. Where a basipterygoid process is absent, the dorsal margin of the palate may be flat, or the metapterygoid may bear a distinct notch.)
0 articulation not obvious
1 via basipterygoid fenestra
2 via metapterygoid process/notch

100. Palatoquadrate ossifications
0 comineralized
1 separate ossification centers

101. Lateral process of ectopterygoid (New character.)
0 absent
1 present

102. Palatoquadrate symphysis hf30 (This character captures whether the palatoquadrates contact at the midline.
)
0 absent
1 present

103. Dorsal margin of palate
0 high posterior extension
1 flat dorsal margin

104. Metapterygoid posterior to quadrate
0 absent
1 present

105. [G 81] Number of dermopalatines (Friedman, 2007.)
0 multiple
1 single

106. Prearticular
0 present
1 absent

107. Vomers (Lopez-Arbarello 2011; Arratia 2013; Xu & Wu, 2012; Xu & Zhao, 2016.)
0 paired
1 single

108. Vomer sutured to parasphenoid (Hurley et al. 2007.)
0 absent
1 present

109. [CH 19; G 50] Accessory operculum (Schultze & Cumbaa, 2001; Cloutier & Arratia, 2004; Friedman & Blom, 2006; Long et al., 2008; Swartz, 2009. This region of the cheek was removed in Coccocephalichthys (Poplin, 1974; Poplin & V?ran, 1996), presumably by Watson (1925) when he first described the specimen. It is unclear from the surviving cast whether a dermohyal and/or accessory operculum were present, and as such this taxon is coded as ???.)
0 absent
1 present

110. [CH 67; G 51] Operculum - relative size (Modified from Lund et al., 1995; Lund, 2000; Lund & Poplin, 2002; Cloutier & Arratia, 2004; Long et al., 2008; Swartz, 2009; Choo, 2011; Xu et al., 2015; Xu & Zhao, 2016Xu & Zhao, 2015. . The coding in Osorioichthys (Taverne, 1997), Mansfieldiscus (Long, 1988), Melanecta (Coates, 1988), Moythomasia nitida (Jessen, 1968), Novagonatodus (Long, 1988; Holland et al., 2007), Woodichthys (Coates, 1998), Cuneognathus (Friedman & Blom,

1006) and Krasnoyarichthys (Prokofiev, 2002) is revised from ?0? to ?1?. The coding in Howqualepis (Long, 1988), Donnrosenia (Long et al., 2008) and Limnomis (Daeschler, 2000) is revised from ?1? to ?0?.)

0 at least twice as high as suboperculum
1 subequal
2 smaller than suboperculum

111. Subopercle (Xu et al. 2014.)

0 present
1 absent

112. [CH 68; G 52] Anterodorsal process of suboperculum (Long et al., 2008; Choo, 2011; Lopez-Arbarello 2011. The coding in Howqualepis (Long, 1988) and Donnrosenia (Long et al., 2008) is changed from '0' to '1'. The anterodorsal process is described as well developed in Gogosardina (Choo et al., 2009), and the coding for this taxon is revised from '?' to '1'. An anterodorsal process is also present in 'semionotiforms'. Although these processes do not appear to be homologous they are coded within the character.)

0 absent
1 present

113. Anteroventral process of suboperculum

0 absent
1 present

114. [G 62] Number of cheek bones bearing pre-opercular canal posterior to jugal (Friedman, 2007; Zhu et al., 2009; Zhu et al., 2013; Xu & Zhao, 2016.)

0 one
1 multiple
2 series of small ossicles

115. Preoperculum orientation (Modified from Gardiner et al., 2005; Swartz 2009. This character is reformulated from its original (compound) formulation, which considered both maxilla and preoperculum shape. Primitively in actinopterygians the preoperculum is wholly or partially developed dorsal to the maxilla as an anterodorsal-posteroventrally oriented bone, either with (e.g. Mimipiscis, Moythomasia) or without (e.g. Cheirolepis) a dorsoventrally oriented limb. The preoperculum may also be near-vertical, with no distinct anterodorsal or anteroventral extensions (e.g. Boreosomus, Peltopleurus), or developed as an anteroventral-posterodorsally-directed bone largely ventral to the maxilla (e.g. Discoserra, Propterus).)

0 prounounced dorsal limb
1 vertical
2 pronounced ventral limb

116. Junction between preopercular and more anterior cheek bones (Modified from Lopez-Arbarello 2011.)

0 Infraorbitals (including jugal) or suborbitals suture with or abut preopercular
1 Infraorbitals (including jugals) and suborbitals broadly overlap preopercular
2 completely obscure

117. Posterior border of preopeculum notched ventrally (Lopez-Arbarello 2011.)

0 absent
1 present

118. Interopercle (Gardiner & Schaeffer 1989; Xu & Gao 2011; Xu et al. 2014, 2015. Gardiner & Schaeffer 1989; Olsen & McCune 1991; Gardiner et al. 1996; Gardiner et al. 2005; Cavin & Suteethorn 2006; Hurley et al. 2007; Lopez-Arbarello 2011; Xu & Zhao, 2016.)

0 absent
1 present

119. [CH 72; G 53] Branchiostegal rays - dorsal-most in series (Lund et al., 1995; Cloutier & Arratia, 2004; Choo, 2011. The coding for Mimipiscis bartrami, M. toombsi (Gardiner, 1984, Choo, 2011), Stegotrachelus (Swartz, 2009), Cheirolepis canadensis (Arratia & Cloutier, 1996), C. schulzei (Arratia & Cloutier, 2004), C. trailli (Pearson & Westoll, 1979) Donnrosenia (Long et al., 2008), Gogosardina (Choo et al., 2009), Howqualepis rostridens (Long, 1988), Novagonatodus (Long, 1988; Holland et al., 2007), Mansfieldiscus (Long, 1988) and Woodichthys (Coates, 1998) is revised from ?1? to ?0?. The coding for Cuneognathus (Friedman & Blom, 2006), Kentuckia hlavini (Dunkle, 1964) and Melanecta (Coates, 1998) is revised from ?1? to ???. The coding for Krasnoyarichthys (Prokofiev, 2002) is changed from ??? to ?1?.)

0 of similar depth to adjacent branchiostegal ray
1 deeper than adjacent branchiostegal ray

120. Lateral gulars (Xu et al., 2014.)
0 present
1 absent

121. [CH 20; G 54] Lateral gulars (Gardiner & Schaeffer, 1989; Cloutier & Ahlberg, 1996; Taverne, 1997; Lund & Poplin, 1997; Coates, 1999; Schultze & Cumbaa, 2001; Zhu & Schultze, 2001; Cloutier & Arratia, 2004; Friedman & Blom, 2006; Long et al., 2008; Swartz, 2009; Brazeau, 2009; Xu & Gao, 2011; Davis et al., 2012; Zhu et al., 2013; Xu et al., 2014; Giles et al., 2015b. The coding for Mansfieldiscus (Long, 1988) is revised from ??? to ?1?. The condition in Boreosomus (Nielsen, 1942) is unique: instead of lateral gulars flanking a median gular, there appears to be a second median gular. This may well represent a fusion of the two, longer lateral gulars, is coded as such. The coding for Moythomasia lineata is revised to '0' (Choo, 2015).)
0 extending most of the length of the lower jaw
1 restricted to the anterior third of the lower jaw (no longer than the width of three branchiostegals)

122. [G 55] Median gular (Lund et al., 1995; Cloutier & Ahlberg, 1996; Coates, 1999; Lund, 2000; Schultze & Cumbaa, 2001; Zhu & Schultze, 2001; Zhu et al., 2001: Lund & Poplin, 2002; Zhu & Yu, 2002; Cloutier & Arratia, 2004; Zhu et al., 2006; Friedman, 2007; Zhu et al., 2009; Xu & Gao, 2011; Zhu et al., 2013; Xu et al., 2014, 2015; Giles et al., 2015b; Xu & Zhao, 2015. Pearson & Westoll (1979: p. 365) state that a median gular is not known in Cheirolepis canadensis. Although a median gular is reconstructed by Cloutier & Arratia (1996: fig. 7), this bone is not present in any specimen photos and is not mentioned in the text. As such, this taxon is coded as ???.)
0 absent
1 present

123. [G 56] Relative length of median gular (Giles et al., 2015b. The condition in Boreosomus (Nielsen, 1942) is unique: instead of lateral gulars flanking a median gular, there appears to be a second median gular. This may well represent a fusion of the two, longer lateral gulars, and is coded as such.)
0 much shorter than jaw length
1 more than half of law length

124. [G 83] Fenestra ventrolateralis (Schultze & Cumbaa, 2001; Zhu & Schultze, 2001; Zhu et al., 2001; Zhu & Yu, 2002; Zhu et al., 2006; Friedman, 2007; Zhu et al., 2009; Zhu et al., 2013.)
0 absent
1 present

125. [G 84] Palatal opening surrounded by premaxilla, maxilla, dermopalatine and vomer (choana) (Zhu & Yu, 2002; Friedman, 2007. Character can only be coded in taxa which possess all of these bones.)
0 absent
1 present

126. [G 85] Internasal cavity (Ahlberg & Johanson, 1998; Zhu & Yu, 2002; Zhu & Ahlberg, 2004; Daeschler et al., 2006; Long et al., 2006; Friedman, 2007; Zhu et al., 2009; Zhu et al., 2013; Giles et al., 2015b.)
0 absent
1 present

127. [G 86] Interorbital septum (Friedman, 2007; Zhu et al., 2009; Brazeau, 2009; Friedman & Brazeau, 2010; Davis et al., 2012; Zhu et al., 2013; Giles et al., 2015b. Cheirolepis trailli is coded '0' (Giles et al., 2015a).)
0 broad
1 narrow

128. Optic foramen (New character. ?Primitively in actinopts, the optic nerve exits the cranial cavity into the orbit through paired foramina approximately halfway up the orbital wall. In many Carboniferous and younger taxa, much of the orbital wall is unossified (the optic fenestra). The optic nerves may exit through openings just posterior to (e.g. Pteronisculus) or confluent with (e.g. Pholidophorus) the optic fenestra. In polypterids and Fukangichthys, the optic nerve exits ventrally through paired foramina that abut the parasphenoid.")
0 dorsally positioned
1 ventrally positioned (i.e. abuts parasphenoid)

129. [G 87] Pronounced median anterior crista on dorsal surface of braincase (Giles et al., 2015b.

Carboniferous and younger actinopts such as Lawrenciella (Hamel & Poplin, 2008) have a median crista anterior to the anterior dorsal fontanelle upon which the skull roof sits.)

0 absent
1 present

130. [G 88] Expanded anterior dorsal fontanelle (Giles et al., 2015b. The anterior dorsal fontanelle of many Carboniferous and younger actinopts is greatly expanded, in contrast to the smaller fontanelle of Devonian taxa such as Mimipiscis (Gardiner, 1984).)

0 absent
1 present

131. [G 89] Endoskeletal intracranial joint (Cloutier & Ahlberg, 1996; Ahlberg & Johanson, 1998; Zhu & Ahlberg, 2004; Zhu et al., 2001; Zhu & Yu, 2002; Daeschler et al., 2006; Long et al., 2006; Friedman, 2007; Brazeau, 2009; Zhu et al., 2009; Friedman & Brazeau, 2010; Davis et al., 2013; Zhu et al., 2013; Giles et al., 2015b. Cheirolepis trailli is coded '0' (Giles et al., 2015a).)

0 absent
1 present

132. [G 90] Eye stalk or unfinished area for similar structure (Zhu & Schultze, 2001; Zhu et al., 2001; Zhu & Yu, 2002; Zhu et al., 2006; Friedman, 2007; Zhu et al., 2009; Zhu et al., 2013; Giles et al., 2015b. This character is coded as absent for taxa that possess a large interorbital fenestra (e.g. Pteronisculus, Coccocephalichthys, Kentuckia deani), as, if present, the eyestalk area would be visible posterior to the opening for the optic nerve.)

0 absent
1 present

133. [G 91] Roof of posterior myodome perforated by palatine branch of facial nerve (VII) (Coates, 1999.)

0 absent
1 present

134. [G 92] Foramen for abducens nerve (VI) dorsally positioned (level with optic foramen (II)) (Coates, 1999.)

0 absent
1 present

135. [G 93] Anterodorsal myodome (Coates, 1999; Gardiner et al. 1996; Hurley et al. 2007; Xu & Gao, 2011; Xu et al., 2014, 2015; Xu & Zhao, 2016.)

0 paired
1 single
2 absent

136. [G 94] Posterior myodome (Modified from Coates, 1999; Xu et al., 2014. Wiley 1976; Gardiner, 1984; Gardiner & Schaeffer, 1989; Gardiner et al. 1996; Hurley et al. 2007; Lopez-Arbarello 2011; Xu & Gao, 2011; Xu et al. 2014, 2015; Xu & Zhao, 2016.)

0 absent
1 paired
2 median

137. [G 96] Basicranial fenestra (Ahlberg & Johanson, 1998; Zhu et al., 2001; Zhu & Yu, 2002; Zhu & Ahlberg, 2004; Friedman, 2007; Zhu et al., 2009; Zhu et al., 2013; Giles et al., 2015b. Cheirolepis trailli is coded '0' (Giles et al., 2015a).)

0 absent
1 present

138. [G 98] Endoskeletal spiracular canal (Patterson, 1982; Gardiner, 1984; Gardiner & Schaeffer, 1989; Taverne, 1997; Coates, 1999; Gardiner et al., 2005; Xu & Gao, 2011; Xu et al., 2014. Taxa that lack a groove on the lateral commissure are coded as inapplicable for this character. . Following Xu et al. (2014), the spiracle in Moythomasia durgaringa is coded '1'. Cheirolepis trailli is coded '0' (Giles et al., 2015a).)

0 open
1 partial closure of spiracular bar
2 complete enclosure in canal

139. [G 100] Basipterygoid process (Gardiner et al., 2005; Xu & Gao, 2011; Xu et al., 2014, 2015; Xu & Zhao, 2016.))

0 present
1 absent

140. [G 101] Basipterygoid process with vertically oriented component (Ahlberg & Johanson, 1998; Zhu & Schultze, 2001; Zhu et al., 2001; Zhu & Yu, 2002; Zhu & Ahlberg, 2004; Zhu et al., 2006; Friedman, 2007; Zhu et al., 2009; Davis et al., 2012; Zhu et al., 2013; Giles et al., 2015b.)

0 absent
1 present

141. [G 103] Dermal component to basipterygoid process (Gardiner, 1984; Gardiner & Schaeffer, 1989; Taverne, 1997; Coates ,1999.)
0 absent
1 present

142. Hyoid facet (Gardiner et al. 2005; Gardiner et al. 1996; Hurley et al. 2007; Xu & Gao 2011; Xu et al. 2015.)
0 directed posteroventrally
1 horizontal

143. [G 104] Fossa bridgei (Gardiner, 1984; Gardiner & Schaeffer, 1989; Taverne, 1997; Coates, 1999; Xu & Gao, 2011; Xu et al., 2014. Cheirolepis trailli is coded '0' (Giles et al., 2015a).)
0 absent
1 present

144. [G 105] Posttemporal fossae (Zhu & Yu, 2002; Friedman, 2007.)
0 absent
1 present

145. [G 106] Vestibular fontanelle (Friedman, 2007; Brazeau, 2009; Zhu et al., 2009; Friedman & Brazeau, 2010; Davis et al., 2012; Zhu et al., 2013; Brazeau & Friedman, 2014; Giles et al., 2015b. Cheirolepis trailli is coded '1' (Giles et al., 2015a).)
0 absent
1 present

146. [G 107] Ventral cranial fissure and vestibular fontanelle (Coates, 1999. We follow Coates (1999) in coding Howqualepis as '0' on the basis of Long 1988 fig. 16 and AMF65495 (pers. obs. S.G.), rather than the braincase reconstruction (Long, 1988: fig. 18). Cheirolepis trailli is coded '0' (Giles et al., 2015a).)
0 separated by bridge of bone
1 conflUent

147. [G 108] Accessory fenestration in otic capsule (Friedman, 2007; Zhu et al., 2009. Cheirolepis trailli is coded '0' (Giles et al., 2015a).)
0 absent
1 present

148. [G 109] Otoccipital fissure (Friedman, 2007; Brazeau, 2009; Davis et al., 2012; Zhu et al., 2013; Giles et al., 2015b. Cheirolepis trailli is coded '1' (Giles et al., 2015a).)
0 absent
1 present

149. [G 110] Median projection overhanging posterior part of posterior dorsal fontanelle (Giles et al., 2015b. Variable in Boreosomus: the posterior dorsal fontanelle is closed in the specimen figured in Nielsen (1942: plate 25F), but developed in the specimen figured in plate 28. This taxon is coded ?0/1? to reflect this polymorphism.)
0 absent
1 present

150. [G 111] Median projection overhanging anterior part of posterior dorsal fontanelle (Giles et al., 2015b. This projection is somewhat reduced in Pteronisculus (Nielsen, 1942), but is coded '1' here. Variable in Boreosomus: the posterior dorsal fontanelle is closed in the specimen figured in Nielsen 1942 plate 25F, but developed in the specimen figured in plate 28. This taxon is coded ?0/1? to reflect this polymorphism. Cheirolepis trailli is coded '0' (2015a).)
0 absent
1 present

151. [G 112] Dorsal aorta (Coates & Sequeira, 1998; Coates & Sequeira, 2001a, b; Coates, 1999; Friedman, 2007; Zhu et al., 2009; Friedman & Brazeau, 2010; Zhu et al., 2013; Giles et al., 2015b. This character is coded as inapplicable in taxa that lack a canal for the dorsal aorta. Cheirolepis trailli is coded '0' (Giles et al., 2015a). The aortic canal of Moythomasia is not figured by Gardiner (1984), but a clear posterior notch in the aortic canal can be seen in Long & Trinajstic (2010:fig 5b). The neurocranium of Gogosardina is not yet described, but this character can be coded on the basis of Choo et al. (2009: fig. 9).)
0 open in groove
1 canal notched posteriorly
2 completely enclosed in canal

152. [G 113] Dorsal aorta pierced by canal/s for exit of eff.a.2 (Giles et al., 2015b. In Mimipiscis bartrami and M. toombsi, a groove for one of the efferent branchial arteries branches off from the

lateral dorsal aorta immediately before the articular area for the first infrapharyngobranchial. However, it is uncertain which, so both taxa coded as '?' for these characters. The neurocranium of Gogosardina is not yet described, but this character can be coded on the basis of Choo et al. (2009: fig. 9).)

0 absent
1 present

153. [G 114] Dorsal aorta pierced by canal/s for exit of eff.a.1 (Giles et al., 2015b. In Mimipiscis bartrami and M. toombsi, a groove for one of the efferent branchial arteries branches off from the lateral dorsal aorta immediately before the articular area for the first infrapharyngobranchial. However, it is uncertain which, so both taxa coded as '?' for these characters. The neurocranium of Gogosardina is not yet described, but this character can be coded on the basis of Choo et al. (2009: fig. 9).)

0 absent
1 present

154. [G 115] Bifurcation of dorsal aorta (Coates & Sequeira, 1998; Coates & Sequeira, 2001a, b; Coates, 1999; Friedman, 2007; Zhu et al., 2009; Friedman & Brazeau, 2010; Zhu et al., 2013; Giles et al., 2015b.)

0 posterior to occiput
1 anterior to occiput

155. [G 116] Birfurcation of dorsal aorta into lateral dorsal aortae (Coates, 1999. This character is coded as inapplicable in taxa that lack a canal for the dorsal aorta. In Mimipiscis toombsi, the bifurcation point of the dorsal aorta can be open (Giles & Friedman, 2014: fig. 2) or closed (Gardiner 1984: fig. 15). This taxon is coded '0/1' to reflect this polymorphism. The aortic canal of Moythomasia is not figured by Gardiner (1984), but the bifucation into the lateral dorsal aortae can be seen in Long & Trinajstic (2010:fig 5b).)

0 open
1 enclosed in canal

156. Braincase ossifications differentiated (New character.)

0 absent
1 present

157. Basisphenoid (Wiley 1976; Lopez-Arbarello 2011.)

0 present
1 absent or very reduced

158. Opisthotic-pterotic relationship (Gardiner et al. 1996; Hurley et al. 2007. This character can only be coded when separate braincase ossifications can be identified.)

0 opisthotic larger than subotic
1 opisthotic and pterotic equal in size

159. Epioccipital (Hurley et al. 2007. This character can only be coded when separate braincase ossifications can be identified.)

0 present
1 absent

160. Forward extension of the exoccipital around the vagus nerve (Olsen & McCune 1991; Gardiner et al. 1996; Cavin & Suteethorn 2006; Hurley et al. 2007; Lopez-Arbarello 2011. This character can only be coded when separate braincase ossifications can be identified.)

0 absent
1 present

161. Spenotic with small dermal component (Grande 2010; Lopez-Arbarello 2011; Xu & Wu 2012; Xu et al. 2014, 2015; Arratia 2013; Xu & Zhao, 2016. This character can only be coded when separate braincase ossifications can be identified.)

0 absent
1 present

162. Pterotic (Gardiner et al. 1996; Grande & Bemis, 1998; Hurley et al. 2007; Xu et al. 2014; Xu & Shen, 2015; Xu & Zhao, 2016. This character can only be coded when separate braincase ossifications can be identified.)

0 present
1 absent

163. Opisthotic bone (Wiley 1976; Cavin & Suteethorn 2006; Hurley et al. 2007; Grande 2010; Lopez-Arbarello 2011; Xu et al., 2014, 2015; Xu & Zhao, 2016. This character can only be coded when separate braincase ossifications can be identified.))

0 present
1 absent

164. Intercalar (Olsen 1994; Gardiner et al. 1996; Lopez-Arbarello 2011; Xu et al. 2014; Xu & Shen,

2015; Xu & Zhao, 2016. This character can only be coded when separate braincase ossifications can be identified.)

0 present
1 absent

165. Supraoccipital bone (Grande 2010; Xu et al. 2014, 2015; Xu & Zhao, 2016. This character can only be coded when separate braincase ossifications can be identified.)

0 absent
1 present

166. Membranous outgrowth of intercalar (Gardiner et al. 1996; Hurley et al. 2007. This character can only be coded when separate braincase ossifications can be identified.)

0 absent
1 present

167. Post-temporal fossa (Gardiner, 1984; Gardiner & Schaeffer, 1989; Coates, 1999; Hurley et al. 2007; Lopez-Arbarello 2011; Xu & Gao, 2011; Xu et al. 2014, 2015; Xu & Zhao, 2016.)

0 absent
1 present

168. Sub-temporal fossa (Gardiner, 1984; Gardiner & Schaeffer, 1989; Gardiner et al. 1996; Hurley et al. 2007; Xu & Gao, 2011; Xu et al. 2014, 2015; Xu & Zhao, 2016.))

0 absent
1 present

169. Dilatator fossa (Gardiner, 1984; Gardiner & Schaeffer, 1989; Coates, 1999; Gardiner et al. 1996; Hurley et al. 2007; Xu & Gao, 2011; Xu et al. 2014, 2015; Xu & Zhao, 2016.))

0 absent
1 present

170. [G 117] Parasphenoid (Gardiner, 1984; Brazeau, 2009; Davis et al., 2012; Zhu et al., 2013; Giles et al., 2015b.)

0 absent
1 present

171. [G 118] Parasphenoid (Coates, 1999; Zhu & Yu, 2002; Gardiner et al., 2005; Friedman, 2007, Xu & Gao, 2011; Xu et al., 2014, 2015; Xu & Zhao, 2016. Cheirolepis trailli is coded '0' (Giles et al., 2015a).)

0 terminates at/anterior to ventral otic fissure
1 extends across ventral otic fissure
2 extends to basioccipital

172. [CH 28; G 120] Ascending process of the parasphenoid (Patterson, 1982; Coates, 1999; Dietze, 2000; Schultze & Cumbaa, 2001; Zhu & Schultze, 2001; Cloutier & Arratia, 2004; Gardiner et al., 2005; Friedman & Blom, 2006; Zhu et al., 2006; Zhu et al., 2009; Choo, 2011; Xu & Gao, 2011; Zhu et al., 2013; Xu et al., 2014; Giles et al., 2015b. The coding in Wendichthys (Lund & Poplin, 1997) is revised from '?' to '1'.)

0 absent
1 present

173. [CH 29; G 121] Parasphenoid with multifid anterior margin (Friedman & Blom, 2006; Friedman, 2007; Zhu et al., 2009; Choo, 2011; Zhu et al., 2013; Giles et al., 2015b.)

0 absent
1 present

174. [G 124] Buccohypophyseal canal pierces parasphenoid (Giles et al., 2015b. The buccohypophyseal canal typically enters the dorsal surface of the parasphenoid, but whether it exits via the ventral surface is more variable, and this distribution is captured by this character.)

0 present
1 absent

175. Parasphenoid teeth (Arratia 2013.)

0 small
1 large
2 absent

176. Parasphenoid pierced by internal carotid artery (Gardiner et al. 1996; Hurley et al. 2007; Xu & Wu, 2012; Xu et al., 2015; Xu & Zhao, 2016.)

0 absent
1 present

177. Parasphenoid pierced by efferent pseudobranchial artery (Gardiner et al. 1996; Hurley et al. 2007; Xu & Wu, 2012; Xu et al., 2015; Xu & Zhao, 2016.)

0 absent

1 present

178. Aortic notch in parasphenoid (Modified from Gardiner et al. 2005.)
0 absent
1 present

179. Parabasal canal (Xu and Gao 2011; Xu et al. 2014.)
0 present
1 absent

180. [G 125] Anterolaterally divergent olfactory tracts (Coates, 1999; Giles & Friedman, 2014. Cheirolepis trailli is coded '1' (Giles et al., 2015a).)
0 absent
1 present

181. [G 126] Elongate olfactory tract(s) (Brazeau, 2009; Friedman & Brazeau 2010; Davis et al., 2012; Zhu et al., 2013; Brazeau & Friedman, 2014; Giles & Friedman, 2014; Giles et al., 2015b. Cheirolepis trailli is coded '0' (Giles et al., 2015a). The olfactory tracts of Osorioichthys are elongate (pers. obs. unpubl. scan data S.G.).)
0 absent
1 present

182. [G 127] Olfactory nerves carried in a single tract (Coates, 1999; Giles & Friedman, 2014. Cheirolepis trailli is coded '1' (Giles et al., 2015a). The olfactory nerves are carried in separate tracts in Osorioichthys (pers. obs. unpubl. scan data S.G.).)
0 present
1 absent

183. [G 128] Hypophyseal chamber (Coates, 1999; Xu & Gao, 2011; Xu et al., 2014.)
0 projects posteroventrally
1 projects ventrally or anteroventrally

184. [G 129] Optic lobes (Giles & Friedman, 2014.)
0 narrower than cerebellum
1 same width or wider than cerebellum

185. Optic lobes (Coates 1999; Hurley et al. 2007; Xu et al. 2014.)
0 smaller than telencephalon
1 larger than telencephalon

186. [G 130] Optic tectum divided into bilateral halves (Coates, 1999.)
0 absent
1 present

187. [G 131] Cerebellar corpus (Giles et al., 2015b. The region posterior to the cerebellar auricles in Lawrenciella was considered to be the area octavolateralis by Hamel & Poplin (2005). However, we interpret it as the corpus cerebellum, and this taxon is coded '1'.)
0 absent
1 present

188. Cerebellar corpus (Coates 1999; Hurley et al. 2007; Xu & Gao 2011; Xu et al. 2014.)
0 divided bilaterally
1 undivided

189. Position of cerebellar corpus (Coates 1999; Hurley et al. 2007; Xu & Gao 2011; Xu et al. 2014.)
0 enters fourth ventricle
1 arches above fourth ventricle

190. Cerebellar corpus with median anteriorly projecting portion (Coates 1999; Hurley et al. 2007; Xu & Gao 2011; Xu et al. 2014.)
0 absent
1 present

191. [G 132] Horizontal semicircular canal (Davis et al., 2012; Zhu et al., 2013; Giles & Friedman, 2014; Giles et al., 2015b.)
0 joins vestibular region dorsal to ampulla for the posterior semicircular canal
1 joins vestibular region level with ampulla for the posterior semicircular canal

192. [G 133] Junction between ampulla of posterior semicircular canal and cranial cavity (Giles et al., 2015b. In certain primitive actinopts, such as Mimipiscis (Giles and Friedman, 2014), a short length of canal lies between the posterior ampulla and the remainder of the labyrinth.)
0 separated by short length of canal
1 confluent

193. [G 134] Crus commune of anterior and posterior semicircular canal (Giles & Friedman, 2014.)
0 dorsal to endocranial roof

1 ventral to endocranial roof

194. [G 135] Lateral cranial canal (Gardiner, 1984; Gardiner & Schaeffer, 1989; Coates, 1999; Cloutier & Arratia, 2004; Gardiner et al., 2005; Zhu et al., 2006; Zhu et al., 2009; Zhu et al., 2013; Giles & Friedman, 2014; Xu et al., 2014; Giles et al., 2015b. The presence of a lateral cranial canal in Ligulalepis and Psarolepis is uncertain, but its presence in Meemannia is confirmed following Lu et al. (2016). Erpetoichthys is conservatively coded as '?'.)
0 absent
1 present

195. Lateral cranial canal connects to cranial cavity anteriorly (New character.)
0 absent
1 present

196. [CH 30 in part; G 147] Enameloid on dermal bones and scales (Characters 147-150 form part of an atomisation of the compound characters 'ganoine' (typically defined as a single or multilayer enamel covering) and 'cosmine' (typically defined as a single layer of enamel with a well defined pore canal network) (e.g. Cloutier & Ahlberg, 1996; Ahlberg & Johanson, 1998; Zhu & Ahlberg, 2004; Schultze & Cumbaa, 2001; Zhu & Schultze, 2001; Zhu et al., 2001; Zhu & Yu, 2002; Daeschler et al., 2006; Long et al., 2006; Zhu et al., 2006; Zhu et al., 2009; Davis et al., 2012; Zhu et al., 2013). A similar approach to atomization was taken by Friedman (2007), Brazeau & Friedman (2010) and Giles et al. (2015b). As detailed histological investigations have not been carried out for the majority of early actinopterygians (rather, they have simply been described as being covered in/bearing ridges of ganoine), many of these characters cannot be coded for a number of taxa. Histological data are only known for specimens of Mimipiscis toombsi (Gardiner, 1984; Choo, 2011), so this and the following characters are coded '?' for Mimipiscis bartrami (Gardiner, 1984; Choo, 2011).)
0 absent
1 present

197. [G 148] Extensive pore-canal network (See notes above for c. 147. C. trailli is coded '1' follwing Lu et al. 2016.)
0 absent
1 present

198. [CH 30 in part; G 149] Enamel (See notes above for c. 147.)
0 single-layered
1 multi-layered

199. [CH 30 in part; G 150] Enamel layers (See notes above for c. 147.)
0 applied directly to one another
1 separated by layers of dentine

200. Scales on body
0 present
1 absent

201. [G 151] Scales (Cloutier & Arratia, 2004; Friedman & Blom, 2006; Long et al., 2008; Swartz, 2009; Zhu et al., 2009; Choo, 2011.)
0 micromeric
1 macromeric

202. [CH 32 in part; G 152] Scales with ?peg and socket articulation' (Maisey, 1986; Gardiner & Schaeffer, 1989; Cloutier & Ahlberg, 1996; Coates, 1999; Dietze, 2000; Poplin & Lund, 2000; Schultze & Cumbaa, 2001; Cloutier & Arratia, 2004; Friedman & Blom, 2006; Friedman, 2007; Long et al., 2008; Brazeau, 2009; Swartz, 2009; Zhu et al., 2009; Friedman & Brazeau, 2010; Lopez-Arbarello 2011; Xu & Gao, 2011; Choo, 2011; Davis et al., 2012; Zhu et al., 2013; Xu et al., 2014; Giles et al., 2015b; Xu & Zhao, 2016. This character is coded only for taxa that possess rhombic scales. The coding for Kentuckia hlavini (Dunkle, 1964) is revised from ?1? to ?0?, and the coding for Limnomis (Daeschler, 2000) from ?0? to ?1?. The coding for Cheirolepis trailli (Giles et al., 2015a) is revised from ?0? to ?1?.)
0 absent
1 present

203. [CH 32 in part; G 153] Peg on rhomboid scale (Patterson, 1982; Cloutier & Ahlberg, 1996; Dietze, 2000; Schultze & Cumbaa, 2001; Zhu & Schultze, 2001; Zhu et al., 2001: Zhu & Yu, 2002; Cloutier & Arratia, 2004; Friedman & Blom, 2006; Zhu et al., 2006; Friedman, 2007; Zhu et al., 2009. Although peg-and-socket articulation of is present between the scales of Limnomis (Daeschler, 2000), the nature of the peg is not described. As such, this taxon is conservatively coded '?'. The coding for

Cheirolepis trailli (Giles et al., 2015a) is revised from ??? to ?0?.)
0 narrow
1 broad

204. [CH 33; G 154] Anterodorsal process on scale (Patterson, 1982; Gardiner, 1984; Gardiner & Schaeffer, 1989; Schultze & Cumbaa, 2001; Zhu & Schultze, 2001; Zhu et al., 2001; Zhu & Yu, 2002; Cloutier & Arratia, 2004; Friedman & Blom, 2006; Zhu et al., 2006; Friedman, 2007; Long et al., 2008; Swartz, 2009; Zhu et al., 2009; Choo, 2011; Zhu et al., 2013; Giles et al., 2015b. The coding for Limnomis (Daeschler, 2000) and Cheirolepis trailli (Giles et al., 2015a) is revised from '0' to '1'.)
0 absent
1 present

205. [CH 35; G 155] Scales with well developed pores on surface (Friedman & Blom 2006; Long et al., 2008; Swartz, 2009; Choo, 2011; Xu et al., 2014. Scale crowns of Cheirolepis schultzei (Arratia & Cloutier, 2004) are not preserved, so this and the following scale characters are coded as '?'. The coding for Donnrosenia (Long et al., 2008) is revised from '1' to '0'. Scales from the posterior half of the flank in Wendichthys bear pores on the enamel surface, whereas those from the anterior part of the flank lack these pores (Lund & Poplin, 1997: fig. 6). This taxon is scored '1'.)
0 absent
1 present

206. Small scales below dorsal fin (New character.)
0 absent
1 present

207. [G 158] Lepidotrichia (Friedman, 2007; Brazeau, 2009; Zhu et al., 2009; Friedman & Brazeau, 2010; Davis et al., 2012; Zhu et al., 2013; Brazeau & Friedman, 2014; Giles et al., 2015b.)
0 absent
1 present

208. [CH 37; G 159] Fringing fulcra (Patterson, 1982; Gardiner & Schaeffer, 1989; Coates, 1999; Dietze, 2000; Schultze & Cumbaa, 2001; Cloutier & Arratia, 2004; Friedman & Blom, 2006; Friedman, 2007; Long et al., 2008; Swartz, 2009; Zhu et al., 2009; Choo, 2011; Xu & Gao, 2011; Zhu et al., 2013; Zhu et al., 2013; Xu et al., 2014, 2015; Xu & Zhao, 2016.)
0 absent
1 present

209. [G 139] Double headed hyomandibular (Cloutier & Ahlberg, 1996; Zhu & Schultze, 2001; Schultze & Cumbaa, 2001; Zhu et al., 2001; Zhu & Yu, 2002; Zhu et al., 2006; Friedman, 2007; Zhu et al., 2009; Friedman & Brazeau, 2010; Zhu et al., 2013; Giles et al., 2015b.)
0 absent
1 present

210. [G 140] Perforate hyomandibula (Friedman, 2007; Zhu et al., 2009; Friedman & Brazeau, 2010; Xu & Gao, 2011; Zhu et al., 2013; Brazeau & Friedman, 2014; Xu et al., 2014, 2015; Xu & Zhao, 2016Xu et al., 2014; Xu & Zhao, 2015. Although Long (1988: p.24) mentions the presence of a depression for the hyomandibular nerve in Howqualepis, it is unclear whether this perforated the hyomandibula. This taxon is conservatively coded as '?'. Cheirolepis trailli is coded '0' (Giles et al., 2015a). Following Friedman (2007), we code Onychodus as '0'.)
0 absent
1 present

211. [G 141] Opercular process (Gardiner & Schaeffer, 1989.)
0 absent
1 present

212. [G 136] Ceratohyal (Gardiner et al., 2005; Xu & Gao, 2011; Xu et al., 2014.)
0 single ossification
1 two ossifications

213. [G 137] Anterior ossification of ceratohyal (Revised from Coates, 1999.The character captures whether the ceratohyal (or the anterior ossification if an anterior and posterior ceratohyal are present) is medially constricted (hourglass-shaped) or plate-like in lateral view.)
0 no medial constriction
1 medial constriction (hourglass-shaped)

214. [G 138] Anterior ceratohyal (Coates, 1999. The groove for the afferent hyoidean artery in the

ceratohyal of Gogosardina is visible in Choo 2009 (fig 6).)

0 no groove
1 groove for afferent hyoidean artery

215. [G 144] Interhyal (Davis et al., 2012; Zhu et al., 2013; Giles et al., 2015b.)

0 absent
1 present

216. Symplectic (Gardiner 1984; Gardiner & Schaeffer 1989; Coates 1999; Hurley et al. 2007; Hurley et al. 2007; Xu & Zhao, 2016.Xu & Zhao, 2015 . The general actinopterygian condition of the hyoid arch seems to comprise four ossifications: hyomandibula, ceratohyal (which may be one or two bones), hypohyal, and an intermediate bone between the hyomandibula and ceratohyal termed, variably, the interhyal or symplectic. In some actinopts (e.g. Amia, Lepisosteus, Hiodon, Dorsetichthys, Macrosemionotus, etc), a second intermediate cartilage is present. The history attached to naming these terms is very complex (see Paterson 1973, Patterson 1982, V?ran 1988, Gardiner et al. 1996, etc), and we have tried here to apply a simple, consistent approach. The ossification that forms an intermediary between the hyomandibula and ceratohyal is termed the interhyal. This is primitively present (and in contact with the quadrate), and may be very reduced (e.g. Watsonulus, Elops), or entirely cartilaginous (e.g. Amia, Lepisosteus) in more derived actinopts. The ossification that contacts the hyomandibula (and typically the quadrate), but does not articulate with the ceratohyal, is termed the symplectic. This element may brace the quadrate, and in Watsonulus, Caturus and Amia additionally articulates with the lower jaw. We follow Grande (2010) in identifying the ?symplectic? of Acipenser as the posterior ceratohyal. V?ran (1988) identified a second intermediate ossification in the hyoid arch in a number of ?palaeoniscids?, which she termed a symplectic. This identification has been disputed on the basis of position (e.g. Gardiner et al. 1996). We have seen no evidence (either through visual examination or CT scanning) for a second intermediate hyoid ossification in any specimens of Boreosomus or Pteronisculus. From examination of Coccocephalichthys, we identify the ?symplectic? of V?ran to be the interhyal and the ?interhyal? of V?ran to correspond to the articular. This casts doubt on the presence of a second element, and we have therefore coded Boreosomus, Pteronisculus and Coccocephalicthys as ?0?.)

0 absent
1 present

217. Symplectic shape c68

0 tube/splint like
1 hatchet
2 l-shaped

218. [G 145] Hypohyal (Friedman & Brazeau, 2010; Brazeau & Friedman, 2014; Giles et al., 2015b.)

0 absent
1 present

219. [G 143] Basihyal (Davis et al., 2012; Zhu et al., 2013; Giles et al., 2015b.)

0 absent
1 present

220. [G 146] Gill arches (Giles et al., 2015b.)

0 largely restricted to area under braincase
1 extend far posterior to braincase

221. Number of ceratobranchials (New character.)

0 five
1 four

222. Number of hypobranchials (Grande, 2010; Xu & Wu, 2012; Xu et al., 2014, 2015; Xu & Zhao, 2016.)

0 three
1 four

223. Uncinate processes on epibranchials (Coates, 1999; Xu & Gao, 2011; Xu et al., 2014, 2015; Xu & Zhao, 2016. An uncinate process is a dorsally-directed extension on the epibranchial that articulates with the pharyngobranchial skeleton.)

0 absent
1 present

224. [G 142] Endoskeletal urohyal (Friedman, 2007; Friedman & Brazeau, 2010; Giles et al., 2015b.)

0 absent
1 present

225. Urohyal formed as a tendon bone of the sternohyoideus muscle (Arratia 2013.)
0 absent
1 present

226. [CH 39; G 162] Presupracleithrum (Patterson, 1982; Gardiner, 1984; Gardiner & Schaeffer, 1989; Taverne, 1997; Lund, 2000; Schultze & Cumbaa, 2001; Zhu & Schultze, 2001; Zhu et al., 2001; Lund & Poplin, 2002; Zhu & Yu, 2002; Cloutier & Arratia, 2004; Gardiner et al., 2005; Friedman & Blom, 2006; Zhu et al., 2006; Friedman, 2007; Long et al., 2008; Swartz, 2009; Zhu et al., 2009; Choo, 2011; Xu & Gao, 2011; Zhu et al., 2013; Xu et al., 2014. Presence of a presupracleithrum is only inferred in Donnrosenia (Long et al., 2008), Gogosardina (Choo et al., 2009) and Kentuckia hlavini (Dunkle, 1964), and the coding for these taxa is revised from ?1? to ???. Similarly, absence is inferred in Krasnoyarichthys (Prokofiev, 2002) and Novagonatodus (Long, 1988; Holland et al., 2007), and the coding is thus changed from '0' to '?'. An elongate bone termed the 'anocleithrum' is variably present in Wendichthys (Lund & Poplin, 1997) in the position occupied by the presupracleithrum in other taxa. We regard this as a positional homologue, and code the taxon '0/1' to reflect this polymorphism. Coded as '?' in C. trailli following arguments in Friedman & Blom (2006). The coding is revised to '0' in Osorioichthys (Taverne, 1997). The coding for Moythomasia lineata is revised to '1' (Choo, 2015).)
0 absent
1 present

227. Presupracleithrum (Xu et al. 2014.)
0 single
1 multiple

228. [G 160] Dorsal margin of cleithrum (Cloutier & Ahlberg, 1996; Schultze & Cumbaa, 2001; Zhu & Schultze, 2001; Zhu et al., 2001; Zhu & Yu, 2002; Cloutier & Arratia, 2004; Zhu et al., 2006; Friedman, 2007; Zhu et al., 2009; Giles et al., 2015b.)
0 pointed
1 broad and rounded

229. Medial wing on cleithrum (Cavin & Suteethorn 2006.)
0 absent
1 present

230. [G 161] Anocleithrum (Gardiner & Schaeffer, 1989; Lund et al., 1995; Cloutier & Ahlberg, 1996; Dietze, 2000; Poplin & Lund, 2000; Schultze & Cumbaa, 2001; Zhu & Schultze, 2001; Zhu et al., 2001; Zhu & Yu, 2002; Cloutier & Arratia, 2004; Zhu et al., 2006; Friedman, 2007; Zhu et al., 2009; Zhu et al., 2013.)
0 bone developed as postcleithrum
1 bone developed as anocleithrum sensu stricto
2 bone absent

231. Clavicle (Coates 1999; Xu & Gao 2011; Xu et al. 2014; Xu & Zhao, 2016.)
0 present as a broad plate
1 much reduced or absent

232. Serrated organ (Arratia 2013. The serrated organ (or appendage) is a small, elongate element, typically ornamented with serrated ridges, present near the anterior margin of the cleithrum.)
0 absent
1 present

233. Interclavicle (Cloutier & Arratia, 2004; Xu et al., 2014.)
0 present
1 absent

234. [CH 40; G 167] Triradiate scapulocoracoid (Zhu & Schultze, 2001; Zhu et al., 2001; Zhu & Yu, 2002; Zhu et al., 2006; Friedman, 2007; Zhu et al., 2009; Xu & Gao, 2011; Zhu et al., 2013; Xu et al., 2014. The endoskeletal shoulder girdle is only described for Mimipiscis toombsi, so the coding for this character is revised from '?' for M. bartrami (Gardiner, 1984; Choo, 2011). The precise morphology of the scapulocoracoid is not known for Cheirolepis canadensis (Arratia & Cloutier, 1996) or Gogosardina (Choo et al., 2009), and as such the coding for these taxa is changed from ?0? to ???. Cheirolepis trailli is coded ?0? (Giles et al., 2015a).)
0 absent
1 present

235. [G 163] Perforate propterygium (Patterson, 1982; Gardiner, 1984; Gardiner & Schaeffer, 1989; Rosen, 1989; Taverne, 1997; Coates, 1999; Zhu &

Schultze, 2001; Zhu et al., 2001; Zhu & Yu, 2002; Zhu et al., 2006; Brazeau, 2009; Zhu et al., 2009; Friedman & Brazeau, 2010; Xu & Gao, 2011; Davis et al., 2012; Zhu et al., 2013; Xu et al., 2014; Giles et al., 2015b.)

0 absent

1 present

236. [CH 41; G 164] Anterior rays embrace propterygium (Patterson, 1982; Gardiner, 1984; Gardiner & Schaeffer, 1989; Taverne, 1997; Coates, 1999; Schultze & Cumbaa, 2001; Zhu & Schultze, 2001; Friedman & Blom, 2006; Long et al., 2008; Swartz, 2009; Choo, 2011; Xu & Gao, 2011. The radials are only described for Mimipiscis toombsi, so the coding for this character is revised from '1? to ??? for M. bartrami (Choo, 2011). The radials are not described in Gogosardina (Choo et al., 2009), so the coding is changed from ?1? to ???.)

0 absent

1 present

2 fused

237. Propterygium fused to first ray

0 absent

1 present

238. [CH 43; G 168] Pectoral fin endoskeleton (Taverne, 1997; Coates, 1999; Friedman & Blom, 2006; Long et al., 2008; Swartz, 2009; Xu & Gao, 2011; Xu et al., 2014. The pectoral fin of Cuneognathus (Friedman & Blom, 2006) and Kentuckia hlavini (Dunkle, 1964) is unknown, and so the coding is revised from ?1? to ???.)

0 extends far beyond body wall (fins lobate)

1 barely extends beyond body wall (fins not lobate)

239. [G 166] Pectoral fin radials (Zhu & Yu, 2002; Friedman, 2007. Two series of pectoral fin radials are described (but not figured) for Cheirolepis candensis (Arratia & Cloutier, 2004). Although we consider this arrangement to be unlikely, for now this taxon is coded '1'. Although Swartz (2009) describes a series of endoskeletal radials in Stegotrachelus, the elements figured in fig. 17 have a scale-like morphology and appear to be made of dermal bone. As such, this taxon is coded '?'.)

0 unjointed

1 jointed

240. [G 169] Fin articulation (Zhu & Schultze, 2001; Zhu et al., 2001; Zhu & Yu, 2002; Zhu et al., 2006; Friedman, 2007; Zhu et al., 2009; Friedman & Brazeau, 2010; Zhu et al., 2013; Giles et al., 2015b.)

0 monobasal

1 polybasal

241. [CH 44; G 171] Pectoral fin-ray segmentation (Coates, 1999; Friedman & Blom, 2006; Long et al., 2008; Choo, 2011; Xu & Gao, 2011; Xu et al., 2014. The pectoral fin in Kentuckia hlavini (Dunkle, 1964) is not preserved, so the coding for this taxon is revised from ?1? to ???. The coding for Osorioichthys (Taverne, 1997) is revised from '0' to '1'. The segmentation of the pectoral fin is not described for Limnomis (Daeschler, 2000), so the coding for this taxon is revised from '0' to '?'.)

0 roughly even segmentation to fin base

1 proximal segments elongate with terminal segmentation

2 no significant segmentation on pectoral fin

3 terminal segments elongate with proximal segmentation

242. [G 170] Pectoral fin

0 [leaf-like]

1 (not leaf-like)

243. [G 172] Paired fin spines (Zhu et al., 2001; Zhu & Yu, 2002; Friedman, 2007; Zhu et al., 2009; Brazeau, 2009; Davis et al., 2012; Zhu et al., 2013; Giles et al., 2015b.)

0 absent

1 present

244. [CH 38; G 173] Pelvic fins (Friedman & Blom, 2006; Friedman, 2007; Brazeau, 2009; Choo, 2011; Davis et al., 2012; Zhu et al., 2013; Brazeau & Friedman, 2014; Giles et al., 2015b.)

0 absent

1 present

245. [CH 45; G 174] Pelvic fin insertion (Gardiner & Schaeffer, 1989; Coates, 1998; Coates, 1999; Lund, 2000; Schultze & Cumbaa, 2001; Cloutier & Arratia, 2004; Friedman & Blom, 2006; Zhu et al., 2006; Long et al., 2008; Swartz, 2009; Zhu et al., 2009; Choo, 2011; Xu et al., 2014. The pelvic fin is incomplete in Novagonatodus (Long, 1988; Holland

et al., 2007), so this taxon is coded '?'. The coding for Moythomasia lineata is revised to '0' (Choo, 2015).)

0 shorter than fin depth (short based)

1 longer than fin depth (long based)

246. [G 177] Basal scutes on fins (Friedman, 2007; Zhu & Yu, 2002.)

0 absent

1 present

247. [CH 48; G 178] Dorsal scutes anterior to dorsal fin (Lund, 2000; Poplin & Lund, 2000; Cloutier & Arratia, 2004; Friedman & Blom, 2006; Long et al., 2008; Swartz, 2009; Choo; 2011. Choo's (2011) codes for this character appear reversed.)

0 absent

1 few limited to region immediately anterior to fin (basal fulcra only)

2 many, extending to posterior of skull roof (complete set of dorsal ridge scales)

248. [CH 49; G 179] Ventral scutes between hypochordal lobe of caudal fin and anal fin (Patterson, 1982; Taverne, 1997; Friedman & Blom, 2006; Long et al., 2008; Choo, 2011. The coding for Howqualepis rostridens (Long, 1988) and Melanecta (Coates, 1998) is revised from ?0? to ?1?.)

0 absent

1 present

249. [CH 50; G 180] Ventral scutes anterior to anal fin (Cloutier & Arratia, 2004; Friedman & Blom, 2006; Long et al., 2008; Swartz, 2009; Choo, 2011. The coding for Gogosardina (Choo et al., 2009) is revised from ?1? to ?0?. Cuneognathus (Friedman & Blom, 2006) possesses several scutes immediately anterior to the anal fin, although it is unclear how far anteriorly they extend. As such, the coding is changed from ??? to ?1?. The coding in Melanecta (Coates, 1998) is revised from ??? to ?1?. Choo (2011) erroneously codes Krasnoyarichthys (Prokofiev, 2002) as state ?2?, which lacks a description; the coding is revised to ?1?. The coding for Moythomasia lineata is revised to '0' (Choo, 2015).)

0 absent

1 present

250. [CH 52; G 181] Dorsal fin(s) (Gardiner & Schaeffer, 1989; Schultze & Cumbaa, 2001; Zhu & Schultze, 2001; Zhu et al., 2001; Zhu & Yu, 2002; Cloutier & Arratia, 2004; Friedman & Blom, 2006; Zhu et al., 2006; Friedman, 2007; Long et al., 2008; Brazeau, 2009; Swartz, 2009; Zhu et al., 2009; Choo, 2011; Davis et al., 2012; Zhu et al., 2013; Giles et al., 2015b.)

0 two

1 one

251. [CH 51; G 182] Relative positions of anal and (second) dorsal fin (Poplin & Lund, 2000; Cloutier & Arratia, 2004; Friedman & Blom, 2006; Long et al., 2008; Swartz, 2009; Choo, 2011. The coding for Stegotrachelus is revised from ?1? to ?2?.)

0 anal shifted anteriorly relative to dorsal

1 fins opposite one another

2 anal shifted posteriorly relative to dorsal

252. Median fins (except caudal fin) (Gardiner et al., 2005; Xu & Gao, 2011; Xu et al., 2014, 2015; Xu & Zhao, 2016.)

0 rays more numerous than radials

1 rays andradials equal

253. Proximal and middle radials of dorsal fin

0 proximal and middle radials of similar size

1 proximal radials substantially enlarged

254. Posteriormost proximal radial of dorsal fin

0 enlarged plate

1 smaller than more anterior radials

255. [CH 46; G 175] Epichordal lobe of caudal fin (Patterson, 1982; Cloutier & Ahlberg, 1996; Coates, 1999; Schultze & Cumbaa, 2001; Zhu & Schultze, 2001; Friedman & Blom, 2006; Long et al., 2008; Swartz, 2009; Choo, 2011.)

0 present

1 absent

256. [CH 47; G 176] Fulcra along dorsal ridge of caudal fin (Patterson, 1982; Taverne, 1997; Gardiner & Schaeffer, 1989; Gardiner et al., 2005; Friedman & Blom, 2006; Long et al., 2008; Choo, 2011. Choo's (2011) codes for this character appear reversed.)

0 absent

1 present

257. Caudal fin geometry (Modified from Gardiner et al., 2005. A long chordal lobe is considered to be present when the notochord reaches the posterior margin of the caudal fin.)
0 long chordal lobe
1 short chordal lobe

258. Posterior margin of caudal fin (Xu & Gao 2011; Xu et al. 2014; Xu & Zhao, 2016.)
0 forked
1 unforked

259. Diplospondyly in mid-caudal region (Arratia 2013.)
0 absent
1 present

260. Median neural spines in caudal region (Coates 1999; Hurley et al. 2007; Xu et al. 2014.)
0 absent
1 present

261. Uroneural (Pinna, 1996; Hurley et al., 2007; Xu & Wu, 2012, Xu et al., 2014; Xu & Zhao, 2016.)
0 absent
1 present

262. Division of hypurals into dorsal and ventral groups (Pinna, 1996, Xu & Wu, 2012, Xu et al., 2014; Xu & Zhao, 2016.)
0 absent
1 present

263. Number of caudal lepidotrichs borne per hypural
0 multiple (single)
1 single

264. Opistocoelous vertebrae (Wiley, 1976; Lopez-Arbarello 2011.)
0 absent
1 present

265. Ossified ribs
0 present
1 absent

266. Antorbital deeper than anteriormost infraorbital
0 absent
1 present

267. Infraorbitals fragmented
0 absent
1 present

268. Suborbitals fragmented
0 absent
1 present

269. Suborbitals extend ventral to orbit
0 absent
1 present

270. Coronoids contribute to lateral dentition field
0 absent
1 present

271. Jaw articulation ventral to orbit
0 absent
1 present

272. Parasphenoid wings around basiocciput
0 absent
1 present

273. Dorsal extension of parasphenoid between orbits
0 absent
1 present

274. Ligament pit on posterior face of braincase
0 absent
1 present

275. 'Hem-like' median fins
0 absent
1 present

276. Anal fin insertion
0 short
1 long

277. Denticulate ridge scales
0 absent
1 present

278. Ossified centra
0 absent
1 present

Phylogenetic analysis scores

MATRIX

Acanthodes_bronni 0??????????????????-?????0?-?????01?-??????-?????-?????????????1?????????????????????-???????0-?-
?021?000?-?-????-?--??0??0-????0000?????00000000???1000--0-?0?????????0000--------1???????????01?0-00--000---?0000010??0-
??1010??-??-????0000101?11100000002????00?????-?---?-?0--?00-?

Acipenser_brevirostrum 111---------00?0000-1-?010000-0101-1----00110-00??1-001001--000--00----------010 ---0-?0-1--
0-0-1001011-1110020002---011-0-0-0100000-?20020--0100--0--0--1-10?100?010-0001211120011101 00001101????0----1----
-01000011010-101000000-00000101?10101110121112000110001000001?0---00000000

Aesopichthys_erinaceus 1101-0000001110010111000010120?0001-00110-1111100101--1101000-0111010000
0000001000012O???2???120?1???????????0100101000010?11???????0??????2?????????1???????00---------?????????????
??????????????????????01101001101 1??????????????100?00??????0??0101002101 2???0100???????10?000???011?

Amia_calva 1101-1000120100011000000101201010 1-1----0001110011000011000 0-10—0100001111001000
01201?1101012011001?0100001000100210101-11000?000001112021--1100-00--0--1-11-0011100110112111000 1
0001110111110010-00--010---?1001110011110101100 0-0001110010101110100000121111011110010010—0000 0 0?01

Amphicentrum_granulosum 11000101000?110?1011?0001-020?0001-1----01?1??000-1100000000-00—111001
00000?1010---1-??20?-0-0-?1200010????020010100000???0001???0????20?0010??0-00??21011?????0 ?????1?01110
0?001?????????????????????????????????010????0?????????0-0??0?????????????????????????0????????-0--00-000?0?

Atractosteus_spatula 11000100-120101011000000101201011 1-1----01211100112--3-10111101110100100 1000
0100001100111020120010010011000101010021001 1-0-000100000-022020011100-00--0--1-11-0110110-101121
1100010?????????????????101?0110000110111101121010110 00-0101110010001110100000?1111111101001100010 0100000-1

Australosomus_kochi 111?????-??-??0??0?????01002010001-1----01011000??0-001--0---0101111000000010100 0 0120??011--
0-0-10200000?000010000100000?100001001001022021--?101101002001001---------0?110101200000 111110????1110-
????011010011011001 10-101001000-00000110?000111010000010010??100100001?0---0-00 01-1

Beagiascus_pulcherrimus 1100000000011100101110001012010001-00110-0210-?0101003111000-?10??111?0
0000???00001101???????-0?1???????????1100000000010110???
??????????????????011?10011?????????????????110?00??????1??2101001 1?11????100???????1010?0???000?

Beishanichthys_brevicaudalis 1100?01000?0110010111000101 20?0??1-1----00111?000-100210020?00101?1100
000000?100001201??2???1?0?????????????0100000000000???1?????????????????????
??????011010?10???????0-????????0-0?0?????????1101000001 2???1011???????-000?0???01-?

Birgeria_groenlandica 1100110000101100101100001 0?2010001-1----0100100010200301020000 0—0110000
0000010000110 1?01???110-1021000000--0100000000001100001 00?0010?202?--010???1--???1?10-?-0????-000 121
0120011?????????????????0????11???001100000?10-101?0?000-00200100—0013101000001200011 000100001?01000 10000-0

Bobosatrania_groenlandica 111----1----000010111-0010120?00{0 1}1-1----0?0011000-2100010000-00—01000
11000001010---0-??2???0-?-?0???0?0????0-1--11000-?-0-???10???0??????0?????????????????1???????????? 121??2?????
??????????????????011???0110?1010?0-1???????0-0001?????????0?0100101121 0?1100??????1-0--00???1100

Boreosomus_piveteaui 1100101100001100111110?01002010011-1----01100-000-2003100000-11010111100
000?010000110?0010300-0-10200001010001000010001011000?1010001?120200101010 01{0 1}{0 1}2111000---------
0001010101000010111111100??110????0110100110011 1?10-1?1??00?0-?020011???0??1?0100010120 0?010000 00?01-00000-
0000-0

Caturus_furcatus 1100010001?1101011000000101201000110-1----0001110011211 02?01200110—0100001111
???0000120??0103012011021001??001000100210?11-1100010??0?????021--1??0-00???????10?000110011??121110
0000?????????????11??????????0110111001111??1??1??1000??1?0????????0100000121111110?10000000000000?0000

Cheirolepis_canadensis 110?01-000000000000??010{0 1}0010?0001-000-0-10011000-1010010000-010? 1111
10000010100001100??10?00-0?????????????1000000000000???0???1?00
??????????????????????????000-0?011?????????????????0-0?00????000110101101011 0???0101???????-0--00???010?

Cheirolepis_schultzei 11000000000?00000000?01010020?00?1-1---0010111?00-1010010000-010?1111?000
0010100001?00????????0??????????0??100000000000?1??0??1????0?????????????????????
??000-0??11?????????????????????0?00??????0??010??0?????????????????-0--?0???????
Cheirolepis_trailli 11000010000000000010010{0 1}001010001-00000-10010000-1010010000-0110111?0
0000010100001100??10100-0-10100000000010000000000001000?0??00?????010000001001?00--1-00---------0001
000000000111?????????????11100010 1?011000????0-????????10000000001000101011011110??? 0100??00??1-0—00 -000000
Chondrosteus_acipenseroides 111---------1????????-?010120????1-1----0?2?0-?0??1?0??00?????0--00-------??01010---0-?0?1--
??0-?0???1??10??02000??-??0?????????????????????000?????????????????????????????1211?200117 ??????????????----1-----
?10000010?0?????????0-0?0?????????12101?00001????110??0000?1?0??-0???00-?
Cladodoides_wildungensis 0?-?-??-----??-??--????-?-??-?????-?????--?????-?-???-???----?????-???-----????-?1??-00?????0---
?0?0-0?-?---??-?---?--?-??-??0000001?0?00010-0000-0100---0-00---------0000--------110100000---0100-????00???????0??????0-
????????--?-?---?????????????????????????????------0--0-?--
Coccocephalichthys_wildi 11????0?????11?0101010?01002010011-1----00110-00112000?0010?01?0?0111?0
0?00??100001101??1???110?1010?00000?0?101?00000?????00?10??000?02020000?01001??2101100---------
0?01010100000?????????????????????01???????0?1????0????????????0?????????????????????????????????????00--00-0?????
Cosmoptychius_striatus 110??1000?00?10010111000101 2??0001-1----?0?1??00101002100000-010?011100
00001?10000?10???2???????1020????????10000000001?110???1?????????0?001???1101??11111?0??00????????101?1?0000?????????
?????1?????01101001 1?????????????????0-0?000????0111100110100 12???1100????0??100000-??000?
Cyranorhis_bergeraci 111---------110010111-001012010001-00100-11111001010021 10000-0101011
10000000?10000120?????????0???20????????000000000000110???
????????011?100110?1?????????????100??0?1????1??1010010112???0100???????1000?0???000?
Dapedium_LIAS 11001100001?1100110?000010---0-??-------1-111100102--3-0-1000?0—0100001101
??11000120??0?0?0120??1???0??00??010100210101-1100010?0001?120?0011100-00??2001?0----------111121012
1010011111?????11011????011??0?110?1????10????????100?01?1???????21010?????????1?11?1?0??00111111111110?
Dapedium_ashley 11?????????????????????010120?00???1----0-??
??0??10?10010?2020011110-00--2001??0?????????111121?021000???111?????11
010???111????
Dapedium_pholidotum 1100110000111100110100001 0---?-01-------1-21110-102--3-0-200010—01000
01?01110100012 0???0030120????0?0?0100101000022 0101-11?????????????????1?????????????0----------????????????
??????????????????????011??0111011?10?1?1???????10??01?1????1??1010020110121??1111???????011111???110?
Dapedium_stollorum 1101010000111000110100001012010011-1----00211100102--3-001000?1010100
0011011101000120???0030??0??1?1????????010100210101-11?????????????????????????????????0?????????????????
??????????????????????????011??0111?????????????????1(0 1)??01?1????101110100201 12???1111???????011111???110?
Dapedium_punctatum 110?010000??10001100000010---?-??-------1-2111?-102--3-0-1101?0--
?100?0110????1000120???0????????1?????????0000012101???1?????????????????
?????????011??9111011?????????????100?01??????1??110??020?12???1111???????011111???110?
Dapedium_caelatum 1100010000?11100110000?01012010?11-1----01?????0102--3-??100000—01000111
0???01000120???0020120??0?1??????0?000000210101-11???????00??????0011??0-?0??2??110----------???1210?2????
?????????????????????011??011?0?????????????????????0?01?1????1???1011020?12???1111???????01?11111?110?
Dapedium_noricum 110?01000???100011?0?0?0100201???1-1----002111?0??2--3-00100??0--
?100?11?00????000120????0?????????????????????010100220101-11???1????(0
2)?????????????????????????011??0?11?????????????????????0-?????????1??110100???12???1111???????000111???1100
Hemicalypterus_weiri 11000100001100-0110???0010020000 11-1----002111001121-3-00100100--?1000
111000???000120???1???1????0?1????????00010?210101-11???
?????????????????????????011??0-11?????????????????(0 1)0??01?1????1??1101002-1121?11111????1??100101???1110
Paradapedium_egertoni 110?010000??1000110000001002 01???1-1----002111?0??2--3-???00??0--
?1?0?01???0?10000120????0???2???0010?10?0??00000021010???
???????????011??0111011?????????????0-0?01??????1??1101002111 21?11111?????????????????1?

Sargodon_tomicus 1?0?0100001?1?0?110001?010120????1-1----0001?1?0??2--3-0??001?0--
?1?0?11??????1?00120???1????????1????????1101010022?10??
??????????????????1?????????????????????(0 1)0??21??????1??1101002111211111111???0????00101???1110
Dandya_ovalis 110??1?00???100?11?0?0?0101201017-1-1----(0 1)02111?0??2?-3-???00??0--
?100?11?0?????000120?????????????0?????????0001012201?????????????????????0?1?????????????????????????????1?1?????????????????
??????????011??0?11?????????????????0-0?2??????????11?100???12???1111????????001?1???11?0
Heterostrophus_phillipsi 110?010000?1110011?1?00010010????101----0???????102--3-01100??0--?1000011
00??10000120???1?????????????????????000000211101-11???1????????? ?????????????
??????011010?11?????????????????100?01?1????1??11?100?011????1111??????0??1101???1100
Tetragonolepis_oldhami 110??1000???1?00?0?????010?20????1-1----0001???0?????3????????0--?1?0?01???0?10
000120?????????????????????????010010210101-11?? ????????011??
??11?????????????????????0??1?1????1??1101002?1121?11111??????0???1?1???111?
Aetholepis_mirabilis ??
??011000?11?????????????
??????????????????1??31010?????????????????????????1?1???1100
Dialipina_salguerioensis 100???1000??01?0?0?????01012100001-1----00?????????103?00????????110??00??????0
0?01000??0?????????????????????????????0???000-???
??????????????????1???011010?10???? ??????????????0?0?????????????0110?0001???0??1???????????00???000?
Dicksonosteus_arcticus 100??1-000000100???????00-00000?0??1?????0010-1???10000??0??-?0???0--------
?????????0?????????????000-00???--0????0????????000000001?????0???0000-00??0--0?00?????????0001000000000?
101???00??????0???0--?0--0????
Diplocercides_kayseri 110?01-000??00?10??000111000010001-1----0?010-0???100?0???00?10--00?-------
00010???00?1010?113010021?000?0?0000?010000-000-0?000?010???0100000010-10??0--1-00---------0001
00000000?111?0?????????????????01---0???1??????10???????????0?????????????10??0??????????1?????????????00-0000??
Dipteronotus_ornatus 110??10000??110010010??010120?000??1----?0??????1?0-00???1--
1?????100000000001000012017??1????0??0?1?????????1000010007?1?????????????????????1?????????????????0????????11101200???
??????????????????????01?0?0?11?????????????????????0?2????????????01002?112????110?100???00---0-0?0100
Discoserra_pectinodon 110000100001010010111000101207?0000-1----002110000-2003001100000--
010000?000001000012007??20??0-0-10?1???0?0??0-1--120000010-????0??00??02?2?--11?0-0????????0----------
1??121?0?0?????????????????????????0110?011101?00010-????????110??1?1???00???10100201120001111?10???1-01101???0110
Donnrosenia_schaefferi 110?001?000011001011100000-01010001-00100-10111?00-???0?10000-0?0?1111?000
001110000110???1???0-0-????????????1001000?0000010?0???
??????????????????011010011???????0-???????????0?00??????1??11011010111????1?????????-?--00???000?
Dorsetichthys_bechei 110?0100100?11001010000010121107?11-1----000110001021011101000000--?101001102
00100000120???1????210?0?1?0???11?0100002101??-11???1??10000020200111010017?0????10100 00001111112100
01111?10?11?????11111????0110?0?1?011????1??????1??0?0??????10??2101000001207??1110111100000000000000-1
Ebenaqua_ritchei 111----1----110010101-0010120?0001-1----001011000-2?00000000-00--0100011?000?? 010---0-
??20?00-0?10?????????0000011000-0-0?????????????????1?????????????????????????????1?1??????????????????
?????????011??001????01?????????????11??21?????????2101002111??11101???????-0--01???0100
Elops_hawaiensis 1101-1001021110010000000101210011 1-1----000111001021000001000 10—1101001102001000
0010010021--1200?021001011110000102101011100010??00???2000--1100-00--0--1-11?0100101111112001010 1
???????????????0-00--000--0011011111?10?11000?10-000101001110101010000012111111001000000 0---000000-1
Entelognathus_primordialis 100??1-100010100??0????0100?00?-0????????0010-????10000??0??-10???100110000 0
?001001?0?-?01?-0-0-?000-0???---0????0?-0??00????0?0??0?????0????0?00-?0??0??0-00---------000?----?--?0?????
??????????????0?????0??0??????0-??0-????0-??0000????????11?????????????1????????0---?-??????
Erpetoichthys_calabaricus 1101-1100000100000001000100201110 1--------2111000-1003000000-01010110100
0000010000120?002030100-1001101000100-1--00000-000-000010000-000011--0001-00--2001110???0?00000001
2101000101010101100001 1?010??01101001000100010-101110010-000001????0?1?100-????1-?111?11????1?0-0000000?0000

Eusthenopteron_foordi 110001-000000000000001110-01010100100000-0010-000-1000001100110—010000
0000000000011000000200-0-1020000-10000100010000-0010110000010???0100100011001--0--1-00--------000
100000000111110000---1100-00--010--001011010110-100010100-1010001---0000101010000200000110100000-0--00-0000-0
Evenkia_eunoptera 110?0010000000?00?01?0001012001111--------?1??000?2002?00200001l?0110000000?
???0???20???1?????0?????????????1100100000000???011
??0110?????????????????100?????????0??0101000?112???100????????-010?0???01-?
Fouldenia_ischiptera 11000101000?11001010?00010110????1-1----0?0111?00-1000?00000-?101?111?000000?1 0100
121???20??0-0??1?0????????0100100000000110???1????????0?????????
???????????01101001l0??????????????????0-0?00?0??1000101010021111???0100???????-0--00???010?
Fukangichthys_longidorsalis 11000?1000??11001?111?0010120?0101-1----011011?0????0310020?0?1010111000
000???00001201001???100?1001101000100100000000000010???01???0????????1?????????????????????????????1?100000?0??????????
??????????011??00110010000?0-??11?1????000?????????1101000001l2????011????????00000?0?01-?
Glyptolepis_groenlandica 110?-1-0000???-0?00?0111110001110010---0-0010-010-1100000000-10--01000?0??
0?0000?10?0?1???2?0-0-0020000-10000101010000000101010O?010???010?1?001???????????00---------000100000
00001111000?---?????????01--00?101???0?10-10011?100-10?00?0???010?00??000?0????0001??????1-0--00-0000-0
Gogonasus_andrewsae 1100-1-0000?00-0000001110-00010100100000-0010-0?0-1000001?00?10—0100000000
0000011020?0000200-0?1020?00-00000100010000?00?011000?010???01001000?1001--0--1-00---------00010001
0000?11110000---1?00-110-010-00?1?110?01???1100??1?0-???0001---000?1???1????????0??1???????-0--00-000 00 ?
Gogosardina_coatesi 11000010000001001011110O0-010100?1-0010?-1?????00-??000?0?0??0100?111100000
01100001101?020?00-0-1010?00000?00101000000000?0?0?????????????000?????????1001??0???????????100??0000?
??????????????????????01101001101001??10-1?10?????-000001????1??1101002101l????10??000??0-0--00-0?0?00
Guiyu_oneiros 1?01-000000100000000000110-00000000001000-0010-110-1000000100100—0111100000
0?000110100?0?0000-0-1????0????000001000000000100010???1???????0?00?????????????0???-????-???100000000??
???????????????1?1101111001????????0-????????100??0???????????11001110l??????????????-0--00-??0?0?
Hiodon_alosoides 11000100100111001100000010120100l1-1----100110000-2000000000-00---10010110001100
001200?021--12001001?0101110000000210001-0-000??000011?2010-01100-00--0----11-010010111?1121011001
0???????????1110-00--010--00101111101101110010l0-000101001110111011000011111101001110O0-0---000001-1
Howqualepis_rostridens 1101-0100000110010111100O-12010001-00100-10111?00-1100010000-01001111?000
000010011110??110?00-0-10100000000000010000000000l0?0????????????1000???10????0--1-?0???-????????101100
0000?????????????????????0110100110?0????0-????????10000000??10001110110111111???0100?000???-0--00-??000?
Hulettia_americana 11000100001111101000000010?2010001-1----00011100102-03100200000—01000011000
?100?0120???10??1200?02100100?1?000100210101-0-???????0?????020?11???-01??0--1-1000?000000?0?111101110
0?????????????????1??-0110?00110111100101O???1?00-0?0101????????10100101121111010100000100001-000001
Ichthyokentema_purbeckensis 1101-100100111001101000010020100O1-1----000110001021011012000l0—010
000110100100001200??0204-1210102100001?11000100210101-1100010??0010?20?0011100-00--0--1?11101?000
11111121001100?????????????????100-011010?110??101?10????????0-0001011???101?10100101l?1??1110?11??00
1000010000001
Kalops_monophyrum 1100010000?11100101110001-12110001-1----00010-001020030002000010 1011100
0000?010000110???20?0??0?????????????000010000010110?????????????????1??????????????0?---------?????1???
??????????????????????????0110100110?0?????????????????100?00?1????0??0101002111l???0100???????101000???000?
Kansasiella_eatoni_ 11?????????????????????00002010O?1-1----0??????0????????0?????????????????????????????? ??????
?0???1? ???????0?????? 000??????0??1011001112?2001010100110111111100-?00000?000101010000001001111 1
0?11110?????????????0???11?????????????0???-00????
Kentuckia_deani 110?001000000100101110O0{0 1}002010001-?--?-?10111000-??000?000?-?10??111?00?0
00?1000011???02?????0-?010?00000??1000000000011?00?100100?11102001010110100110100O---------000101?
0000?0010011?100?111101????????0???011????0-?????????????????????????0?????????????????????-?--00-00????

Lawrenciella_schaefferi ??????????????????????0?????????-????????????0????????????????????????????????????
??????????????????0??????????????0??1011001002020010101001111101100--------000101?100000010011?110011
110?????????????0??-00????
Lepisosteus_osseus 11000100-120101001010000100201011 1-1----00211100112-031001111011001000001000
011000011001110301200100100110001010100210011-0-????0??????22020011101-00--0--1-11-0110110-0011201
100010001110111110111011100110100110111101121010110 00-01011001000111010000010111111101001100 0 00100
000-1
Leptolepis_bronni 11000100101111100100??0001012110011-1----00010-000-2-01110100000--?100011
1020010000120???2???121??0210010?11?010000210101-11???10??0010?2??0011??0-00--2111?10??000001 11?
?12101?1111?????????????11?????????0100111111?101???110-0?0111???1?011101000001211011100111000-0000100000-?
'"Ligulalepis'" 11?????????????1?1???00??00000?01?00000-0?????0???????00????????0??????????????????
??????????????????-??????????????????00?0010??0?000?0?01?01???????00---------0000--------1101?????????????
???????????0??--?????
Luederia_kempi ??0?????0??0????????????1???? ?????
??????????????0??????????????0??10?100???20200101010010?211?100---?-----0??111???000??1?????????????????
?????????0??-00????
Luganoia_lepidosteoides 11001100001011-01000??0011--11-000?1----1-1111-00-0-0200120?0?1010100102?0
0000100001201?02?????0??0?1?01???110100002000012??0????????1??0????????????????????
????011010?1?01101????????????0-0?21??001?101110100000121??1111???????-00001???00-?
Macrepistius_arenatus 110??10001??10????0?0?0010120????1-00000-10111?0112-03?012001?0--?100?01? 0? ???
0000120???1???1?0???????????0?000100210102???????10??0010120?0011?00-00???????101001000011111121?1210
01?????????????????10??01???0?11????????????-????0-0??1?????????????????????1110???????000101100???1
Macrosemimimus_lennieri 110001000???1110110?000010120?0???-1----00010-?0112-?10012111?0--0100?0
1100???0000120???10????0010?10000????00010021010????????0??00???202001???0-00??0--1?11-0101110-11?121
10?0?10?????????????10????011??0011???????10????????0-0?01?1????1???101000001 2?????????????000101?????-?
Macrosemius_rostratus 11000100012110?01?00?000101210 0?11-1----00011010112--0-00001-?0—0101001100
0?10000120??01040120?1001?00000010001002-1101-0-???????0????2??0011??0-00???????11-010011?-1?01211??0
0?????????????????1?????011??0?1101111?1??1????1?00-01?101000??011?0100?10121111110?00?0000—0100010 ?1
Meemannia_eos 11??????????0??????????0{0 1}002000??1-1----01?0???????????00????????0????????????0000
11???0?0?00-0-1?????????????????????????????0???0??????1???000???1?0?????0?---------000?????????????????00---
0?0101111?????????????????0-??0????????
Melanecta_anneae 1101-01000?011001011100010 02?10001-1----0??????00-1?0?0?0000-0?0?1111?00000?
?100001?0?????????0?????????????0100000000??????0???1?????????????????????????????00?
??0?11?????????????????0-0?00??????1??11011011112???1100???????-0??00???000?
Mesopoma_planti 110?001?00??1100101110?01012010??1-1----001?1??00-?0?1?{0 1}0000-?1?10111??000
0??100001?0?????????0?????????????0100000000010????0??0??????1?????????????????????0?????????????????????????01111000 1?1?0?
???011010011???011?????????????0?00?????????11010011111????000???????-00000???000?
Miguashaia_bureaui 110001-0000010-10100000110000100000001000-?010-001?1?0000110-010--00?-------
0001000120?0020?113-100???????0?000000100 00-000-???1?0?0????0????
????????????10??01---0010???????10????????0-0010?1????0??0101?000001???0001????0?1?0--00????0-0
Mimipiscis_bartrami 11000010000001001011100 00-01010011-00001-10111000-1000010000-01001111100
0000110000110100 20?00-0-?0100000000001010000000001000?10?00?00?001000000 1001??2001000---------00 010 010000-
0?11???????????1?????0110100110??00110-111010001000000??1?0101110100211120?0?1000000?01-0--00-000000
Mimipiscis_toombsi 11000010000011001011110 00-02010011-00001-10111000-1000010000-010011111 0000
0011000011010020100-0-10100000000001010000000001000?10?0000000010000001001002001{0 1}00---------00 010010000-
011100100---100101010011010011010001 10-11101000100000001110101?10100211110?01100 0000? 0 1-0--00-000000
Moythomasia_durgaringa 1101-01000?01100101110000-12010011-00010-110??100-1110011000-010011111
0000000100001101001010 0-0-10100000000001010000001001000?10?0001101010000001001001001000---------0

001011000000??1???????????1?1?1001101101101000110-1110100010000000111?1?1110100211110??11?00100?0 1-0--00-
000000
Moythomasia_lineata 1100001100011100101110000-02010??1-00000-1101?100-1000110000-010?1111?000
0010100001107??1???0-0?1???????????0001000?0010010??
???????????10100110107?11?????????????????100?00??11??101010?0021012???11?0???????-0--?0???000?
Moythomasia_nitida 1100011000011100101110000-02010001-00000-11111100-1102010000-01001111?
0000010100000110???1?????0????????????1100000000010110???
??1?10011011?11?????????????????100?00?????01??1101002111 1???1100??????0-000?0???000?
Obaichthys_decoratus 110?01000?2010?0??0???0010020?0??1-1----001110?0??2--3-0?1111?0--?100001100??
?00???2010110??120010?100?1?001000100210101-0-???????0???????001???0-00??0--1-1?-?11?110-???120110??1
??????????????????????01101001101?110?12??1??1??0-010011?0?0001110100000011?????1?01?0?10?0000100?00-1
Onychodus_jandemarrai 1100000000000000000100111000010?0011---000010-010-110000-100111010111
1000000000001010007?00100-?-100-000?00--0100010000-000-??100?010???0??000??01?11?????1??0????????????10 0000000
0???????????11???00--01---001000001010-10??00??101010010---0?0??01?0000020??00110????01-0--00-0?0?-?
Osorioichthys_marginis 1100001000?0110010110100100111 0?01-00000-?1010000-1001010000-
010?1111?00?00101000011 0???1??????????????????0100000000100107?0??0???0??0??????????????????????????????????????11
1?????????????????01101001 1????????????????????0-0?00?0?11000111 0??02?????????????????-000?0???????
Osteolepis_macrolepidotus 110011-000-000000?-001110-00010100100000-0010-010-1000001000-?0—010000
000000000001?00???0200-0-?0???0????000100010000100101???0?01??????????0?1???????????00---------000????????
0??????????????????????010101?101??????0-???????00-1?10??????0??0101010000 2???0001????0?1-0--00?0?00-?
Ozarcus_mapesae 0?-?-??-----??-??--?????????-???????????--???????-???-???----?????-???-----????-?1??-??????? ?---?0?0-
00??---??-?------?-??-??0000001???0001??0?00-01??---0-00---------0000--------1?????????????????????????? ? ??00000000-
1010000??-?-?---?????????????????????????????------0--0-?--
Peltopleurus_lissocephalus 110?0011000111001011000010120100 01-1----00010-000-1002000200101 0?010001
00000?100001201???0????0??0?????????0100001000017???0?????????????????????????????
????01???0?11????????????-????0-0021?1????1??1101000011 2???1000???????-00000???000?
Platysomus_superbus 111--10?----010010111-001012010001-1----001111000-1000000000-00--01110?000
00010?0012????2?????0?????????????0100001000001?????????????????0?1?????????????????????????????12100?001?????????????????
??011010?11?????????????????0-0?00??????0??0?01000001 2???110????????-0--?0???010?
Polypterus_bichir 1100011000001000000010001002011101--------2111000-10030000---01010110100000
0010000120100203010 0-1001101000100001000000-000-00001??00-000011--0001-00???????10???0?000000012 101
0001?10101011000?????10100110100100010 0100-101110010-0000010000001010100000120111011010010 0-0000000000-0
Porolepis_sp. 1100100000-00000??-?0111110001110010---0-0010-010-1000000000-10--0100000000007
000102001??0200-0-?000?00-?000010001000000010101007?10???01000000?10????0--1-00---------00010000100 0?111?000?---
?????110-011101010110000 10-?00???100-1010??0???0???0010?00001???100????????-0--?0-?000-?
Propterus_elongatus 11000100???1101?1100?00?1002110101-1----00????1?112--0-002010?0—01010011000
?10000120?????????0??0?1?0?0??0?0001002-1001-0-???????????????0?1?????????????????????0??? ?????1????????
??????????????????????011????11???11???01???????0-00?0110??0?011?0100???02?111110?1??100?0--0100?0001
Psarolepis_romeri 1101-1-000?0??-0???001?10-120100?????????0??0-??0-????????00?0?--??111000000000
01101001000000-??1????0???0000?0??00?00?????00100??11???0?10000????01???????00---------000100000000????
?????????????1111011111?????????????????????????0?0??0?????1??1?????????????????????-0??00-0?????
Pteronisculus_stensioi 1100001000011107101110?01012010001-1----01111000102002100000-010?0?1110
0000101000011 0?0010200-0-1020000000001100000000001100 0?10?1001102020010101101012101100---------
000101010000011111111110011110????01101001101101110-1110100010000001 1?101??0101001111200001000000?01100000-
000000
Raynerius_splendens 11?????????????????1????00-01?10001-000??-?111?00????1001??????1101111?0000?0010
00011010010?00-0-1010000000???0000000100001 1??0100000???10100000010010010010 00--------000100?0000
00???0010????100101???011011???010001?0-11101000100 0?000?????????????????????????????????0--00-00????

Saurichthys_madagascarensis 111--000----11-010100-00?-02100??1-1----0?0011?00-?0?1?00100001 0?01110000 000?10000120 1?01?????0?10000000??000-1--00000-1-0-00010?000???2021-0?100-00???????0----------??0121?00?? ?00110111?????????????010-00011?????????????????0-0020011?1000111010021111011111 1???0??1-00000???0000

Scanilepis_dubia 110??010????11??1?0???00100001???1-1----01111??0??1?0310-20?0?10?0111?00?00???00 ???20?????????0?????????????1100?00000000???1010011010 110?????????????????0-0?????????????0100???12????0??????????000?0????10?

Semionotus_elegans 1100010001211-1-11010000101200 0?11-1----00011100112-010002111?0—01000001010 01000012010?10?0120010?1?0?00001000100210101-0-?????????????????1?????????????1??01?111?-??1111100001? ???????????????101001????011011?10110111011000-010111000??0111010020112111111101001000001 01-0?0000

Styloichthys_changae 1???-????0????-??0??????0-0?0100?0???????0?????????????????????????010000000??0010??? 200???0??0-010????0???0?0?????0000??????1?100??11???0100000??0-1???0--1-00---------000100000000?????????? ???????1111?????????1??????1???????????00????1?????0??0?????????????????????0??00-00????

Styracopterus_fulcratus 111--101----11001010?-0010120????1-1----010111?00-1000?00000-?101?111?000000 ? 1010012 11?? 20??0-0??1??????????020010000010110???1????????0????? ??????????????0110100110?1??????????????0-0?00?0????0???2101002111 2???0100???????-0--00???000?

Tanaocrossus_kalliokoskii ?????????????????????????????????1??????1?????????????????????11??????0?????????? ?????????????????????100????00???1??0110?????? ?????????????????????????????10?????????1?11?????????????????000?

Tegeolepis_clarki 11000000?0?01100101???0010010?0001-00000-1101??011?000010000-0????111?00?000? 10010110??11?????0?????????????1??0000?000110?0???1?100?00?????????????????????00 101???0?00?????????????????0?????????0??110??001011????1????????010--00?0?00-?

Tetragonolepis_semicincta 11000100001011001001000010020?0011-1----000110001021030011000 00—01000 011000?10000120???104-??0010?100101?1?000100210101-11?0?10??00?????20011??0-00???????0?????????? ???1? 1 ??211?0?????????????????????011??0011011?101111???????0-000101?11010111010020112111111?100000100101? ??1111

Venusichthys_comptus 11000100000111001011000010121?0??1-1----00011?00102-03000000000—0101 000000001000012 0?????????0??0??????????000001110001-1?? ?????????????????????????011?10011?????????????????0-0?01?1????1??11010000012???1100????????00001???00-?

Watsonulus_eugnathoides 1100000011111-1-100000001012000011-1----000101001121000101001 00--0101001111001000012 0??0102012011021?01010?1011100110110-110001??000111202001 1??1101--0--1-1010010000011112101000 00?????????????10????01???0?1?011101?10101???0?100020?11???1??21010000012?-?1110??00?0010--0000?0?-1

Wendyichthys_dicksoni 111---------11001011?-001012010001-00110-1111100111102111000-110?0111?00000 0010000120??0????0-0???2?????????000000000010110?0??????0???2????0???1??1???????? ?????????????1 01????????? ?????????????????01???1011?????????????????{0 1}-0?00?1????1??0101001011 2???1100???????1000?0???0000

Woodichthys_bearsdeni 1100001000?0110010111000101201 0001-00100-1111?000-1000100000-010?1111? 000000010000110???1???0-0??000?0000???0100000000010??0?????0?????0?0?10??1001??1101100---------000101 00?0000?????????????????????0110110110?????????????????0-0?00???1101??11010011112???1100???????-0--00-??00??

Chapter 4 Lepidosaur Semicircular Canals

4.1 Phylogeny not habit predicts semicircular canal morphology of limbed lepidosaurs

Ashley E. Latimer[1], Emma Sherratt[2], Torsten M. Scheyer[1]

1University of Zurich, Department of Paleontology, Karl Schmid-Strasse 4, Zurich, CH-8006, Switzerland
2The University of Adelaide, Adelaide SA 5005Australia

Image: Eastern blue-tongue (*Tiliqua scincoides scincoides*)
Ashley Latimer, Canberra 2017
Photograph

Author contributions AEL designed the study, collected data, did analyses, wrote the paper, ES provided data, TMS and ES read and contributed comments

ABSTRACT

Morphology of the semicircular canals of the inner ear of squamate reptiles has been used to infer phylogenetic relationships, habitat, and mode of locomotion among extinct members of this group largely based on analysis for the inner ears of mammals. Our understanding of this sensory systems in squamates would be advanced by an overview of the interactions between the morphology, habit, and phylogeny while accounting for size and evolutionary allometry for a broadly representative sample of squamates. Here the semicircular canals of 94 species of extant limbed lepidosaurs are examined using three-dimensional landmark-based geometric morphometrics in a phylogenetic context to evaluate the relative contributions of life habit, size, and phylogeny on canal shape. We find that phylogeny is correlated the largest component of semicircular canal shape change, size effects are non-trivial, and habit has little correlation or effect with semicircular canal shape. Only size of the semicircular canals correlates with habit; semiaquatic taxa have larger inner ears than most taxa that do not swim, but must be tested with body mass and phylogeny or risk over-estimating the effect. Centroid size and body mass have a strong correlation, and semiaquatic taxa are known to be heavier to better retain heat, and that is reflected in these results. Habit is not predictable from inclusive phylogenetic samples of limbed squamates and may require much more restricted clades to see any effect, therefore suggesting reconstructions with extinct animals consider their extant comparative counterparts carefully. Centroid size may prove a better estimator for body mass than body length for extinct organisms.

INTRODUCTION

All animals with backbones, whether they run, swim, fly, crawl, or burrow must be able to orient themselves in a three-dimensional (3D) environment. This ability is mediated by the inner ear, particularly the semicircular canals, which are vital to balance, orientation, head position, and gaze stabilization. This system is exceptionally never lost among vertebrates, and for all its necessary functions, semicircular canal morphology has been shown to relate to ecology, posture, locomotion, as well as phylogeny [1–3]. While the semicircular canals of mammals are the best studied (e.g. [4–9]), a recent surge in research of the semicircular canals of living and extinct squamates [2,10–13], other reptiles including birds [14], as well as amphibians [15] and fishes [16] has improved our understanding of those groups.

Semicircular canal morphology has been shown distinct and convergent in vertebrates with life habits including burrowing [2,12,15] and gliding [11], the morphology varies with the degree of aquatic adaptation[10,17], and differs among arboreal and terrestrial

taxa[13,18]. Unique locomotion is also associated with unique morphology, where tail-assisted walking in dwarf chameleons is associated with bulbus semicircular canal morphology [18]. Because of this ecomorphological relationship, comparative anatomy of semicircular canals of extant species is used to infer life habit of extinct taxa [2,10,12,17,19]. Is ecomorphological convergence visible on in inclusive living clades (e.g. 'squamates'), and is it sensitive enough to estimate habit in extinct members of those groups? Some studies on restricted clades suggest not [2,13], but it has not been tested for total group squamates.

The semicircular canal system consists of soft tissue and surrounding bone; the soft tissue semicircular ducts are filled with fluid and receptor hair cells, whereas the semicircular canals are the bony anatomy surrounding the soft tissue [20,21]. The bones comprising the semicircular canals in reptiles also form the side wall of the braincase, and the sutures between these bones remain unfused in many taxa until adulthood, a large body size is achieved, or until death [22,23], leaving the potential for shape change in the semicircular canal system through life. Ontogenetic change in skull shape between clades, and correlations between environmental factors (e.g. rainfall) and head shape have been investigated for only a few clades [e.g. 22,24]. Whether the shape of the inner ear covaries with size across clades (evolutionary allometry [25]) has likewise not been tested. Thanks to the position of the ducts inside bony canals, undamaged skulls of living or extinct animals preserve the passage of the semicircular canal system, and potentially the sensory ecology of those animals, all accessible with computed tomography (CT).

The combination of cheaper and faster micro-CT scanning with new morphometric approaches has resulted in 3D datasets for large scale geometric morphometric analysis. Here we investigate the relative contribution of phylogeny, four life habit groups (semiaquatic, arboreal, fossorial, and terrestrial), and size on semicircular canal morphology across living squamates that are limbed (thus excluding limbless lizards and snakes, which have different effects of size on ecology [26] and have been studied elsewhere[2]).

METHODS

Specimens, data, and reconstruction

The endocasts of the bony labyrinth of 93 species of squamates and *Sphenodon punctatus* and were digitally sectioned and extracted from X-ray micro computed tomographs as a proxy for the soft tissue semicircular canals in VG StudioMax 2.2 (Supplemental Figure 2). Tomographs were from 3 sources: 1) *Amevia amevia*, *Iguana iguana*, *Saara hardwickii*, *Varanus griseus*, *V. niloticus*, *V. rudicollis*, *V. salvator* were scanned by A.L. at the University of Zurich; 2) Australian varanids (*V. brevicauda*, *V. bushi*, *V. caudolineatus*, *V. eremius*, *V.*

giganteus, *V. gilleni*, *V. glauerti*, *V. mitchelli*, *V. panoptes*, *V. rosenbergi*, *V. scalaris*, *V. storri*, *V. tristis*) were scanned at the Australian National University for J. Scott Keogh; 3) Digimorph, originally part of the deep scaly project[27]. The left semicircular canals were extracted, or right where necessary and mirrored since left-right asymmetry is negligible. Literature information for mass and snout vent length measurements [28] were used for all taxa except where the values were outliers in a length-mass plot, where typographical errors were identified in the latest version and corrected from a prior version [26].

Habit

To test for an association between lifestyle as proxy for locomotion and the morphology of the semicircular canals, the lifestyle habit of each species was recorded in four categories, using binary coding (yes or no): fossorial, arboreal, semiaquatic, terrestrial. Frequently, a taxon's life habits cannot be described adequately by a single category, therefore taxa may have to one, two or three habits in combination, however no taxon has all four habits. For example, although marine iguanas *Amblyrhynchus cristatus* forage in water, they spend 95% of their time on land [29] to sun themselves on coastal rocks, compete for mating territories, and reproduce. Therefore, Marine iguana are coded as terrestrial and semiaquatic. Not all semiaquatic taxa are terrestrial, for example the green iguana, *Iguana iguana* lives mainly in trees overhanging rivers, and if threatened, drops into the water to swim to safety [30]. The green iguana is coded here as arboreal and semiaquatic. It would be misleading to code the marine iguana as aquatic and the green iguana as arboreal when both taxa swim regularly, but one inhabits trees and the other spends time on land. Taxa spending time in and on trees are classified as arboreal, and likewise those spending time on the ground are terrestrial, and taxa which are accomplished swimmers and spend time in water are semiaquatic. Those taxa which stay for an extended time either in burrows of their own creation, or dig in leaf litter are classified as fossorial. This method also allows for comparison of the overall complexity of environments each species may inhabit as a number from one to four, representing the sum of habits of that species. Characterization of each species' habit comes from a variety of sources, listed in the supplementary materials.

Phylogeny

To correct all analyses for phylogeny, an ultrametric calibrated time-tree for squamate phylogeny [31] was pruned using R (ape: drop.tip) [32] to the 94 species of squamates with legs and *Sphenodon* in this study (Figure 1). This pruned tree was used to estimate

phylogenetic influence in all analyses. All R functions used are listed as (package: function), e.g. (ape: drop.tip), where ape is the package and drop.tip is the function.

Landmarks

Midline streamlines [9] were landmarked to quantify the orientation and direction of each canal as opposed to surface landmarking which can be affected by surface irregularities of each canal and low-resolution scans. Surface files (.ply or .stl) representing the semicircular canals of each specimen were imported into Meshtools [33] where the midline streamline endocasts of each canal were landmarked manually (Figure 2) using an arbitrary number of points starting. The anterior and posterior canals were landmarked from the junction of their ampulla to the canal's junction with the common crus. The horizontal canal was landmarked from the ampulla to the last visible portion of the canal on the sacculus. The common crus were landmarked from the lowest visible point on the sacculus to the junction with the anterior and posterior canals. These hand-placed points were then resampled into curves comprising twenty evenly-spaced semilandmarks. The 3D coordinates of these semilandmarks were exported and imported into R statistical environment v. 3.3.2 [32] and processed as follows using a flexible script provided in the supplementary materials.

To standardize the semilandmarks for comparison across species they were aligned using procrustes superimposition and allowed to slide along tangents to the curves between the first and last point to minimize bending energy, centered around the origin, and scaled to size (geomorph: gpagen, [34]). These points, the Procrustes residuals, without the common crus were used in the following analyses and visualized using principal components analysis (PCA) (geomorph: plotTangentSpace).

Integration

First, we assessed the degree of evolutionary integration (covariation) in shape among the three canals. To do this, the procrustes residuals of the three semicircular canals (without the common crus) were examined using three-block partial least squares analysis with 1000 permutations in a phylogenetic framework (geomorph: integration.test)[34] to assess the null hypothesis that the canals are not integrated. Three-block partial least squares analysis allowed for the anterior, posterior, and horizontal canals to be treated as separate units.

Phylogenetic signal and shape

Next, we assessed the amount of shape difference in the morphology of the semicircular canals between species correlated to phylogenetic signal. The amount of phylogenetic signal held within Procrustes residuals was estimated using the K_{mult} statistic

(geomorph: physignal)[35], a multivariate version of K [36]. Like K, K_{mult} estimates the phylogenetic signal in a dataset assuming a Brownian motion model of evolution. Values near zero are explained by a star tree where the variation is explained by things other than phylogeny, values closer to one suggest there is as much phylogenetic signal as would be expected under a Brownian motion model, and higher values are explained by more phylogenetic signal in the morphology than predicted under a Brownian motion model of evolution.

Allometry

To test if squamate semicircular canal shapes (Procrustes residuals) follow the same allometric principals as mammal semicircular canals, we tested SVL, body mass, and centroid size. We ran a multivariate regression (geomorph: procD.pgls) to test for evolutionary allometry, the change in shape associated with evolutionary change in size across a phylogeny, with a null hypothesis of no correlation between size variation and shape variation along branches of the tree. Covariation of shape and size are evaluated independently using a PGLS (Procrustes residuals ~ metric) for Snout-vent length (SVL), centroid size, and body mass. SVL is a measure from the tip of the snout to the vent, and centroid size, the distance of the semilandmarks of the semicircular canals from the center of their distribution, were included in the model as covariates to account for size variation. Maximum SVL from large sizes on record may correspond to SVL related allometry and it is a commonly available measurement. Centroid size captures an estimate of the actual size of the semicircular canals of that specimen as a proxy for head length. Because the included specimens are not as long as the maximum recorded lengths of their species, however, we included centroid size as a better indicator of individual size, and as an indicator for the part of the organism undergoing the motion most likely to be translated to the semicircular canals, the head. Finally, because body mass is correlated to ear size in mammals, we test that relationship in limbed squamates, and used it as a correcting factor in analysis with habit. The allometric relationship was visualized using a regression score [37] (geomorph: procD.allometry) independently for SVL, body mass, and centroid size.

Habit

Then, to test for an association between habit and semicircular canal shape, we used a phylogenetic least squares (PGLS) analysis for high dimensional data (geomorph: procD.PGLS), which evaluates the input model while accounting for phylogenetic influence [34,38]. The hypothesis of a relationship between habit and semicircular canal morphology

was tested with each habit independently and controlling for body mass (Procrustes residuals ~ log body mass), and with 1000 permutations.

To assess the association of SVL, mass, and centroid size with a particular habit, we performed a univariate PGLS (caper: pgls) Centroid size is the log of uncorrected distance of the semilandmarks points from the centroid (centroid size) as well as log snout-vent length (SVL).

RESULTS

Integration

The shapes of the three canals are integrated (r-PLS = 0.789, p = 0.001) and thus changes in shape of one canal are correlated with changes in shape in the others. All three semicircular canals are used together for subsequent analysis.

Principal components and major axes of shape variation

The first three axes from the PCA account for 60.2% of the proportion of total variance (PC1: 35.492%, PC2: 16.543%, PC3: 8.163%). The closest squamate to average shape (0,0) on PC1 and PC2 is *Phymaturus palluma* a terrestrial pleurodont, nearby to both *Lacerta viridis* and *Varanus panoptes*. Each clade investigated here generally occupies a restricted portion of the morphospace on the principal components, but that space is not unique and overlaps with other clades (Figure 4). Gekkota, Scincomorpha, and Anguimorpha excepting *Varanus* overlap in the same morphospace in negative values of PC1. *Varanus* is at the mean of PC1, and Lacertoidea, Acrodonta and Pleurodonta occupy morphospace in the positive direction of PC1. *Varanus* and Lacertoidea are on the positive end of PC2, while Acrodonta are in the negative direction on PC2. *Sphenodon* falls furthest from the group on negative PC2.

Shape change of the semicircular canals along each PC axis away from the mean shape is best viewed in three dimensions (Figure 3). Mean shape of PC1 is a rounded and slightly inflected anterior semicircular canal, the positive direction has more rounded shapes and taller overall semicircular canals, and the anterior and posterior semicircular canals begin further below the horizontal canal, whereas shape change in the negative direction the inflection of the anterior canal increases and the semicircular canals elongate rostro-caudally. The mean shape of PC2 has balanced canals above and below the inflection point, for increasingly negative values the canals move dorsal to the horizontal canal (exemplified by the rhynchocephalian *Sphenodon punctatus*), in the positive direction the proportion of the anterior and posterior semicircular canals ventral to the horizontal canal increases. Shape change on the third principal component emphasizes the inflection point (concavity) in the

anterior canal and the length of the horizontal canal in the positive direction, and roundness (convexity) in the negative direction.

Phylogeny

There is significant phylogenetic signal in the morphology of the semicircular canals among limbed squamates (K_{mult}=0.615, p= 0.001) (Appendix table 1). Therefore, the Procrustes residuals have phylogenetic signal but less than would be assumed under a Brownian motion model of evolution. Clades cluster visibly on the first principal component, but less on the second and third principal components (Figure 4).

Size

Tests for allometric relationships between semicircular canal shape and size revealed that, although semicircular canal shape does not covary with log SVL, there is an allometric relationship between semicircular canal shape and centroid size, as well as body mass (Table 4). Furthermore, body mass predicts centroid size (R^2=0.6439, F=173.2, p< 2.2e-16). Limbed squamate SVL does not predict the values of Procrustes residuals or the PC axes. Additionally, the smallest semicircular canals are found in the Mexican horned lizard (*Phrynosoma taurus*) and the largest in the Asian Water Monitor, *Varanus salvator*.

Habit

PGLS of the Procrustes residuals shows no support for convergent shape change due to life habit (Table 1). Species sharing similar habits do not cluster visibly in the morphospace (Figure 5). Furthermore, generalist taxa with more than one life habit did not cluster in shape space, on any principal component, and do not predict centroid size.

DISCUSSION

Our results do not support the hypothesis that distantly related taxa with similar life habit have convergent semicircular canal shape. We did not recover a fossorial type ear, and while we did not include legless taxa and had few obligate fossorial taxa, there nevertheless does not appear to be a convergent morphotype on taxa that dig or move through leaf litter among squamates with legs. Furthermore, there is no semicircular canal shape associated with semiaquatic squamates, the semicircular canals do not appear flatter or a more antero-posteriorly expanded as has been hypothesized elsewhere. There is no correlation between habit and canal shape, the values of those differences overlap and even though the models pick

up differences between species with a particular habit and the rest, it cannot distinguish between different habits.

Instead of habit, phylogeny appears to be the primary driver of shape. Related species cluster in morphospace by phylogenetic group particularly on the largest principal component. This leads us to conclude that analysis of semicircular canal shape for squamates should always be considered in a phylogenetic framework.

After phylogeny, the strongest correlation with canal shape is body mass and centroid size (Table 4, Figure 7). Centroid size and body mass correlated and are larger in semiaquatic taxa. Semiaquatic taxa are heavier than their length would predict, likely aiding in heat retention while swimming, and that correlation is reflected in the centroid size. The relationship of centroid size to body mass may help identify semiaquatic squamates, but also estimate body mass from centroid size. Unlike mammals, where the bony labyrinth ossifies early, in many squamates these bones grow during adulthood, and these results suggest the semicircular canals of squamates scale with the increasing mass of the skull as opposed to length.

Some features of squamate semicircular canals may offer some suggestions for future research. Particularly strange methods of locomotion as well as body morphology may override the phylogenetic signal. Interesting phylogenetic outliers include *Brookesia brygooi* (Figure 4), which has bulbous semicircular canal morphology typical of dwarf chameleons with assisted walking [18]. Dwarf chameleons use their tail like an extra leg and move very slowly, locomotion quite unlike the actions of varanid lizards occupying that region. Also, the tiny semicircular canals of genus of *Phrynosoma* plot outside the normal allometric relationship of semicircular cana size and body mass of squamate reptiles and may be due to their shortened skulls. The inner ears of that clade may arrest development early, and there may be a unique functional aspect to the posterior region of the skull in these taxa. These results suggest two further suggestions for methods in future analyses are. First, the shapes of the canals are highly integrated, likely due to skull shape constraints, and so the three canals should be considered together. And second, due to the poor definition and varying degrees of visibility, the common crus are not reliable to landmark across large groups of squamates from endocasts alone because it introduces noise from landmarking imprecision.

CONCLUSIONS

Phylogeny is the main source of shape difference in semicircular canals among large scale groups of limbed squamates, and therefore semicircular canal shape should be a better predictor of phylogeny than of habit, and a poor predictor of habit. Unlike among legless

squamates[2], this analysis of squamates with legs does not show a correlation between shape of the canals and ecological group. This sample included fewer of the typical 'burrowing' morphology of legless lizards, and further work including taxa with legs and without is needed to fully assess this morphology.

Centroid size and body mass, but not SVL, correlate with semicircular canal shape and semiaquatic habit. Larger taxa with a semiaquatic habit have a larger centroid size than and body mass than squamates of similar length and no semiaquatic habit. Centroid size is a better predictor of semiaquatic habit than other metrics, but should be analyzed with phylogeny and a metric of body size or risk overestimating the likelihood of that habit, in agreement with best practices [39].

Among squamates with legs, ecological implication of semicircular canals would only, at best, be applicable at smaller clade-scale investigations[13]. In any case, inferring the ecology of extinct taxa without a well sampled set of close relatives seems unlikely.

The relationship between centroid size and body mass could also be used to estimate body mass in extinct squamates where only a skull is known and shows potential for a metric of semiaquatic habit.

ACKNOWLEDGEMENTS

Thanks to Jessie Maisano (Digimorph) and Matthew Colbert (Digimorph), Renaud Lebrun (Montpellier), Alexandra Wegman (UZH), Madlen Stange (UZH), Beat Scheffold (UZH), Timothée Bonnet (ANU), Damien Esquerre (ANU), J. Scott Keogh(ANU), Simon P. Blomberg, Anita Schweizer. Funding from Swiss National Science Foundation grant 31003A-149506 and 173173 to Torsten M. Scheyer, M. Sánchez, and T. Rowe's NSF Digital Libraries Grant.

REFERENCES

1. Georgi J. 2008 Semicircular Canal Morphology as Evidence of Locomotor Environment in Amniotes. *J. Vertebr. Paleontol.* **28**, 83a–83a.

2. Palci A, Hutchinson MN, Caldwell MW, Lee MSY. 2017 The morphology of the inner ear of squamate reptiles and its bearing on the origin of snakes. *R. Soc. Open Sci.* **4**, 170685. (doi:10.1098/rsos.170685)

3. Hullar TE. 2006 Semicircular canal geometry, afferent sensitivity, and animal behavior. *Anat. Rec. Part a-Discoveries Mol. Cell. Evol. Biol.* **288a**, 466–472. (doi:10.1002/ar.a.20304)

4. Malinzak MD, Kay RF, Hullar TE. 2012 Locomotor head movements and semicircular canal morphology in primates. *Proc. Natl. Acad. Sci. U. S. A.* **109**, 17914–17919. (doi:10.1073/pnas.1206139109)
5. Jeffery N, Spoor F. 2006 The primate subarcuate fossa and its relationship to the semicircular canals part I: prenatal growth. *J. Hum. Evol.* **51**, 537–549. (doi:10.1016/j.jhevol.2006.07.003)
6. Gray AA. 1907 The labyrinth of animals : including mammals, birds, reptiles and amphibians. London: J. {&} A. Churchill.
7. Ekdale EG. 2016 Form and function of the mammalian inner ear. *J. Anat.* **228**, 324–337. (doi:10.1111/joa.12308)
8. Spoor F, Bajpal S, Hussaim ST, Kumar K, Thewissen JGM. 2002 Vestibular evidence for the evolution of aquatic behaviour in early cetaceans. *Nature* **417**, 163–166. (doi:DOI 10.1038/417163a)
9. Gunz P, Ramsier M, Kuhrig M, Hublin JJ, Spoor F. 2012 The mammalian bony labyrinth reconsidered, introducing a comprehensive geometric morphometric approach. *J. Anat.* **220**, 529–543. (doi:10.1111/j.1469-7580.2012.01493.x)
10. Cuthbertson RS, Maddin HC, Holmes RB, Anderson JS. 2015 The Braincase and Endosseous Labyrinth of Plioplatecarpus peckensis (Mosasauridae, Plioplatecarpinae), With Functional Implications for Locomotor Behavior. *Anat. Rec.* **298**, 1597–1611. (doi:10.1002/ar.23180)
11. Boistel R, Herrel A, Lebrun R, Daghfous G, Tafforeau P, Losos JB, Vanhooydonck B. 2011 Shake rattle and roll: The bony labyrinth and aerial descent in squamates. *Integr. Comp. Biol.* **51**, 957–968. (doi:10.1093/icb/icr034)
12. Yi H, Norell MA. 2015 The burrowing origin of modern snakes. *Sci. Adv.* **1**, 1–5. (doi:10.1126/sciadv.1500743)
13. Dickson B V., Sherratt E, Losos JB, Pierce SE. 2017 Semicircular canals in *Anolis* lizards: ecomorphological convergence and ecomorph affinities of fossil species. *R. Soc. Open Sci.* **4**, 170058. (doi:10.1098/rsos.170058)
14. Georgi JA, Sipla JS. 2008 Comparative and Functional Anatomy of Balance in Aquatic Reptiles and Birds. *Sens. Evol. Threshold Adapt. Second. Aquat. Vertebr.* , 233–256.
15. Maddin HC, Sherratt E. 2014 Influence of fossoriality on inner ear morphology: Insights from caecilian amphibians. *J. Anat.* **225**, 83–93. (doi:10.1111/joa.12190)
16. Giles S, Rogers M, Friedman M. 2016 Bony labyrinth morphology in early neopterygian fishes (Actinopterygii: Neopterygii). *J. Morphol.* **0**, 1–15. (doi:10.1002/jmor.20551)

17. Neenan JM, Reich T, Evers SW, Druckenmiller PS, Voeten DFAE, Choiniere JN, Barrett PM, Pierce SE, Benson RBJ. 2017 Evolution of the Sauropterygian Labyrinth with Increasingly Pelagic Lifestyles. *Curr. Biol.* , 1–7. (doi:10.1016/j.cub.2017.10.069)
18. Boistel R, Herrel A, Daghfous G, Libourel P-A, Boller E, Tafforeau P, Bels V. 2010 Assisted walking in Malagasy dwarf chamaeleons. *Biol. Lett.* **6**, 740–743. (doi:10.1098/rsbl.2010.0322)
19. Neenan JM, Scheyer TM. 2014 New specimen of Psephoderma alpinum (Sauropterygia, Placodontia) from the Late Triassic of Schesaplana Mountain, Graubünden, Switzerland. *Swiss J. Geosci.* **107**, 349–357. (doi:10.1007/s00015-014-0173-9)
20. Sipla JS, Spoor F. 2008 The Physics and Physiology of Balance. In *Sensory Evolution on the Threshold: Adaptations in Secondarily Aquatic Vertebrates* (eds JGM Thewissen, S Nummela), pp. 227–232. Berkeley: University of California Press.
21. Federative Committee on AnatomicalTerminology. 1998 *Terminologia Anatomica.* Stuttgart: Georg Thieme Verlag.
22. Hipsley CA, Müller J. 2017 Developmental dynamics of ecomorphological convergence in a transcontinental lizard radiation. *Evolution (N. Y).* **71**, 936–948. (doi:10.1111/evo.13186)
23. Frýdlová P, Nutilová V, Dudák J, Žemlička J, Němec P, Velenský P, Jirásek T, Frynta D. 2017 Patterns of growth in monitor lizards (Varanidae) as revealed by computed tomography of femoral growth plates. *Zoomorphology* **136**, 95–106. (doi:10.1007/s00435-016-0338-3)
24. Openshaw GH, Keogh JS. 2014 Head shape evolution in monitor lizards (Varanus): Interactions between extreme size disparity, phylogeny and ecology. *J. Evol. Biol.* **27**, 363–373. (doi:10.1111/jeb.12299)
25. Klingenberg CP. 2016 Size, shape, and form: concepts of allometry in geometric morphometrics. *Dev. Genes Evol.* **226**, 113–137. (doi:10.1007/s00427-016-0539-2)
26. Meiri S. 2010 Length-weight allometries in lizards. *J. Zool.* **281**, 218–226. (doi:10.1111/j.1469-7998.2010.00696.x)
27. Gauthier JA, Kearney M, Maisano JA, Rieppel O, Behlke ADB. 2012 Assembling the Squamate Tree of Life : Perspectives from the Phenotype and the Fossil Record Assembling the Squamate Tree of Life : Perspectives from the Phenotype and the Fossil Record. *Bull. Peabody Museum Nat. Hist.* **53**, 3–308. (doi:10.3374/014.053.0101)
28. Feldman A, Sabath N, Pyron RA, Mayrose I, Meiri S. 2016 Body sizes and diversification rates of lizards, snakes, amphisbaenians and the tuatara. *Glob. Ecol. Biogeogr.* **25**, 187–197. (doi:10.1111/geb.12398)
29. Trillmich KGK, Trillmich F. 1986 Foraging strategies of the marine iguana, Amblyrhynchus cristatus. *Behav. Ecol. Sociobiol.* **18**, 259–266. (doi:10.1007/BF00300002)
30. Köhler G. 2003 *Reptiles of Central America.* Offenbach: Herpeton Verlag.

31. Zheng Y, Wiens JJ. 2016 Combining phylogenomic and supermatrix approaches, and a time-calibrated phylogeny for squamate reptiles (lizards and snakes) based on 52 genes and 4162 species. *Mol. Phylogenet. Evol.* **94**, 537–547. (doi:10.1016/j.ympev.2015.10.009)
32. R core team. 2014 R: A Language and Environment for Statistical Computing.
33. Lebrun R. 2014 ISE-Meshtools, a 3D interactive fossil reconstruction freeware. In *12th Annual Meeting of EAVP, Tornio, Italy*,
34. Adams DC, Otarola-Castillo E. 2013 geomorph: an R package for the collection and analysis of geometric morphometric shape data. *Methods Ecol. Evol.* **4**, 393–399.
35. Adams DC. 2014 A generalized K statistic for estimating phylogenetic signal from shape and other high-dimensional multivariate data. *Syst. Biol.* **63**, 685–697. (doi:10.1093/sysbio/syu030)
36. Blomberg SP, Jr TG, Ives AR. 2003 Testing for Phylogenetic Signal in Comparative Data: Behavioral Traits are More Labile. *Evolution* **57**, 717–745. (doi:10.1111/j.0014-3820.2003.tb00285.x)
37. Drake AG, Klingenberg CP. 2008 The pace of morphological change: historical transformation of skull shape in St Bernard dogs. *Proc. R. Soc. B Biol. Sci.* **275**, 71–76. (doi:10.1098/rspb.2007.1169)
38. Orme D, Freckleton R, Thomas G, Petzoldt T, Fritz S, Isaac N, Pearse W. 2013 caper: Comparative Analyses of Phylogenetics and Evolution in R.
39. Outomuro D, Johansson F. 2017 A potential pitfall in studies of biological shape: Does size matter? *J. Anim. Ecol.* **86**, 1447–1457. (doi:10.1111/1365-2656.12732)

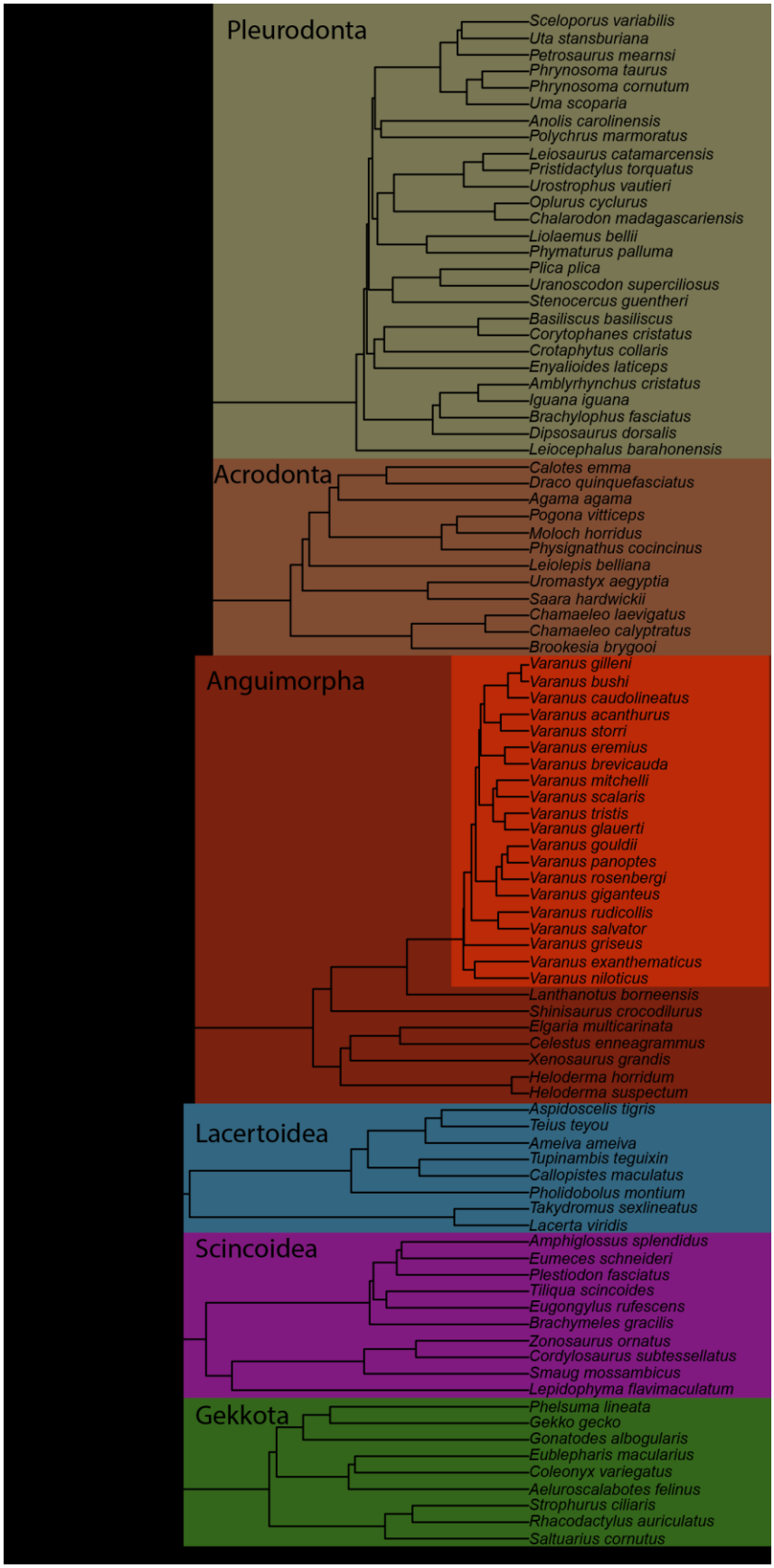

Figure 1 Tree of taxa included in the phylogenetic analysis, pruned from [31] . Colors correspond to the indicated taxonomic group, bright red are *Varanus*.

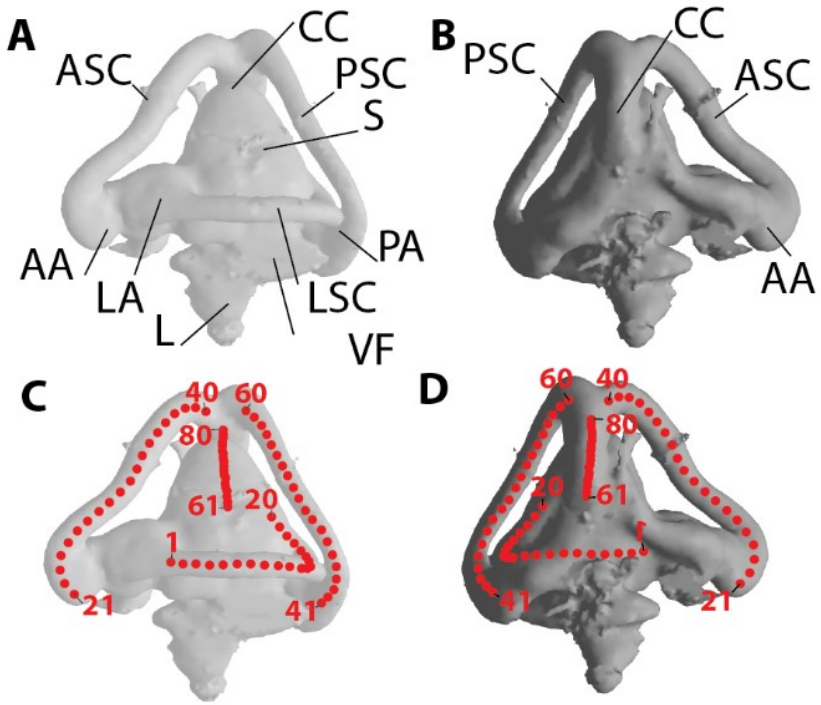

Figure 2. Landmarks on *Varanus niloticus* (PIMUZ A/III0225), each canal is described by 20 landmarks along a central streamline. Abbreviations: AA anterior ampulla, ASC anterior semicircular canal, CC common crus, L lagena, LA lateral ampulla, LSC lateral semicircular canal, PA posterior ampulla, PSC posterior semicircular canal, S sacculus, VF vestibular fontanelle,

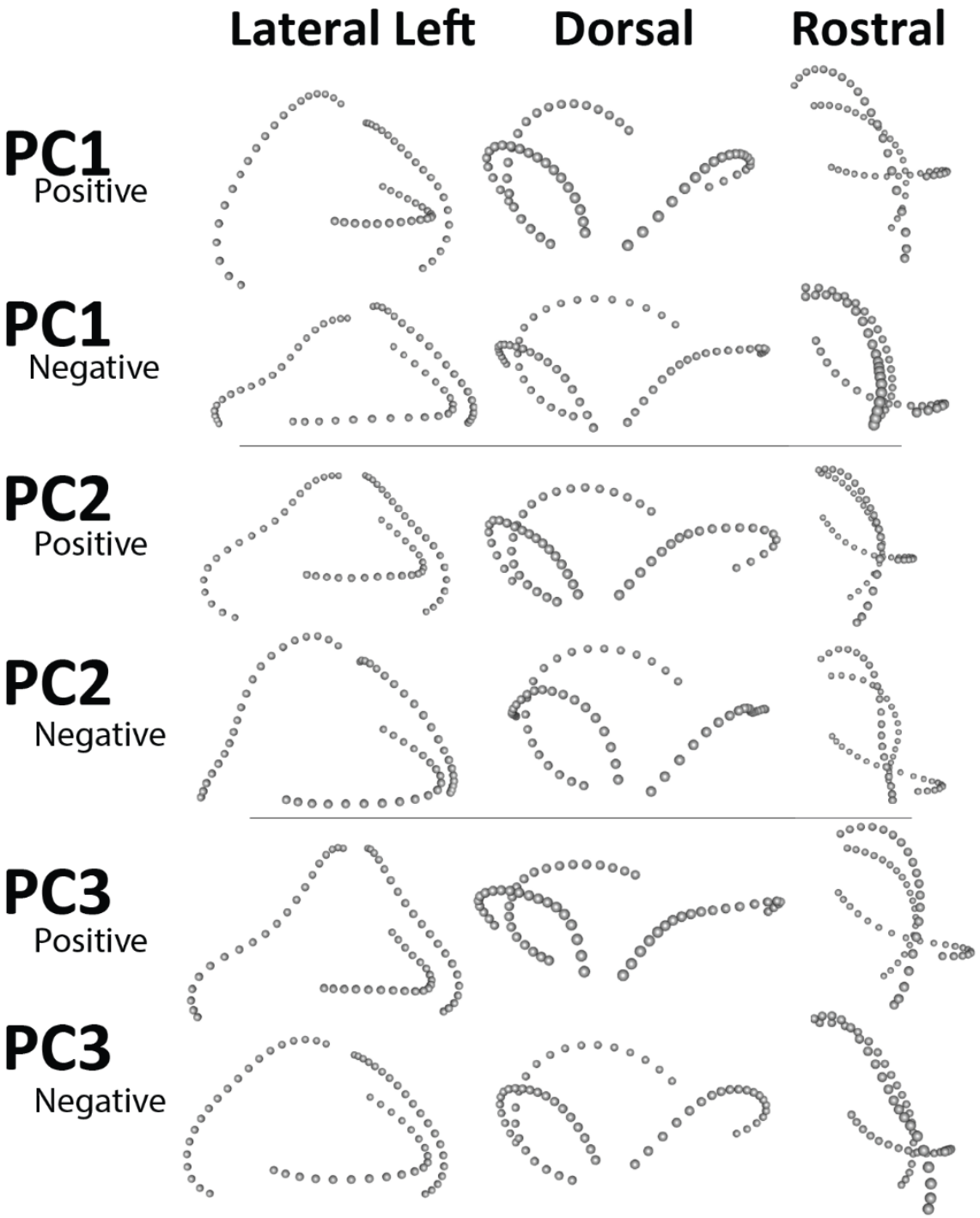

Figure 3. Shape change on the first three principal component axes in three views.

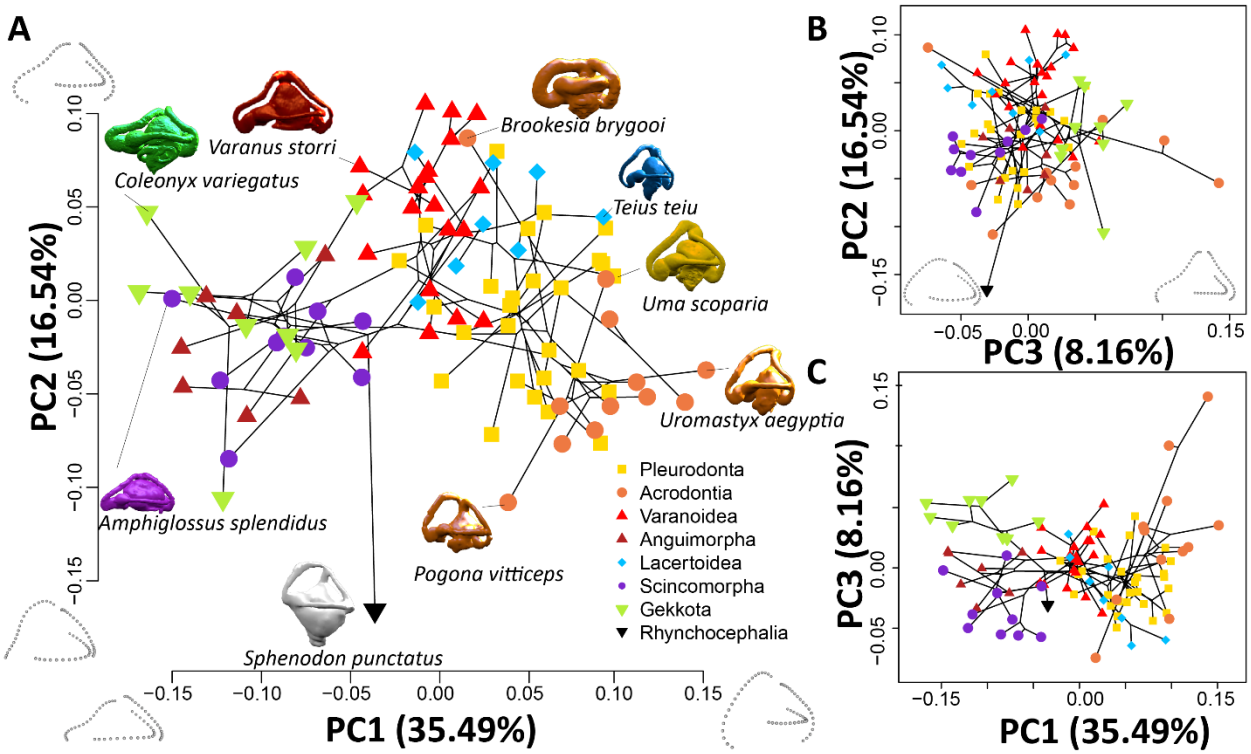

Figure 4. Taxa plotted on A) PC1 and PC2, B) PC3 and PC2, C) PC1, PC3 for the landmark coordinates of three semicircular canals together, for each species, colored by clade.

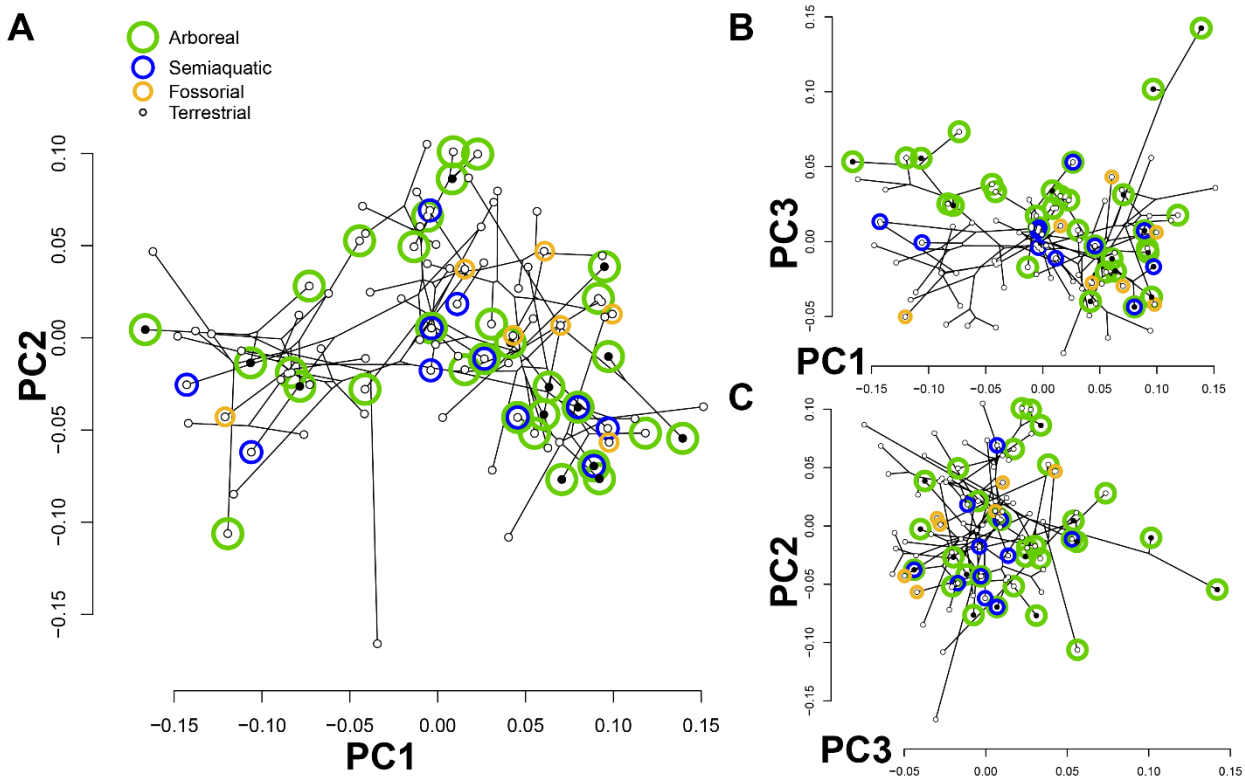

Figure 5. The habits of each species are plotted on A) PC1 and PC2, B) PC1 and PC3, and C) PC2 and PC3. Each species may have more than one habit, and multiple habits are plotted as concentric circles Black circles are species that are not terrestrial, and are just the location of those species.

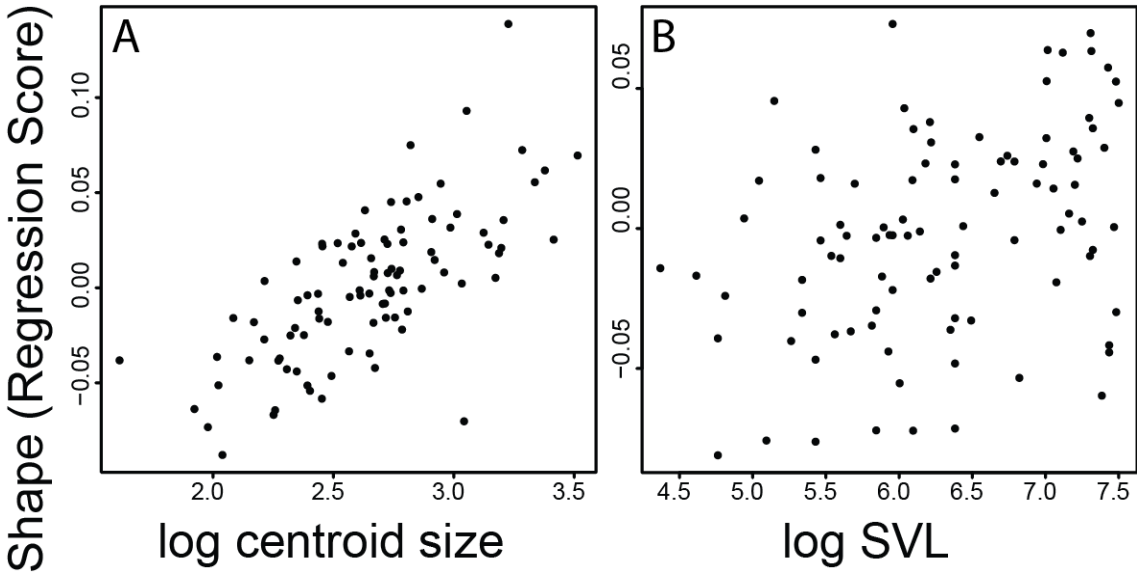

Figure 6. Allometric relationship between shape and (A) centroid size, and (B) lack of a relationship with snout vent length.

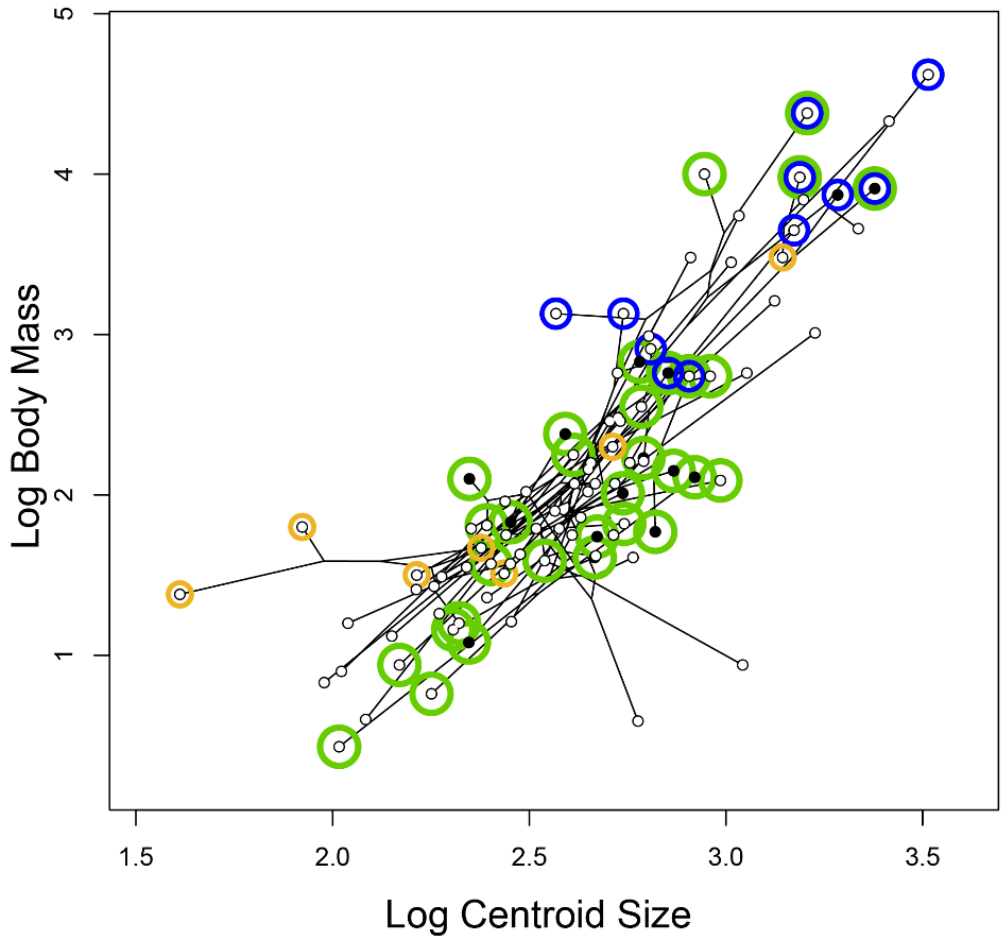

Figure 7. Relationship between centroid size, habit, and body mass.

PGLS: Shape~ log body mass+ habit

	Rsq	F	Pr(>F)
logmass	0.060961	6.0331	0.000999
fossorial	0.019531	1.9329	0.207792
logmass	0.060961	6.0371	0.000999
semiaquatic	0.02014	1.9945	0.44955
logmass	0.060961	6.0654	0.000999
arboreal	0.024431	2.4308	0.213786
logmass	0.060961	6.0314	0.000999
terrestrial	0.019281	1.9076	0.948052
logmass	0.060961	6.0383	0.003
Generalist	0.020317	2.0124	0.751

Table 1. Results of PGLS of the Procrustes Residuals accounting for log body mass and habit, run independently for each habit with mass correction, and generalist, a sum of total habits for each species with mass correction.

PGLS: Log Centroid size ~ Habitat

	R	F	P
Fossorial	-0.005298	1.49	0.2245
Semiaquatic	0.05525	6.439	0.01285
Arboreal	-2.26E-05	0.998	0.3204
Terrestrial	-0.005268	0.513	0.4758
Generalist	-0.001125	0.895	0.3465

Table 2. Results of a PGLS test to determine the correlation between centroid size and habit.

PGLS: Log Body Mass ~ Habitat

	R	F	P
Fossorial	-0.006289	0.418	0.5192
Semiaquatic	0.1748	20.7	1.64E-05
Arboreal	-0.000229	0.979	0.3251
Terrestrial	0.0198	2.879	0.09315
Generalist	-0.007437	0.314	0.5769

Table 3. Results of a PGLS test to determine the correlation between Body mass and habit.

PGLS: Shape ~ Metric

	R	F	P
Log mass	0.060961	5.9725	0.003
Log centroid size	0.05272	5.1202	0.001
Log length	0.019999	1.8775	0.139

Table 4. Allometric relationships between semicircular canal shape and body measures of mass, centroid size, and length.

4.2 Supplemental Material for "Contribution of phylogeny and habit to endosseous labyrinth shape in limbed squamates"

Habits

Habit categories for each taxon are based on literature cited in the supplementary materials and expanded here [1–45].

Inclusion tests

To test if sliding semilandmarks should be included in the analysis, and if the common crus brings information or noise, generalized procrustes analyses (package:geomorph, function: gpagen) and phylogenetic signal (package:geomorph, function:physignal) were implemented.

The Common Crus vary in visibility by clade, and their extent is poorly defined. The proportion of variance from each of the three principal components for analyses with the common crus (Figure 1 B and D) were lower than without them (Figure 1 A and B), and the amount of phylogenetic signal was likewise lower (Figure 2 B and D vs A and B). Therefore, including the common crus increases the amount of noise in the dataset, and was excluded.

Sliding semilandmarks were developed for two dimensional (2D) landmarking to reduce the amount of artifact from evenly spaced space landmarks on 2D surface [46]. We tested this in three cases, without sliders, with curve sliders using bending energy, and third, curve sliders using procrustes distances. They are evaluated by looking at the recovered phylogenetic signal, and we assume that a larger phylogenetic signal would not be recovered by chance.

Bending energy recovers a greater phylogenetic signal than no sliders when the common crus is excluded and included (Figure 1). Procrustes distances, surprisingly are worse than excluding sliders when the common crus is excluded, but performed better than bending energy when it the common crus was included (Figure 1). The overall higher phylogenetic signal recovered by sliding the semilandmarks with bending energy and the unpredictable performance of Procrustes distances show bending energy is the better choice for semilandmarks sliding here. The curious performance of procrustes distances here suggests it may be better to use unslid data than the procrustes distances, but if bending energy is an option it should be used instead.

Common Crus	Sliders	K	PC1	PC2	PC3	Sum of PC1-3
	BE	0.607	33.59	15.56	8.86	58.008
CC	BE	0.559	26.98	16.91	9.12	53.01
		0.557	28.71	21.49	9.06	59.26
CC		0.549	24.31	21.16	9.1	54.568
	PD	0.554	26.78	20.14	8.91	55.82
CC	PD	0.583	25.51	17.85	8.68	52.039

Table 1. The phylogenetic signal and proportion of variance in each of the three principal component axes with and without the common crus, bending energy (BE), or procrustes distances (PD). K is the phylogenetic signal in the data as a proportion of 1 (Adams).

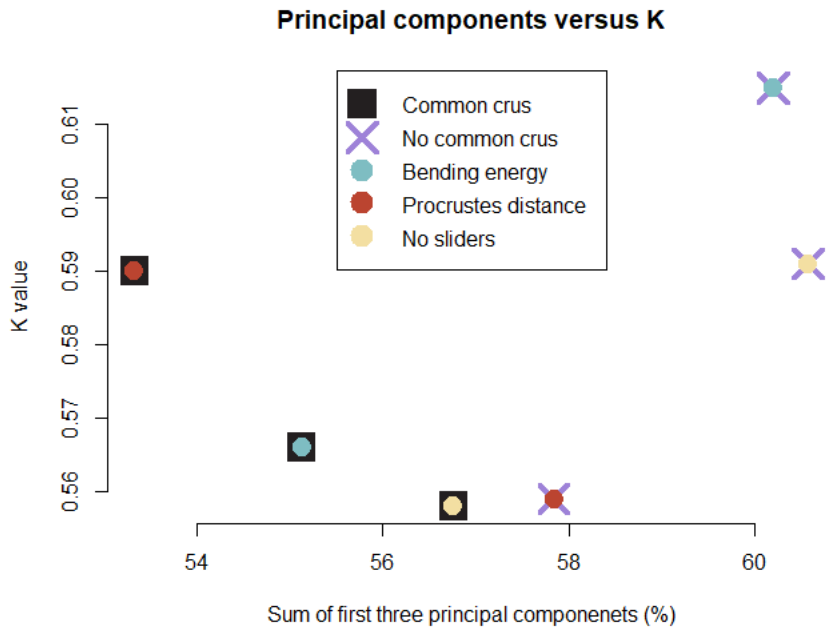

Supplemental Figure 1. Graph of the different outputs for the aligned coordinates under different conditions, K is the proportion of phylogenetic influence. The principal components are shown as

Supplemental Figure 2. Inner ears of all specimens to scale, box is 1mm square, in alphabetical order with row numbers. Taxon numbers below correspond to the principal components in the supplement Figure 3. Colors correspond to the taxon colors; Gekkota green, Scincoidea purple, Lacertoidea blue, Anguimorpha red, Acrodonta orange, Pleurodonta yellow, *Sphenodon* white. ROW 1: 1 *Aeluroscalabotes felinus*, 2 *Agama agama*, 3 *Amblyrhynchus cristatus*, 4 *Ameiva ameiva*, 5 *Amphiglossus splendidus*, 6 *Anolis carolinensis*, 7 *Aspidoscelis tigris*, 8 *Basiliscus basiliscus*, 9 *Brachylophus fasciatus*, 10 *Brachymeles gracilis.* ROW 2: 11

Brookesia brygooi, 12 *Callopistes maculatus*, 13 *Calotes emma*, 14 *Celestus enneagrammus*, 15 *Chalarodon madagascariensis*, 16 *Chamaeleo calyptratus*, 17 *Chamaeleo laevigatus*, 18 *Coleonyx variegatus*, 19 *Cordylosaurus subtessellatus*, 20 *Corytophanes cristatus*. ROW3: 21 *Crotaphytus collaris*, 22 *Dipsosaurus dorsalis*, 23 *Draco quinquefasciatus*, 24 *Elgaria multicarinata*, 25 *Enyalioides laticeps*, 26 *Eublepharis macularius*, 27 *Eugongylus rufescens*, 28 *Eumeces schneideri*, 29 *Gekko gecko*, 30 *Gonatodes albogularis*. *ROW 4:* 31 *Heloderma horridum*, 32 *Heloderma suspectum*, 33 *Iguana iguana*, 34 *Lacerta viridis*, 35 *Lanthanotus borneensis*, 36 *Leiocephalus barahonensis*, 37 *Leiolepis belliana*, 38 *Leiosaurus catamarcensis*, 39 *Lepidophyma flavimaculatum*, 40 *Liolaemus bellii*. ROW 5: 41 *Moloch horridus*, 42 *Oplurus cyclurus*, 43 *Petrosaurus mearnsi*, 44 *Phelsuma lineata*, 45 *Pholidobolus montium*, 46 *Phrynosoma cornutum*, 47 *Phrynosoma taurus*, 48 *Phymaturus palluma*, 49 *Physignathus cocincinus*, 50 *Plestiodon fasciatus*. ROW 6: 51 *Plica plica*, 52 *Pogona vitticeps*, 53 *Polychrus marmoratus*, 54 *Pristidactylus torquatus*, 55 *Rhacodactylus auriculatus*, 56 *Saara hardwickii*, 57 *Saltuarius cornutus*, 58 *Sceloporus variabilis*, 59 *Shinisaurus crocodilurus*, 60 *Smaug mossambicus*, ROW 7: 61 *Sphenodon punctatus*, 62 *Stenocercus guentheri*, 63 *Strophurus ciliaris*, 64 *Takydromus sexlineatus*, 65 *Teius teyou*, 66 *Tiliqua scincoides*, 67 *Tupinambis teguixin*, 68 *Uma scoparia*, 69 *Uranoscodon superciliosus*, 70 *Uromastyx aegyptia*, ROW 8: 71 *Urostrophus vautieri*, 72 *Uta stansburiana*, 73 *Varanus acanthurus*, 74 *Varanus brevicauda*, 75 *Varanus bushi*, 76 *Varanus caudolineatus*, 77 *Varanus eremius*, 78 *Varanus exanthematicus*, 79 *Varanus giganteus*, 80 *Varanus gilleni*. ROW 9: 81 *Varanus glauerti*, 82 *Varanus gouldii*, 83 *Varanus griseus*, 84 *Varanus mitchelli*, 85 *Varanus niloticus*, 86 *Varanus panoptes*, 87 *Varanus rosenbergi*. ROW 10: 88 *Varanus rudicollis*, 89 *Varanus salvator*, 90 *Varanus scalaris*, 91 *Varanus storri*, 92 *Varanus tristis*, 93 *Xenosaurus grandis*, 94 *Zonosaurus ornatus*.

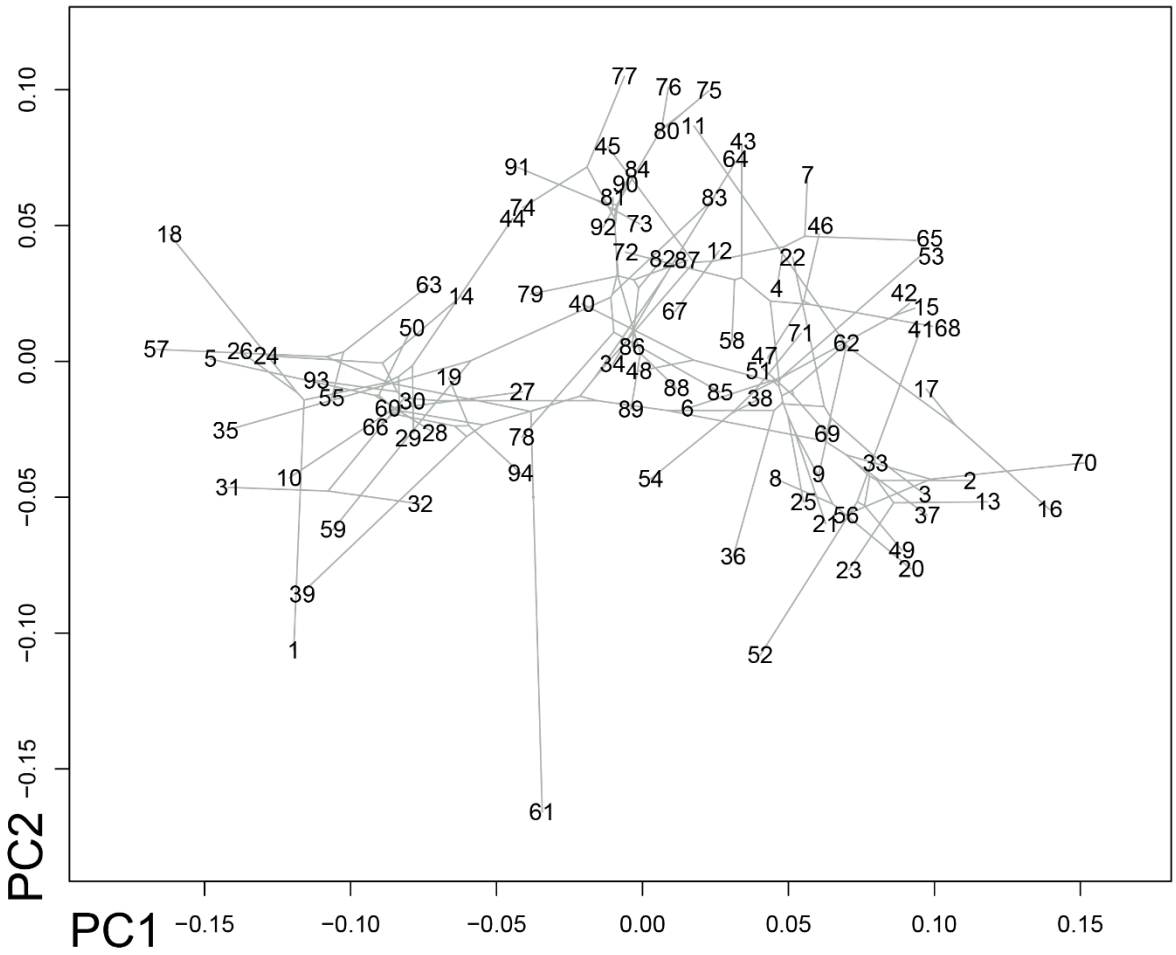

Supplemental Figure 3. Species spread on principal components 1 and 2 overlaying a phylogenetic tree. Species numbers are in alphabetical order and correspond to the caption of Supplemental Figure 2.

CITATIONS

1. Zaaf A, Van Damme R. Limb proportions in climbing and ground-dwelling geckos (Lepidosauria, Gekkonidae): A phylogenetically informed analysis. Zoomorphology. 2001;121:45–53.

2. Das I. Lizards of Borneo. Kota Kinabalu: Natural History Publications (Borneo) Sdn. Bhd.; 2004.

3. Yeboah S. Observations on territory of the rainbow lizard, Agama agama. Afr. J. Ecol. 1982;20:187–92.

4. Wiens JJ, Brandley MC, Reeder TW. Why Does a Trait Evolve Multiple Times Within a Clade? Repeated Evolution of Snakeline Body Form in Squamate Reptiles. Evolution (N. Y). [Internet]. 2006;60:123–41. Available from: http://www.ncbi.nlm.nih.gov/pubmed/16568638
5. La Marca E, Soriano P. Reptiles de los andes de venezuela. Mijares A, Esqueda LF, Perez JEG, Navarrete LF, editors. Merida: BIOGEOS; 2004.
6. Greenberg N, Crews D. Endocrine and behavioral responses to aggression and social dominance in the green anole lizard, Anolis carolinensis. Gen. Comp. Endocrinol. 1990;77:246–55.
7. Mitchell JC. Ecology of southeastern Arizona whiptail lizards (Cnemidophorus: Teiidae): population densities, resource partitioning, and niche overlap. Can. J Zool. 1979;57:1487–99.
8. Ord TJ, Blumstein DT, Evans CS. Ecology and signal evolution in lizards. Biol. J. Linn. Soc. 2002;77:127–48.
9. Tolley KA, Herrel A, editors. The biology of chameleons. Berkeley: University of California Press; 2014.
10. Fuentes ER. Ecological Convergence of Lizard Communities in Chile and California. Ecol. Soc. Am. 1976;57:3–17.
11. Esquerré D, Núñez H. Reptiles de la región metropolitana de Chile. 1st ed. Pedreros AM, editor. Valdiva: CEA Ediciones; 2017.
12. Campbell JA, Camarillo R. JL. A New Lizard of the Genus *Diploglossus* (Anguidae : Diploglossinae) from Mexico , with a Review of the Mexican and Northern Central American Species Author (s): Jonathan A . Campbell and José L . Camarillo R . Published by : Allen Press on behalf. Herpetologica. 1994;50:193–209.
13. Higham TE, Jayne BC. Locomotion of lizards on inclines and perches: hindlimb kinematics of an arboreal specialist and a terrestrial generalist. J. Exp. Biol. [Internet]. 2004;207:233–48. Available from: http://jeb.biologists.org/cgi/doi/10.1242/jeb.00763
14. Grismer LL. Amphibians and Reptiles of Baja California. Berkeley: University of California Press; 2002.
15. Branch. A Photographic Guide to Snakes and Other Reptiles of Southern Africa. Cape Town: Struik Publishers; 2002.
16. Badger D, Netherton J. Lizards : A Natural history of Some Uncommon creatures - Extraordinary Chameleons, Iguanas, Geckos, & More. Cornell K, editor. St. Paul: Voyageur Press; 2006.
17. Irschick DJ, Jayne BC. Comparative Three-Dimensional Kinematics of the Hindlimb for High-Speed Bipedal and Quadrupedal Locomotion of Lizards. J. Exp. Biol. 1999;202:1047–1065.

18. Duellman WE. The lives of Amphibians and reptiles in an Amazon rainforest. Bauer AM, editor. Ithica: Comstock Publishing Associates; 2005.
19. Cogger H. Reptiles and Amphibians of Australia. 7th ed. Collingswood: Csiro Publishing; 2014.
20. McCoy M. Reptiles of the Solomon Islands. Sofia: Pensoft Publishers; 2006.
21. Miranda JP, Ricci-Lobão A, Rocha CFD. Influence of structural habitat use on the thermal ecology of Gonatodes humeralis (Squamata: Gekkonidae) from a transitional forest in Maranhão, Brazil. Zool. (Curitiba, Impresso). 2010;27:35–9.
22. Tulli MJ, Cruz FB, Herrel A, Vanhooydonck B, Abdala V. The interplay between claw morphology and microhabitat use in neotropical iguanian lizards. Zoology [Internet]. Elsevier; 2009;112:379–92. Available from: http://dx.doi.org/10.1016/j.zool.2009.02.001
23. Glaw F, Vences M. A field guide to the amphibians and reptiles of Madagascar. Vences & Glaw; 2007.
24. Adolphs K, Bates MF. Cordylosaurus subtessellatus [Internet]. IUCN Red List Threat. Species 2010 e.T178341A7526963. 2010 [cited 2018 Jan 25]. Available from: http://dx.doi.org/10.2305/IUCN.UK.2010-4.RLTS.T178341A7526963.en
25. Davis DD. Behavior of the Lizard Corythophanes Cristatus. Fieldiana Zool. 1953;35:1–8.
26. Sunyer J. CGPLWLW, Solórzano A. Lepidophyma flavimaculatum [Internet]. IUCN Red List Threat. Species 2013 e.T197495A2490538. 2013 [cited 2018 Jan 25]. Available from: http://dx.doi.org/10.2305/IUCN.UK.2013-2.RLTS.T197495A2490538.en.
27. Nunez H. EP, Mella J. Liolaemus bellii [Internet]. IUCN Red List Threat. Species 2016 e.T56051706A56051708. 2016 [cited 2018 Jan 25]. Available from: http://dx.doi.org/10.2305/IUCN.UK.2016-1.RLTS.T56051706A56051708.en
28. Vences M. Phelsuma lineata [Internet]. IUCN Red List Threat. Species 2011 e.T172826A6925369. 2011 [cited 2018 Jan 25]. Available from: http://dx.doi.org/10.2305/IUCN.UK.2011-2.RLTS.T172826A6925369.en
29. Münchenberg T, Wollenberg KC, Glaw F, Vences M. Molecular phylogeny and geographic variation of Malagasy iguanas (Oplurus and Chalarodon). Amphibia-Reptilia. 2008;29:319–27.
30. Tikader BK, Sharma RC. Handbook of Indian Lizards. Calcutta: Zoological Survey of India; 1992.
31. Blanc CP, Carpenter CC. Studies on the Iguanidae of Madagascar III. Social and reproductive behavior of Chalarodon madagascariensis. J. Herpetol. JSTOR; 1969;125–34.
32. Vitt L, Magnusson W, Pires TCA, Lima AP. Guide to the lizards of Reserva Adolpho Ducke. Manaus: Áttema Design Editorial; 2008.

33. de Lisle HF. Behavioral ecology of the banded rock lizard (Petrosaurus mearnsi). Bull. South. Calif. Acad. Sci. 1991;90:102–17.
34. Breckenridge WJ. Reptiles and Amphibians of Minnesota. Minneapolis: The University of Minnesota Press; 1944.
35. Swan M, Watharow S. Snakes , Lizards and Frogs. Collingwood: Csiro Publishing; 2005.
36. Chester SR. A wildlife guide to Chile : continental Chile, Chilean Antarctica, Easter Island, Juan Fernández Archipelago. 1st ed. Princeton: Princeton University Press; 2008.
37. Laspiur A, Acosta JC, Abdala CS. A new species of Leiosaurus (Iguania: Leiosauridae) from central-western Argentina. Zootaxa. 2007;1470:47–57.
38. Bauer AM, Sadlier RA. The Herpetofauna of New Caledonia. Society for the Study of Amphibians and Reptiles, in cooperation with the Institut de recherche pour le développement; 2000.
39. Savage JM. The amphibians and reptiles of Costa Rica: A Herpetofauna between Two Continets, between Two Seas. Chicago: Uuniversity of Chicago Press; 2002;934.
40. Nguyen TQ, Hamilton P, Ziegler T. Shinisaurus crocodilurus [Internet]. IUCN Red List Threat. Species 2014 e.T57287221A57287235. 2014 [cited 2017 Aug 18]. Available from: http://dx.doi.org/10.2305/IUCN.UK.2014-1.RLTS.T57287221A57287235.en
41. Pianka ER, Pianka HD. Comparative Ecology of Twelve Species of Nocturnal Lizards (Gekkonidae) in the Western Australian Desert. Copeia. 1976;1976:125–42.
42. Auliya M. Takydromus sexlineatus [Internet]. IUCN Red List Threat. Species 2010 e.T178424A7544274. 2010. Available from: http://dx.doi.org/10.2305/IUCN.UK.2010-4.RLTS.T178424A7544274.en
43. Wilms, T., Eid, E.K.A., Al Johany, A.M.H., Amr, Z.S.S., Els, J., Baha El Din, S., Disi, A.M., Sharifi, M., Papenfuss, T., Shafiei Bafti, S. & Werner YL. Uromastyx aegyptia (errata version published in 2017) [Internet]. IUCN Red List Threat. Species 2012 e.T164729A115304711. 2017 [cited 2017 Aug 18]. Available from: http://dx.doi.org/10.2305/IUCN.UK.2012.RLTS.T164729A1071308.en
44. Köhler G. Reptiles of Central America. Offenbach: Herpeton Verlag; 2003.
45. Winton WM. Habits and Behavior of the Texas Horned Lizard, Phrynosoma cornutum, Harlan. I. Copeia. 1916;36:81–4.
46. Perez SI, Bernal V, Gonzalez PN. Differences between sliding semi-landmark methods in geometric morphometrics, with an application to human craniofacial and dental variation. J. Anat. 2006;208:769–84.

Chapter 5 Semicircular Canals of Reptiles

5.1 Shape and size of semicircular canals correlate with clade and body mass in reptiles

Ashley E. Latimer[1,2], Timothée Bonnet[2], Emma Sherratt[3], Torsten M. Scheyer[1]

[1]University of Zurich, Department of Paleontology, Karl Schmid-Strasse 4, Zurich, CH-8006, Switzerland

[2] Australian National University, Canberra ACT 0200 Australia

[3] The University of Adelaide, Adelaide SA 5005Australia

Image: Saltwater Crocodile (*Crocodylus porosus*)
Ashley Latimer, Daintree 2017
Photograph

Author contributions AEL designed the study, collected data, did analyses, wrote the paper, ES provided data, TB contributed to statistical analysis and interpretation, TMS and TB read and contributed to the paper.

ABSTRACT

The semicircular canals, also called the bony labyrinth, are the sensory system responsible for balance in all vertebrates. The shape and size of these canals have been associated with life habits including environment and locomotion. Few predictive models associating life history traits with labyrinth size and shape exist for reptiles. Here we investigate the association between labyrinth size and shape with phylogeny, habit, and body mass of 119 extant and extinct reptiles including lepidosaurs, archosaurs, turtles, and Sauropterygians. Three-dimensional morphometrics and linear models suggest the major components of semicircular canal shape are phylogenetic and do not predict semiaquatic life habit in reptiles. Habit also fails to predict labyrinth size, as a measure of labyrinth length. Labyrinth length predicts body mass in all reptiles, confirming previous studies. We use labyrinth length to predict body mass for extinct taxa and unknown taxa, and highlight the limitations predicting body mass in taxa of different body morphology. We show habit is not a good predictor for labyrinth shape and our results support the idea that habit should not be inferred from labyrinth shape across disparate reptilian lineages. We argue that labyrinth length alone does not predict locomotor style, but instead when combined with body mass estimates may reveal convergence on pelagic lifestyles.

INTRODUCTION

Comparative anatomy of living species is necessary to reconstruct life history and organism morphology of extinct species from fossils. Semicircular canals are popularly used for such inferences. Semicircular ducts are the soft tissue sensory system responsible for balance and orientation in the inner ear. Head rotations, body movement and jostling from the environment all cause fluid to move inside ducts, displacing a jelly-like cup over sensitive hairs that register the motion, which is sent to the brain and interpreted together with eye movement [1]. The semicircular canals are the trace of the ducts, and their surrounding fluid, in the bones of the skull, and the mazelike structure is frequently called the bony labyrinth. The semicircular canals fossilize when a skull is preserved, and are readily visible to three-dimensional computed tomography imaging, all without harming the sample.

Morphology of semicircular canals has been associated with locomotion, life history, and phylogeny in mammals both living and extinct e.g. [2–18]. The inner ears of living reptiles are less frequently studied [19–27] and lack models relating phylogeny, morphology, and life history. Like mammals, previous studies of reptiles suggest that ducts of different shape are purportedly sensitive to different motions and thus the shape of the canals should correspond with how an organism lives and moves, its life habits [19,20,28]. Chapter 3 and other work [22] suggest phylogenetic signal in squamates semicircular canal shape dominates contributions from life habit, and histology of the lagenar soft tissues correspond with strong

phylogenetic signal [29]. In Chapter 3, the only habit corresponding with the inner ear was semiaquatic habit, e.g. taxa that live near water and swim sometimes.

The Semicircular canals carry information in size as well as shape. Length of the bony labyrinth has also been associated with the water depth and locomotor activity in the habitat used by extinct marine reptiles [24]. In that study, taxa with larger labyrinths are correlated to deeper water and free-swimming locomotion, using labyrinth lengths from disparately related reptiles. Elsewhere, dimensions of the inner ears have been correlated to body mass of vertebrates which is under phylogenetic control [30,31], and body mass has been further related to semiaquatic habit in reptiles [32]. Chapter three also found specifically that semiaquatic squamates may have larger centroid sizes than non-semiaquatic taxa. We suggest the interaction between body mass and locomotor activity should be further investigated with a larger taxonomic sampling of living taxa with similar body proportions.

Here we investigate the first order differences in canal shape in reptiles and test if they are predicted by habit, size, or phylogeny. Based on semicircular canal shape, we make phylogenetic predictions for Sauropterygia. Second, we identify a relationship between mass and labyrinth length, and use that relationship to propose a model predicting body mass for reptiles. We compare the real body mass of extant species with the predicted values, and predict body mass for extinct and extant reptiles. We account for the influence of semiaquatic habit on labyrinth length in body mass estimates, and discuss validity of various interpretations of the data.

METHODS

We investigate semicircular canals of reptiles from the Triassic to the present including lepidosaurs, turtles, archosauromorphs, and sauropterygians. Endocasts from 95 squamates, *Sphenodon punctatus*, five turtles (*Agrionemys horsfieldii*, *Apalone mutica*, *Chrysemys picta*, *Malacochersus tornieri*, *Chelus fimbriata*), and five extant crocodylians (*Caiman crocodilus*, *Mecistops cataphractus*, *Crocodylus moreletii*, *Osteolaemus tetraspis*, *Tomistoma schlegelii*) were digitally sectioned and extracted as a proxy for the soft tissue semicircular canals in VG StudioMax 2.2 and Slicer 4.8.0 (Appendix). The extant *Malacochersus* was included from [33,34]. Labyrinth endocasts from turtles *Lepidochelys olivacea* and *Macrochelys temminckii*, the marine reptiles *Augustasaurus hagdorni, Callawayasaurus colombiensis, Libonectes morgani, Macroplata tenuceps, Microcleidus homalospondylus, Nothosaurus sp., Peloneustes philarcus, Placodus gigas, and Simosaurus gaillardoti*, and the Triassic archosauriform *Euparkeria capensis* were sourced from published work [24,35,36], and right labyrinths were mirrored. Labyrinth length was measured from the rostral-most point of the anterior canal to the caudal-most point of the posterior canal, along a line parallel to the horizontal canal. The

central streamline of each semicircular canal were landmarked using the methods described in (Chapter 3, Latimer) using the Meshtools program [37].

Species were split in two categories, semiaquatic/aquatic, or not, depending on their lifestyle. Semiaquatic/aquatic taxa spend time around and swimming in water or spend most of their lives in water. Information for each species' habit came from a variety of sources, cited in the appendix. For extinct taxa these habits are approximated from body morphology and geology in the literature according to [24,36]. Measurements for body mass and snout-vent length (SVL) for each species are listed in the supplement. In lieu of SVL, curved carapace length was used for turtles where available.

All analyses were run using R [38]. To identify contribution of habit and phylogeny to shape we imported landmarked streamlines for the semicircular canals of each species to R in a three-dimensional array, and used the package geomorph for a generalized procrustes analysis to align the landmarks and remove effects of size. Next, we used the function plotTangentSpace, from the package geomorph, to visualize of habit and phylogeny on the first two principal components which explain the most variation [39]. Then, to test for an association between semiaquatic/aquatic habit and semicircular canal shape, we used a phylogenetic least squares (PGLS) analysis for high dimensional data (geomorph: procD.PGLS), to see if semiaquatic habit predicts labyrinth shape [39,40].

To test for phylogenetic signal in labyrinth shape, ultrametric Phylogenetic trees from crocodylians [41], turtles [42], and squamates [43] were pruned to the taxa listed in the appendix using the package ape and function drop.tip in R. A supertree was then assembled by hand in the same topology to remain ultrametric, arbitrarily increasing the length of the branch below Crocodylia to match the length of the turtle tree, and increasing the branch leading to squamates to equal the length of Archelosauria [44]. Phylogenetic signal in the shape of the semicircular canals was identified using physignal in the package geomorph, resulting in a value of K which shows how well a model fits a Brownian motion model of evolution. Values close to one suggest a variation is as expected under Brownian motion.

To test if labyrinth length predicts body mass or SVL in reptiles, we used linear models. Our most simple model predicted the natural log body mass as a linear function of labyrinth length (slope with an intercept). To test the effect of semiaquatic habit on the relationship between labyrinth length and log body mass, we fitted the interaction between labyrinth length and habit (semiaquatic/aquatic or not). Two outliers, *Chrysemys picta* and *Coleonyx variegatus*, identified by the model were excluded from the following predictive models. Two more models were tested in order to find a better prediction for the relationship between body mass and labyrinth length: a quadratic model of labyrinth length predicting log body mass (quadratic: natural log body mass as a function of labyrinth length and Labyrinth length squared); and a model log body mass and log labyrinth length (natural log body mass

as a function of natural log labyrinth length). In particular, these models allowed us to test whether the effect of habit on the relationship between labyrinth length and body mass is genuine, or whether it is an artifact of the larger sizes of semi-aquatic species. All models were compared using AICc, a version of the Akaike information criterion corrected for small sample sizes [45]. We retained a final model based on AICc and ability to extrapolate body mass above the range observed in our dataset.

To test the predictive ability of the final model with taxa of known body mass, we predicted the body mass for two squamates, *Leiolepis triploida* and *Platysaurus imperator*, that were not used to create the predictive model. Finally, we used the final model to predict body mass of living and extinct taxa where body mass is unknown using labyrinth length.

RESULTS

Taxa clustered by clade on the first two principal components from shape of the semicircular canals (proportion of variance PC1= 58.01%, PC2= 11.591%, PC3= 7.248%). Shape is predicted by phylogenetic relatedness, as is readily seen in (Figure 1). The phylogenetic signal in the aligned coordinates ($K=1.065$ $p<.001$) is consistent with a Brownian motion model of evolution. Clear phylogenetic groups are seen primarily on PC1 for the large clade differentiation (lepidosaurs, sauropterygians, archelosaurs). Smaller clades are differentiated on principal component 2 (squamate clades, testudines vs. crocodylians) which account for less variation.

When corrected for phylogeny, PGLS reports in no power of semiaquatic habit to predict semicircular canal shape (R^2=4.568% $p=0.324$) among extant taxa represented in the tree (Figure 2), revealing the concentration of semiaquatic taxa for positive values of PC1 is a phylogenetic and sampling artifact.

Results of the ΔAICc are shown on Table 1. Although the ΔAICc finds the quadratic model the best fit for the data, and thus the best predictor for body mass of taxa that fall within the sampled body range, estimates of body mass outside that range, such as for large marine reptiles are biologically improbable (Figure 3). A more biologically probable model for body mass estimation is log mass predicted by log labyrinth length (Figures 3 and 4) used in the subsequent models for body mass estimation. Linear models of log body mass and labyrinth length for semiaquatic and non-semiaquatic taxa differ in slope and intercept (Figure 3). These differences however may be due to the size difference between semiaquatic and non-semiaquatic taxa in that sample, semiaquatic taxa are larger (R^2 = 22.13%, $P < 0.001$). Habit does not improve the predictive ability of the quadratic models (change in AICc when including habit: 0.04) and log models (change in AICc when including habit: 1.45).

Body masses predicted by the log model for *Platysaurus imperator* and *Leiolepis triploida,* known extant squamates, are in Table 2A. Body mass predictions for species of unknown body mass are on Table 2B, including the extant crocodile *Crocodylus moreletii*, the extinct archosauriform *Euparkeria capensis,* and sauropterygian reptiles. A comparison of the real body masses and predicted body masses for the taxa used to make the model is available in the supplement.

DISCUSSION

Semicircular canal shape

Further extending the conclusions of Latimer (Chapter 2 and 3) and in agreement with published literature, semicircular canal shape is a good predictor of phylogenetic group across distantly related taxa, in this case reptiles. The species clusters predict phylogenetic sister groups of all taxa consistent with current phylogenetic hypotheses [43,44,46]: *Euparkeria* with crocodylians, turtles and crocodylians within Archelosauria, and squamates and tuatara within Lepidosauria. Using qualitative visual distances between the point clusters, the data suggest that sauropterygians are more closely related to Archelosauria than to Lepidosauria. The results proposed here, while qualitative, could be quantitively tested using a time calibrated ultrametric tree for reptiles including all taxa, which was not available for this study.

Semicircular canal shape does not converge across distantly related reptiles by habit. Although a greater proportion of aquatic taxa are on the right-hand size of principal component 1 (Figure 2), PGLS shows this is related to phylogeny; all crocodiles are semiaquatic and all sauropterygian reptiles are marine. As highlighted elsewhere [25], reptiles lack a comparative sample of diverse, extant marine species with which to contrast convergent pelagic morphologies. This reduces the predictive power of the current dataset for pelagic-only species, and forces us to group all swimming and semiaquatic species in one. With this dataset, however, we can state there is no convergent ear morphology for all reptiles that swim.

Labyrinth length

Semicircular canal size, as measured by labyrinth length, is not correlated with habit in our dataset. The interaction between habit and labyrinth length in linear models is an artifact of sampled semiaquatic taxa having larger body mass than non-aquatic species, partitioning size classes between those parts of the dataset (Figure 3). Semiaquatic and aquatic reptiles are larger than their non-aquatic counterparts, likely due to thermal benefits (Chapter 3) [32]. This artifact is removed by modeling a non-linear relationship between labyrinth length and size with a quadratic or a logarithmic mode. Model selection criterion AICc does not support including habit as a predictor for body mass in non-linear models. Labyrinth length alone,

therefore, should not be used to predict semiaquatic habit across large phylogenetic groups of reptiles.

Instead, labyrinth length predicts body mass in reptiles. While the log model has a lower fit (R^2= 83.92) than the quadratic model (R^2= 86.12%), the log model can predict biologically informative body mass estimates for taxa exceeding the largest extant reptiles used to create the model (e.g. sauropterygians). Given that labyrinth length predicts body mass, and the extinct pelagic taxa are larger, we would expect pelagic taxa to have large labyrinths, however body mass estimates for the marine reptiles show some striking irregularities. This is exemplified by the case of long-necked plesiosaur *Libonectes morgani* with a smaller estimated body than the short-necked mosasaur *Simosaurus gaillardoti*, despite a larger skull and a body potentially twice the length of *S. gaillardoti*.

One explanation for shrinking labyrinth length in larger taxa could be body proportions. Extant taxa in the log model for body mass estimation all have a similar body plans and proportions; they are quadrupedal and have necks rarely exceeding the length of the head, although turtles have a shell. We may expect less efficacy of body mass predictions for taxa that differ from this, e.g. long necked marine reptiles. While effects of neck-body proportions are not known for estimates of body mass from labyrinth length, hypotheses in the literature suggest taxa with shorter necks may result in smaller canal radii [24,25] or long necks may have a smaller head to body ratio, and therefore may have smaller labyrinth lengths in proportion to the body. These ideas are not supported by the current data. Basicranial lengths of the marine reptiles [24] suggest that the inner ear is smaller than the skull length alone would predict, suggesting it is not just a shrinking skull. Neck length also appears unrelated. Convergent reductions in semicircular canal radius in the Ross seal are not associated with an increase or decrease in neck length [18], whales are associate with decreasing neck length [47], and pelagic Sauropterygians with long necks. This evidence from mammals and relative skull morphology suggests the cause is not body morphology, but may be something related to pelagic habit.

The second explanation is pelagic taxa convergently reduce the radius of the semicircular canals of the inner ears, seen in *Libonectes morgani*, *Macroplata tenuiceps* (Supplemental Figure 1), cetaceans [47], and the Ross seal [18], independent of neck length. Pelagic reptiles in this dataset have semicircular canals characterized by reduced canal radius and canal length as seen in pelagic mammals, although they retain the taxonomic shape of their canals. The reduced canal radius changes shape and size in a way unique to each taxon based on existing size and morphology. This is not detected by landmarks of the streamline, but could be detected by comparing the ratios of labyrinth length to the internal radius of the semicircular canals of close relatives to the pelagic taxa. *Lepidochelys olivacea* is the only extant pelagic reptile in this dataset, limiting comparisons of body mass and habit of living taxa. The

morphological convergence of the inner ears is indisputable, and most likely cause appears to be convergent pelagic adaptation independent of body morphology.

Labyrinth length as a predictor for locomotor strategy

If labyrinth lengths of pelagic taxa are convergently large as suggested [24], we would expect pelagic taxa to have larger labyrinths than their non-pelagic relatives, and show similar trends versus body mass. In the pelagic sea turtle, the olive Ridley (*Lepidochelys olivacea*), the labyrinth is long relative to its body mass among turtles, but in pelagic Sauropterygian *Libonectes morgani* the labyrinth is short for the body mass compared to less-pelagic sauropterygians (e.g. *Simosaurus gaillardoti*). These opposite relationships suggest locomotion type does not cause uniform changes across groups of reptiles.

Furthermore, the results of [24] paper may be interpreted differently. First, the locomotor groups overlap with the phylogenetic groups. Even if any predictive power of labyrinth size was attributed to this locomotor style, the effects of locomotor style and phylogeny would be indistinguishable in that model, particularly because the model is not corrected for phylogeny. In Chapter 3 we showed that phylogenetic signal in shape is strong, as is phylogenetic signal in body size, further suggesting that phylogeny predict size better than locomotor group. This nullifies the results that locomotor style is related to labyrinth length. Second, the results of that paper do not contain a clear signal of an effect of swimming or neck length on labyrinth length as evidenced by AICc scores- the null model has better predictive power than models including swimming and neck length. We argue here that labyrinth size is likely a function of body mass and not a function of locomotor style.

Error and limitations

There is measurement error in this dataset, particularly because body mass and labyrinth length are not from the same individual. We used opportunistic CT data and scanned without associated wet mass information. Instead, maximum weights from the literature were used with ears that are likely from individuals smaller than the maximum record. The correlation between body mass and labyrinth length could be improved if both measurements came from the same individual for each clade in the predicted model. This could help answer a fundamental developmental and allometric question: do the semicircular canals of reptiles reach maximum size early in development, or does it scale with body mass during life. With that questioned answered, estimates of body mass from labyrinth length would better predict the size of individuals. Additionally, adding large taxa to the dataset, particularly large crocodylians, would improve estimates for the largest taxa. For this reason, the body masses predicted by this model for the larger marine reptiles as shown in Figure 4 have an exceptionally wide confidence interval.

We include this further comment on body morphology. While reptiles in this dataset are limbed and mostly quadrupedal, *Euparkeria* and *Basilisk* are believed to be occasionally bipedal. They both fit the general trends expected from phylogeny and Basilisk fits directly on the line of best fit for body mass estimation in the log model. This suggests occasional bipedalism does not prevent recovery of the observed trends. Greater inclusion of obligatory bipedal taxa could confirm that labyrinth length can predict body mass those taxa.

A final note concerns the time from which these taxa are sampled, taxa in this dataset span from Triassic to the present. The influence of phylogeny on shape is related to the time taxa have been evolving independently. Among extant taxa, all species have been evolving for the same amount of time, and precisely equal to their sister groups. The comparison between Cretaceous *Libonectes morgani* is millions of years removed from Triassic *Simosaurus gaillardoti*. *L. morgani* and *S. gaillardoti* inherited an inner ear from a common ancestor, but *Libonectes* had millions of years longer to innovate on that morphology. *Lepidochelys olivacea* has had the same amount of time as its most recent common ancestor with other turtles to innovate on its own ear. Phylogenetic correction relies on ultrametric trees to remove the effect of shared phylogeny, but it is not possible with unequal branch lengths, and the interpretation of such morphology should be carefully considered when contrasting convergence within one lineage, here Sauropterygia.

CONCLUSIONS

We tested the ability of shape and size of the inner ear in reptiles to predict phylogeny, habit, and body mass. Our results exclude habit as a useful predictor of shape and size of the semicircular canals in our dataset. Labyrinth shape may be used as a predictor for phylogenetic relationship in reptiles but should not be used to infer swimming or semiaquatic habits of extinct taxa without living close relatives. Labyrinth length is a powerful predictor of body mass for both living and extinct reptiles. The models could be further improved with more taxa and better estimates of body mass for the individuals included, and has the potential to estimate body masses for species known only by partial skull material without any destructive sampling. Head-body proportions remain to be tested among the dinosaur-bird clade to extend the usefulness of labyrinth length as a predictor for body mass for those taxa.

A benefit of using labyrinth length over centroid size or shape is the measurement is its technical simplicity. A measurement only requires a CT scan, and would not require the entire labyrinth to be preserved or sectioned in order to measure the length from reptiles to predict their body mass.

ACKNOWLEDGEMENTS

Semicircular Canals of Reptiles

Thanks to Jessie Maisano and Matthew Colbert (Digimorph) and Alexandra Wegman (Zurich) for scan data, and Gabriela Sobral for the semicircular canal surface model of *Euparkeria capensis*. Thanks to J. Scott Keogh (ANU), Swiss National Science Foundation grant 31003A-149506 and 173173 to Torsten M. Scheyer, M. Sánchez, and T. Rowe's NSF Digital Libraries Grant.

REFERENCES

1. Henn V. 1988 Visual-Vestibular Interaction. In *Sensory Systems I Vision and Visual Systems* (ed G Aldeman), pp. 114–115. Basel: Birkhäuser. (doi:978-1-4899-6647-6)
2. Hullar TE. 2006 Semicircular canal geometry, afferent sensitivity, and animal behavior. *Anat. Rec. Part a-Discoveries Mol. Cell. Evol. Biol.* **288a**, 466–472. (doi:10.1002/ar.a.20304)
3. Grohe C, Tseng ZJ, Lebrun R, Boistel R, Flynn JJ. 2016 Bony labyrinth shape variation in extant Carnivora: a case study of Musteloidea. *J. Anat.* **228**, 366–383. (doi:10.1111/joa.12421)
4. Grohé C, Lee B, Flynn JJ. 2018 Recent inner ear specialization for high-speed hunting in cheetahs. , 1–8. (doi:10.1038/s41598-018-20198-3)
5. Kemp AD, Kirk EC. 2014 Eye Size and Visual Acuity Influence Vestibular Anatomy in Mammals. *Anat. Rec. Integr. Anat. Evol. Biol.* **297**, 781–790. (doi:10.1002/ar.22892)
6. Kirk EC, Hoffmann S, Kemp AD, Krause DW, O'Connor PM. 2014 Sensory Anatomy and Sensory Ecology of *Vintana Sertichi* (Mammalia, Gondwanatheria) from the Late Cretaceous of Madagascar. *J. Vertebr. Paleontol.* **34**, 203–222. (doi:10.1080/02724634.2014.963232)
7. Gunz P, Ramsier M, Kuhrig M, Hublin JJ, Spoor F. 2012 The mammalian bony labyrinth reconsidered, introducing a comprehensive geometric morphometric approach. *J. Anat.* **220**, 529–543. (doi:10.1111/j.1469-7580.2012.01493.x)
8. Ekdale EG. 2016 Form and function of the mammalian inner ear. *J. Anat.* **228**, 324–337. (doi:10.1111/joa.12308)
9. Davies KTJ, Bates PJJ, Maryanto I, Cotton JA, Rossiter SJ. 2013 The Evolution of Bat Vestibular Systems in the Face of Potential Antagonistic Selection Pressures for Flight and Echolocation. *PLoS One* **8**, 8–10. (doi:10.1371/journal.pone.0061998)
10. Graf W, Vidal P-P. 1996 Semicircular canal size and upright stance are not interrelated. *J. Hum. Evol.* **30**, 175–181. (doi:10.1006/jhev.1996.0017)
11. Schmelzle T, Sánchez-Villagra MR, Maier W. 2007 Vestibular labyrinth diversity in diprotodontian marsupial mammals. *Mammal Study* **32**, 83–97. (doi:10.3106/1348-6160(2007)32[83:VLDIDM]2.0.CO;2)

12. Costeur L. 2014 The petrosal bone and inner ear of Micromeryx flourensianus (Artiodactyla, Moschidae) and inferred potential for ruminant phylogenetics. *Zitteliana R. B Abhandlungen der Bayer. Staatssammlung fur Palaontologie und Geol.* **32**, 99–114.
13. Lebrun R, de León MP, Tafforeau P, Zollikofer C. 2010 Deep evolutionary roots of strepsirrhine primate labyrinthine morphology. *J. Anat.* **216**, 368–380. (doi:10.1111/j.1469-7580.2009.01177.x)
14. David R, Droulez J, Allain R, Berthoz A, Janvier P, Bennequin D. 2010 Motion from the past. A new method to infer vestibular capacities of extinct species. *Comptes Rendus Palevol* **9**, 397–410. (doi:10.1016/j.crpv.2010.07.012)
15. Ekdale EG. 2013 Comparative Anatomy of the Bony Labyrinth (Inner Ear) of Placental Mammals. *PLoS One* **8**, 27–28. (doi:10.1371/journal.pone.0066624)
16. Alloing-Séguier L, Sánchez-Villagra MR, Lee MSY, Lebrun R. 2013 The Bony Labyrinth in Diprotodontian Marsupial Mammals: Diversity in Extant and Extinct Forms and Relationships with Size and Phylogeny. *J. Mamm. Evol.* **20**, 191–198. (doi:10.1007/s10914-013-9228-3)
17. Crumpton N, Kardjilov N, Asher RJ. 2015 Convergence vs. Specialization in the ear region of moles (mammalia). *J. Morphol.* **276**, 900–914. (doi:10.1002/jmor.20391)
18. Loza CM, Latimer AE, Sánchez-Villagra MR, Carlini AA. 2017 Sensory anatomy of the most aquatic of carnivorans: the Antarctic Ross seal, and convergences with other mammals. *Biol. Lett.* **20170489**. (doi:http://dx.doi.org/10.1098/rsbl.2017.0489)
19. Boistel R, Herrel A, Lebrun R, Daghfous G, Tafforeau P, Losos JB, Vanhooydonck B. 2011 Shake rattle and roll: The bony labyrinth and aerial descent in squamates. *Integr. Comp. Biol.* **51**, 957–968. (doi:10.1093/icb/icr034)
20. Boistel R, Herrel A, Daghfous G, Libourel P-A, Boller E, Tafforeau P, Bels V. 2010 Assisted walking in Malagasy dwarf chamaeleons. *Biol. Lett.* **6**, 740–743. (doi:10.1098/rsbl.2010.0322)
21. Dickson B V., Sherratt E, Losos JB, Pierce SE. 2017 Semicircular canals in *Anolis* lizards: ecomorphological convergence and ecomorph affinities of fossil species. *R. Soc. Open Sci.* **4**, 170058. (doi:10.1098/rsos.170058)
22. Palci A, Hutchinson MN, Caldwell MW, Lee MSY. 2017 The morphology of the inner ear of squamate reptiles and its bearing on the origin of snakes. *R. Soc. Open Sci.* **4**, 170685. (doi:10.1098/rsos.170685)
23. Witmer LM, Ridgely RC. 2009 New insights into the brain, braincase, and ear region of tyrannosaurs (Dinosauria, Theropoda), with implications for sensory organization and behavior. *Anat. Rec.* **292**, 1266–1296. (doi:10.1002/ar.20983)

Semicircular Canals of Reptiles
24. Neenan JM, Reich T, Evers SW, Druckenmiller PS, Voeten DFAE, Choiniere JN, Barrett PM, Pierce SE, Benson RBJ. 2017 Evolution of the Sauropterygian Labyrinth with Increasingly Pelagic Lifestyles. *Curr. Biol.* , 1–7. (doi:10.1016/j.cub.2017.10.069)
25. Spoor F, Thewissen JGM. 2008 Comparative and Functional Anatomy of Balance in Aquatic Mammals. *Sens. Evol. Threshold Adapt. Second. Aquat. Vertebr.* , 257–284.
26. Yi H, Norell MA. 2015 The burrowing origin of modern snakes. *Sci. Adv.* **1**, 1–5. (doi:10.1126/sciadv.1500743)
27. Brusatte SL, Muir A, Young MT, Walsh S, Steel L, Witmer LM. 2016 The Braincase and Neurosensory Anatomy of an Early Jurassic Marine Crocodylomorph: Implications for Crocodylian Sinus Evolution and Sensory Transitions. *Anat. Rec.* **299**, 1511–1530. (doi:10.1002/ar.23462)
28. Georgi JA, Sipla JS. 2008 Comparative and Functional Anatomy of Balance in Aquatic Reptiles and Birds. *Sens. Evol. Threshold Adapt. Second. Aquat. Vertebr.* , 233–256.
29. Schmidt RS. 1964 Phylogenetic Significance of Lizard Cochlea Author. *Am. Soc. Ichthyol. Herpetol.* **1964**, 542–549.
30. Bernacsek GM, Carroll RL. 1981 Semicircular canal size in fossil fishes and amphibians. *Can. J. Earth Sci.* **18**, 150–156. (doi:10.1139/e81-012)
31. Jones GM, Spells KE. 1963 A theoretical and comparative study of the functional dependence of the semicircular canal upon its physical dimensions. *Proc. R. Soc. London. Ser. B* **157**, 403–419. (doi:10.1098/rspb.1963.0019)
32. Meiri S. 2010 Length-weight allometries in lizards. *J. Zool.* **281**, 218–226. (doi:10.1111/j.1469-7998.2010.00696.x)
33. Mautner A-K, Latimer AE, Uwe F, Schey. 2017 3D data and models related to the publication: An updated description of the osteology of the pancake tortoise Malacochersus tornieri (Testudines: Testudinidae) with special focus on intraspecific variation. *MorphoMuseuM* **2**, 2–4.
34. Mautner A-K, Latimer AE, Fritz U, Scheyer TM. 2017 An updated description of the osteology of the pancake tortoise *Malacochersus tornieri* (Testudines: Testudinidae) with special focus on intraspecific variation. *J. Morphol.* **278**, 321–333. (doi:10.1002/jmor.20640)
35. Neenan JM, Reich T, Evers SW, Druckenmiller PS, Voeten DFAE, Choiniere JN, Barrett PM, Pierce SE, Benson RBJ. 2017 3D models related to the publication: Evolution of the sauropterygian labyrinth with increasingly pelagic lifestyles. *MorphoMuseuM* **4**, 1–3. (doi:10.18563/journal.m3.62)
36. Sobral G, Sookias RB, Bhullar B-AS, Smith R, Butler RJ, Müller J. 2016 New information on the braincase and inner ear of *Euparkeria capensis* Broom: implications for diapsid and archosaur evolution. *R. Soc. Open Sci.* **3**, 160072. (doi:10.1098/rsos.160072)

37. Lebrun R. 2014 ISE-Meshtools, a 3D interactive fossil reconstruction freeware. In *12th Annual Meeting of EAVP, Tornio, Italy*,
38. R core team. 2014 R: A Language and Environment for Statistical Computing.
39. Adams DC, Otarola-Castillo E. 2013 geomorph: an R package for the collection and analysis of geometric morphometric shape data. *Methods Ecol. Evol.* **4**, 393–399.
40. Orme D, Freckleton R, Thomas G, Petzoldt T, Fritz S, Isaac N, Pearse W. 2013 caper: Comparative Analyses of Phylogenetics and Evolution in R.
41. Oaks JR. 2011 A time-calibrated species tree of crocodylia reveals a recent radiation of the true crocodiles. *Evolution (N. Y).* **65**, 3285–3297. (doi:10.1111/j.1558-5646.2011.01373.x)
42. Pereira AG, Sterli J, Moreira FRR, Schrago CG. 2017 Multilocus phylogeny and statistical biogeography clarify the evolutionary history of major lineages of turtles. *Mol. Phylogenet. Evol.* **113**, 59–66. (doi:10.1016/j.ympev.2017.05.008)
43. Zheng Y, Wiens JJ. 2016 Combining phylogenomic and supermatrix approaches, and a time-calibrated phylogeny for squamate reptiles (lizards and snakes) based on 52 genes and 4162 species. *Mol. Phylogenet. Evol.* **94**, 537–547. (doi:10.1016/j.ympev.2015.10.009)
44. Crawford NG, Parham JF, Sellas AB, Faircloth BC, Glenn TC, Papenfuss TJ, Henderson JB, Hansen MH, Simison WB. 2015 A phylogenomic analysis of turtles. *Mol. Phylogenet. Evol.* **83**, 250–257. (doi:10.1016/j.ympev.2014.10.021)
45. Burnham KP, Anderson DR. 2003 Model selection and multimodel inference: a practical information-theoretic approach. Springer Science & Business Media.
46. Chiari Y, Cahais V, Galtier N, Delsuc F. 2012 Phylogenomic analyses support the position of turtles as the sister group of birds and crocodiles (Archosauria). *BMC Biol.* **10**. (doi:10.1186/1741-7007-10-65)
47. Spoor F, Bajpal S, Hussaim ST, Kumar K, Thewissen JGM. 2002 Vestibular evidence for the evolution of aquatic behaviour in early cetaceans. *Nature* **417**, 163–166. (doi:DOI 10.1038/417163a)

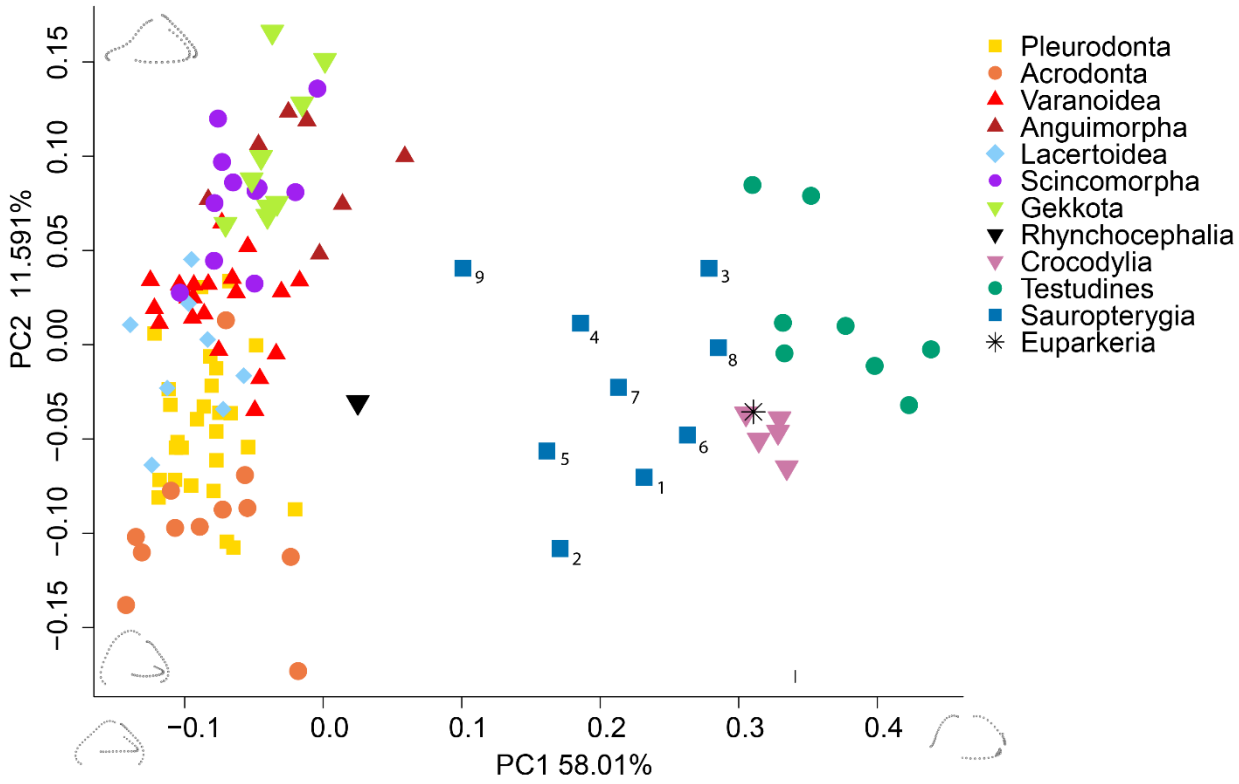

Figure 1. Species cluster by clade on the first two principal components of semicircular canal shape. Species are colored according to phylogenetic group. Marine reptiles (blue): 1 *Augustasaurus hagdorni, 2 Callawayasaurus colombiensis, 3 Libonectes morgani,* 4 *Macroplata tenuiceps, 5 Microcleidus homalospondylus, 6 Nothosaurus sp., 7 Peloneustes philarcus, 8 Placodus gigas, 9 Simosaurus gaillardoti*

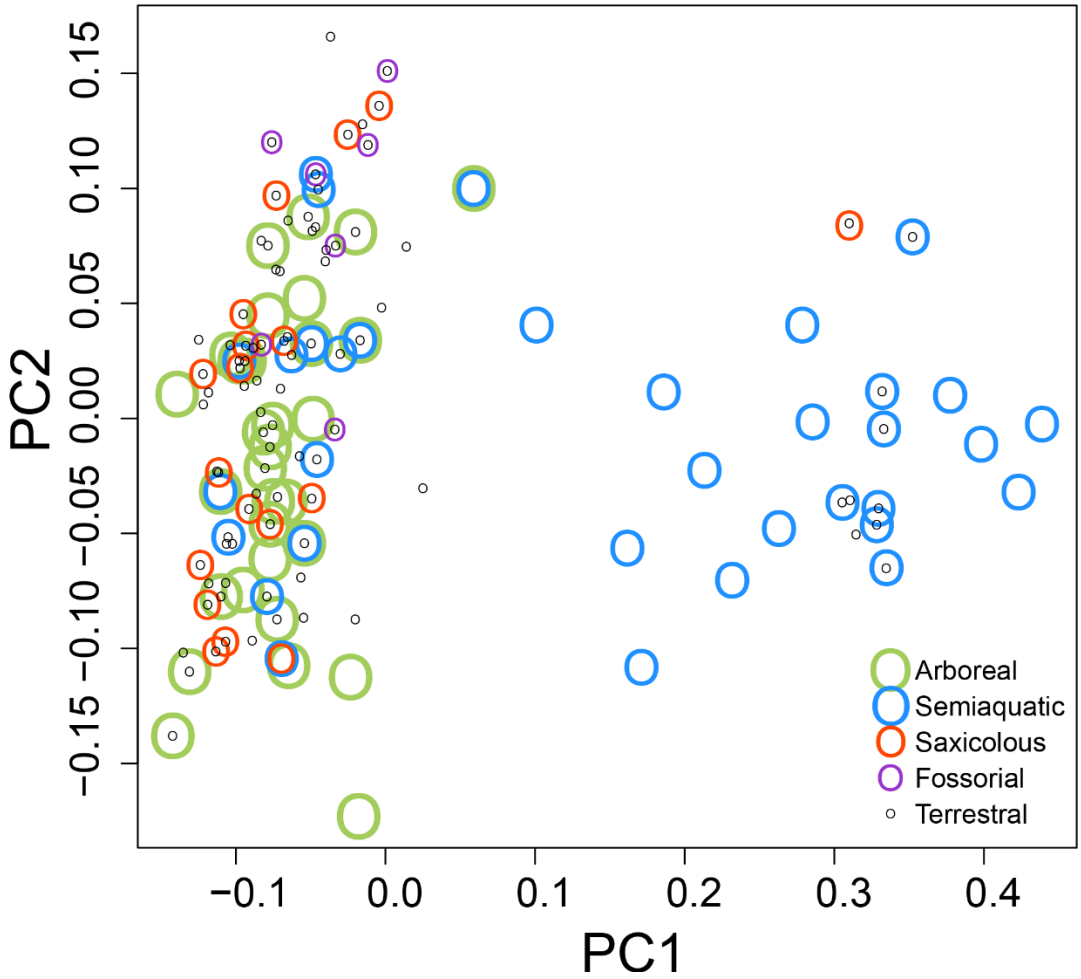

Figure 2. Habits of reptiles, a species may have more than one habit, represented by concentric circles in the location of each species.

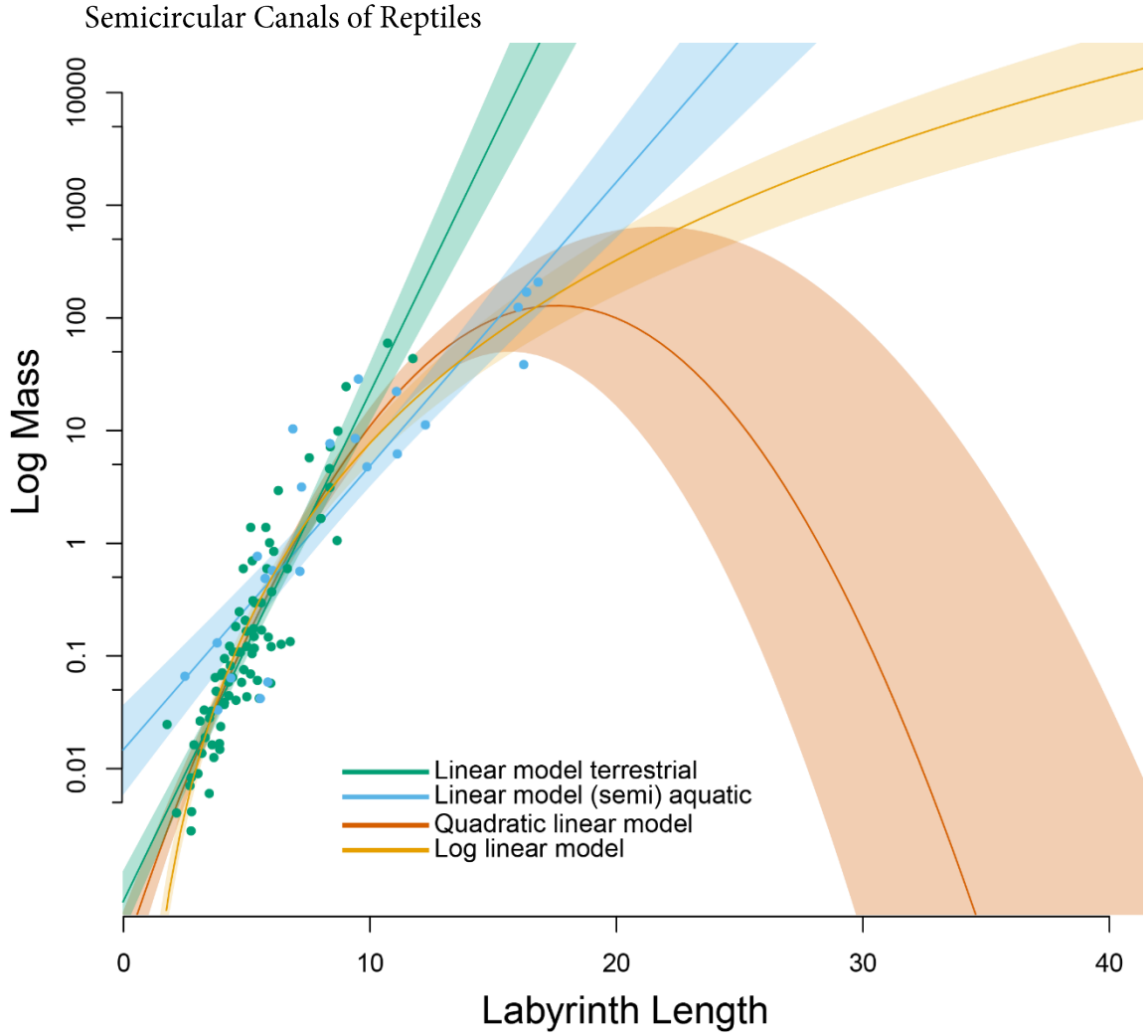

Figure 3: Blue points are semiaquatic taxa, with a linear regression for the relationship between the log mass and labyrinth length of semiaquatic taxa with blue 95% confidence interval. The red dots are taxa which are not semiaquatic, with their corresponding red line and 95% confidence interval. The gold line is the line of best fit for a log equation best describing the fit between log body mass and labyrinth length with its 95% confidence interval. The quadratic linear model is orange and shown with its 95% confidence interval, also orange.

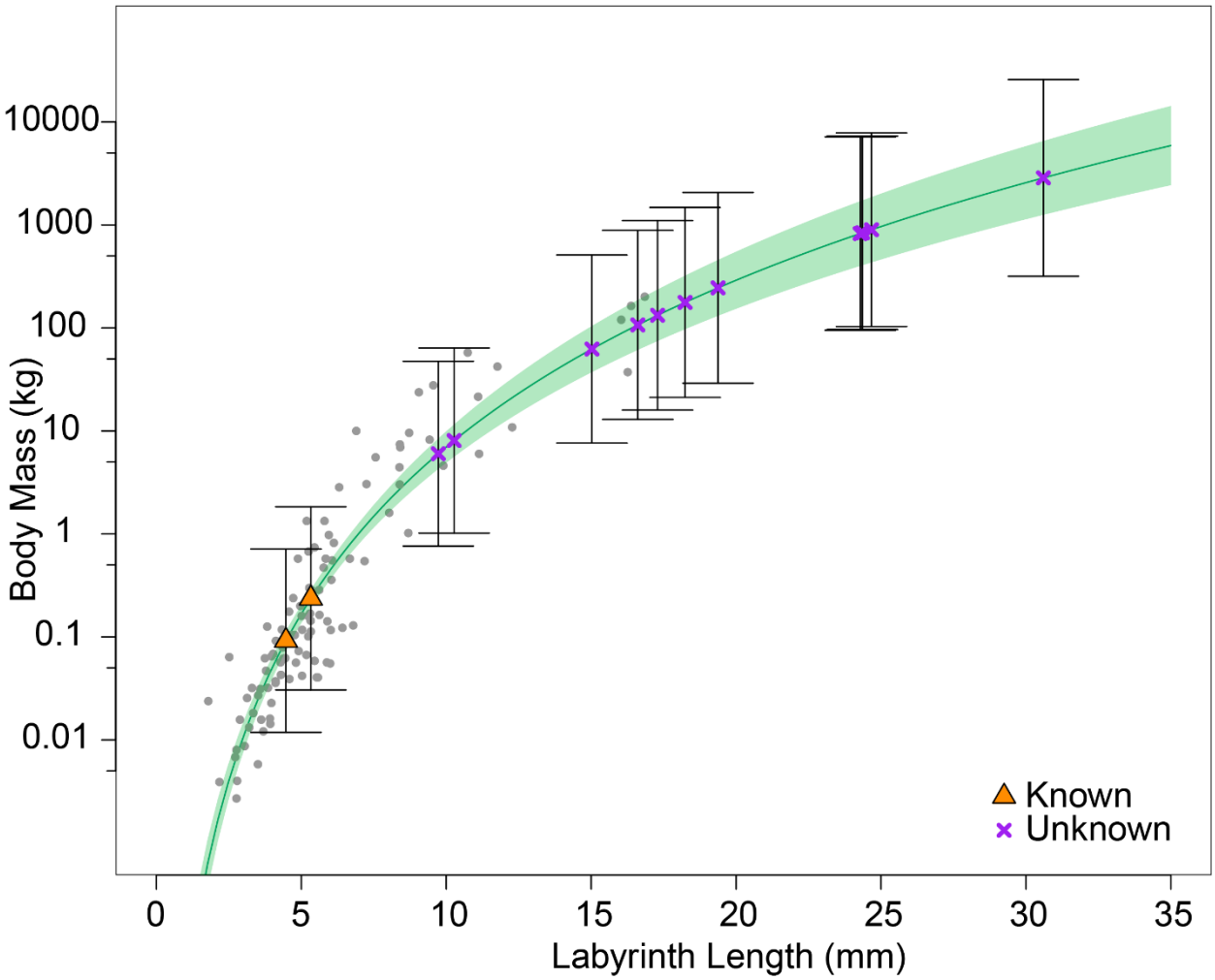

Figure 4. The formula for predicting log body mass and from log body length plotted in green, with the green shading indicating the 95% confidence interval for that model with grey dots for each species used to make the model. Predicted body masses for taxa with known maximum mass (orange Δ) and without known mass (purple x) placed on the confidence interval, brackets indicate the 95% confidence interval for body mass estimates for possible weights for those taxa given the noise in the present sample.

	parameters	R^2	AICc	ΔAICc	Biologically appropriate estimates at large values
Labyrinth length	2	80.99	320.90	31.26	Yes
with Semiaquatic	4	85.92	292.25	2.61	Yes
Quadratic labyrinth length	3	86.12	289.64	0.00	No
with Semiaquatic	6	86.61	289.60	-0.04	No
Log Labyrinth Length*	2	83.92	303.62	13.98	Yes
with Semiaquatic	4	84.05	305.15	15.51	Yes

Table 1 Results of linear models predicting body mass using various parameters, each with and without semiaquatic habit. Parameters are number of parameters used to predict body mass in the linear model. Adjusted R^2 and AICc, as well as the difference between the AICc and the best model. The models preferred for mass estimation is indicated by a star.

A) Taxa of known mass	Clade	Body mass(g)	Lower Estimate	Upper Estimate	Known Mass (g)
Platysaurus imperator	Squamate	91.90	11.84	713.41	104.90
Leiolepis triploida	Squamate	236.38	30.50	1831.94	199.50
B) Taxa of unknown mass		Body mass(Kg)			
Euparkeria capensis †	Archosauriform	6.01	0.76	47.46	-
Puppigerus camperi †	Testudine	8.06	1.02	63.83	-
Microcleidus homalospondylus †	Plesiosaur	62.39	7.63	510.49	-
Nothosaurus sp †	Nothosaur	106.94	12.93	884.47	-
Mecistops cataphractus	Crocodylian	132.76	15.98	1103.07	-
Augustasaurus hagdorni †	Pistosaur	176.90	21.16	1479.27	-
Placodus gigas †	Placodont	245.06	29.09	2064.69	-
Callawayasaurus colombiensis †	Plesiosaur	825.17	94.95	7170.89	-
Libonectes morgani †	Plesiosaur	838.46	96.44	7289.53	-
Peloneustes philarcus †	Plesiosaur	839.18	96.52	7295.95	-
Simosaurus gaillardoti †	Nothosaur	898.79	103.18	7829.04	-
Macroplata tenuceps †	Plesiosaur	2863.62	317.77	25806.06	-

Table 2 Predicted body mass from log labyrinth length for extant and extinct taxa of known and unknown body masses. Dagger symbol (†) indicates extinct species.

5.2 Supplement for "Shape and size of semicircular canals correlate with clade and body mass in reptiles"

Ashley E. Latimer[1,2], Timothée Bonnet[2], Emma Sherratt[3], Torsten M. Scheyer[1]

[1]University of Zurich, Department of Paleontology, Karl Schmid-Strasse 4, Zurich, CH-8006, Switzerland

[2] Australian National University, Canberra ACT 0200 Australia

[3] The University of Adelaide, Adelaide SA 5005Australia

Surface Models

Most squamate inner ears are figured in Latimer chapter 3. Inner ears from other reptiles new to this study are figured to scale in Supplemental Figure 1, including two squamates not figured in the previous study.

Body Length and Masses

Snout vent length and mass of *caiman crocodilus* is the upper range taken from [1], derived from equations using the largest skull size of *Crocodylus moreletii* [2], *Mecistops cataphractus* [4], two formulae, one for mass and one for SVL (snout-vent length) of *Osteolaemus tetraspis* was derived from the measurements in [3] using linear regression to log values, and applied to the record total length from [4] for mass ((27720g):

Mass= exp((ln(Total Length)-2.4426)/.2661) (estimate)
SVL = exp((ln(Total Length)-0.8710)/0.9355)

SVL is not widely available for turtles, so curved carapace length was used instead. Large carapace lengths were used from the literature as follows: *Apalone mutica* and *Chrysemys picta* [5], *Macrochelys temminckii* [6], *Lepidochelys olivacea* [7], *Testudo horsfieldii* [8], *Chelus fimbriata* [9], *Malacochersus tornieri* [10].

Body mass and labyrinth lengths for all taxa used to created the model predicting body mass are shown in Supplemental Figure 2, colorized by clade. Masses predicted by the log-log model (Supplemental Figure 3) for species used to create that model were plotted with input body mass to visualize the correspondence between the two.

Phylogeny

An estimate of phylogenetic signal (Supplemental Figure 4) was run including taxa which were present in the trees used and the dataset (Supplemental Figure 6).

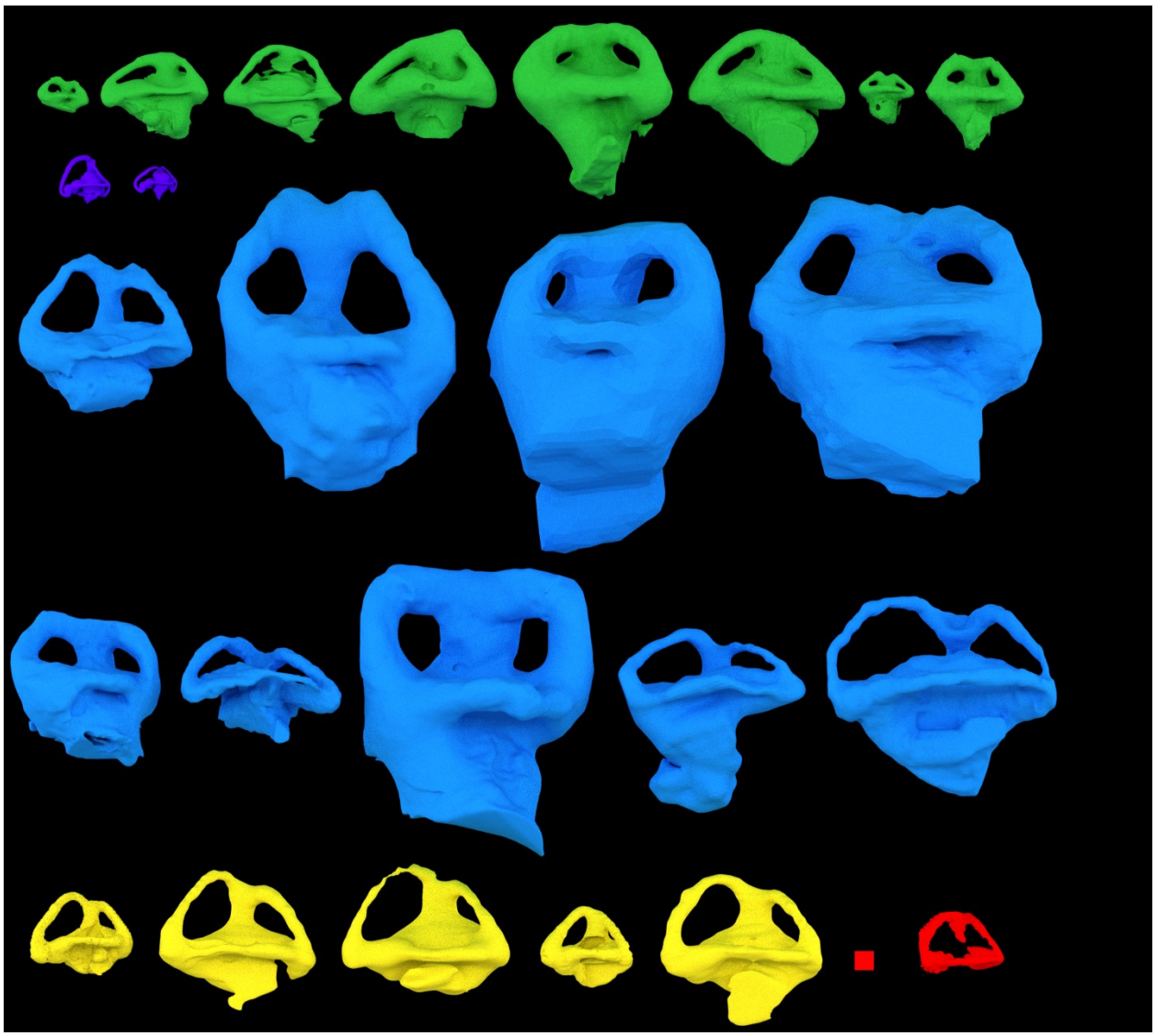

Supplemental Figure 1. Reptile semicircular canals to scale not figured in Chapter 3, including surfaces from [11,12]. Sides of the red cube are 1mm. In alphabetical order by group 1) Testudines (green): *Agrionemys horsfieldii*, *Apalone mutica*, *Chelus fimbriata*, *Chrysemys picta*, *Lepidochelys olivacea*, *Macrochelys*, *Malacochersus*, *Puppigerus* 2) Squamates (violet): *Leiolepis triploida*, *Platysaurus imperator* 3) Marine reptiles (blue): *Augustasaurus hagdorni*, *Callawayasaurus colombiensis*, *Libonectes morgani*, *Macroplata tenuiceps* 4) Marine reptiles (blue): *Microcleidus homalospondylus*, *Nothosaurus sp.*, *Peloneustes philarcus*, *Placodus gigas*, *Simosaurus gaillardoti* 5) Crocodilians (yellow): *Caiman crocodilus*, *Crocodylus moreleti*, *Mecistops cataphractus*, *Osteolaemus tetraspis*, *Tomistoma schlegelii* 6) Archosauromorph (red): *Euparkeria capensis*

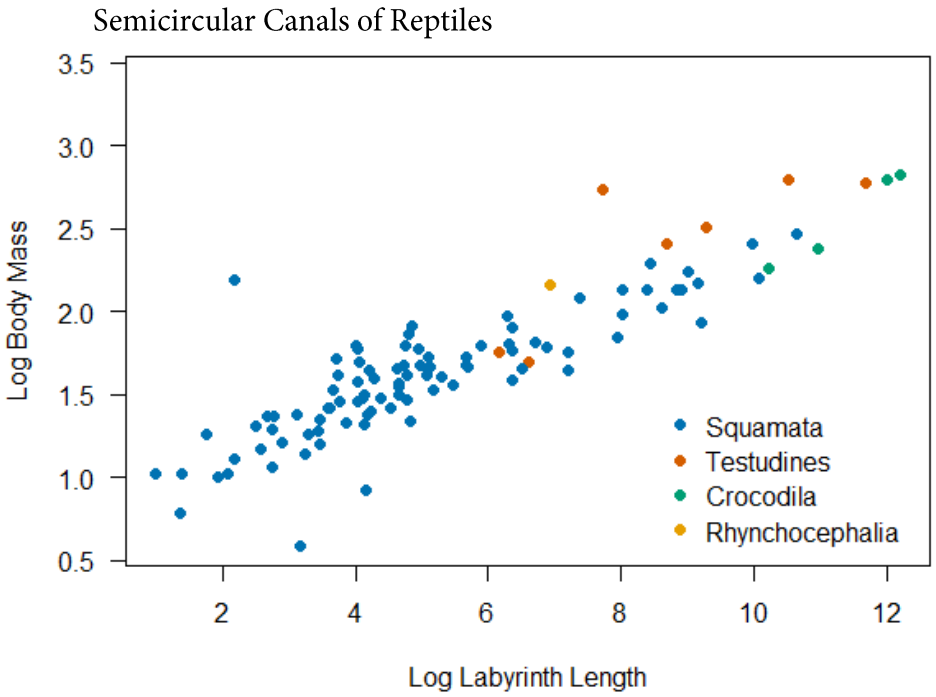

Supplemental Figure 2. Distribution of clades between real species maximum body masses and labyrinth length.

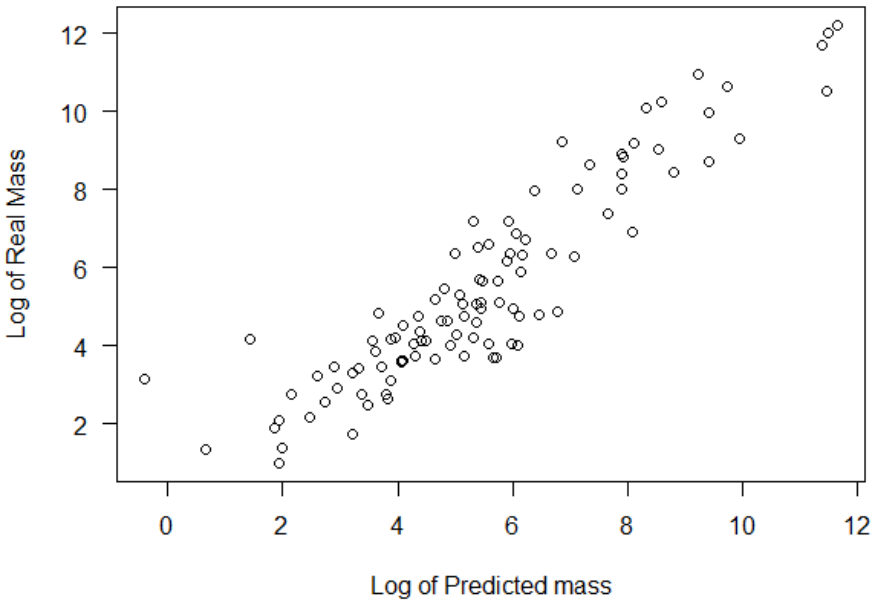

Supplemental Figure 3. Graph showing log body mass estimate from the linear model predicted by log labyrinth length against the input body mass values for the taxa used to create the log-log model.

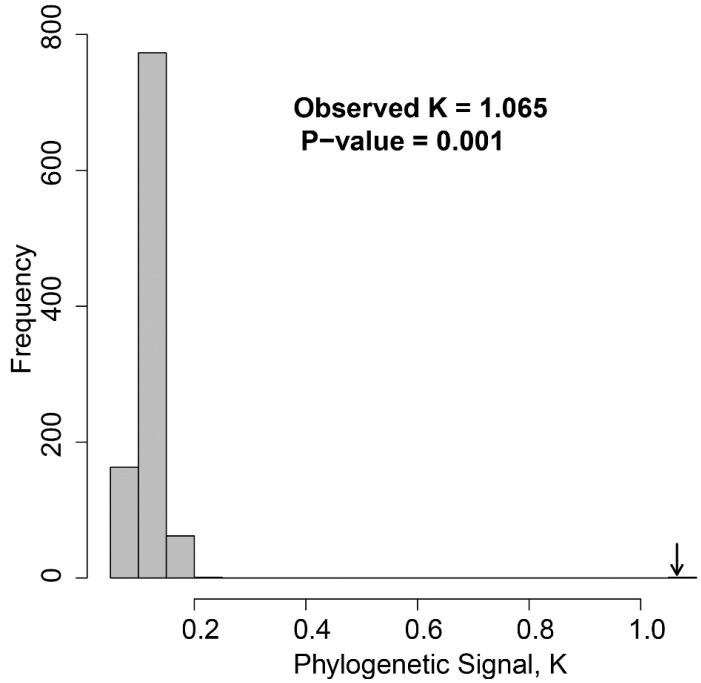

Supplemental Figure 4 Phylogenetic signal for all taxa with ear shape.

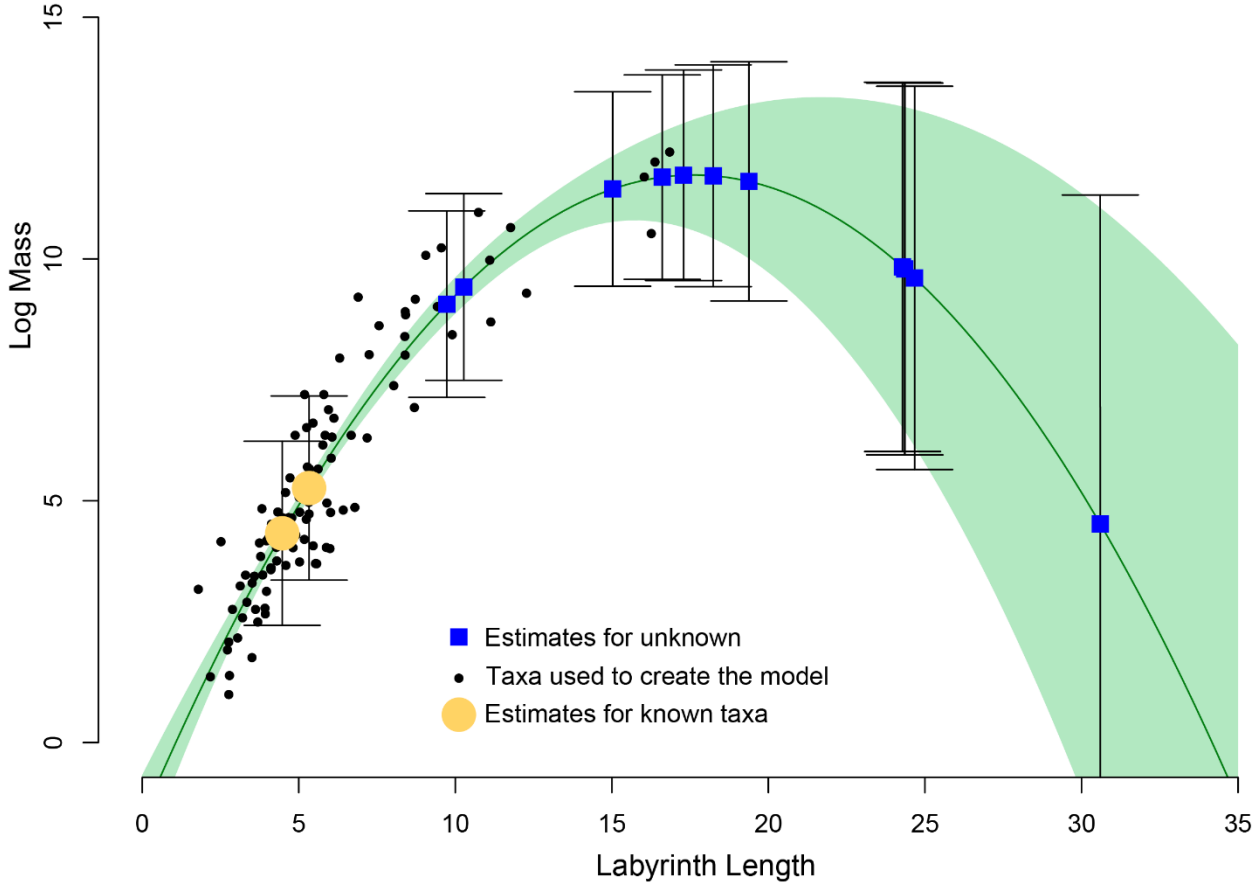

Supplemental Figure 5. The green line is the graph of the quadratic model estimating body mass with 95% confidence interval (green shape). While this model is more accurate to estimate the body mass of taxa within the size of taxa used to build the model, it predicts impossible decreasing body mass for larger labyrinth size.

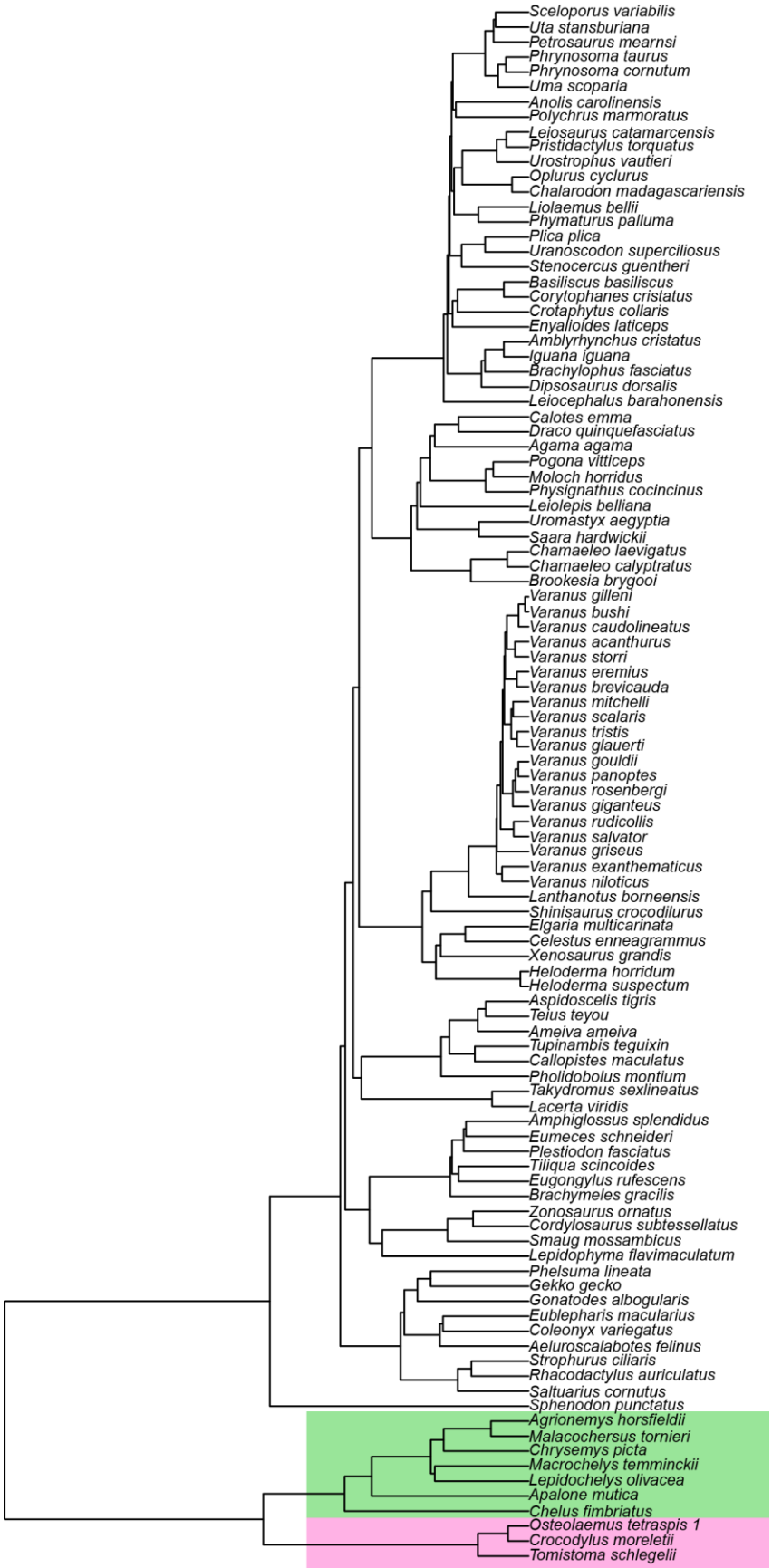

Supplemental Figure 6. Phylogenetic tree of the taxa used in the analyses correcting for phylogenetic relationship. Turtles are in the green box, crocodylians in pink, lepidosaurs in white. The taxa included are *Aeluroscalabotes felinus*, *Agama agama*, *Agrionemys horsfieldii*, *Amblyrhynchus cristatus*, *Ameiva ameiva*, *Amphiglossus splendidus*, *Anolis carolinensis*,

Apalone mutica, *Aspidoscelis tigris*, *Basiliscus basiliscus*, *Brachylophus fasciatus*, *Brachymeles gracilis*, *Brookesia brygooi*, *Callopistes maculatus*, *Calotes emma*, *Celestus enneagrammus*, *Chalarodon madagascariensis*, *Chamaeleo calyptratus*, *Chamaeleo laevigatus*, *Chelus fimbriatus*, *Chrysemys picta*, *Coleonyx variegatus*, *Cordylosaurus subtessellatus*, *Corytophanes cristatus*, *Crocodylus moreletii*, *Crotaphytus collaris*, *Dipsosaurus dorsalis*, *Draco quinquefasciatus*, *Elgaria multicarinata*, *Enyalioides laticeps*, *Eublepharis macularius*, *Eugongylus rufescens*, *Eumeces schneideri*, *Gekko gecko*, *Gonatodes albogularis*, *Heloderma horridum*, *Heloderma suspectum*, *Iguana iguana*, *Lacerta viridis*, *Lanthanotus borneensis*, *Leiocephalus barahonensis*, *Leiolepis belliana*, *Leiosaurus catamarcensis*, *Lepidochelys olivacea*, *Lepidophyma flavimaculatum*, *Liolaemus bellii*, *Macrochelys temminckii*, *Malacochersus tornieri*, *Moloch horridus*, *Oplurus cyclurus*, *Osteolaemus tetraspis*, *Petrosaurus mearnsi*, *Phelsuma lineata*, *Pholidobolus montium*, *Phrynosoma cornutum*, *Phrynosoma taurus*, *Phymaturus palluma*, *Physignathus cocincinus*, *Plestiodon fasciatus*, *Plica plica*, *Pogona vitticeps*, *Polychrus marmoratus*, *Pristidactylus torquatus*, *Rhacodactylus auriculatus*, *Saara hardwickii*, *Saltuarius cornutus*, *Sceloporus variabilis*, *Shinisaurus crocodilurus*, *Smaug mossambicus*, *Sphenodon punctatus*, *Stenocercus guentheri*, *Strophurus ciliaris*, *Takydromus sexlineatus*, *Teius teyou*, *Tiliqua scincoides*, *Tomistoma schlegelii*, *Tupinambis teguixin*, *Uma scoparia*, *Uranoscodon superciliosus*, *Uromastyx aegyptia*, *Urostrophus vautieri*, *Uta stansburiana*, *Varanus acanthurus*, *Varanus brevicauda*, *Varanus bushi*, *Varanus caudolineatus*, *Varanus eremius*, *Varanus exanthematicus*, *Varanus giganteus*, *Varanus gilleni*, *Varanus glauerti*, *Varanus gouldii*, *Varanus griseus*, *Varanus salvator*, *Varanus mitchelli*, *Varanus niloticus*, *Varanus panoptes*, *Varanus rosenbergi*, *Varanus rudicollis*, *Varanus scalaris*, *Varanus storri*, *Varanus tristis*, *Xenosaurus grandis*, *Zonosaurus ornatus*

REFERENCES

1. Gorzula SJ. 1978 An ecological study of *Caiman crocodilus crocodilus* inhabiting savanna lagoons in the Venezuelan Guayana. *Oecologia* **35**, 21–34. (doi:10.1007/BF00345539)

2. Platt SG, Rainwater TR, Thorbjarnarson JB, Martin D. 2009 Size estimation, morphometrics, sex ratio, sexual size dimorphism, and biomass of Morelet's crocodile in northern Belize. *Caribb. J. Sci.* **45**, 80–93. (doi:10.18475/cjos.v45i1.a12)

3. Pauwels OSG, Barr B, Sanchez ML, Burger M. 2007 Diet records for the dwarf crocodile, *Osteolaemus tetraspis tetraspis* in Rabi oil fields and Loango National Park, Southwestern Gabon. *Hamadryad* **31**, 258–264.

4. Waitkuwait WE. 1989 Present knowledge on the west African slender-snouted crocodile, *Crocodylus cataphractus* Cuvier 1824 and the west African dwarf crocodile *Osteolaemus tetraspis*, Cope 1861. *IUCN Publ. NEW Ser.* , 259–275.

5. Edmond BS, Daniel RE. 2001 Maximum size record for Amphibians and Reptiles in Missouri. *Missouri Herpetol. assoication Newsl.* , 15–16.

6. Boundy J, Kennedy C. 2006 Trapping survey results for the alligator snapping turtle (*Macrochelys temminckii*) in southeastern Louisiana, with comments on exploitation. *Chelonian Conserv. Biol.* **5**, 3–9. (doi:10.2744/1071-8443(2006)5[3:TSRFTA]2.0.CO;2)

7. Cogger H. 2014 *Reptiles and Amphibians of Australia.* 7th ed. Collingswood: Csiro Publishing.

8. Bonnet X, Lagarde F, Henen BT, Corbinl J, Nagy KA, Naulleau G, Balhoull K, Legrand A, Cambag R. 2001 Sexual dimorphism in steppe tortoises (*Testudo horsfieldii*): influence of the environment and sexual selection on body shape and mobility. *Biol. J. Linn. Soc.* **72**, 357–372.

9. Barrio-Amorós CL, Narbaiza Í. 2008 Turtles of the venezuelan estado Amazonas. *Radiata* **17**, 2–19.

10. Ewert MA, Hatcher RE, Goode JM. In press. Sex Determination and Ontogeny in Malacochersus tornieri , the Pancake Tortoise. *J. Herpetol.* **38**, 291–295.

11. Neenan JM, Reich T, Evers SW, Druckenmiller PS, Voeten DFAE, Choiniere JN, Barrett PM, Pierce SE, Benson RBJ. 2017 Evolution of the Sauropterygian Labyrinth with Increasingly Pelagic Lifestyles. *Curr. Biol.* , 1–7. (doi:10.1016/j.cub.2017.10.069)

12. Neenan JM, Reich T, Evers SW, Druckenmiller PS, Voeten DFAE, Choiniere JN, Barrett PM, Pierce SE, Benson RBJ. 2017 3D models related to the publication: Evolution of the sauropterygian labyrinth with increasingly pelagic lifestyles. *MorphoMuseuM* **4**, 1–3. (doi:10.18563/journal.m3.62)

Chapter 6 Supplemental Chapter

6.1 An Updated Description of the Osteology of the Pancake Tortoise *Malacochersus torneri* (Testudines:Testudinidae) with Special Focus on Intraspecific variation

Ana-Katharina Mautner[1], Ashley E. Latimer[1], Uwe Fritz[2], Torsten M. Scheyer[1]

[1]University of Zurich, Department of Paleontology, Karl Schmid-Strasse 4, Zurich, CH-8006, Switzerland
[2] Museum of Zoology (Museum fur Tierkunde) A. B. Meyer Building, Dresden, D-01109, Germany

Art: Turtle in the garden
Ashley Latimer, 1996
Pencil

Author contributions Conception and design of study: TS, UF. Acquisition of data: TS A-KM. Analysis and interpretations of the data: A-KM, AEL, TS. Drafting the manuscript: A-KM, AEL, TS. Critical revision of the article: TS, UF . Approval of the manuscript to be published: A-KM, AEL, UF, TS.

JOURNAL OF MORPHOLOGY 278:321–333 (2017)

An Updated Description of the Osteology of the Pancake Tortoise *Malacochersus tornieri* (Testudines: Testudinidae) with Special Focus on Intraspecific Variation

Anna-Katharina Mautner,[1] Ashley E. Latimer,[1] Uwe Fritz,[2] and Torsten M. Scheyer[1]*

[1]*University of Zurich, Palaeontological Institute and Museum, Karl Schmid-Strasse 4, Zurich, CH-8006, Switzerland*
[2]*Museum of Zoology (Museum für Tierkunde), A. B. Meyer Building, Dresden, D-01109, Germany*

ABSTRACT Exceptional variability in the shell of the pancake tortoise *Malacochersus tornieri*, both in the keratinous surficial scutes and the underlying bones, in addition to its remarkably fenestrated bony shell are unique among tortoises. Based on 14 individuals of different sizes and ages, the observed variation in *M. tornieri* was described in detail, with additional notes on the typically testudinid skull, inner ear and brain endocast using microCT-scan data, as well as the limbs. Similar degrees of variation have not yet been described in any other extant turtle species and therefore seem notable in *M. tornieri*, and might be related to the species' unique lifestyle. Within the carapace, the peripherals and suprapygals are most variable in number. Furthermore, different combinations of peripherals are participating in the central plastral fontanelle and in some individuals additional bones take part in the formation of the plastron. J. Morphol. 278:321–333, 2017. © 2017 Wiley Periodicals, Inc.

KEY WORDS: brain endocast; chelonian shell; microcomputed tomography; morphology; variability

RESEARCH HGHLIGHTS

Malacochersus tornieri shows exceptional variability in shell bones and scutes. This stands in contrast to a conservative configuration of the typical testudinid skull, for which the brain endocast and inner ear was reconstructed using microCT-scan data.

INTRODUCTION

The typical chelonian shell is a closed, completely ossified bony capsule consisting of a dorsal carapace and a ventral plastron connected via an inflexible bony bridge, enclosing most of the animal except for limbs, tail and head. The carapacial and plastral bones are usually covered by epidermal keratinous shields, which margins do not overlap with the underlying bone boundaries (Zangerl and Johnson, 1957; Zangerl, 1969). This general structure is present in all tortoises (all members of Testudinidae), with the exception of the bony shell of *Malacochersus tornieri* (Siebenrock, 1903), the African pancake tortoise. In this species, the typical compact and closed bony shell is fenestrated and flexible, even in adult individuals. The scutes still enclose the complete shell, which makes the fenestration invisible in a living animal.

Malacochersus tornieri has thus one of the most remarkable shell structures among turtles; the carapace and plastron show an almost "pathological" shell bone reduction in superficial appearance. Indeed, Siebenrock (1903: 443), when describing the species as "*Testudo tornieri* nov. spec." based on a dried specimen in the Berlin Museum collection, thought the individual with its flat and soft shell must have been either ill prepared or suffered from osteomalacia, impeding realistic size measurements (see also Loveridge and Williams, 1957). His view changed by 1904 when he had the chance to study another specimen from the museum collection in Munich (Siebenrock, 1904), in which he assumed the fenestrated condition of the shell was related to a partial constraint in development. This interpretation was also adopted later by Procter (1922: 521), who provided the first comprehensive study of the osteology and development of *M. tornieri*.

With its flat and flexible shell, highly unusual for a land tortoise of the family Testudinidae, *M. tornieri* inhabits arid shrub and thorny brush

Additional Supporting Information may be found in the online version of this article.

Contract grant sponsor: Swiss National Science Foundation; Grant number: 31003A-149506 (to T.M.S.).

*Correspondence to: T. M. Scheyer, University of Zurich, Palaeontological Institute and Museum, Karl Schmid-Strasse 4, CH-8006 Zurich, Switzerland. E-mail: tscheyer@pim.uzh.ch

Received 26 September 2016; Revised 23 November 2016; Accepted 4 December 2016.

Published online 25 January 2017 in Wiley Online Library (wileyonlinelibrary.com).
DOI 10.1002/jmor.20640

© 2017 WILEY PERIODICALS, INC.

environments on rocky outcrops, so called kopjes, in Tanzania, Kenya and adjacent areas in northeastern Zambia (Procter, 1922; Chansa and Wagner, 2006). It was widely assumed that *M. tornieri* could inflate the shell to some degree to wedge itself in rocky crevasses (Boulenger, 1920; Procter, 1922; Pritchard, 1979) until laboratory experiments indicated that no intrapulmonary pressure increase is present that would allow this kind of wedging (Ireland and Gans, 1972). Later, however, it was proposed that *M. tornieri* does display two different ways of wedging into the kopjes. In the first case, the tortoise either uses its hind legs to press its ossified slightly humped rear part of the shell against the ceiling in wider crevasses, whereas in the second case, individuals can "inflate" a balloon-like unossified area in the plastron (Moll and Klemens, 1996) by drawing the legs back into the shell, which according to those authors, supports the original observation (Boulenger, 1920; Procter, 1922; Pritchard, 1979). The species appears neither long-lived nor very productive, with females laying only a single egg, or occasionally two, up to twice a year in the wild (Pritchard, 1979; Ernst and Barbour, 1989; Bonin et al., 2006; see Supporting Information Table S1).

Boulenger (1920: 265), while describing a new species, *Testudo loveridgii* (based on four specimens of *M. tornieri* sent to Boulenger by Loveridge; see Loveridge and Williams, 1957: 288–289), also recognized the extreme reduction of shell bone as a nonpathological condition.

Loveridge (1923) was thought by many others to have erected yet another synonym of *M. tornieri*, *Testudo procterae*, based on a single distinctively colored and apparently juvenile specimen from Tanzania, housed at the Natural History Museum in London. Loveridge and Williams (1957) provided genus and species descriptions for *Malacochersus tornieri* and also for *T. procterae*. Following those authors, there is little evidence, apart from coloration, that the type specimen of *T. procterae* represents a distinct species; instead it was proposed that it belongs to a different population of *M. tornieri*. As discussed by Crumly (1988), *T. loveridgii* and *T. procterae* were declared junior synonyms of *M. tornieri* (Siebenrock, 1903) by Loveridge and Williams (1957; contra Mertens and Müller, 1934; Mertens and Wermuth, 1955). Today, however, *T. procterae* is generally identified as a specimen of the hinge-backed tortoise *Kinixys spekii* (Fritz and Havaš, 2007; Turtle Taxonomy Working Group, 2014).

Gibbons and Lovich (1990), using mean plastron length, and Moll and Klemens (1996) described males of *M. tornieri* as smaller than females, and Procter (1922) noted that males have longer and thicker tails in *Malacochersus*. Ewert et al. (2004), however, found significant differences in the carapace length in growing juvenile males and females, whereas studied adults differed significantly only in live mass and not in carapace length. Additionally, Malonza (2003) noted no significant sexual dimorphism in size or coloration between populations from Kenya. Further details on external morphology are described elsewhere (Siebenrock, 1904; Procter, 1922; Loveridge and Williams, 1957; Pritchard, 1979, 2008; Ernst and Barbour, 1989; Lovich and Ernst, 1989).

The first attempts to solve the relationships between *M. tornieri* and other tortoises were based on morphological characters. Loveridge and Williams (1957: 284–285) interpreted *M. tornieri* to have arisen "quite independently from the ancestral stock of testudinines." Crumly (1984a: 212) listed three shared derived characters supporting a *Malacochersus-Testudo* clade: " 'Supranasal' scales present" [see Loveridge and Williams (1957: 284)], "inguinal scute does not contact the femoral scute", and "ventral tip of the intrafenestral process exposed to view and sutures between the process and the surrounding bones are still present." Gaffney and Meylan (1988: 212) also combined the genera *Malacochersus* and *Testudo* in the subtribe Testudinina, based on the same three morphological characters. More recent studies employing molecular techniques resolved the phylogeny of *M. tornieri* in a more testable way. Using a five-gene dataset including mitochondrial and nuclear DNA, *M. tornieri* was found either closely related to a *Testudo* clade (including the species *horsfieldii*, *graeca* and *kleinmanni*) or to *Indotestudo* (Le et al., 2006). Two other analyses, using whole mitochondrial genome sequences (Parham et al., 2006) and using a modified and expanded "Le et al. (2006)" dataset data (Fritz and Bininda-Emonds, 2007), both recovered a weakly supported *Malacochersus* + *Indotestudo* clade. Yet, whereas the first analysis (Parham et al., 2006) found *Testudo* paraphyletic with respect to *Malacochersus* + *Indotestudo*, the second one (Fritz and Bininda-Emonds, 2007) revealed a monophyletic *Testudo* sister to *Malacochersus* + *Indotestudo* (Fig. 1).

Individual variation in the scutation of turtles is frequent, whereas variation in the bony shell is less common (Zangerl and Johnson, 1957; Zangerl, 1969). There are several studies on variation in the scutes of the turtle shell (Zangerl and Johnson, 1957; MacCulloch, 1981; Hewavisenthi and Parmenter, 2001; Bell et al., 2006; Moustakas-Verho and Cherepanov, 2015; Loehr, 2016; Packard et al., 2016) showing that abnormalities in the scutes are relatively frequent. Concerning variation in scutation, Zangerl and Johnson (1957) for instance found 43% of abnormal specimens in a sample of 2,220 individuals and Loehr (2016) found 44% of a wild population of *Homopus signatus* (Gmelin, 1789) deviating from the normal carapacial scute pattern. Several reasons have been proposed, like high levels of pollutants (Bell et al., 2006), drying of the eggs during incubation (Lynn and Ullrich, 1950) incubation temperatures (Hewavisenthi and Parmenter, 2001; Packard

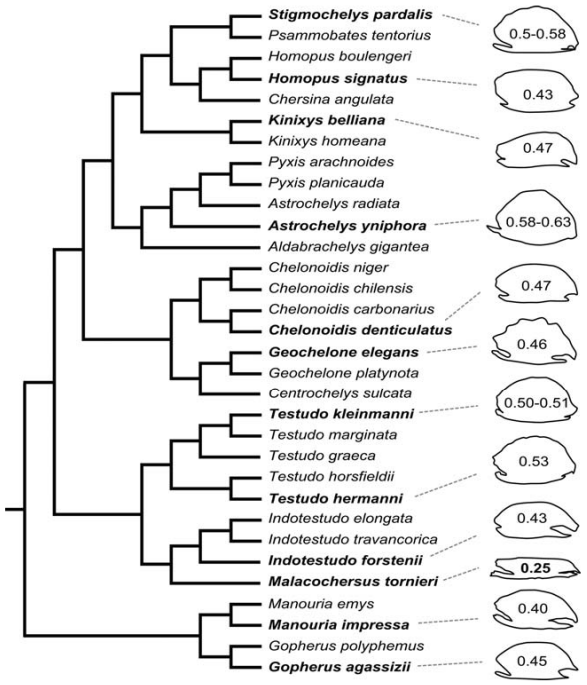

Fig. 1. Phylogenetic relationships of land tortoises (Testudinidae) based on Fritz and Bininda-Emonds (2007), showing shell contours and height/length ratios (Supporting Information Table S2).

et al., 2016), genetic defects, or consequences of accidents or trauma during the embryonic stage (Pritchard, 2008).

Variation in the bony shell is much less obvious among living species and also less studied among extant taxa. Concerning such shell bone variation, abnormalities in two individuals of *Glyptemys insculpta* (Le Conte, 1830) (Parker, 1901), high variation in the neural formula of *Testudo hermanni* (Gmelin, 1789) on Golem Grad Island (Đorđević, 2014), geographic variation in the scutation and neural and costal bones of *Chelus fimbriatus* (Schneider, 1783) (Sánchez-Villagra et al., 1995), variation in the neural number and pleural shape of *Testudo kleinmanni* (Lortet, 1883) (Delfino et al., 2009), variation in the neural formula of chelid turtles from Australia and New Guinea (Rhodin and Mittermeier, 1977; Thomson and Georges, 1996), a *Pelusios sinuatus* (Smith, 1838) specimen lacking mesoplastra (Broadley, 1997), abnormal absence of mesoplastra in *Podocnemis erythrocephala* (Spix, 1824) (Pritchard, 2008), as well as variation in the number of neurals of *Dipsochelys*, now *Aldabrachelys* (Loveridge and Williams, 1957), have been described (Gerlach, 1999), just to name a few examples. More aberrant morphological shell conditions and anomalies have been compiled by Rothschild et al. (2013, table 27.5). There is still a lack of knowledge on this topic for most species, however, which makes a detailed description of variation in *M. tornieri* more valuable.

Here, we provide novel information about the general osteology of the species, as well illustrate the virtual brain endocast and the bony labyrinth. In addition, we set out to study the variability of shell bones in this modern turtle species, which is useful in discussing species recognition in the fossil record, which are often based only on shell material.

MATERIALS AND METHODS

Eleven of the fourteen specimens studied were used from the Museum of Zoology, Senckenberg Natural History Collections Dresden, Germany (MTD 10622, 14777, 17162, 19333, 19334, 24315, 24917, 30989, 31408, 31606 and 47600), one from the Field Museum, Chicago (FMNH 5616), one from the Natural History museum of Vienna, Austria (NHM 39289) and one from the Museum Collection of the Zoological Museum of the University of Zurich, Switzerland (ZM 100.102). The MTD specimens were alcohol-preserved specimens that were initially macerated, followed by careful manual removal of soft tissue (integument and muscles) by the preparator. This way all the limb bones, especially the autopodial elements, were preserved and held in situ by sinews. MTD 10622, 14777, 17162, 19333, 19334 were all males and from Kenya, whereas MTD 47600 was also a male but without locality information. FMNH 5616 came from Dodoma, Tanzania (collected together with three other specimens by Arthur Loveridge in 1921) and the Zurich specimen was collected close to Mount Kilimanjaro, Tanzania. All specimens analyzed were wild-caught, thus captivity biases (e.g., malformations and pathologies) related to the sometimes unfavorable keeping conditions of pet trade or zoo animals, can be ruled out. The specimens were photographed and measured with sliding calipers to the first decimal place in mm. The pictures were then edited using Adobe Creative Suite. The skull of ZM 100.102 was also scanned at the Anthropological Institute of the University of Zurich. Its external morphology was also compared to the six skulls of the MTD series (i.e., MTD 14777, 17162, 24315, 30989, 31606 and 47600). The skull of ZM 100.102 was scanned 1,024 × 1,024 resolution producing 967 slices, at 36 μm slice thickness and increment. The skull was modeled in Aviso, and the resulting images were processed with Adobe Photoshop CS6 and figures were assembled in Adobe Illustrator CS6. Diagrams were generated using R (version 3.2.5) and edited using Inkscape 0.91. The 3d skull model and accompanying dataset are available at MorphoMuseuM (Mautner et al., 2016; doi: 10.18563/m3.2.2.e4).

Institutional Abbreviations

FMNH, The Field Museum, Chicago, Illinois, USA; **MTD**, Museum of Zoology, Senckenberg Natural History Collections Dresden, Germany; **NHM**, Naturhistorisches Museum Wien, Austria; **ZM**, Zoological Museum of the University of Zurich, Switzerland.

RESULTS

Taxonomy

Testudines Batsch, 1788
Cryptodira Cope, 1868
Testudinidae Batsch, 1788
Malacochersus tornieri (Siebenrock, 1903)

Synonymy

Testudo tornieri (Siebenrock, 1903: 443)
Testudo loveridgii (Boulenger, 1920: 263), *Malacochersus loveridgii*

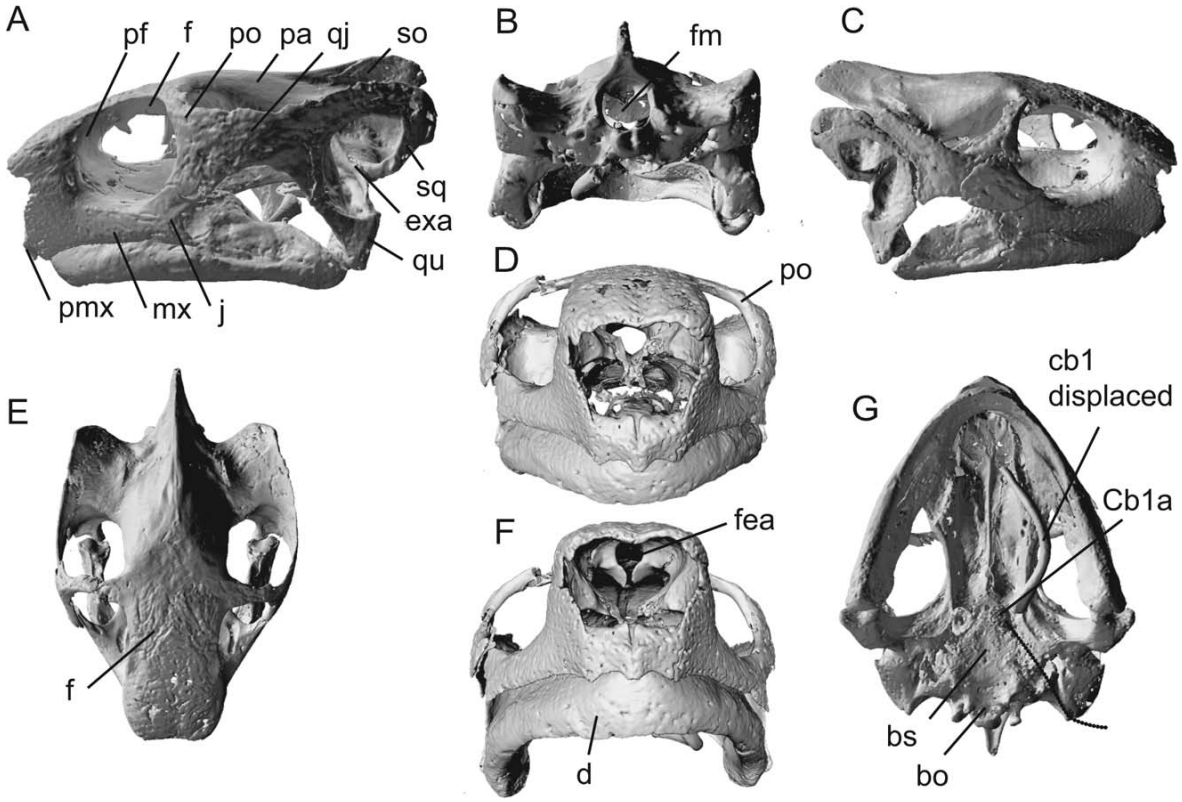

Fig. 2. *Malacochersus tornieri* ZM 100.102, skull. Views as follows: **A**) left lateral, **B**) occipital, **C**) right lateral, **D**) rostral, **E**) dorsal, **F**) higher rostral, **G**) ventral. The dotted line is in the correct location for cb1. Abbreviations: bo, basioccipital; bs, basisphenoid; cb1, cornu branchiale 1; Cb1a, anterior calcified portion of cornu branchiale 1; D, dentary; exa, external auditory meatus with stapes; f, frontal; fea, fissura ethmoidales; fm, foramen magnum; j, jugal; mx, maxilla; pa, parietal; pf, prefrontal; pmx, premaxilla; po, postorbital; po, postorbital; qj, quadratojugal; qu, quadrate; so, supraoccipital; sq, squamosal. Skull length (anterior tip of pf to posterior margin of so crest) is 5.9 cm.

Skull

Little description of the skull osteology can be found in Procter (1922: 485, 490), who noted for example that the prefrontals are larger than the frontals and the maxilla carries three "alveolar" ridges, with the inner one being comparatively weak and the outer one, that is, the maxillary edge, being denticulated. Later, Loveridge and Williams (1957: 284) noted that the head, limbs and vertebrae of *Malacochersus tornieri* are "thoroughly testudinine and differ but little from those of *Geochelone*." The authors (p. 283) also provided the following set of osteological skull and mandible characters for the species: "skull with triturating surface of maxilla strongly ridged; median premaxillary ridge absent; maxillary not entering roof of palate; anterior palatine foramina small, concealed in ventral view; prootic well exposed dorsally; quadrate enclosing stapes; surangular sometimes markedly lower than prearticular, exposing the latter to view externally."

Gaffney (1979) also presented a detailed drawing with a description of all the bones participating in the skull formation, yet some views were omitted. The observations of Loveridge and Williams (1957) and Gaffney (1979) can be affirmed by the specimens studied here.

Additional information on the osteology of the skull of *Malacochersus tornieri* (Fig. 2; Supporting Information Fig. S1): prefrontals are not or only slightly expanded compared to frontals; frontals of wide rectangular shape in dorsal view without anterior or posterior processes, postorbitals lacking an anterolateral process but having posterolateral processes forming about half of the anterior lower orbital margin; suture between jugal and postorbital extending almost horizontally; pointed contact between basisphenoid and vomer in ventral view. Skulls measured in this study ranged from 21.3 to 32.3 mm in condylobasal length, 7.4 to 12 mm in cranial height and 8.3 to 17.5 mm in maximum skull width (Table 1).

The endocranial space in turtles does not closely correspond to the morphology of the brain tissue, however, the space is of phylogenetic importance (e.g., Carabajal et al., 2013). The endocast of *Malacochersus tornieri* is tubular, tapering rostrally (Fig. 3). The thicker posterior portion of the

TABLE 1. Measurements and bones participating in the carapace and plastron of 14 individuals of Malacochersus tornieri

	Specimen no. (arranged with increasing SCL)													
Character	MTD 47600	MTD 30989	MTD 19334	MTD 24917	MTD 14777	MTD 31606	MTD 17162	MTD 31408	NHM 39289	MTD 19333	FM 5616	ZM 100. 102	MTD 24315	MTD 10622
Straight carapace length (SCL)	94.9	99.8	109.2	127.0	127.7	134.5	135.6	137.8	138.6	142.9	144.7*	151.0	164.0	164.5
Straight carapace width (SCW)	78.3	81.3	82.6	98.1	94.9	103.4	100.0	96.0†	97.2	110.6	106.4*	105.3	113.4	124.4
Straight plastron length (SPL)	88.3	95.5	108.1	124.5	127.1	136.8	136.5	127.0†	124‡	136.9	142.0*	145.0†	158.7	153.5
Peripherals participating in central plastral fontanella (left)	5 + 6	5 + 6	5 + 6	none	5 + 6	5 + 6	5 + 6	5 + 6	5 + 6 + 7	6 + 7	5 + 6	5 + 6	5 + 6	6 + 7
Peripherals participating in central plastral fontanella (right)	5 + 6	5 + 6	5 + 6	5 + 6	5 + 6	5 + 6	none	5 + 6	5 + 6 + 7	5-7	5 + 6	5 + 6	5 + 6	6 + 7
Additional bone participating in central plastral fontanella (left)	no	no	no	yes	no	no	yes	no	no	no	no	no	no	no
Additional bone participating in central plastral fontanella (right)	no	no	no	no	no	no	yes	no	no	no	no	no	no	no
Number of peripherals (left)	12	11	11	12	12	11	11	12	12	12	11	11	11	12
number of peripherals (right)	12	11	11	11	12	11	11	12	11	12	11	10	11	12
Number of suprapygals	2	1	2	2	2	2	2	NA	NA	2	1	2	1	2
Condylobasal length	7.5	7.4	9.9	9.9	10.7	11.0	11.2	10.7	10.2	12.0	NA	9.9	11.0	10.8
Maximum skull width	17.4	17.6	20.9	23.0	25.5	25.3	24.5	25.1	23.0	28.0	NA	22.8	28.7	27.0

*Measured on images using ImageJ 1.47k; NA, not available.
†Measurable only after the plastral lobes were brought in articulation with the carapacial parts.
‡Approximate measurement only due to preparation bias.

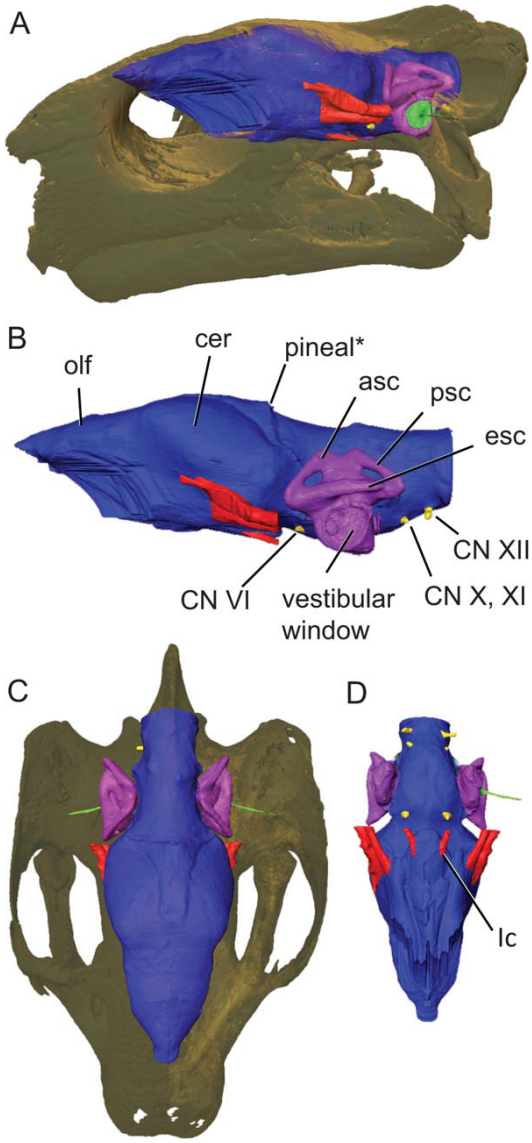

Fig. 3. *Malacochersus tornieri* ZM100.102, endocranial spaces. Specimen presented in **A**) and **B**) left lateral, **C**) dorsal and **D**) ventral views. Blue, endocranium; red, blood vessels; bright green, stapes; purple, semicircular canals; yellow, cranial nerves. Abbreviations of endocranial impressions of the following structures: olf, olfactory tract; cer, cerebrum; ic, internal carotid; CN VI, abducens nerve; CN X, XI, vagus and spinal accessory nerves; CN XII, hypoglossal nerve. Pineal* corresponds to the attachment of the pineal, but like in most modern turtles it usually does not penetrate the skull roof, although it might occur in some individuals (Zangerl, 1957; Gaffney, 1979; Crumly, 1982). Skull length (anterior tip of pf to posterior margin of so crest) is 5.9 cm. [Color figure can be viewed at wileyonlinelibrary.com]

endocast, corresponding to the hindbrain, lies on a horizontal plane. The attachment site of the pineal to the parietal results in a thinned portion of the skull roof. The middle ear is modeled here with the stapes (Fig. 3).

Carapace

The bony carapace is very flat (Fig. 1; Supporting Information Fig. S2; see also Dosik and Stayton, 2016), with striking shell bone reduction, which has been thoroughly described by Procter (1922). The straight carapace length (SCL) in the specimens treated in this study ranges from 94.4 to 164.5 mm and the straight carapace width (SCW) from 16.3 to 28.1 mm.

Typically it consists of 1 nuchal, 8 neurals, 8 costals (per side), 11 peripherals (per side), 1 suprapygal and 1 pygal, 49 bones in total (Procter, 1922). In the specimens studied here, however, there is a high variability in the number of peripherals and suprapygals among the different individuals. Six of the 14 studied specimens have 11 peripherals as proposed by Procter (1922), 5 specimens have 12 on each side, two have 12 on the left and 11 on the right and one has 11 on the left and 10 on the right side (Table 1). A young specimen of *M. tornieri* that is shown in text figure 21 in Procter (1922) has 10 peripherals on the left side and 11 on the right side as well, although the author does not mention this explicitly in the text.

Furthermore, there is variability in the number of suprapygals within this set of specimens (Table 1). Most of the specimens have two suprapygals, of which the first is very small, rectangular and horizontally slender and the second is diamond-shaped, elongated and approximately twice as wide as the first suprapygal. In two of the specimens one suprapygal was visible, which is the state originally reported (Procter, 1922).

In the smaller individuals (MTD 47600, MTD 30989, MTD 24917, MTD 14777, MTD 17162) the costals are only partly and less strongly connected to the marginals when compared to the larger individuals (MTD 19334, MTD 31606, MTD 19333, MTD 24315, MTD 10622, ZM 100.102; Table 1; Fig. 4). The relationship with size is not distinct with some smaller individuals having more developed costals than larger ones, but when comparing the smallest individual with the largest there is definitely a difference in the thickness of costals and the area of connection with the peripherals. The costals 6, 7 and 8 are especially less developed in smaller individuals than in larger ones. In smaller individuals the sixth and seventh costal are still completely or partly separate from each other, whereas in the two largest individuals (MTD 24315 and 10622) they are almost entirely fused. Furthermore the connection between the sixth, seventh and eighth costal with the peripherals solidifies the larger *Malacochersus tornieri* becomes.

Plastron

The bony plastron has been described as consisting of very thin bone and a large central diamond-shaped fontanelle reaching from ento- to xiphiplastron and from the left peripherals to the right peripherals (Procter, 1922). In the specimens studied by Procter, peripherals 5, 6 and 7 took part in the formation of the plastron on both sides, 5 and 6 participated in the central plastral fontanelle, symmetrical on the left and right side. The specimens treated in this study, however, show a great variability in the composition of the plastron and the central plastral fontanelle (Table 1). Most of the specimens still have the fifth and sixth peripheral taking part in the central plastral fontanelle (MTD 47600, MTD 30989, MTD 19334, MTD 14777, MTD 31606, MTD 31408, MTD 24315, ZM 100.102), but there was considerable variation noted in this composition. In MTD 24917 (Fig. 5) no peripherals on the left side and 5 and 6 on the right side, in MTD 17162 5 and 6 on the left side and only 6 on the right side, in MTD 19333 6 and 7 on the left side and 5, 6 and 7 on the right side, in NMW 39289 5, 6 and 7 on both sides and in MTD 10622 6 and 7 on both sides take part in the formation of the central plastral fontanelle. Four of the 14 specimens (28.6%) therefore deviate from the general bone formula found for *M. tornieri* (see Procter, 1922). Furthermore some of the individuals have additional bones in the plastron. MTD 24917 (Fig. 5) for instance has an additional bone attached to the left fifth and sixth peripheral, between the hyoplastron and hypoplastron. MTD 17162 (Fig. 5) has an additional bone attached to the right fifth and sixth peripheral, between hyoplastron and hypoplastron, which is only connected to the hyoplastron. On the left side it has an additional bone too, which is only attached to the hyoplastron and the fifth peripheral.

The hatchlings of *Malacochersus tornieri* have been described as almost circular and becoming more rectangular when they mature (Moll and Klemens, 1996). To visualize the degree of roundness in the series of *M. tornieri* specimens studied here, the ratio between straight carapace length (SCL) and straight carapace width (SCW) was calculated (Table 1). The trend reported earlier (Moll and Klemens, 1996), however, cannot be confirmed in our sample. The smallest individual is rounder than the largest, but there are several outliers (MTD 10622, MTD 19333) within the intermediate stages.

Vertebral Column

The first eight vertebrae, as observed in MTKD 24315, form the S-shaped cervical vertebral column as is typical in other cryptodiran turtles. The joints between the fifth and sixth and the eighth cervical and the first thoracic vertebra enable the neck and head retraction into the shell. Thoracic vertebrae have been thoroughly described by Procter (1922). Two sacral vertebrae and at least 20 caudal vertebrae are present in MTKD 47600, 3 sacral and 23 caudal vertebrae in MTKD 31606.

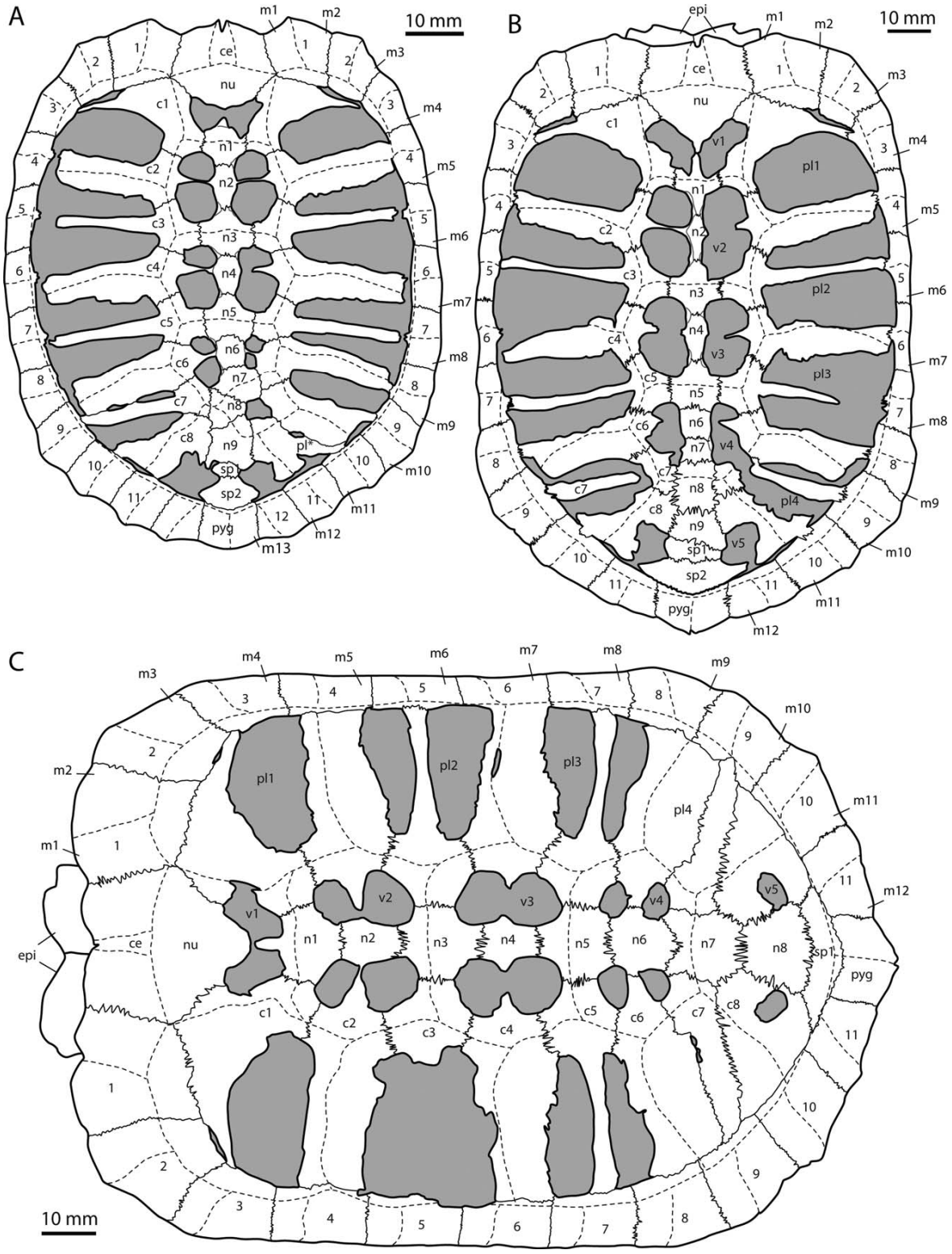

Fig. 4. *Malacochersus tornieri* **A**) MTD 47600 in dorsal view, carapace. **B**) MTD 17162 in dorsal view. **C**) MTD 24315 in dorsal view. Full lines: boundaries of the bony plates, dotted lines: boundaries of the scutes. Abbreviations: ce, cervical; v, vertebral, pl, pleural; m, marginal; nu, nuchal; n, neural; c, costal; sp, suprapygal; pyg, pygal; epi, epiplastron.

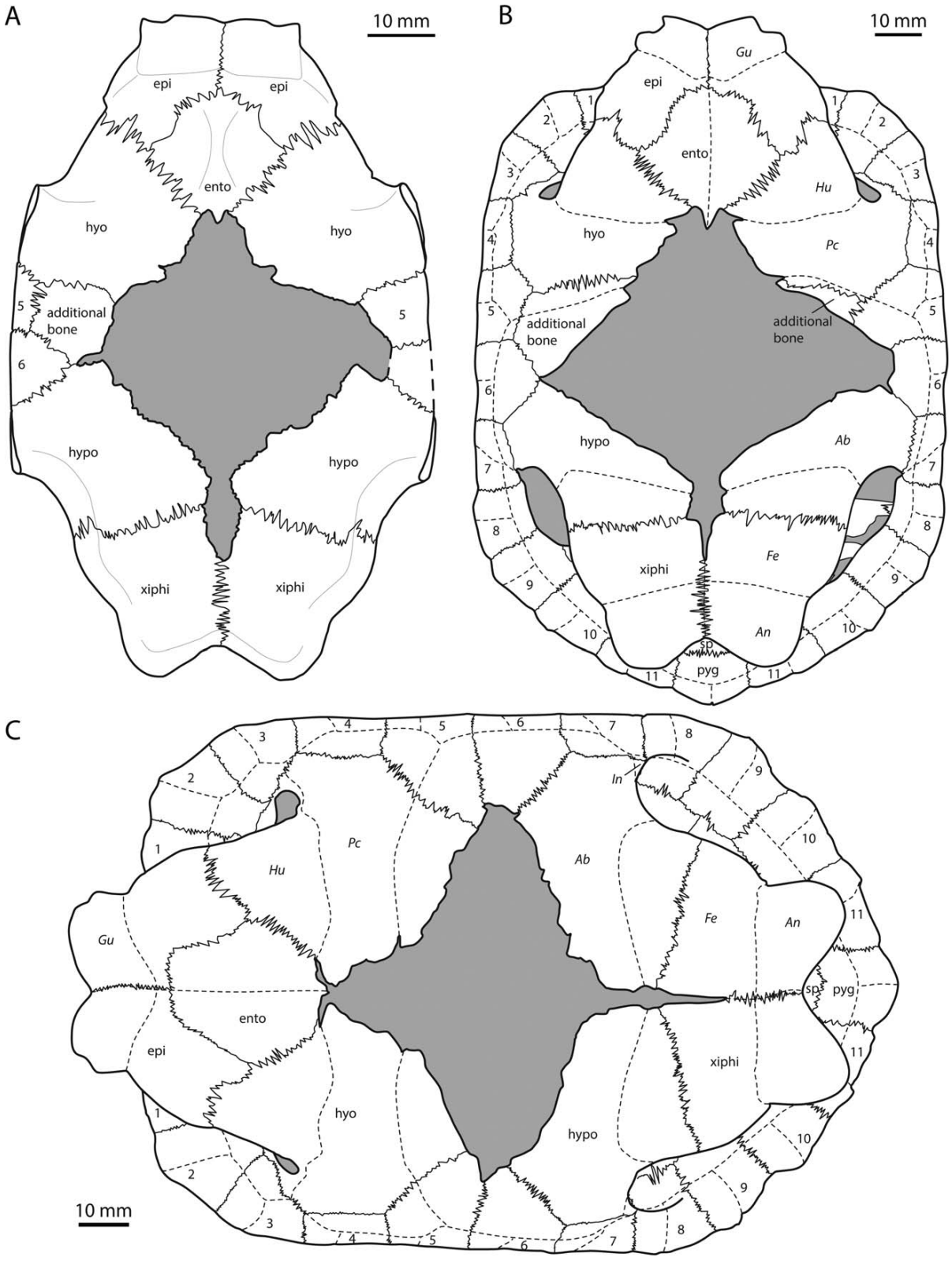

Fig. 5. *Malacochersus tornieri* **A**) MTD 24917, plastron in dorsal view. **B**) MTD 17162 in ventral view. **C**) MTD 24315 in ventral view. Full lines: boundaries of shell bones; dotted lines: keratinous scute boundaries. Abbreveations: Ab, Abdominal; Gu, gular; Hu, Humeral, Pc, Pectoral; Fe, Femoral; An, Anal; epi, epiplastron; ento, entoplastron; hyo, hyoplastron; hypo, hypoplastron; xiphi, xiphiplastron; sp, suprapygal; pyg, pygal.

Shoulder Girdle

In our sample, only specimen ZM 100.102 preserves the shoulder girdle, and it is still articulated to the shell and humeri on both sides. It consists of a dorsal scapular prong, a ventral anterior acromial process and a ventral posterior coracoid, as is typical for extant turtles (Walker, 1973; Lee, 1996; Depecker et al., 2006). The scapular prong is quite short compared to testudinids with a high-domed shell such as *Testudo hermanni* and *Stigmochelys pardalis* (Bell, 1828).

Pelvic Girdle

The pelvic girdle is present in specimens ZM 100.102, MTKD D14777, MTKD D24315, MTKD D31606, MTKD D47600 and MTKD D31408. It consists of three bony elements: ilium, ischium and pubis, each participating to the acetabular fossa, and the ilium connected to two sacral ribs (Fig. 6, see also Zug, 1971). Similar to the pectoral girdle, the pelvic girdle is not as high as in tortoises with a domed carapace, for example, *Testudo hermanni*. The ilium is approximately the same length as the pubis in *Malacochersus tornieri* whereas the ilium is almost twice as long as the pubis in *Testudo hermanni*. The foramen obturatum between the pubis and ischium is elliptical, whereas it is nearly circular in *Testudo hermanni*.

Limbs

The fore-limb consists of humerus, radius, ulna that are shaped similar to those of other tortoises. The tibia in the hind-limbs is longer than the radius in the fore-limbs (Procter, 1922). In contrast to that, the humerus in the fore-limbs is generally longer than the femur in the hind-limbs. Five digits are present in the fore- and hind-limbs, but the especially small fifth digit of the hind-limb is not present in most of the macerated specimens (Fig. 7).

The manus consists of the ulnare, intermedium, lateral and medial centrale, five distal carpals, five metacarpals and the phalanges. The phalangeal formula is 2-2-2-2-1 in all specimens except for specimen MTD 31408 which seems to have a phalangeal formula of 2-2-2-2-2 and an additional sixth digit (Fig. 7). Crumly (1984b) described the lateral and medial central in *M. tornieri* as fused with a visible suture and this observation can be confirmed by this new study.

The pes consists of the astragalocalcaneum complex (in which the astragalus and calcaneum are fused, but a suture is still visible) four distal tarsals, an ansulate bone (fifth hooked element, a fusion of the fifth distal tarsal with the fifth metatarsal sensu Joyce et al., 2013), four metatarsals and two phalanges per digit (Fig. 7). Crumly and Sánchez-Villagra (2004) found the phalangeal formula to be 2-2-2-2-1, which is the formula that would be found, if the fifth hooked element is interpreted as the fifth distal tarsal and not a fusion of the fifth tarsal and metatarsal. If it represents a fusion (sensu Joyce et al., 2013), however, the two attached elements are interpreted as two phalanges and not one metatarsal and one phalanx. Another exception in specimen MTD 31408 is an additional bone present between the first and second distal tarsal.

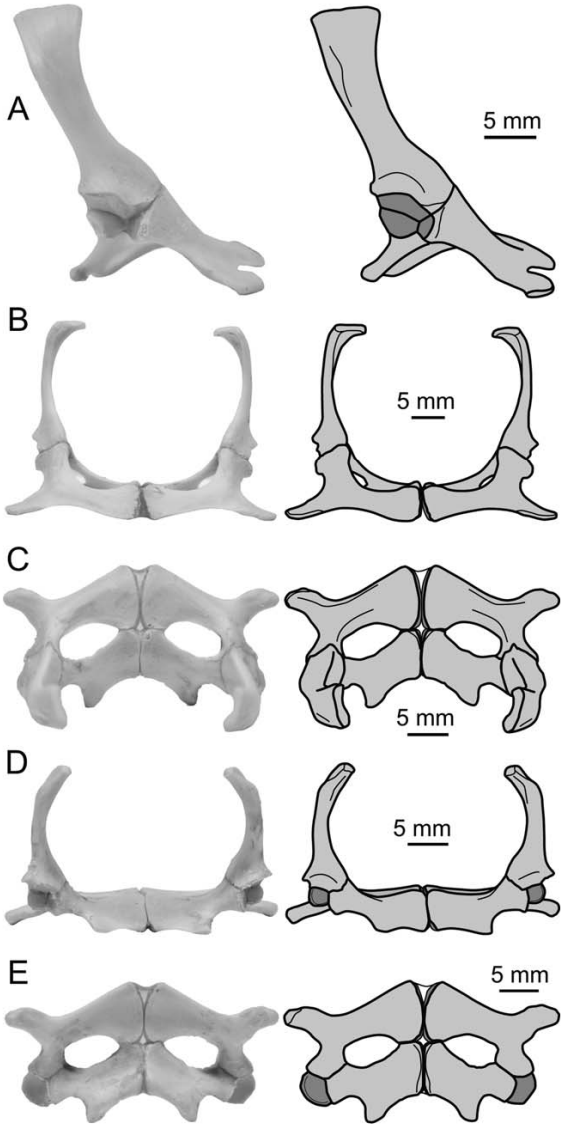

Fig. 6. *Malacochersus tornieri*, photographs and schematic interpretative drawings of pelvic girdle elements [**A**, **B**) MTD 24315; **C**–**E**) MTD 31606]. A, right lateral view. B, anterior view. C, posterior view. D, posterior view. E, ventral view.

Based on eleven individuals, the phalangeal formula of *M. tornieri* was reported to be 2-2-2-2-2/1

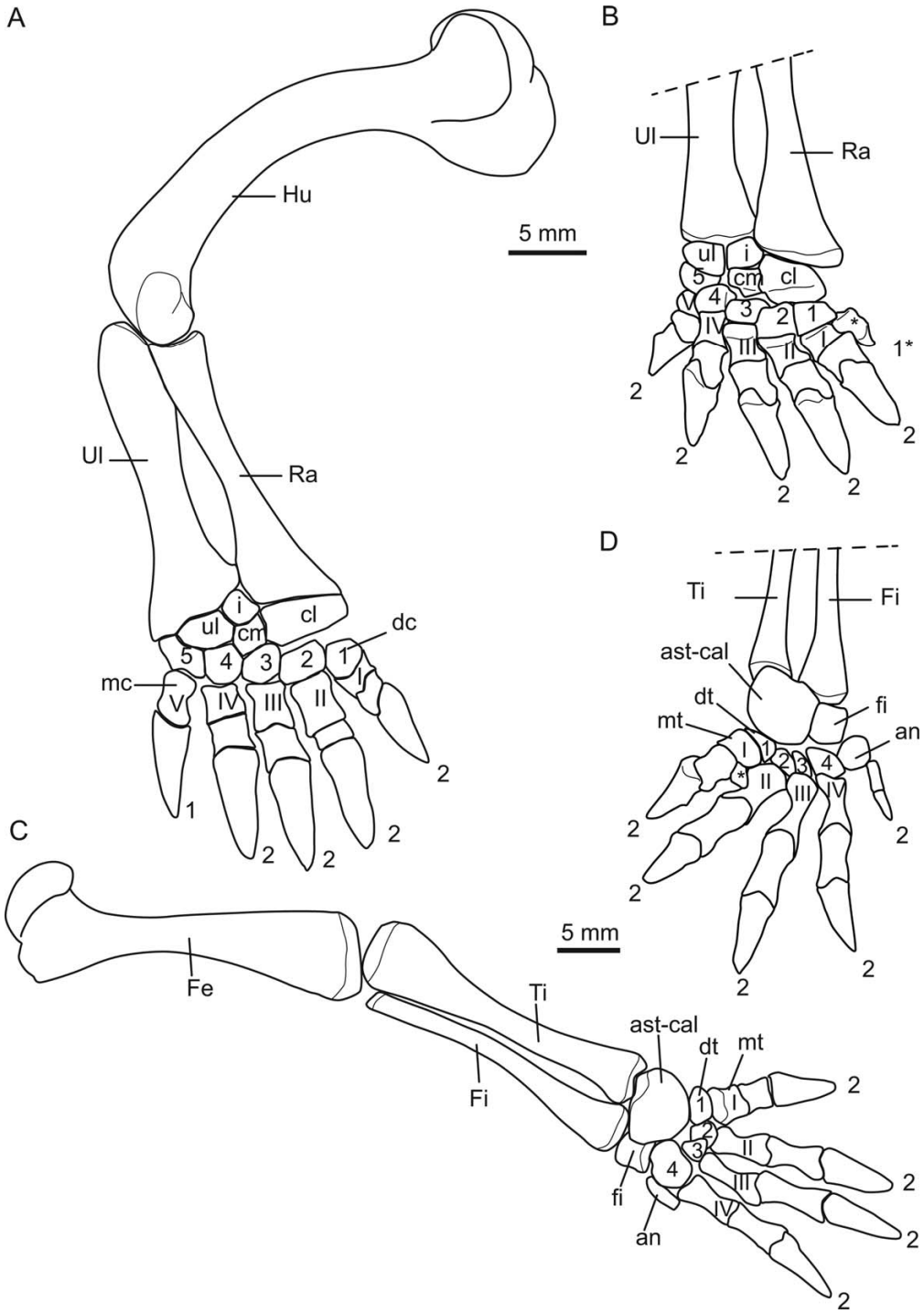

Fig. 7. *Malacochersus tornieri*, fore- and hindlimb bone morphology. **A**) Right forelimb of MTD 24315 in dorsal view. **B**) Detail of right manual autopodium of MTD 31408 in dorsal view. **C**) Left hindlimb of MTD 17162 in dorsal view. **D**) Detail of right pedal autopodium of MTD 31408 in dorsal view. Abbreviations: an, ansulate bone; ast-cal, astragalocalcaneum complex; cl, lateral centrale; cm, medial centrale; dc, distal carpal; Fe, femur; Fi, fibula; fi, fibulare; Hu, humerus; i, intermedium; mc, metacarpal; mt, metatarsal; Ra, radius; Ti, tibia; Ul, ulna; ul, ulnare; *, supernumerary bony elements. Roman numerals are used for identifying metacarpals/metatarsals, Arabic numerals for digit elements.

for the manus and 2-2-2-2-1 for the pes respectively (Crumly and Sánchez-Villagra, 2004). The addition of a second phalanx on the fifth digit in the manus was interpreted as a peramorphic condition, which occurs also in other testudinid taxa, such as *Geochelone*, *Indotestudo*, *Kinixys* and *Pyxis*. The phalangeal formula of the manus as given by Crumly and Sánchez-Villagra (2004) can be verified by the additional specimens studied herein, but only a single specimen (MTD 31408) has the fifth digit in the pes. The phalangeal formula in the pes, however, has to incorporate the fifth hooked element (ansulate bone sensu Joyce et al., 2013) and therefore should be 2-2-2-2-2. The fore- and hindlimbs of the observed specimens did not show evidence of osteoderms, nor were there osteoderms mentioned or visible in the X-rays provided by Procter (1922).

Scutes

According to Procter (1922) there is high variability between scutes observed on individuals. The general formula for the carapacial scutes is one cervical (on the nuchal bone), five vertebrals (over the neurals), four pairs of pleurals (situated on the costal bones) and 12 pairs of marginals (the last pair of marginals is called a paired supracaudal). One of the 23 specimens treated by Procter (1922) has 13 marginals on the left side, one 13 on both sides, one only four vertrebrals, one has the third vertebral divided longitudinally and three individuals possess an intergular.

The specimens studied here also have some variation in the scutes. ZM 100.102 has one cervical, 11 marginals on the right side, 12 marginals on the left, six vertebrals, five pleurals on the left side and four pleurals on the right (Supporting Information Fig. S3). Furthermore the second vertebral is divided horizontally and it is also deformed and not hexagonal (see Procter, 1922), but indented on the left side. MTD 19333 has 13 marginals on both sides, but except from that, follows the general formula and MTD 47600 deviates with six pleurals on the left side. The rest of the specimens used in this study follow the formula reported originally (Procter, 1922) and only FMNH 5616 shows an intergular.

DISCUSSION

Our study provides complementary information on the osteology and scutation pattern found in *Malacochersus tornieri*, particularly of the striking morphological variation of the bony shell and the appendicular skeleton. Furthermore it includes a novel description of the inner ear and brain endocast. Comparing the shell height of tortoises with reproductive (number of eggs in a clutch) and ecological factors (natural habitat preference) did not reveal clear trends (Supporting Information Table S1). High-domed forms living in open or forested environments can have many eggs per clutch (e.g., the African *Stigmochelys pardalis*) or only very few (e.g., the Madagascar tortoise *Astrochelys yniphora*); flat-shelled taxa such as the North American fossorial gopher tortoise *Gopherus polyphemus* can have also many eggs or only a single egg, as evidenced by the small padloper species *Homopus signatus*. The latter species also lives in rocky environments, where it often seeks cracks for hiding; however, the way of wedging itself into the cracks is still unique behavior of *Malacochersus tornieri*. Furthermore, the *Testudo-Indotestudo-Malacochersus* clade is, with the exception of *M. tornieri*, neither particularly flat nor high-domed (see Fig. 1).

Conversely, *M. tornieri* is characterized by a unique shell structure and bone composition, which is atypical for turtles (Zangerl and Johnson, 1957; Zangerl, 1969). In 11 of the 14 studied specimens the carapacial bone formula differs from the typical formula found by previous authors (Table 1; see also Procter, 1922). Eight out of 10 specimens had two suprapygals present instead of one. Therefore, we suggest two suprapygals as the typical number instead of one. The number of specimens available in the first in-depth osteological study (Procter, 1922), was larger (23 dead individuals and 2 live ones), but not many were complete and only used the complete skeleton of one adult, X-rays of the two type specimens, one young and one individual that decomposed during transit were used for the osteological description. Therefore, it is possible that most specimens have two suprapygals, and that there is considerable variation between the individuals. With our results the typical carapacial bone formula would be one nuchal, eight neurals, eight paired costals, 11 paired peripherals, two suprapygals and one pygal bone.

The plastron is less variable with only five out of 14 individuals deviating from the typical bone formula. This amount of variation in such a small sample is still high. In two specimens additional bones participate in the plastron and the central plastral fontanelle. Similar additional bones were already observed and interpreted as mesoplastra (Pritchard, 1979, 2008). If they are actually homologous to the true mesoplastra, which are usually paired, is not clear.

Most publications on variation in the turtle shell are related to the scutes, where variation is more frequently noted and easier to study than in the underlying bony shell (Zangerl and Johnson, 1957; MacCulloch, 1981; Hewavisenthi and Parmenter, 2001; Bell et al., 2006; Moustakas-Verho and Cherepanov, 2015; Loehr, 2016; Packard et al., 2016). Similar factors that influence the scutation, however, also likely influence the shell bone composition beneath, but to support this statement, further specific developmental studies are necessary. Although *Malacochersus tornieri* seems to stand out among

other testudinids (Fig. 1) and other turtles in general, given its high levels of shell (both bone and scute) variability, a more general comparative study covering several species to show that other species do not show a similar amount of variation as *M. tornieri* is deemed necessary. In comparison to its shell, no abnormalities or conspicuous variation was noticed in the axial and proximal appendicular elements. In the distal appendicular skeleton, however, which was already studied previously (Crumly and Sánchez-Villagra, 2004), we noticed additional variation in the manus and pes that was previously not reported. Besides the known manual formula 2-2-2-2-2/1 and pedal formula of 2-2-2-2-1 for the species, we report on a specimen (MTD 31408) with a supernumerary ossification, interpreted here as an additional digit anterior to the first normal digit in the manus. The same specimen was the only one in the whole series that, following the interpretation of the ansulate bone sensu Joyce et al. (2013), has two phalanges in the fifth pedal digit, leading to the formula 2-2-2-2-2, as well as a supernumerary ossification between digit 1 and 2. In contrast, the lack of elements of the fifth digit in several specimens (MTD 14777, 17162, 19334, 24315 and 31606), although the ansulate bone was always well developed, is interpreted here as a preservation bias during maceration and preparation rather than indicating a potential loss of the fifth digit in this species which frequently occurs in some other testudinids (Crumly and Sánchez-Villagra, 2004).

The skull bone composition noted herein was constant over all observed skulls, corroborating that already described earlier (Gaffney, 1979). In addition, the inner ear of *M. tornieri* has characteristics common in many turtles, the canals are broad with straight anterior and posterior semicircular canals, and separated by a notch above the common crus. The space for the external semicircular canal is confluent with the sacculus along most of its length.

AUTHOR CONTRIBUTIONS

Conception and design of study: Torsten Scheyer, Uwe Fritz

Acquisition of data: Torsten Scheyer, Anna-Katharina Mautner

Analysis and interpretations of the data: Anna-Katharina Mautner, Ashley Latimer, Torsten Scheyer

Drafting the manuscript: Anna-Katharina Mautner, Torsten Scheyer, Ashley Latimer

Critical revision of the article: Torsten Scheyer, Uwe Fritz

Approval of the version of the manuscript to be published: Anna-Katharina Mautner, Ashley Latimer, Uwe Fritz, Torsten Scheyer

ACKNOWLEDGMENTS

Henry Heidecke (MTD) is thanked for the preparation of *Malacochersus* specimens. Raffael Ernst and Markus Auer (MTD), Heinz Grillitsch (NMW), as well as Barbara Oberholzer and Marianne Haffner (ZM UZH) granted and provided access to specimens. Alexandra Wegmann (PIMUZ) is acknowledged for scanning the skull and Andreas Bedorf (former Bonn University) for creating the virtual endocast and endosseous labyrinth. Ingmar Werneburg (GPIT) and Massimo Delfino (Univ. Torino) are thanked for discussions. Tristan Stayton (Bucknell Univ.) is thanked for providing images of the Field Museum specimen used. We thank the editor and two anonymous reviewers for their valuable comments and suggestions. The authors declare to have no conflict of interest.

LITERATURE CITED

Bell B, Spotila JR, Congdon J. 2006. High incidence of deformity in aquatic turtles in the John Heinz National Wildlife Refuge. Environ Pollut 142:457–465.

Bell T. 1828. Descriptions of three new species of land tortoises. Zool J 3:419–421.

Bonin F, Devaux B, Dupré A. 2006. Turtles of the World. Baltimore: Hopkins University Press. 416 p.

Boulenger GA. 1920. Une Tortue extraordinaire: *Testudo Loveridgii*, sp. n. C R Hebd Seances Acad Sci, Paris 170:263–265.

Broadley DG. 1997. An anomalous specimen of *Pelusios sinuatus* lacking mesoplastra. Celonian Conserv Biol 2:610–611.

Carabajal AP, Sterli J, Müller J, Hilger A. 2013. Neuroanatomy of the marine Jurassic turtle *Plesiochelys etalloni* (Testudinata, Plesiochelyidae). PLoS One 8:1–12.

Chansa W, Wagner P. 2006. On the status of *Malacochersus tornieri* (Siebenrock, 1903) in Zambia. Salamandra 42:187–190.

Crumly CR. 1982. The "parietal" foramen in turtles. J Herpetol 16:317–320.

Crumly CR. 1984a. The Evolution of Land Tortoises (family Testudinidae). PhD thesis, Department of Zoology and Physiology, Rutgers, The State University of New Jersey, Newark, NJ. 584 p.

Crumly CR. 1984b. The cranial morphometry of Galapagos tortoises. Proc California Acad Sci 43:111–121.

Crumly CR. 1988. A nomenclatural history of tortoises (Family Testudinidae). Smithson Herpetol Inf Serv 75:1–17.

Crumly CR, Sánchez-Villagra MR. 2004. Patterns of variation in the phalangeal formulae of land tortoises (Testudinidae): Developmental constraint, size and phylogenetic history. J Exp Zool (Mol Dev Evol) 302B:134–146.

Delfino M, Chesi F, Fritz U. 2009. Shell morphology of the Egyptian tortoise, *Testudo kleinmanni* Lortet, 1883, the osteologically least-known *Testudo* species. Zool Stud 48:850–860.

Depecker M, Berge C, Penin X, Renous S. 2006. Geometric morphometrics of the shoulder girdle in extant turtles (Chelonii). J Anat 208:35–45.

Dorđević S. 2014. Carapace peculiarities of Hermann's tortoises (*Testudo hermanni*) in several Balkan populations. North West J Zool 11:16–26.

Dosik M, Stayton T. Size, shape, and stress in tortoise shell evolution. Herpetologica 72. doi: 10.1655/Herpetologica-D-16-00031.

Ernst CH, Barbour RW. 1989. Turtles of the World. Washington, DC: Smithsonian Institution Press. 313 p.

Ewert MA, Hatcher RE, Goode JM. 2004. Sex Determination and ontogeny in *Malacochersus tornieri*, the pancake tortoise. J Herpetol 38:288–291.

Fritz U, Bininda-Emonds ORP. 2007. When genes meet nomenclature: Tortoise phylogeny and the shifting generic concepts of *Testudo* and *Geochelone*. Zoology 110:298–307.

Fritz U, Havaš P. 2007. Checklist of chelonians of the world. Vertebr Zool 57:149–368.
Gaffney ES. 1979. Comparative cranial morphology of recent and fossil tortoises. Bull Am Mus Nat Hist 164:67–376.
Gaffney ES, Meylan PA. 1988. A phylogeny of turtles. In: Benton MJ, editor. The Phylogeny and Classification of the Tetrapods. Volume 1: Amphibians, Reptiles, Birds. Oxford: Clarendon Press. pp 157–219.
Gerlach J. 1999. Distinctive neural bones in *Dipsochelys* giant tortoises: Structural and taxonomic characters. J Morphol 240:33–37.
Gibbons JW, Lovich JE. 1990. Sexual dimorphism in turtles with emphasis on the slider turtle (*Trachemys scripta*). Herpetol Monogr 4:1–29.
Gmelin JF. 1789. Caroli a Linné, Systema naturae per regna tria naturae secundum classes, ordines, genera species, cum characteribus, differentiis, synonymis, locis. Ed. 13. Leipzig: Tom.I Pars III. pp 1033–1516.
Hewavisenthi S, Parmenter CJ. 2001. Influence of incubation environment on the development of the flatback turtle (*Natator depressus*). Copeia 2001:668–682.
Ireland LC, Gans C. 1972. The adaptive significance of the flexible shell of the tortoise *Malacochersus tornieri*. Anim Behav 20:778–781.
Joyce WG, Werneburg I, Lyson TR. 2013. The hooked element in the pes of turtles (Testudines): A global approach to exploring primary and secondary homology. J Anat 223:421–441.
Le M, Raxworthy CJ, McCord WP, Mertz L. 2006. A molecular phylogeny of tortoises (Testudines: Testudinidae) based on mitochondrial and nuclear genes. Mol Phylogenet Evol 40: 517–531.
Le Conte J. 1830. Description of the new species of North American tortoises. Ann Lyceum Nat Hist New York 3:91–131.
Lee MSY. 1996. The homologies and early evolution of the shoulder girdle in turtles. Proc R Soc Lond B 263:111–117.
Loehr VJT. 2016. Wide variation in carapacial scute patterns in a natural population of speckled tortoises, *Homopus signatus*. African J Herpetol 65:47–54.
Lortet L. 1883. Poissons et reptils du lac de Tibériade et de quelques autres parties de la Syrie. Arch du Mus Hist Nat Lyon 3:99–194.
Loveridge A. 1923. Notes of East African tortoises collected 1921-1923 with the description of a new species of land tortoise. Proc Zool Soc Lond 1923:923–933.
Loveridge A, Williams EE. 1957. Revision of the African tortoises and turtles of the suborder Cryptodira. Bull Mus Comp Zool 115:163–557.
Lovich JE, Ernst CH. 1989. Variation in the plastral formulae of selected turtles with comments on taxonomic utility. Copeia 1989:304–318.
Lynn WG, Ullrich MC. 1950. Experimental production of shell abnormalities in turtles. Copeia 1950:253–262.
MacCulloch RD. 1981. Variation in the shell of *Chrysemys picta belli* from southern Saskatchewan. J Herpetol 15:181–185.
Malonza PK. 2003. Ecology and distribution of the pancake tortoise, *Malacochersus tornieri* in Kenya. J East African Nat Hist 92:81–96.
Mautner A-K, Latimer AE, Fritz U, Scheyer TM. 2016. 3D data and models related to the publication: An updated description of the osteology of the pancake tortoise *Malacochersus tornieri* (Testudines: Testudinidae) with special focus on intraspecific variation. MorphoMuseuM 2 (2)-e4. doi:10.18563/m3.2.2.e4.
Mertens R, Müller L. 1934. Systematische Liste der lebenden Schildkröten. Blätt Aquar- Terrarienkunde 45:42–45, 59–67.
Mertens R, Wermuth H. 1955. Die rezenten Schildkröten, Krokodile und Brückenechsen. Zool Jahrb, Abt Syst 83:323–440.
Moll D, Klemens MW. 1996. Ecological characteristics of the pancake tortoise, *Malacochersus tornieri*, in Tanzania. Chelonian Conserv Biol 2:26–35.
Moustakas-Verho JE, Cherepanov GO. 2015. The integumental appendages of the turtle shell: An evo-devo perspective. J Exp Zool Part (Mol Dev Evol) 324B:221–229.
Packard GC, Packard MJ, Miller K, Bordman TJ. 2016. Influence of moisture, temperature, and substrate on snapping turtle eggs and embryos. Ecology 68:983–993.
Parham JF, Macey JR, Papenfuss TJ, Feldman CR, Turkozan O, Polymeni R, Boore J. 2006. The phylogeny of Mediterranean tortoises and their close relatives based on complete mitochondrial genome sequences from museum specimens. Mol Phylogenet Evol 38:50–64.
Parker GH. 1901. Correlated abnormalities in the scutes and bony plates of the carapace of the sculptured tortoise. Am Nat 35:17–24.
Pritchard PCH. 1979. Encyclopedia of Turtles. Encycl Turtles. Neptune: T. F. H. Publications. 895p.
Pritchard PCH. 2008. Evolution and structure of the turtle shell. In: Wyneken J, Godfrey MH, Bels V, editors. Biology of Turtles Boca Raton: CRC Press. pp 45–83.
Procter JB. 1922. A study of the remarkable tortoise, *Testudo loveridgii* Blgr., and the morphology of the chelonian carapace. Proc Zool Soc Lond 1922:483–1276.
Rhodin AGJ, Mittermeier R. 1977. Neural bones in chelid turtles from Australia and New Guinea. Copeia 1977:370–372.
Rothschild BM, Schultze H-P, Pellegrini R. 2013. Osseous and other hard tissue pathologies in turtles and abnormalities of mineral deposition. In: Brinkman DB, Holroyd PA, Gardner JD, editors. Morphology and Evolution of Turtles [Proceedings of the Gaffney Turtle Symposium (2009) in Honor of Eugene S Gaffney. Vertebrate Paleobiology and Paleoanthropology Series]. Dordrecht: Springer. pp 501–534.
Sánchez-Villagra MR, Pritchard PCH, Paolillo A, Linares OJ. 1995. Geographic variation in the matamata turtle, *Chelus fimbriatus*, with observations on its shell morphology and morphometry. Chelonian Conserv Biol 1:293–300.
Schneider JG. 1783. Allgemeine Naturgeschichte der Schildkröten, nebst einem systematischen Verzeichnisse der einzelnen Arten und zwey Kupfern. Leipzig: J.G. Müller. 364 p.
Siebenrock F. 1903. Über zwei seltene und eine neue Schildkröte des Berliner Museums. Sitzungsber Akad Wissensch Wien, Math-Naturw Cl 112:439–445.
Siebenrock F. 1904. Über partielle Hemmungs-Erscheinungen bei der Bildung einer Rückenschale von *Testudo tornieri*, Siebenrock. Sitzungsber Akad Wissensch Wien, Math-Naturw Cl 113:29–34.
Smith A. 1838. Illustrations of the Zoology of South Africa; consisting chiefly of Figures and Descriptions of the Objects of Natural History collected during an Expedition into the Interior of South Africa in the years 1834, 1835 and 1836. London: Smith, Elder and Co. 23 p.
Spix JB. 1824. Animalia nova sive species novae testudinum et ranarum, quas in itinere per Brasiliam annis MDCCCXVII - MDCCCXX jussu et auspiciis Maximiliani Josephi I. Bavariae Regis suscepto collegit et descripsit. Munich, Hübschmann. 53 p.
Thomson S, Georges A. 1996. Neural bones in Australian chelid turtles. Chelonian Conserv Biol 2:82–86.
Turtle Taxonomy Working Group. 2014. Turtles of the World, 7th Edition: Annotated Checklist of Taxonomy, Synonymy, Distribution with Maps, and Conservation Status. In: Rhodin AGJ, Pritchard PCH, Van Dijk PP, Saumure RA, Buhlmann KA, Iverson JB, Mittermeier RA, eds. Conservation Biology of Freshwater Turtles and Tortoises: A Compilation Project of the IUCN/SSC Tortoise and Freshwater Turtle Specialist Group. Chelonian Res Monogr 5:329–479.
Walker WFJ. 1973. The locomotory apparatus of testudines. In: Gans C, Parsons TS, editors. Biology of the Reptilia, Vol. 4: Morphology D. London: Academic Press. pp 1–100.
Zangerl R. 1957. A parietal foramen in the skull of a recent turtle. Proc Zool Soc Calcutta 1957:273.
Zangerl R. 1969. The turtle shell. In: Gans C, Bellairs A d'A., Parsons TS, editors. Biology of the Reptilia, Vol. 1 Morphology A. London: Academic Press. pp 311–339.
Zangerl R, Johnson RG. 1957. The nature of shield abnormalities in the turtle shell. Fieldiana Geol 10:341–362.
Zug GR. 1971. Buoyancy, locomotion, morphology and the pelvic girdle and hindlimb, and systematics of Cryptodiran turtles. Misc Publ Museum Zool Univ Michigan 142:1–98.

6.2 3D data and models related to the publication: An Updated Description of the osteology of the pancake tortoise *Malacochersus tornieri*

Ana-Katharina Mautner[1], Ashley E. Latimer[1], Uwe Fritz[2], Torsten M. Scheyer[1]

[1]University of Zurich, Department of Paleontology, Karl Schmid-Strasse 4, Zurich, CH-8006, Switzerland
[2] Museum of Zoology (Museum fur Tierkunde) A. B. Meyer Building, Dresden, D-01109, Germany

morphoMuseum

Volume 02, issue 2
January 2017

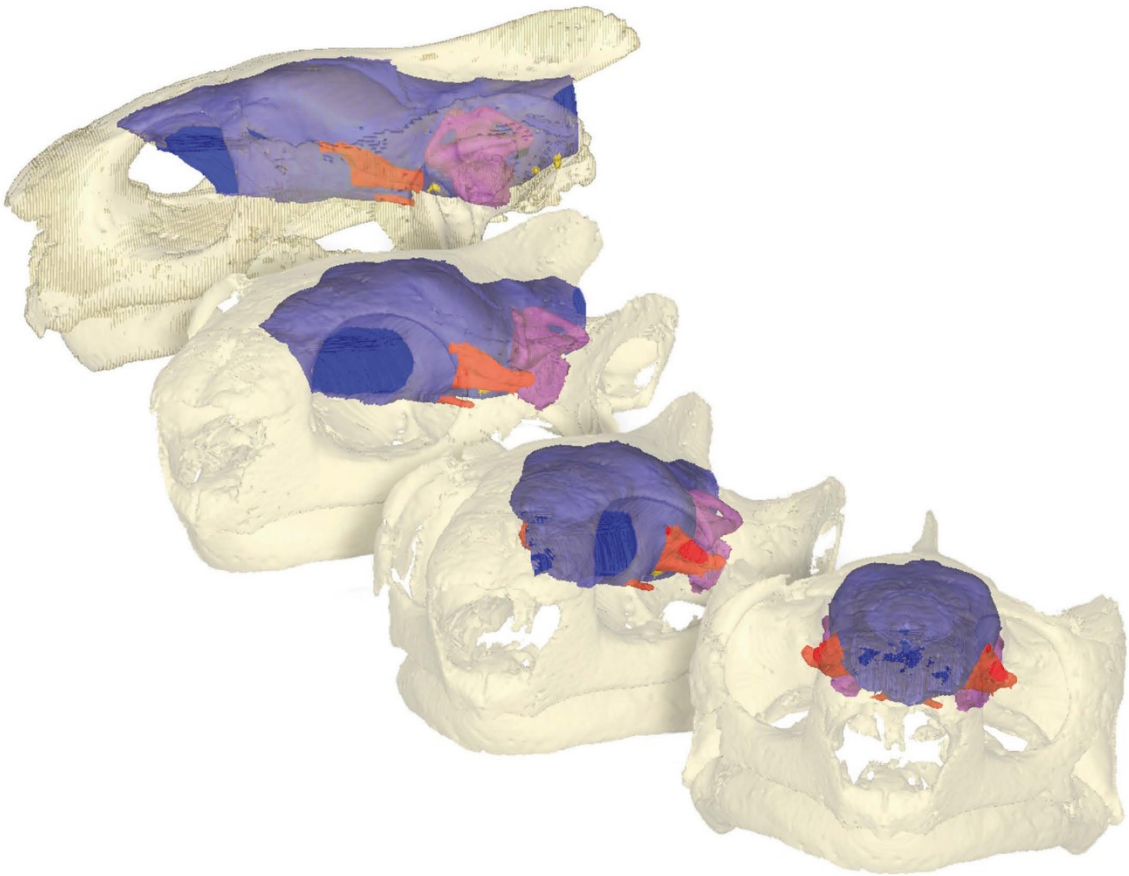

Featured dataset:

Anna-Katharina Mautner , Ashley E. Latimer, Uwe Fritz and Torsten M. Scheyer

3D data and models related to the publication: An updated description of the osteology of the pancake tortoise *Malacochersus tornieri* (Testudines: Testudinidae) with special focus on intraspecific variation.

Dataset

3D data and models related to the publication: An updated description of the osteology of the pancake tortoise *Malacochersus tornieri* (Testudines: Testudinidae) with special focus on intraspecific variation

Mautner Anna-Katharina[1], Latimer Ashley E.[1], Fritz Uwe[2], Scheyer Torsten M.[1]*

[1] *University of Zurich, Palaeontological Institute and Museum, Karl Schmid-Strasse 4, CH- 8006 Zurich, Switzerland.*
[2] *Museum of Zoology (Museum für Tierkunde), A. B. Meyer Building, D-01109 Dresden, Germany.*
***Corresponding author**: tscheyer@pim.uzh.ch*

Abstract
The present publication contains the µCT dataset and the 3D models analyzed in the following publication: Mautner, A.-K., A. E. Latimer, U. Fritz, and T. M. Scheyer. An updated description of the osteology of the pancake tortoise *Malacochersus tornieri* (Testudines: Testudinidae) with special focus on intraspecific variation. Journal of Morphology. https://doi.org/10.1002/jmor.20640

Keywords: brain endocast, chelonian shell, micro computed tomography, morphology, variability

Submitted:2016-12-09, published online:2017-01-25. https://doi.org/10.18563/m3.2.2.e4

Model IDs	Taxon	Description
M3#129_ZM 100.102	*Malacochersus tornieri*	Virtual brain and inner ear endocast.
M3#130_ZM 100.102	*Malacochersus tornieri*	µCT data set (resolution: 36µm)

Table 1. List of models

INTRODUCTION

The inner ear and brain endocast (Fig. 1) using micro CT scan data is part of a revised osteological analysis of the pancake tortoise *Malacochersus tornieri* (Mautner et al., 201X). This tortoise has a very flat shell, which allows the animal to hide in cracks and under rocks in its natural habitat, i.e. rocky arid shrub and thorny brush environments in Tanzania and adjacent countries in eastern Africa (e.g., Procter, 1922).

METHODS

The 3D surfaces were extracted by manually labeling cranial spaces within AVIZO (FEI). The 3D surface models are provided in .ply format that can be opened with a wide range of freeware viewers. In addition the 3D dataset that was used for the 3D modeling is provided as well.

ACKNOWLEDGEMENTS

Grant sponsor: Swiss National Science Foundation. Grant number: 31003A-149506 to TMS

BIBLIOGRAPHY

Mautner, A.-K., A. E. Latimer, U. Fritz, and T. M. Scheyer (201X). An updated description of the osteology of the pancake tortoise *Malacochersus tornieri* (Testudines: Testudinidae) with special focus on intraspecific variation. Journal of Morphology. https://doi.org/10.1002/jmor.20640

Procter, J. B., 1922. A study of the remarkable tortoise, *Testudo loveridgii* Blgr., and the morphogeny of the chelonian carapace. Proceedings of the Zoological Society of London Pt. 3 No. 34, 483-526. https://doi.org/10.1111/j.1096-3642.1922.tb02155.x

Figure 1. Virtual brain and inner ear endocast of *Malacochersus tornieri* (ZM 100.102; Zoological Museum of the University of Zürich). Blue, endocranium; red, blood vessels; purple, semicircular canals; yellow, cranial nerves.

Chapter 7 Discussion

As we have seen, the semicircular canals are shaped by their evolutionary history, phylogeny rather than habit predicts the shapes of the central streamlines in reptiles. Habit should not be estimated from labyrinth shape when sampling across distantly related reptiles.

Critical examination of the literature on ecomorph and inner ear morphology show that relationships to habit are often not supported when phylogeny is included [1], for taxa with unknown relationship to living related taxa [2], and here, after size is accounted for. Amphibians, snakes, and birds should be subjected to the same cross-clade analyses like the reptiles studied here to determine if phylogeny and semicircular canal morphology have the same relationship. If so, predicting ecology from inner ear shape in those species for distantly related taxa is equally dubious.

As in whales, semicircular canals are smaller and shorter than would be predicted from body mass in the Ross seal *Ommatophoca rossi* and large sauropterygians. Unlike whales, this morphology is not associated with a change in neck length to body mass in seals, appears with an extreme shortened neck in sauropterygians, and the semicircular canals actually overpredict body mass in the olive Ridley sea turtle *Lepidochelys olivacea*. Therefore, the shortened semicircular canals of pelagic marine taxa may not be related to shortened necks, nor is it simply acquired as taxa become semiaquatic, nor is it uniformly acquired by pelagic taxa. Although the morphology may not reflect ecology, it may be related to dorso-ventral motion during locomotion also known as head-digging.

Fish, although undeniably aquatic, lack the inner ear morphology that is seen in aquatic tetrapods. This suggests that typical bulbous appearance of pelagic tetrapods is not related to the environment, but perhaps related to the difference between morphology between bony fishes and tetrapods. One striking feature that has evolved for amniote tetrapods is the atlas-axis complex in the neck, which allows for dorso-ventral motion impossible in fishes. Taxa that move with a head-digging dorso-ventral motion develop reduced canals length. Independent evolution of that motion in caecilian amphibians, coupled with fossorial head-digging habit results in that same morphology [3]. The shortened semicircular canals of reptiles and the Ross seal look superficially similar such as fossorial snakes [4,5] and caecilians. Furthermore, taxa that exhibit lateral undulations, sea snakes [4] and fish, and do not have the small canal morphology. This suggests that dorso-ventral motion has a large influence on semicircular canal morphology irrespective of ecology but present with convergent dorso-ventral motion.

Further directions for this research, aside from what is listed above, include testing specific aspects of body morphology and quantifying aspects of the semicircular ducts such as number of hair receptors and fluid viscosity of vertebrates. Aspects of body morphology of

particular interest include leg length, neck length, relative size of the head, changes in braincase side-wall associated with different mouth-gapes in both fishes and reptiles, and developmental arrest of the semicircular canals in mammals. Leg lengths and presence or absence of legs would determine if legless taxa undergo the same types of morphological changes as those with them. Investigations into the soft tissue would reveal how changes in semicircular canals are related to changes in semicircular ducts. Each of these features would provide insight into the constraints on inner ear morphology and potentially provide background to predicting more of life history and soft tissue morphology from semicircular canals.

Semicircular canals have an untapped utility as body mass estimators. We show here that a simple measure of inner ear size, labyrinth length, predicts body mass across reptiles even when the sampled semicircular canals and literature provided body mass estimates come from disparate individuals. With both pieces of data from the same individual, and samples to more restricted clades, the predictive power for body mass will be even closer to true values.

Further research avenues opened by these wide-ranging chapters suggest change our view on the applicability of inner ear size and shape for addressing questions of life history. While semicircular canal shape is not predicted by habit, it is predicted by phylogeny. Therefore, it may be used for secondary tests of phylogenetic hypotheses, which has not yet been attempted. Because we show that the inner ear is conserved phylogenetically and does not converge on life habit, it provides the perfect universal comparator for phylogeny without convergent ecological issues. Attempts should begin with fishes, where uncertain phylogenetic relationships of extinct taxa producing poorly supported trees are a very real problem. Additionally, body size estimates from inner ears might be another useful independent nondestructive metric for taxa where this information is unknown. Labyrinth length proves a powerful metric of size that does not require perfect preservation and is universally present in all vertebrates. Convergent evolution of bulbous inner ears likely come from dorso-ventral motion associated with head-digging in any medium. This semicircular canal appearance does not detract from the phylogenetic signal in inner ear shape in our samples. Although some uses of inner ear shape are no longer supported, these new applications will further our understanding of vertebrate body size deep time phylogenetic relationships.

REFERENCES

1. Grohe C, Tseng ZJ, Lebrun R, Boistel R, Flynn JJ. 2016 Bony labyrinth shape variation in extant Carnivora: a case study of Musteloidea. *J. Anat.* **228**, 366–383. (doi:10.1111/joa.12421)

2. Dickson B V., Sherratt E, Losos JB, Pierce SE. 2017 Semicircular canals in *Anolis* lizards: ecomorphological convergence and ecomorph affinities of fossil species. *R. Soc. Open Sci.* **4**, 170058. (doi:10.1098/rsos.170058)
3. Maddin HC, Sherratt E. 2014 Influence of fossoriality on inner ear morphology: Insights from caecilian amphibians. *J. Anat.* **225**, 83–93. (doi:10.1111/joa.12190)
4. Palci A, Hutchinson MN, Caldwell MW, Lee MSY. 2017 The morphology of the inner ear of squamate reptiles and its bearing on the origin of snakes. *R. Soc. Open Sci.* **4**, 170685. (doi:10.1098/rsos.170685)
5. Yi H, Norell MA. 2015 The burrowing origin of modern snakes. *Sci. Adv.* **1**, 1–5. (doi:10.1126/sciadv.1500743)

Curriculum Vitae

LATIMER, ASHLEY EMILIE
Email: ashley.latimer@pim.uzh.ch or latimer.ae@gmail.com
Date of birth: 19 September, 1989
Nationalities: French, New Zealander

Education

2014-2018: PhD, The University of Zurich, Department of Paleontology
Supervisor: Torsten Scheyer
Title:

2011-2014: MSc in Geological Sciences (Paleontology)
The University of Texas at Austin, Jackson School of Geosciences
Title: Redescription of teeth and epithelial plates from the platypus (*Ornithorhynchus anatinus*): morphological and evolutionary implications

2008-2011: BS in Geological Sciences, Environmental Geology, August 2011
The University of Texas at Austin, Jackson School of Geosciences

Research interests

Paleozoic and Mesozoic marine faunas
Sensory adaptations
3D modeling techniques
Novel morphology

Skills

Fluent in French

Technical operation of scanning electron microscopes(SEM), Nikon 3D Computed Tomography scanner (CT)

Software proficiencies in VG Studio Max, Aviso, Slicer, Mimics, Meshlab, MeshTools, Arc GIS, Geomapper, PAUP*, R, Mesquite, TKS, Adobe and Microsoft packages

Field Experience

Collected Jurassic and Triassic invertebrates, Eastern and Northern **France** 8/2015
Collected Devonian invertebrates, Tafilalt Basin, **Morocco** 3/2015
Overview of Triassic vertebrate localities in Southern **Germany** 8/2014
Collected Miocene vertebrates, Devil's Graveyard badlands in **West Texas**, 1/2014
Collected Cambrian to Silurian echinoderms, localities in **Oklahoma**, 8/2013
Controlled excavation of Pleistocene vertebrate material from a stratified deposit in a **West Texas** cave, Crockett Co. 3/2013

Collected Cambrian to Devonian invertebrate communities in Western **Utah** 7/2011
Led undergraduate student field trips for classes in Austin, **Texas** focusing on geology and fossils of the local area 2013, 2012, 2011

Collections and Curatorial Experience

Vertebrate Paleontology Laboratory, The University of Texas at Austin Pickle Campus, 2012

Responsibilities included cataloging and moving a section of the vertebrate collection, conserving and cross-checking information with the database, physically relocating specimens to new cabinets, accessioning new field material to the collections.

Nonvertebrate Paleontology Laboratory, The University of Texas at Austin Pickle Campus, 2010

Responsibilities included photographing collection materials with a light box and camera stand, entering data in collections databases using Specify and Microsoft Access, cleaning and conserving recent endangered and extinct mussel collections, identifying and curating fossil invertebrate material.

Teaching Appointments

The University of Zurich
Miscellaneous Lectures – Sensory Systems and Skulls, Spring 2014, Fall 2015, Fall 2016

Teaching Assistant Vertebrate morphology, Spring 2015, Spring 2016, Spring 2017

Responsibilities included writing a lecture and assignment for students, designing and supervising multiple student projects

The University of Texas at Austin

Teaching Assistant Introductory **Geology**, Spring 2013

Responsibilities included coordinating two large separate lab groups meeting twice per week, rewriting and updating fossil lab section, driving students to field sites and leading field trips, grading assignments.

Head Teaching Assistant, **Paleobiology**, Fall 2012, Fall 2011

Responsibilities included teaching classes of 20 students twice a week on topics across the tree of life, driving students to field sites, designing and writing quizzes and tests, preparing laboratory sections, grading assignments.

Head Teaching Assistant, **Plate Tectonics and Earth History**, Spring 2012

Responsibilities included teaching classes across the tree of life and geological principals, designing and writing quizzes and tests, preparing laboratory sections, grading assignment, driving students to field sites.

Geology Internship

Imagine Resources, LLC, Summer 2009, Winter 2009, Summer 2010
Responsibilities included creating digital cross sections used in publication

(Cornish, F. G. 2011. Incised Valleys of the Upper Wilcox, Middle Texas Gulf Coast: Additional Pathways for Wilcox Sand Delivery to the Deep Gulf of Mexico. South Texas Geological Society Bulletin 52:15-48), copying, rectifying, and importing maps to TKS, digitizing and correlating well logs, retrieving well logs from various sources, integrating physical and digital media to create attractive prospect presentations, providing technical support for programs and devices.

Honors, Awards, and Achievements

2014: MS Tech Sessions speaker award
2012, 2013: Lundelius Scholarship; UT
2012: Dorothy Ogden Carsey Memorial Scholarship Fund; UT
2011: Bloomer Fund for Motivated Students; UT
2010: The Louis and Elizabeth Scherck Geology Scholarship; UT
2008-2013: Jackson School Scholarship; UT
2008: Daughters of the American Revolution Scholarship
2008: Ms Pete Scholarship

Professional Memberships and Service

2016 – Present American Society of Naturalists
2014 – Present European Association of Vertebrate Paleontology
2011 – Present Society of Vertebrate Paleontologists

Presentations and Outreach

2017: Invited lecture to Neuroanatomy group in the University of Zurich
2016: Public talk - Balance and Orientation-Lange Nacht der Museen, Zurich Switzerland
2015: Public talk - Skulls and sensory systems -Lange Nacht der Museen, Zurich Switzerland
2014: Lange Nacht at the Museum
2013: Explore UT, annual public event at the university, Presented on fossils, anatomy and, evolution
2008: Representative of the Texas Coastal Bend, Presented on ocean literacy and conservation at the Second National Student Summit on Oceans and Coasts in Washington D.C.

Abstracts and Professional Society Talks

Latimer, A. E. 2016. Neurocranial morphology of a new large Late Triassic neopterygian fish and deep bodied fishes on the teleost stem. Society of Vertebrate Paleontologists 76th annual meeting, Berlin, Germany (talk).

Latimer, A. E. 2016. 3D reconstruction of a Late Triassic Neopterygian braincase – ecological implications of the neurocranium, and the phylogeny of Neopterygii. Evolution (talk)

Latimer, A. E. 2015 Digital endocranial reconstruction of a large Triassic actinopterygian from Schesaplana, Switzerland, European Association of Vertebrate Palaeontologists 13th annual meeting, Opole, Poland (poster presentation).

Latimer, A. E. and T. Rowe. 2014 Structure and function of thickened epithelial plates (cornules) in the extant platypus (Ornithorhynchus anatinus) revisited with SEM and CT. European Association of Vertebrate Palaeontologists 12th annual meeting, Torino, Italy (poster presentation).

Latimer, A. E, T. Rowe. 2014. Juvenile platypus (Ornithorhynchus anatinus) teeth are diverse: morphological and features and evolutionary implications of a reduced dentition. p 166. Society of Vertebrate Paleontologists 74th annual meeting, Berlin, Germany (poster presentation).

Burroughs, R. W., C. J. Bell, A. E. Latimer, and E. C. Kirk. 2011. Fossil turtles from the Devil's Graveyard Formation of southwest Texas: Large terrestrial turtles and a geographic range extension for carettochelyid turtles. Pp. 91-92 in Texas Academy of Science 114th Annual Meeting Program, March 3-5th 2011 St. Edward's University.

Publications

Latimer AE, Loza CM, Sánchez-Villagra MR, Carlini AA. 2017 Supplemental information for "Sensory anatomy of the most aquatic of carnivorans: the Antarctic Ross seal, and convergences with other mammals".

Loza CM, Latimer AE, Sánchez-Villagra MR, Carlini AA. 2017 Sensory anatomy of the most aquatic of carnivorans: the Antarctic Ross seal, and convergences with other mammals. Biol. Lett. 20170489. MorphoMuseuM *in press.*

Mautner A-K, Latimer AE, Fritz U, Scheyer TM. 2017 An updated description of the osteology of the pancake tortoise Malacochersus tornieri (Testudines: Testudinidae) with special focus on intraspecific variation. J. Morphol. 278, 321-333. (doi:10.1002/jmor.20640)

Mautner A-K, Latimer AE, Uwe F, Scheyer. 2017 3D data and models related to the publication: An updated description of the osteology of the pancake tortoise Malacochersus tornieri (Testudines: Testudinidae) with special focus on intraspecific variation. MorphoMuseuM 2, 2-4.

Prepared Manuscripts

Latimer AE. Platypus (*Ornithorhynchus anatinus*) puggles chew with the teeth of adults, in review *Journal of Mammalian Evolution*

Latimer AE, Giles S. A giant dapediid from the Late Triassic of Switzerland and insights into neopterygian phylogeny, in review *Royal Society Open Science*

Latimer AE, Sherratt E, Scheyer TM. Phylogeny not habit predicts semicircular canal morphology of limbed lepidosaurs

Latimer AE, Bonnet T, Sherratt E, Scheyer TM. Shape and size of semicircular canals correlate with clade and body mass in reptiles